Dissertation zur Erlangung des Doktorgrades

der Fakultät für Chemie und Pharmazie

der Ludwig-Maximilians-Universität München

Reactions of Carbanions with Michael Acceptors and Electron-deficient Arenes: Quantifying Polar Organic Reactivity

Dipl. Chem. Florian Seeliger

aus

Hamburg

2008

Erklärung

Diese Dissertation wurde im Sinne von § 13 Abs. 3 bzw. 4 der Promotionsordnung vom 29. Januar 1998 von Herrn Prof. Dr. Herbert Mayr betreut.

Ehrenwörtliche Versicherung

Diese Dissertation wurde selbständig und ohne unerlaubte Hilfe erarbeitet.

München, 13.03.2008

……..…………………………...

Florian Seeliger

Dissertation eingereicht am   13.03.2008

1.Gutachter   Prof. Dr. Herbert Mayr
2.Gutachter   Prof. Dr. Hendrik Zipse

Mündliche Prüfung am   24.04.2008

Für Birgit

Danksagung

Ich möchte mich an dieser Stelle ganz herzlich bei Herrn Prof. Dr. Herbert Mayr für seine herausragende und beispielhafte Betreuung während der Durchführung meiner Arbeit, die interessante Themenstellung und seine stete Hilfs- und Diskussionsbereitschaft bedanken.

Weiterhin gilt mein Dank Herrn Prof. Dr. Mieczyslaw Makosza, der es mir ermöglichte, für 2 Monate in Warschau zu forschen und Prof. Dr. Hendrik Zipse, der mir als Ratgeber für die quantenchemischen Rechnungen hilfreich zur Seite stand.

Den Mitgliedern des Arbeitskreises danke ich für ein äußerst angenehmes Arbeitsklima mit vielen abwechslungsreichen Diskussionen über Chemie und andere Dinge.

Meinen Laborkollegen Oliver Kaumanns, Heike Schaller, Markus Horn und Erik Breuer sei für ihre Hilfsbereitschaft und das tolle Arbeitsklima besonders gedankt. Es war eine sehr schöne Zeit! Ferner möchte ich mich bedanken bei Sylwia Blazej, die mir in meiner Zeit in Warschau hilfreich zur Seite stand.

Meinen F-Praktikanten, Barbara Körner, Florian Hofbauer und Sebastian Bernhard danke ich für ihren großen Einsatz bei der Durchführung der experimentellen Arbeiten und die humorvolle Zusammenarbeit und wünsche ihnen für ihre Zukunft alles Gute!

Für die kritische und zügige Durchsicht dieser Arbeit danke ich Nicolas Streidl, Markus Horn, Dorothea Richter, Roland Appel, Tobias Nigst, Martin Breugst und Barbara Seeliger.

Zuletzt danke ich aber vor allem meiner Familie, insbesondere meiner Mutter und meinem Vater, die mich nicht nur während meiner Promotion, sondern Zeit meines Lebens unterstützt haben.

Publikationen

(1) S. T. A. Berger, F. H. Seeliger, F. Hofbauer, H. Mayr, *Org. Biomol. Chem.* **2007**, *5*, 3020-3026: *"Electrophilicity Parameters for 2-Benzylidene-indan-1,3-diones - a systematic extension of the benzhydrylium based electrophilicity scale"*

(2) F. Seeliger, S. T. A. Berger, G. Y. Remennikov, K. Polborn, H. Mayr, *J. Org. Chem.* **2007**, *72*, 9170-9180: *"Electrophilicity of 5-Benzylidene-1,3-dimethyl-barbituric and – thiobarbituric Acids"*

(3) F. Seeliger, S. Blazej, S. Bernhardt, H. Mayr, M. Makosza, *Chem. Eur. J.* **2008**, accepted.: *" Reactivity of Nitro-(hetero)arenes with Carbanions: Bridging Aromatic, Heteroaromatic, and Vinylic Electrophilicity"*

(4) F. Seeliger, H. Mayr, *Org. Biomol. Chem.* **2008**, submitted: *"Nucleophilic Behavior of Sulfonyl-stabilized Carbanions"*

Konferenzbeiträge

(1) 08/2006 18. IUPAC Konferenz „Physical Organic Chemistry", Warschau, Polen
Vortrag: *„Quantifying Electrophilicity and Nucleophilicity"*
Poster Präsentation: *"Electrophilicities of Benzylidenebarbituric Acids"*

Table of Contents

List of Abbreviations

aq.	aqueous
Ar	aryl
Bn	benzyl
bp	boiling point
Bu	butyl
calc.	calculated
conc.	concentrated
dma	4-(dimethylamino)phenyl
d	doublet
DMF	*N,N*-dimethyl formamide
DMSO	dimethyl sulfoxide
E	electrophilicity parameter
e.g.	exempli gratia
elec	electrophile
eq.	equation
equiv.	equivalent(s)
Et	ethyl
EtOAc	ethyl acetate
exp.	experimental
HPLC	high pressure liquid chromatography
i.e.	id est
i.v.	in vacuo
k	rate constant
K	equilibrium constant
KO*t*Bu	potassium *tert*-butoxide
lil	lilolidin-8-yl (= 1,2,5,6-tetrahydro-4*H*-pyrrolo[3,2,1-*ij*]quinolin-8-yl)
lit.	literature
M	mol/L
m	*meta*
Me	methyl
min	minute(s)

mp	melting point
MPLC	medium pressure liquid chromatography
MS	mass spectrometry
N	nucleophilicity parameter
NMR	nuclear magnetic resonance
no.	number
nuc	nucleophile
o	*ortho*
p	*para*
Ph	phenyl
ppm	parts per million
Pr	propyl
q	quartet
s	nucleophile-specific slope parameter
s	singlet
t	triplet
*t*Bu	*tert.* butyl
THF	tetrahydrofuran
vs.	versus

Chapter 0

Summary

0.1   Introduction

The linear-free-energy-relationship 0.1 is a versatile and powerful tool to predict polar organic reactivity. The reactions of carbocations with various nucleophiles as well as the reactions of carbanions with quinone methides and Michael acceptors are described by equation 0.1

$$\log k_2(20\ ^\circ\mathrm{C}) = s(N + E) \tag{0.1}$$

Electrophiles are characterized by the electrophilicity parameter E and nucleophiles are characterized by a nucleophilicity parameter N and a nucleophile-specific slope-parameter s.

0.2   Electrophilicity   of   5-Benzylidene-1,3-dimethyl-barbituric   and   -thiobarbituric Acids

Kinetics of the reactions of acceptor-stabilized carbanions **2** (e.g., anions of Meldrum's acid, dimedone, acetylacetone, ethyl acetoacetate, ethyl cyanoacetate) with benzylidenebarbituric and -thiobarbituric acids **1a-e** have been determined in dimethyl sulfoxide solution at 20 °C. ^{1}H- and ^{13}C-NMR analysis of the addition products **3⁻** confirmed the reaction course depicted in Scheme 0.1.
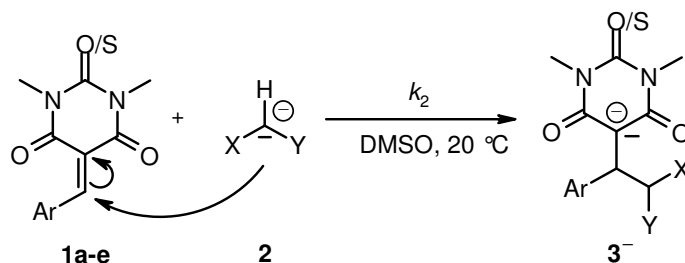
SCHEME 0.1: Reactions of the Michael acceptors **1a-e** with carbanions **2** in DMSO.
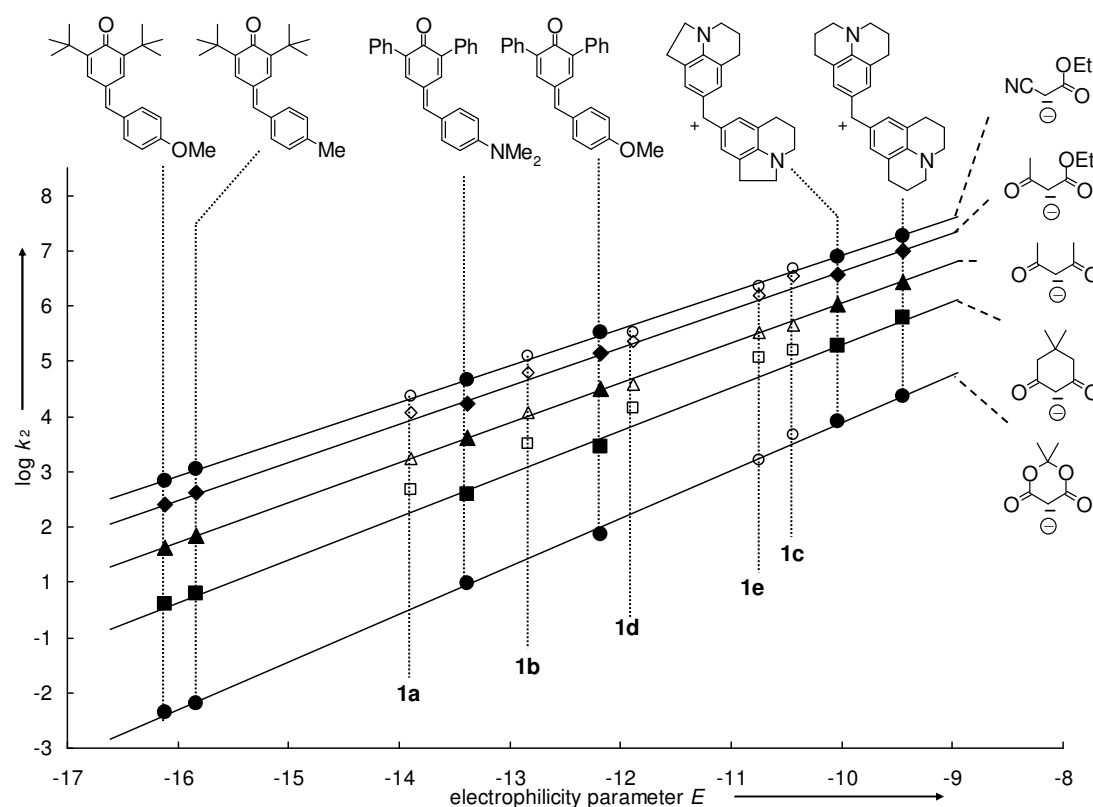
FIGURE 0.1: Logarithmic rate constants for the reactions of selected carbanions **2** with benzylidene(thio)barbituric acids **1a**-**e** compared with the reactivities toward reference electrophiles.
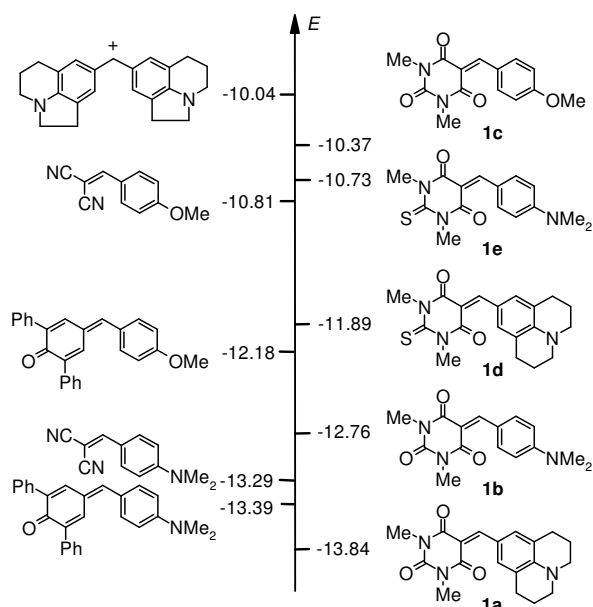
FIGURE 0.2: Comparison of electrophilicity parameters E of Michael acceptors, quinone methides and diarylcarbenium ions.

The second-order rate constants are employed to determine the electrophilicity parameters E of the benzylidenebarbituric and -thiobarbituric acids **1a**-**e** according to the correlation equation 0.1 (Figure 0.1). With E parameters in the range of -10.4 to -13.9 the electrophilicities of **1a**-**e** are comparable to those of analogously substituted benzylidenemalononitriles and quinone methides (Figure 0.2)

2

0.3   Electrophilicities of 2-Benzylidene-indan-1,3-diones

The kinetics of the reactions of the 2-benzylidene-indan-1,3-diones **4a-d** with the acceptor-stabilized carbanions **2** have been studied photometrically in DMSO at 20 °C. The obtained second-order rate constants have been used to determine the electrophilicity parameters E of **4a-d**, according to the linear free energy relationship 0.1. In several cases the anionic reaction products **5⁻** and their conjugate acids **5** have been characterized by ^{1}H- and ^{13}C-NMR spectroscopy (Scheme 0.3).
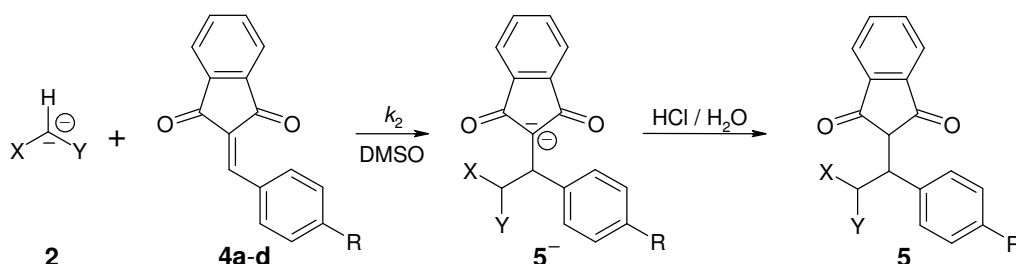
SCHEME 0.3: Reactions of 2-benzylidene-indan-1,3-diones **4a-d** with carbanions **2** in DMSO at 20 °C.
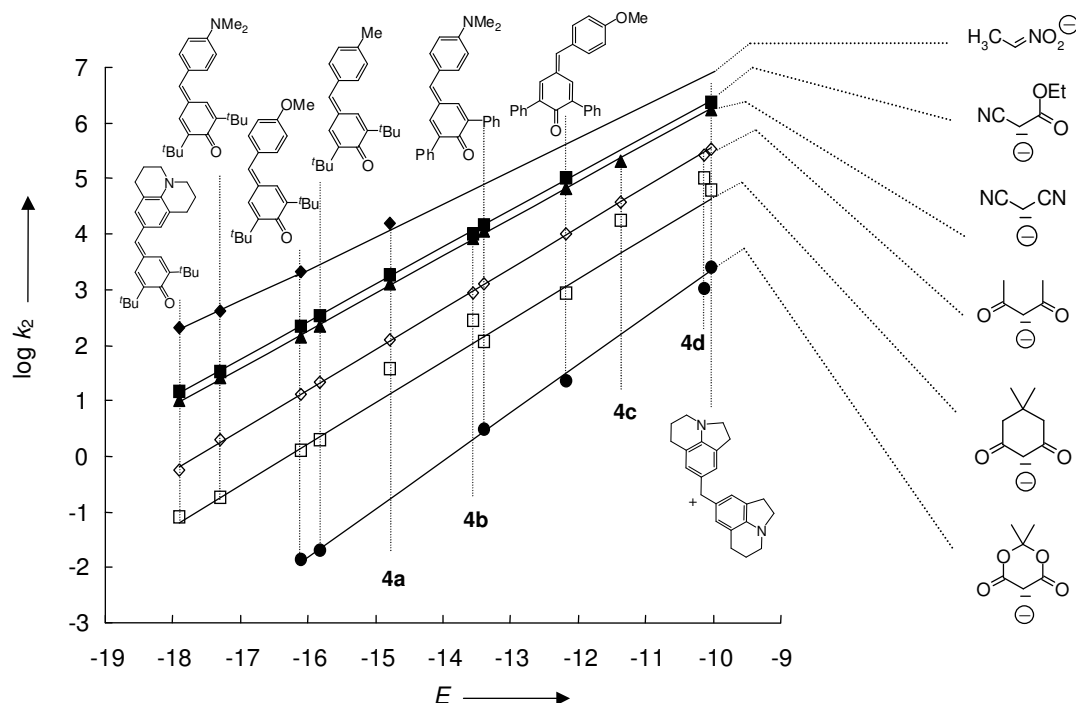
FIGURE 0.3: Logarithmic rate constants for the reactions of carbanions **2** with the 2-benzylidene-indan-1,3-diones **4a-d** (for structures see Figure 0.4) and with reference electrophiles (quinone methides and diarylcarbenium ions) in DMSO at 20 °C.

The determined electrophilicity parameters E of the 2-benzylidene-indan-1,3-diones **4a-d** are in the range of $-10 > E > -15$ and comparable with those of quinone methides (Figure 0.4).
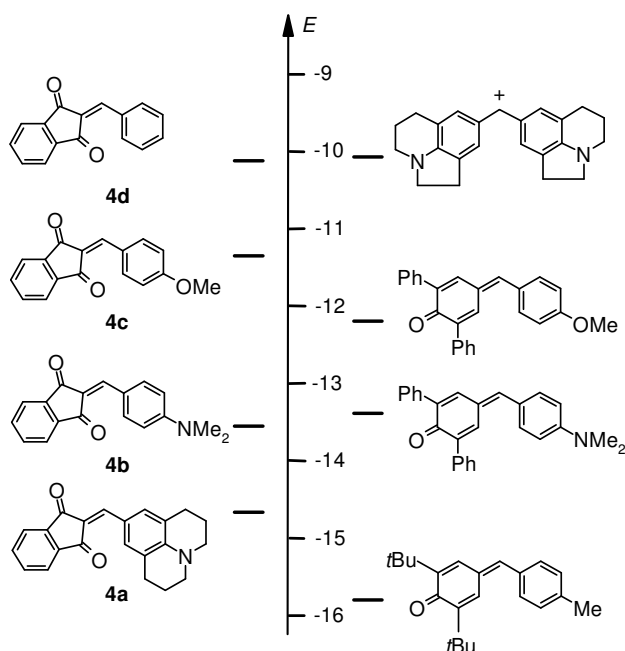
FIGURE 0.4: Comparison of the electrophilicity parameters E of the 2-benzylidene-indan-1,3-diones **4a-d** with reference electrophiles in DMSO.

0.4 Reactions of Nitro(hetero)arenes with Carbanions – Bridging Aromatic, Heteroaromatic, and Vinylic Electrophilicity
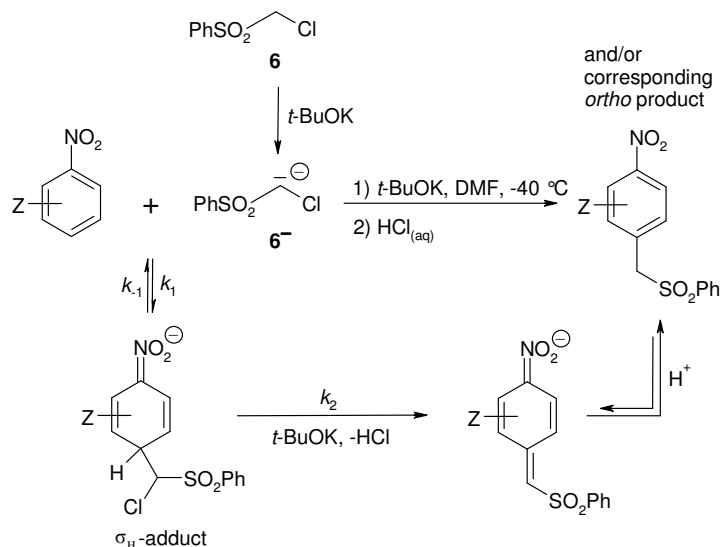
SCHEME 0.4: Mechanism of the Vicarious Nucleophilic Substitution in nitroarenes with the anion of chloromethyl phenyl sulfone (**6⁻**).

k_{rel} competition experiments

Structure	k_{rel}
(87000) NO$_2$, Cl pyridine	8.7×10^4
(72000 / 6000) NO$_2$ pyridine	7.8×10^4
(18000) NO$_2$ thiophene	1.8×10^4
MeO (17000) NO$_2$ pyridine	1.7×10^4
(4600) NO$_2$ naphthalene	4.6×10^3
OEt, NO$_2$ (670 / 330) pyridine	1.0×10^3
NO$_2$ (550) imidazole	5.5×10^2
Cl (125 / 125) NO$_2$	2.5×10^2
NO$_2$ (93) pyrazole	9.3×10^1
F (50 / 50) NO$_2$	1.0×10^2
(9.0 / 9.0) NO$_2$ imidazole	1.8×10^1
NO$_2$ (5.0) pyrrole	5.0
(0.7 / 1.0 / 1.0) NO$_2$ nitrobenzene	2.7
MeO (0.89 / 0.89) NO$_2$	1.8
(1.0) NO$_2$ pyrrole	1.0

Competition experiment partial values: 3.9 (4.1), 3.7 (3.7), 4.8, 17 (13), 19 (21), 4.5 (4.2), 1.8, 5.7 (6.2), 1.0 (1.1), 2.7, 7.0, 2.8 (3.1), 11 (9.9), 5.0, 2.2

The relative rate constants for the Vicarious Nucleophilic Substitution (VNS, Scheme 0.4) of the anion of chloromethyl phenyl sulfone (**6**⁻) with a variety of nitroheteroarenes, for example nitropyridines, nitropyrroles, nitroimidazoles, 2-nitrothiophene, and 4-nitropyrazole, have been determined by competition experiments (Figure 0.5).

It has shown that nitropyridines are approximately four orders of magnitude more reactive than nitrobenzene. Among the five-membered heterocycles 2-nitrothiophene is the most active followed by nitroimidazoles and 4-nitropyrazole. Nitropyrroles are the least electrophilic nitroheteroarenes with reactivities comparable to nitrobenzene (Figure 0.5). Quantum chemically calculated methyl anion affinities (B3LYP/6-311G(d,p) //B3LYP/6-31G(d)) of the nitro(hetero)-arenes correlate only moderately with the partial relative rate constants.

FIGURE 0.5: Overall relative reactivities k_{rel} (−40 °C) of nitro(hetero)arenes toward the anion of chloromethyl phenyl sulfone (**6**⁻) in relation to nitrobenzene (k_{rel} = 2.7). The numbers in the formula give the relative reactivities of the corresponding positions with respect to one *ortho*-position of nitrobenzene. The numbers in parentheses indicate HPLC results, all other numbers result from GC analysis.

By measuring the second-order rate constants of the addition of **6**⁻ to nitroarenes and to diethyl arylidenemalonates it was possible to link the electrophilic reactivities of nitro(hetero)arenes with the comprehensive electrophilicity scale based on the linear-free-energy-relationship 0.1 (Figure 0.6).
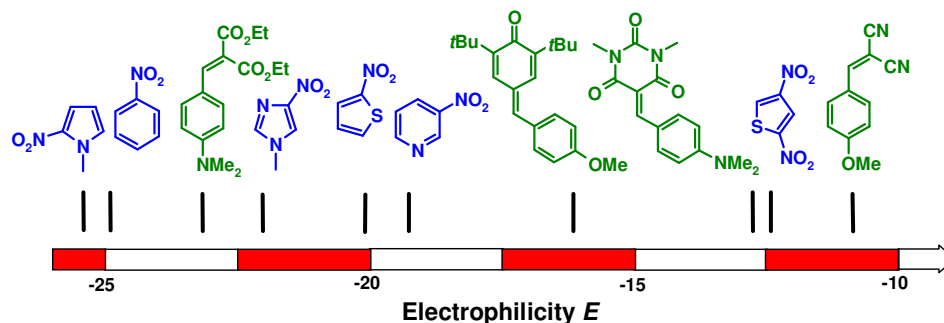
FIGURE 0.6: Comparison of the reactivities of (hetero)aromatic and vinylic electrophiles.

0.5   Nucleophilic Behavior of Sulfonyl-stabilized Carbanions

Kinetics of the reactions of sulfonyl-stabilized carbanions (**7a-d**)⁻ with reference electrophiles (quinone methides **8a-e** and diarylcarbenium ions **9a-b**) and with Michael acceptors (benzylidene Meldrum's acid **10**, benzylidenebarbituric acids **1a-c**, and benzylidene-indan-1,3-diones **4a-d**) have been determined in DMSO solution at 20 °C (Scheme 0.5). In several cases the anionic addition products and their conjugate acids have been characterized by ^{1}H- and ^{13}C-NMR spectroscopy, in order to prove the reaction course.
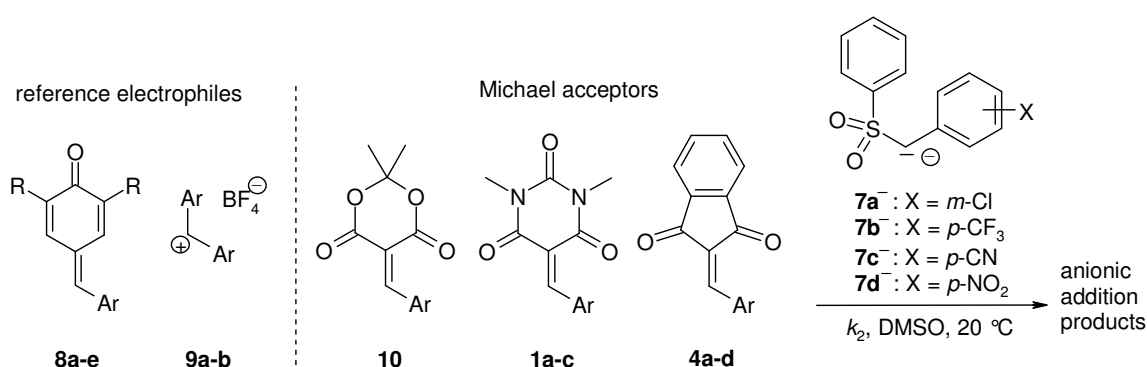
SCHEME 0.5: Reactions of sulfonyl-stabilized carbanions (**7a-d**)⁻ with reference electrophiles **8**-**9** and Michael acceptors **1**, **4**, and **10** in DMSO at 20 °C.

Plots of the logarithmic second-order rate constants log k_2 versus the electrophilicity parameters E for the reactions of sulfonyl-stabilized carbanions $(7a\text{-}d)^-$ with the reference electrophiles **8** and **9** yielded straight correlations (exemplarily depicted in Figure 0.7 for $7b^-$ and $7d^-$). However, the rate constants of $(7a\text{-}d)^-$ with Michael acceptors **1**, **4**, and **10** are about one order of magnitude lower than expected and, therefore, deviate from the correlation line of the reference electrophiles **8-9**.
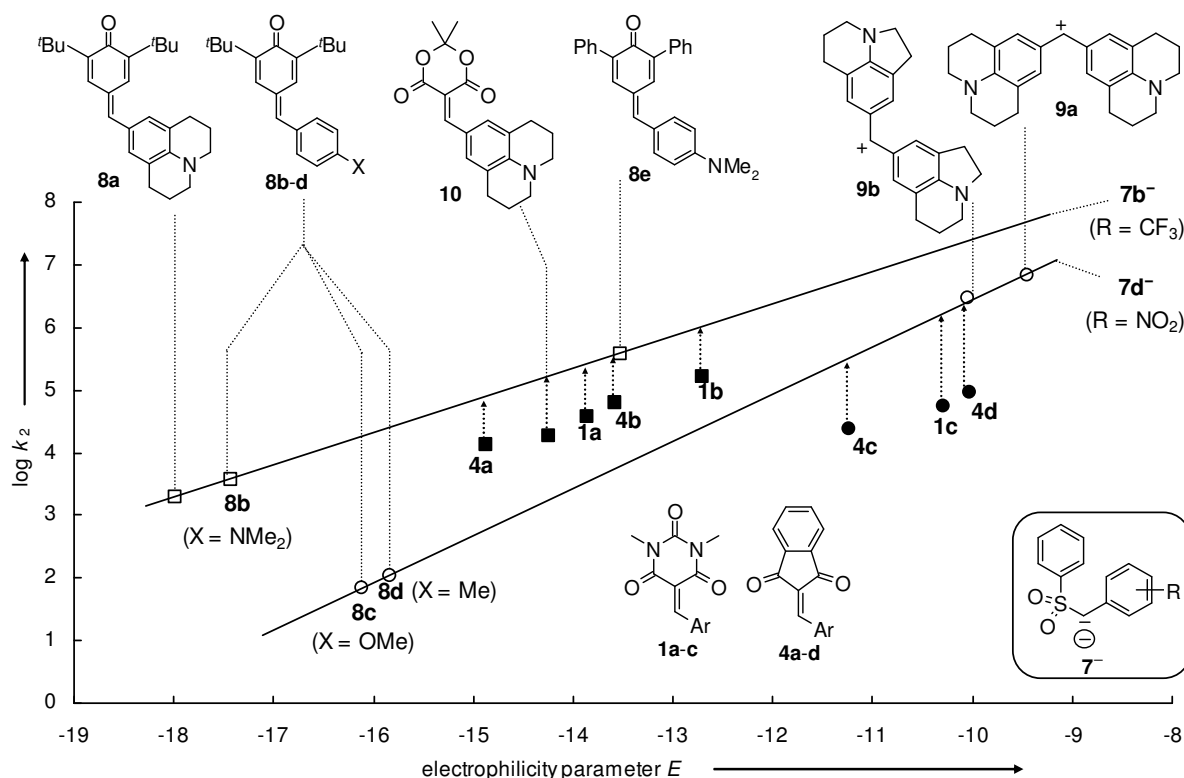
FIGURE 0.7: Plot of log k_2 versus the electrophilicity parameters E for the reactions of the sulfonyl-stabilized carbanions $7b^-$ and $7d^-$ with reference electrophiles **8**, **9** and Michael acceptors **1**, **4**, and **10**.

The nucleophilicity parameters N and s determined for the sulfonyl-stabilized carbanions $(7a\text{-}d)^-$ can be used to predict roughly the rates of their reactions with the ordinary Michael acceptors **1**, **4**, and **10** within the postulated error limit of equation 0.1 (i.e., a factor of 10-100). The deviations from equation 0.1, found for the additions of $(7a\text{-}d)^-$ to the electrophiles **1**, **4**, and **10**, are presently not interpretable.

0.6 Solvent Effects on the Rates of Electrophile-Nucleophile Combinations

Kinetics of the addition reactions of anionic and neutral nucleophiles to both carbocations and uncharged Michael acceptors were studied in various solvents (Figure 0.8).
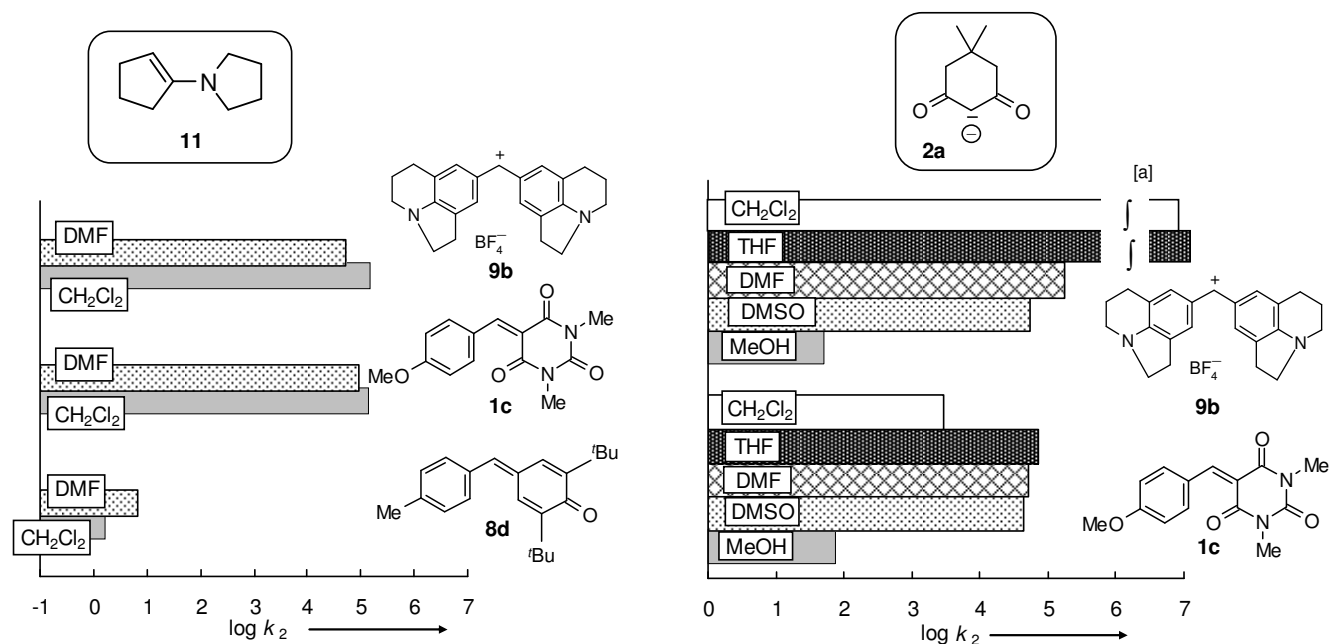
FIGURE 0.8: Left: solvent effects on the rate of the reaction of 1-pyrrolidinocyclopentene (**11**) with diarylcarbenium ion **9b,** benzylidenebarbituric acid **1c**, and quinone methide **8d** at 20 °C. Right: solvent effects on the rate of the reactions of dimedone anion (**2a**) with diarylcarbenium ion **9a** and benzylidenebarbituric acid **1c** at 20 °C. − [a] The reactions of **2a** with **9b** in THF and CH$_2$Cl$_2$ are too fast to be measured with the stopped-flow method.

The reactions of 1-pyrrolidinocyclopentene (**11**) with benzylidenebarbituric acid **1c**, diarylcarbenium ion **9a**, and quinone methide **8d** in CH$_2$Cl$_2$ and DMF confirm the negligible solvent effect on the rates of the reactions of π-nucleophiles with diarylcarbenium ions observed previously. On the other side, the reaction rates of the addition of dimedone anion (**2a**) to the uncharged Michael acceptor **1c** considerably depend on the hydrogen-bond donor abilities of the used solvent and can be properly correlated with the solvent acidity scale of Catalan (Figure 0.9). The high reactivity of the carbanion-carbocation combination **2a** + **9b** in the more apolar solvents dichloromethane and THF can be rationalized in terms of electrostatic interactions.
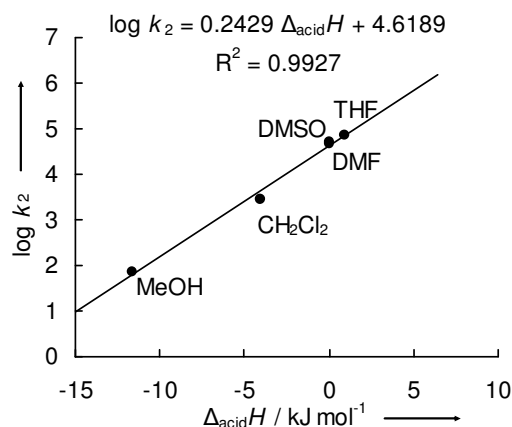
FIGURE 0.9: Correlation of log k_2 versus Catalan's hydrogen-bond acidity $\Delta_{acid}H$ for the reaction of dimedone anion (**2a**) with benzylidenebarbituric acid **1c** in different solvents.

0.7   Miscellaneous Experiments

0.7.1 Combinatorial Kinetics

The kinetics of the reactions of dimedone anion (**2a**) with Michael acceptors **1b-c** and diarylcarbenium ion **9b** have been determined simultaneously (Figure 0.10).
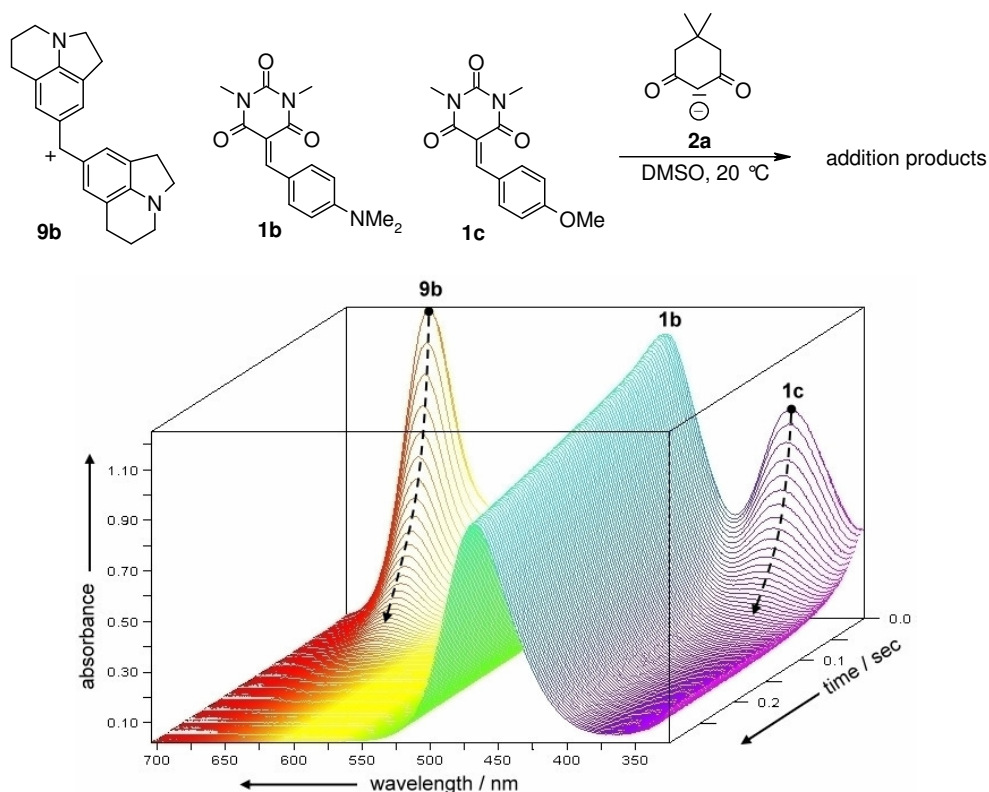
FIGURE 0.10: The first 0.3 s of the multicomponent reaction of **2a** with electrophiles **9b** and **1b-c** monitored by stopped-flow UV-Vis spectroscopy.

The obtained second-order rate constants are in agreement with those of single measurements. Therefore, it is generally possible to perform kinetic investigations, for example determination of reactivity parameters, faster and more efficient particularly for screening experiments.

0.7.2 The Reactivity of the 2-(p-Nitrophenyl)-propionitrile Anion

The kinetics of the reactions of 2-(p-nitrophenyl)-propionitrile anion ($\mathbf{12}^-$) with benzylidene-barbituric acids **1b-c** and benzylidene-indan-1,3-diones **4b-d** have been studied in DMSO at 20 °C, in order to characterize this nucleophile according to equation 0.1.
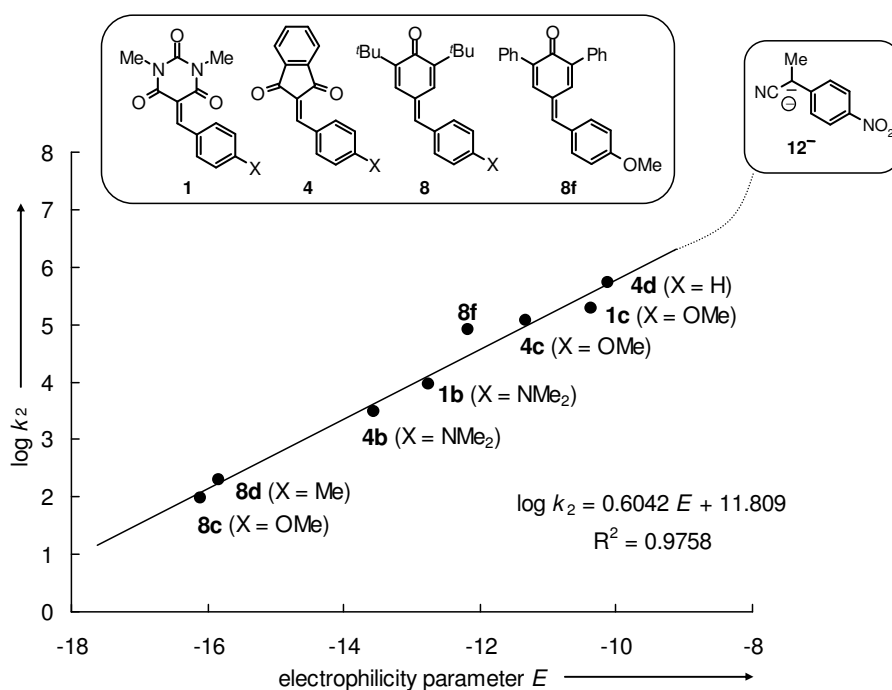
FIGURE 0.11: Plot of log k_2 versus E for the reactions of the 2-(p-nitrophenyl)-propionitrile anion ($\mathbf{12}^-$) with electrophiles **1**, **4**, and **8**.

From the plot of log k_2 versus E depicted in Figure 0.8 one derives $N = 19.54$ and $s = 0.60$ for the anion of 2-(p-nitrophenyl)-propionitrile ($\mathbf{12}^-$).

Chapter 1

Introduction and Objectives

1.1 Introduction

In the 1930s Ingold introduced the terms "electrophile" and "nucleophile", which are associated with electron-deficient and electron-rich species, respectively for systemizing the course of polar organic reactions.[1-3] Since then, there have been a number of attempts to quantify electrophilicity and nucleophilicity as general concepts. The first systematic effort was reported by Swain and Scott.[4] These authors investigated the rates of S_N2 reactions and characterized nucleophiles by one parameter (n) and electrophiles by two parameters (s, $\log k_{water}$) according to equation 1.1.

$$\log (k/k_{water}) = sn \qquad (1.1)$$

The Swain-Scott equation (1.1) describes the change in rates for the reactions of a given electrophile with different nucleophiles. n characterizes the nucleophilicity of a reagent and s represents the sensitivity of the electrophile towards variation of nucleophiles [the S_N2 reactions of nucleophiles with CH_3Br in water were used as reference reactions ($s = 1$)].

About 20 years later, Ritchie proposed a concept called "constant selectivity relationship" based on the reactions of carbocations and diazonium ions with nucleophiles.[5-7] He found that the relative rate constants of two nucleophiles do not depend on the absolute reactivities of the electrophiles. With Ritchie's nucleophilicity scale − covering a range of about 13 orders of magnitude − it was possible to calculate the rates of these reactions from only one parameter for electrophiles ($\log k_0$) and a single parameter for nucleophiles (N_+), (equation 1.2).

$$\log (k/k_0) = N_+ \qquad (1.2)$$

It was later shown that equation 1.2 is not strictly valid and that better correlations are obtained, when different families of electrophiles are treated separately.[8]

The additions of diarylcarbenium ions to terminal double bonds, where the formation of the new C–C bond is the rate-determining step, showed also constant selectivity relationships over a wide reactivity range.[9-11] However, the introduction of a second parameter for nucleophiles (*s*) was considered essential to cover a larger variety of nucleophiles.[12-14] In 1994 Mayr and Patz introduced the linear-free-energy relationship 1.3:[12]

$$\log k_{(20\ °C)} = s\ (N + E) \tag{1.3}$$

where *E* and *N* are the electrophilicity and nucleophilicity parameters, respectively, and *s* is the nucleophile-specific slope parameter.

Up to now, more than 400 nucleophiles, like enamines,[15-17] amines,[18, 19] alkoxides,[18, 20] silyl enol ethers and ketene acetals,[16, 21, 22] hydride donors,[16, 23] carbanions,[23-27] and heterocyclic arenes[16, 17, 28] have been characterized according to equation 1.3. On the other hand, about 100 electrophiles have been parameterized, including carbocations and cationic metal-pi-complexes,[16, 17] quinone methides,[23] and Michael acceptors.[29]

1.2 Objectives

The goal of this thesis was to characterize highly reactive carbanions (e.g., sulfonyl-stabilized carbanions), in order to extend the nucleophilicity scale (chapter 4). On the other side new reference electrophiles of lower reactivity were needed [e.g., Michael acceptors (chapters 2 and 3)]. Because of the extent of this project, Stefan Berger, Oliver Kaumanns and I were supposed to reach this goal in a collaborative effort.

Another major objective of this thesis was bridging aromatic and aliphatic electrophilicity (chapter 5). Part of this work was done by me at the Institute of Organic Chemistry, Polish Academy of Sciences, Warsaw, Poland under the guidance of Prof. Mieczyslaw Makosza.

Because the major parts of this thesis have already been published or submitted for publication, individual introductions will be given at the beginning of each chapter. In order to identify my contributions to the multiauthor publications, the Experimental Sections report exclusively the experiments, which were performed by me. Unpublished investigations are given in chapters 5-7.

For a more detailed review on equation 1.3 see ref.[30] and visit the webpage http://cicum92.cup.uni-muenchen.de/mayr/reaktionsdatenbank/.

1.3 References

[1]   C. K. Ingold, *Recl. Trav. Chim. Pays-Bas* **1929**, *42*, 797-812.

[2]   C. K. Ingold, *J. Chem. Soc.* **1933**, 1120-1127.

[3]   C. K. Ingold, *Chem. Rev.* **1934**, *15*, 225-274.

[4]   C. G. Swain, C. B. Scott, *J. Am. Chem. Soc.* **1953**, *75*, 141-147.

[5]   C. D. Ritchie, *Acc. Chem. Res.* **1972**, *5*, 348-354.

[6]   C. D. Ritchie, J. E. van Verth, P. O. I. Virtanen, *J. Am. Chem. Soc.* **1982**, *104*, 3491-3497.

[7]   C. D. Ritchie, *J. Am. Chem. Soc.* **1984**, *106*, 7187-7194.

[8]   C. D. Ritchie, *Can. J. Chem.* **1986**, *64*, 2239-2250.

[9]   H. Mayr, R. Schneider, U. Grabis, *Angew. Chem.* **1986**, *98*, 1034-1036; *Angew. Chem., Int. Ed. Engl.* **1986**, *25*, 1017-1019.

[11]   H. Mayr, R. Schneider, U. Grabis, *J. Am. Chem. Soc.* **1990**, *112*, 4460-4467.

[12]   H. Mayr, M. Patz, *Angew. Chem.* **1994**, *106*, 990-1010; *Angew. Chem. Int. Ed.* **1994**, *33*, 938-957.

[13]   H. Mayr, O. Kuhn, M. F. Gotta, M. Patz, *J. Phys. Org. Chem.* **1998**, *11*, 642-654.

[14]   H. Mayr, M. Patz, M. F. Gotta, A. R. Ofial, *Pure Appl. Chem.* **1998**, *70*, 1993-2000.

[15]   A. D. Dilman, S. L. Ioffe, H. Mayr, *J. Org. Chem,* **2001**, *66*, 3196-3200.

[16]   H. Mayr, T. Bug, M. F. Gotta, N. Hering, B. Irrgang, B. Janker, B. Kempf, R. Loos, A. R. Ofial, G. Remennikov, H. Schimmel, *J. Am. Chem. Soc.* **2001**, *123*, 9500-9512.

[17]   H. Mayr, B. Kempf, A. R. Ofial, *Acc. Chem. Res.* **2003**, *36*, 66-77.

[18]   S. Minegishi, H. Mayr, *J. Am. Chem. Soc.* **2003**, *125*, 286-295.

[19]   F. Brotzel, Y. C. Chu, H. Mayr, *J. Org. Chem,* **2007**, *72*, 3679-3688.

[20]   T. B. Phan, H. Mayr, *Can. J. Chem.* **2005**, *83*, 1554-1560.

[21]   T. Tokuyasu, H. Mayr, *Eur. J. Org. Chem.* **2004**, 2791-2796.

[22]   A. D. Dilman, H. Mayr, *Eur. J. Org. Chem.* **2005**, 1760-1764.

[23]   R. Lucius, R. Loos, H. Mayr, *Angew. Chem.* **2002**, *114*, 97-102; *Angew. Chem. Int. Ed.* **2002**, *41*, 91-95.

[24]   T. Bug, H. Mayr, *J. Am. Chem. Soc.* **2003**, *125*, 12980-12986.

[25]   T. Bug, T. Lemek, H. Mayr, *J. Org. Chem.* **2004**, *69*, 7565-7576.

[26]   T. B. Phan, H. Mayr, *Eur. J. Org. Chem.* **2006**, 2530-2537.

[27]   S. T. A. Berger, A. R. Ofial, H. Mayr, *J. Am. Chem. Soc.* **2007**, *129*, 9753-9761.

[28]   S. Lakhdar, M. Westermaier, F. Terrier, R. Goumont, T. Boubaker, A. R. Ofial, H. Mayr, *J. Org. Chem,* **2006**, 9088-9095.

[29]   T. Lemek, H. Mayr, *J. Org. Chem.* **2003**, *68*, 6880-6886.

[30]   H. Mayr, A. R. Ofial, *Pure Appl. Chem.* **2005**, *77*, 1807-1821.

Chapter 2

Electrophilicity of 5-Benzylidene-1,3-dimethyl-barbituric and -thiobarbituric Acids

F. Seeliger, S. T. A. Berger, G. Y. Remennikov, K. Polborn, and H. Mayr, *J. Org. Chem.* **2007**, *72*, 9170-9180.

2.1 Introduction

Benzylidenebarbituric and -thiobarbituric acids are characterized by their strongly polarized exocyclic double bond with a positive partial charge on the arylidene carbon.[1, 2] They have been termed as "electrically neutral organic Lewis acids"[3, 4] because they react with typical Lewis bases,[5] such as alkoxides,[3, 6] amines,[6-9] thiols,[10] water,[11] and the hydrogensulfite ion.[12] Benzylidenebarbituric and -thiobarbituric acids also react with carbon nucleophiles, e.g., compounds containing an active methylene group,[13, 14] isonitriles,[15] phosphacumulene ylids,[16, 17] or organo zinc reagents.[18-20] Due to the fact that the active double bond in benzylidenebarbituric acids can easily be reduced,[21-23] these compounds can be used for the synthesis of unsymmetrical disulfides[24, 25] and for the mild oxidation of alcohols.[26, 27] Furthermore, benzylidenebarbituric and -thiobarbituric acids are important building blocks in the synthesis of pyrazolo[3,4-d]pyrimidine derivatives,[28, 29] which show broad biological activity.[30-32] Benzylidenethiobarbituric acids also trap radicals and, therefore, can be used as thermal stabilizers in rigid PVC.[33]

Some years ago we showed that the reactions of diarylcarbenium ions with nucleophiles can be described by the linear-free-energy-relationship (2.1) and suggested a set of diarylcarbenium ions and nucleophiles as reference compounds for determining the reactivity of further nucleophiles and electrophiles.[34]

$$\log k_2(20\ °C) = s(N + E) \tag{2.1}$$

E = electrophilicity parameter, N = nucleophilicity parameter, s = nucleophile-specific slope parameter

Equation (2.1) also holds for the reactions of carbanions with quinone methides, which can be considered as uncharged analogs of diarylcarbenium ions,[35, 36] and with typical Michael acceptors, like benzylidenemalononitriles[37] or 2-benzylidene-indan-1,3-diones.[38]

Previously, Bernasconi has studied the kinetics of the additions of carbanions, alkoxides, and amines to 2-benzylidene-indan-1,3-diones,[41] benzylidene Meldrum's acids,[42, 43] and other electrophiles with polarized double bonds in 50 % aqueous DMSO.[44] We have now investigated analogous reactions with benzylidenebarbituric and -thiobarbituric acids in order to examine scope and limitations of equation (2.1). For this purpose we studied the kinetics of the addition reactions of the potassium salts of different CH-acids (**2a** to **2m**, Table 2.1) to the Michael acceptors **1a**-**e**.
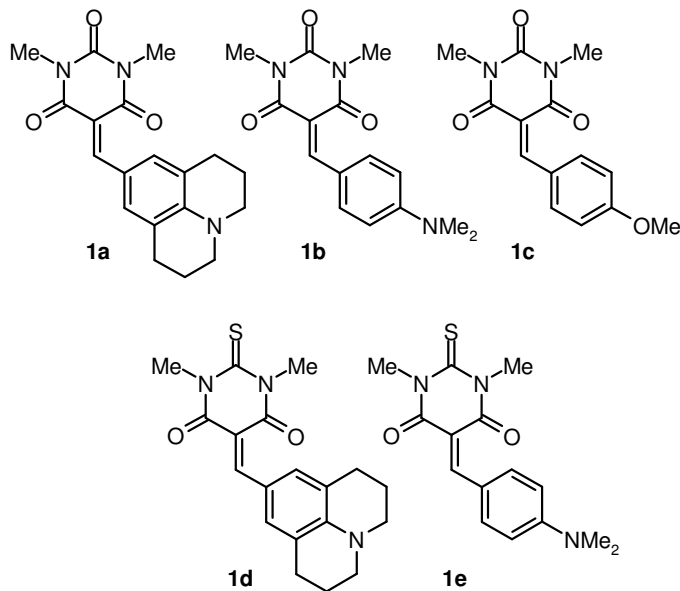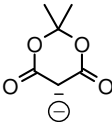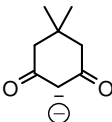
TABLE 2.1: Reactivity parameters N and s of the carbanions **2a** to **2m** in DMSO.

	X	Y	N / s
2a			13.91 / 0.86[a]
2b			16.27 / 0.77[a]
2c	4-NC-	SO_2CF_3	16.28 / 0.75[b]
2d	4-NC-	NO_2	16.96 / 0.73[c]
2e	COMe	COMe	17.64 / 0.73[a]
2f	C_6H_5	SO_2CF_3	18.67 / 0.67[b]
2g	COMe	CO_2Et	18.82 / 0.69[a]
2h	CN	CN	19.36 / 0.67[a]
2i	CN	CO_2Et	19.62 / 0.67[a]
2k	CO_2Et	CO_2Et	20.22 / 0.65[a]
2l	H	NO_2	20.71 / 0.60[c]
2m	Me	NO_2	21.54 / 0.62[d]

[a] Ref.[36]. [b] Ref.[39]. [c] Ref.[40]. [d] Ref.[37].

2.2 Results

2.2.1 Product Studies

When equimolar amounts of the benzylidene(thio)barbituric acids **1a-e** and the potassium salts **2** were combined in d_6-DMSO, quantitative formation of the adducts **3** was observed by ^{1}H- and ^{13}C-NMR spectroscopy (Scheme 2.1). Because in many cases analogous reaction products can be expected, product studies have not been performed for all reactions, which have been studied kinetically. In the following, the first letter of the adducts identifies the electrophile, while the second letter identifies the nucleophile, for example, **3ah** is an adduct from **1a** and **2h**.
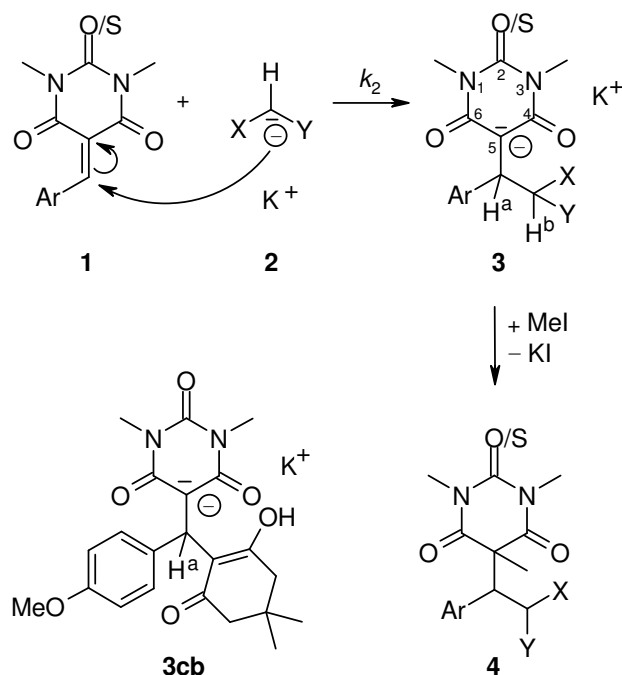
SCHEME 2.1: Products of the additions of the carbanions **2** to the active double bond of benzylidene(thio)barbituric acids **1a-e**.

Protons H^a and H^b, which absorb as doublets between δ 4.43–4.81 ppm (H^a) and δ 5.11–6.20 ppm (H^b), are characteristic for the addition products **3** (Table 2.2). The high upfield shifts of the ^{1}H-NMR signals of the vinylic protons H^a in compounds **1a-e** (δ 8.30–8.47 ppm)[45] to δ 4.43–4.81 ppm in products **3** indicate the nucleophilic attack in β-position of the Michael acceptor.[6] This interpretation is also confirmed by the ^{13}C-NMR spectra, which show an upfield shift of the benzylidene carbon from δ 159–160 ppm in **1a-e** to δ 31–46 ppm in **3**. The upfield shift of C-5 by an average of 27 ppm from δ 108–115 ppm in **1a-e** to δ 83–86 ppm in **3** reflects the increase of electron density in the pyrimidine rings.

The observation of two signal sets in the ^{1}H-NMR spectra of compounds **3cg**, **3ci**, and **3cm** indicates the formation of two diastereomers in these cases (**3cg**, 5:3; **3ci**, 2:1; **3cm**, 9:2). The enol structure of the dimedone ring of **3cb** (from **1c** and **2b**; Scheme 2.1) is indicated by its ^{13}C-NMR spectrum and the OH signal at δ 14.60 ppm. As a consequence, proton H^a absorbs as a singlet at δ 6.08 ppm.

18

TABLE 2.2: ^{1}H- and ^{13}C-NMR spectroscopic analysis of products **3**.[a]

	δ H^a / ppm	δ H^b / ppm	$^3J_{(H^a\text{-}H^b)}$ / Hz	δ (C-H^a) / ppm	δ (C-5) / ppm
3ah	4.43	6.02	11.9	43.2	83.7
3bh	4.57	6.08	11.9	43.2	83.6
3cb	6.08	14.60[b]	-	31.0	89.6
3ce	4.81	5.48	12.3	40.5	86.0
3cg[c]	4.78	5.11	12.6	40.5	85.7
3cg[d]	4.76	5.28	12.2	40.4	86.1
3ch	4.61	6.12	12.2	43.2	83.7
3ci[c]	4.59	5.37	12.3	40.3	85.1
3ci[d]	4.65	5.35	12.2	40.3	83.9
3ck	4.70	5.14	12.3	40.5	85.9
3cm[c]	4.45	6.00	11.4	45.8	85.0
3cm[d]	4.43	6.20	11.4	45.7	83.8
3de	4.67	5.41	12.3	40.3	91.5
3dh	4.43	5.96	12.1	43.2	88.9
3ee	4.78	5.47	12.5	40.4	91.4

[a] For assignment of structures see Scheme 2.1 and Table 2.3, **3ah** means product from **1a** and **2h**. [b] See text. [c] Major diastereomer. [d] Minor diastereomer.

Treatment of the potassium salts **3ck** and **3cm** with methyl iodide yields **4ck** and **4cm** by methylation of the 5-position of the pyrimidine ring. After separation of the diastereomers (9:2) of **4cm** by crystallization from ethanol, the structure of the major diastereomer was determined by x-ray crystallography (Figure 2.1).
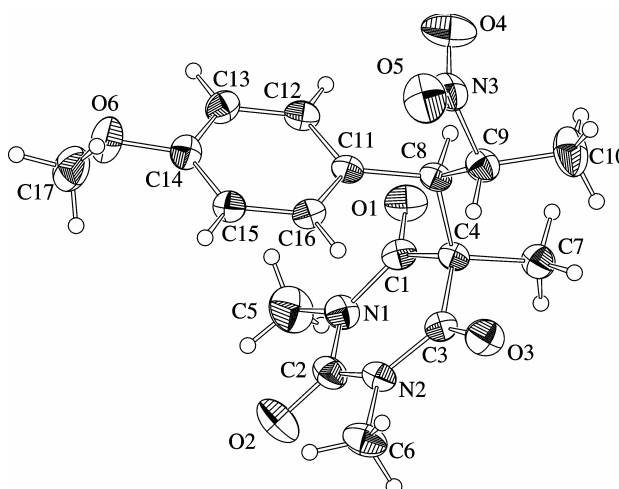
FIGURE 2.1: X-ray crystal structure (ORTEP projektion) of the major diastereomer of **4cm**. Atom numbers refer to the x-ray analysis.

The anionic adducts **3** obtained from arylidenebarbituric acids **1b** and **1c** were also treated with aqueous hydrochloric acid. The adducts **3ce**, **3cg**, **3cm** and **3bm** derived from acetylacetone (**2e**), ethyl acetoacetate (**2g**), and nitroethane (**2m**), respectively, yielded the protonated species **5** as depicted in Scheme 2.2. On the other hand, protonation of **3cb**, the product from **1c** and dimedone (**2b**), gave **5cb**, where the dimedone group as well as the barbituric acid group adopted an enol structure in CDCl$_3$, as shown by two OH resonances at δ 12.83 (sharp) and δ 11.32 (very broad). This difference is also evident in the ^{13}C-NMR spectrum of **5cb**, where C-5 of the barbituric acid group absorbs at δ 92.8, while this carbon absorbs at δ 50.6−52.2 in all other adducts **5**.

Protonation of **3ch** (from malononitrile) and **3ci** (from ethyl cyanoacetate) under the same conditions resulted in retro-Michael additions with formation of the cyanostyrenes **7ch** and **7ci** (Scheme 2.2). Acidification of **3bh** (malononitrile adduct to **1b**) also gave rise to the formation of the corresponding benzylidenemalononitrile **7bh**. Analogous retro-Michael additions have previously been observed by Patai and Rappoport when treating α-cyano-β-phenylacrylates with malononitrile in 95 % ethanol[46] and by us when benzylidene-malononitriles were combined with the carbanion of ethyl cyanoacetate in DMSO.[37] Szántay observed this so-called aryl methylene transfer when methoxy-substituted β-nitro styrenes were treated with ethyl cyanoacetate or malononitrile in the presence of a basic catalyst.[47]

In addition to the retro-Michael adduct **7ch**, just discussed, acid hydrolysis of **3ch** (from malononitrile anion **2h** and **1c**) yields 47 % of the dihydropyrano[2,3-d]pyrimidine **8ch**. Syntheses of analogous pyrano[2,3-d]pyrimidines via reaction of benzylidenemalononitriles with 1,3-dimethylbarbituric acid[48] or via microwave irradiation of barbituric acids, benzaldehyde, and cyanoacetates or malononitriles[49] have been reported. In these reactions the Michael adducts **5** are probably formed as intermediates, which then undergo cyclization by attack of an enolic hydroxy group at one of the cyano functions.
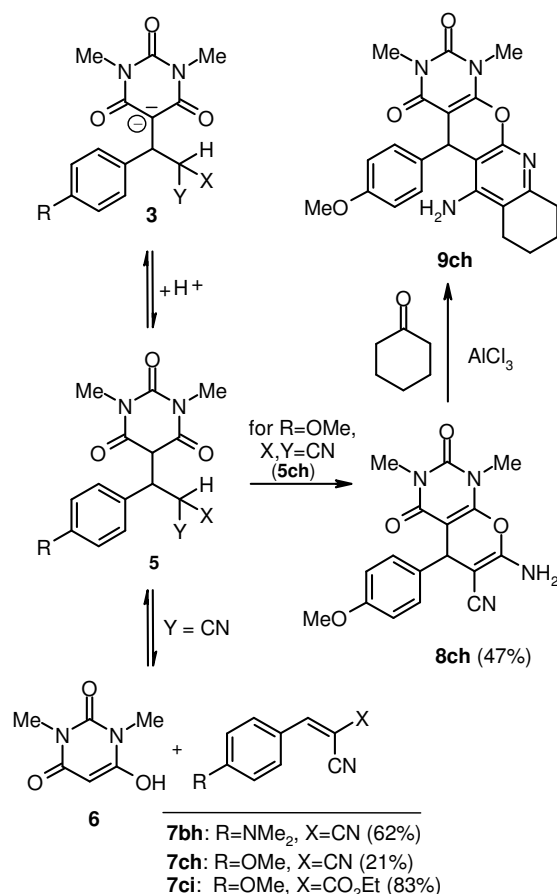
SCHEME 2.2: Protonation of the potassium salts **3** leads to compounds **5**. The salts **3bh**, **3ch**, **3ci** undergo a retro Michael addition upon protonation to form cyanoolefins **7bh**, **7ch**, **7ci**. Under these conditions compound **5ch** forms also the cyclic dihydropyrano[2,3-d]pyrimidine **8ch**, which reacts with cyclohexanone via Friedlander reaction to pyrano[2,3-b]quinoline **9ch**.

Because of the structural analogy to tacrine,[50, 51] which is an inhibitor of acetyl cholinesterase and a drug that proved to have a beneficial effect on cognition in patients with Alzheimer's disease,[52, 53] dihydropyran **8ch** was used as starting material for the synthesis of a new pyrano[2,3-b]quinoline. In a Friedlaender reaction the acid catalyzed condensation of **8ch** with cyclohexanone gave 69 % of the tacrine analogue **9ch**.

2.2.2 Kinetics

Benzylidene(thio)barbituric acids **1a**-**e** show strong absorption bands in the UV-Vis spectra (375–525 nm).[1] By nucleophilic attack at the benzylidene carbon the chromophore is destroyed, and the reaction can be followed by the decrease of the absorbance. All reactions proceeded quantitatively, so that the solutions were completely decolorized. The kinetic

experiments were performed under pseudo-first-order conditions using a high excess of the nucleophiles. From the exponential decays of the UV-Vis absorbances of the electrophiles the pseudo-first-order rate constants were obtained (Figure 2.2).

In previous work we demonstrated that the potassium salts of the carbanions studied in this work are not paired under the conditions used for the kinetic experiments.[36, 39, 40] The second-order rate constants k_2 (Table 2.3), which are obtained as the slopes of $k_{1\Psi}$ versus [2] correlations (Figure 2.2, insert), can therefore be considered to reflect the reactivities of free carbanions.
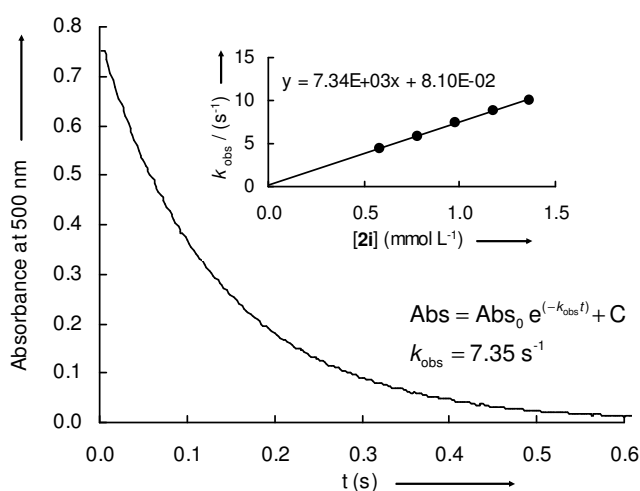
FIGURE 2.2: Exponential decay of the absorbance at 500 nm during the reaction of **1a** ($c_0 = 2.90 \times 10^{-5}$ mol L^{-1}, $\lambda = 500$ nm) with **2i** ($c_0 = 9.78 \times 10^{-4}$ mol L^{-1}) in DMSO at 20 °C.

TABLE 2.3: Second-order rate constants k_2 (DMSO, 20 °C) and characterized products of the reactions of benzylidene(thio)barbituric acids **1a-e** with the potassium salts of different carbanions **2**.

elec	nuc	k_2 (L mol^{-1}s^{-1})	products	elec	nuc	k_2 (L mol^{-1}s^{-1})	products
1a	**2b**	1.49×10^2	-	**1c**	**2g**	1.08×10^6	**3cg**,[a] **5cg**[b]
	2c	5.37×10^1	-		**2h**	1.80×10^6	**3ch**,[a] **7ch**[b]
	2d	1.88×10^2	-				**8ch**[b]
	2e	5.45×10^2	-		**2i**	1.49×10^6	**3ci**,[a] **7ci**[b]
	2f	1.01×10^3	-		**2k**	1.41×10^6	**3ck**,[a] **4ck**[b]
	2g	3.78×10^3	-		**2m**	-	**3cm**,[a] **4cm**[b]
	2h	1.27×10^4	**3ah**[a]				**5cm**^{b}
	2i	7.34×10^3	-				
	2k	7.66×10^3	-	**1d**	**2b**	4.36×10^3	-
	2l	1.54×10^4	-		**2e**	1.17×10^4	**3de**[a]
	2m	2.98×10^4	-		**2g**	7.41×10^4	-
					2h	1.64×10^5	**3dh**[a]
1b	**2b**	1.04×10^3	-		**2i**	1.06×10^5	-
	2c	2.18×10^2	-		**2k**	1.13×10^5	-
	2e	3.72×10^3	-				
	2f	5.71×10^3	-	**1e**	**2a**	4.97×10^2	-
	2g	2.03×10^4	-		**2b**	3.72×10^4	-
	2h	5.88×10^4	**3bh**,[a] **7bh**[b]		**2e**	1.03×10^5	**3ee**[a]
	2i	4.00×10^4	-		**2g**	4.89×10^5	-
	2k	3.49×10^4	-		**2i**	7.05×10^5	-
	2m	-	**5bm**[b]		**2k**	6.71×10^5	-
1c	**2a**	1.42×10^3	-				
	2b	4.83×10^4	**3cb**,[a] **5cb**[b]				
	2e	1.44×10^5	**3ce**,[a] **5ce**[b]				
	2f	1.97×10^5	-				

[a] Potassium salts of **3** produced in d_6-DMSO were characterized by ^{1}H- and ^{13}C-NMR. [b] Characterization of isolated products.

2.3 Discussion

2.3.1 Reactions with Carbanions

Equation 2.1 was used to calculate the E parameters of **1a-e** from the rate constants given in Table 2.3 and the previously reported N and s parameters of the carbanions **2a-m**.[36, 37, 39, 40] A least-squares fit of calculated and experimental rate constants (minimization of $\Delta^2 = \sum(\log k_2 - s(N + E))^2$ with the What's *Best!* nonlinear solver) gave the E parameters of the benzylidene(thio)barbituric acids **1a-e**, which are close to the arithmetic means of the E values calculated for each individual electrophile-nucleophile combination.

However, the reactivities of some carbanions deviate slightly but systematically from the correlation lines. Figure 2.3 shows that the triflinate stabilized carbanion **2f** reacts two to three times slower with each of the electrophiles **1a-c** than expected from its previously published reactivity parameters N and s.[39] On the other hand, the malononitrile anion **2h** reacts two to four times faster with the electrophiles **1a-d** than expected (Figure 2.3 and 2.4).
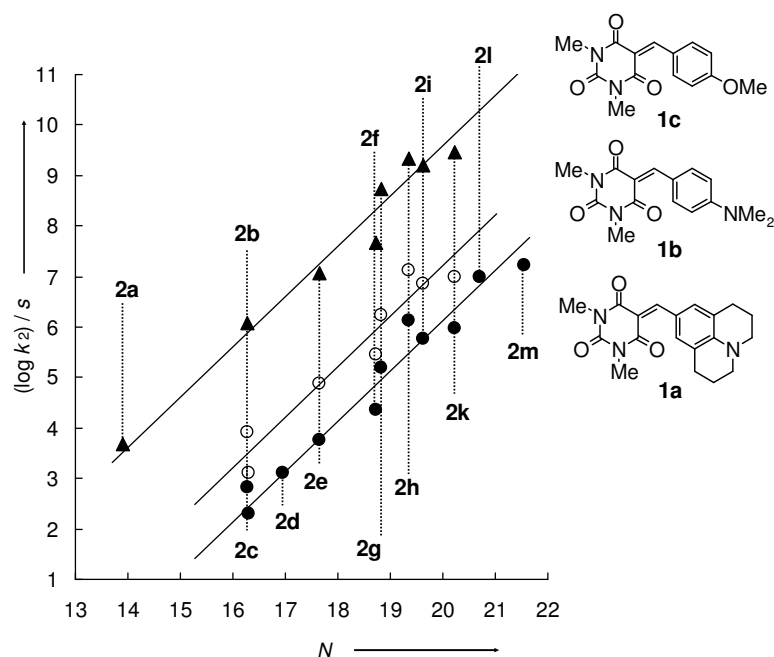
FIGURE 2.3: Plot of (log k_2)/s versus N for the reactions of **1a-c** with selected carbanions **2**. The correlation lines are fixed at a slope of 1.0, as required by equation 2.1.
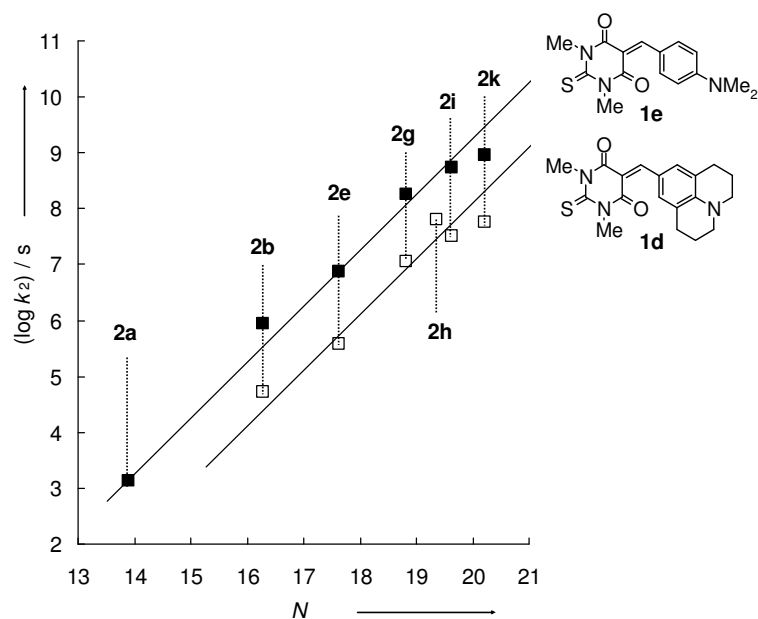
FIGURE 2.4: Plot of (log k_2)/s versus N for the reactions of **1d** and **1e** with different carbanions **2**. The correlation lines are fixed at a slope of 1.0, as required by equation 2.1.

A comparison of the electrophilicities of diarylcarbenium ions, quinone methides, and benzylidene(thio)barbituric acids (**1a**-**e**) is given in Figure 2.5.
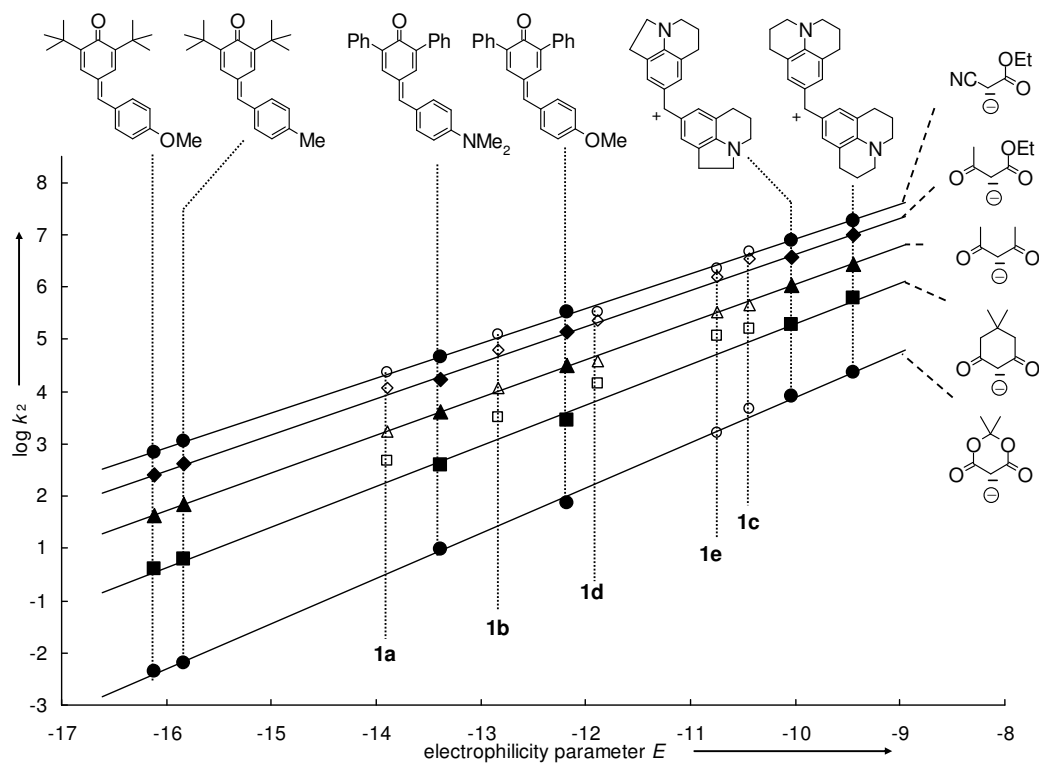
FIGURE 2.5: Rate constants for the reactions of selected carbanions **2** with benzylidene(thio)barbituric acids **1a-e** compared with the reactivities toward reference

25

electrophiles. The rate constants for the reactions of **1a-e** with **2** were not used for the construction of the correlation lines.

The good fit demonstrates that the nucleophilic reactivity order of carbanions, which was derived from the rates of their reactions with diarylcarbenium ions and quinone methides in DMSO, also holds for the reactions with typical Michael acceptors. In agreement with the conclusions drawn from Figures 2.3 and 2.4, Figure 2.5 also shows that **2b**, the anion of dimedone, reacts faster with the benzylidene(thio)barbituric acids **1a-e** than expected from the rates of the reactions of **2b** with the reference electrophiles (diarylcarbenium ions and quinone methides).
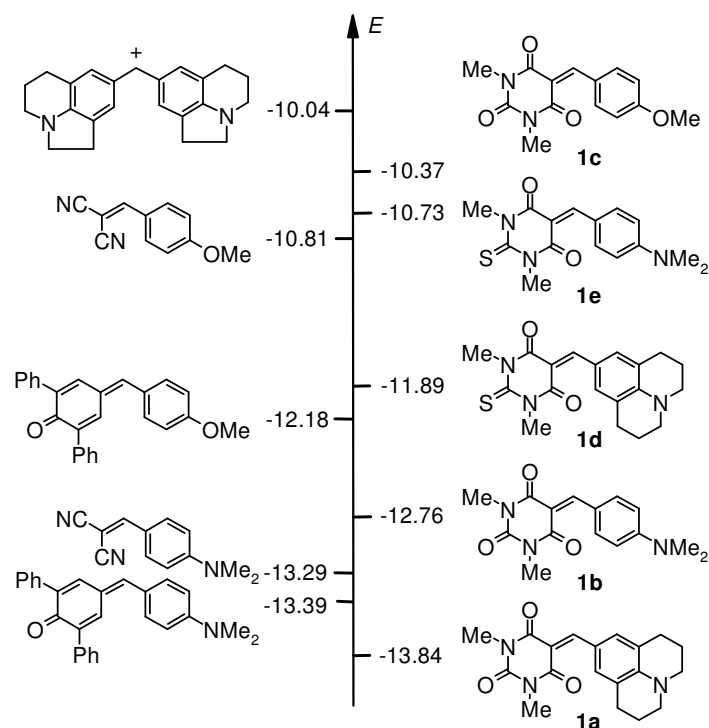
FIGURE 2.6: Comparison of electrophilicity parameters E of Michael acceptors, quinone methides and diarylcarbenium ions.

As summarized in Figure 2.6, benzylidene(thio)barbituric acid derivatives have similar electrophilicities as the corresponding benzylidenemalononitriles. It is found that the thiobarbiturates are more reactive than the corresponding oxa analogues. This observation may be surprising because oxygen is more electronegative than sulfur. Obviously different resonance effects in amides and thioamides are responsible for this ranking of reactivity. It has been reported that thiolactams possess greater dipole moments than lactams.[54] The

higher rotational barrier for the C–N bond in thioformamides – compared with formamides – also indicates the high contribution of a resonance structure with C=N double bond.[55] *Ab initio* MO calculations by Wiberg and Rablen showed that more electron density is transferred from nitrogen to sulfur in thioformamides than from nitrogen to oxygen in formamides.[56] If one assumes that the thioamide structure with a C=N double bond also has a greater importance in the thiobarbituric acids, one can conclude that the positive polarization of nitrogen in the resonance structures **1d'** and **1e'** (Scheme 2.3) is responsible for the increased electron accepting abilities of the thiobarbituric acids.

1d, **1e**   **1d'**, **1e'**
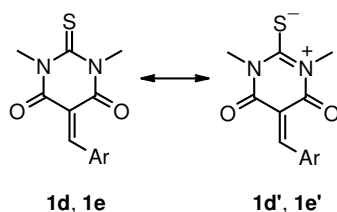
SCHEME 2.3: Resonance effects of benzylidenethiobarbituric acids **1d** and **1e**.

2.3.2 Reactions with other Types of Nucleophiles

From the reactivity parameter of **1c** ($E = -10.37$) one can derive that this electrophile should also be capable of undergoing reactions with electron rich π-systems with $N > 5$ (e.g., silyl enol ethers or electron-rich arenes). In accord with this conclusion **1c** was found to react with 1-phenyl-1-(trimethylsiloxy)ethene (**10a**, $N = 6.22$, $s = 0.96$)[57] and 1-(trimethylsiloxy)-cyclopentene (**10b**, $N = 6.57$, $s = 0.93$)[57] in DMSO at 20 °C to give **11ca** and **11cb**, respectively, after aqueous workup (Scheme 2.4). Compound **11ca** has previously been synthesized by base catalyzed addition of 1,3-dimethylbarbituric acid to 3-(4-methoxyphenyl)-1-phenylprop-2-en-1-one.[58] Attempts to follow the reaction of **1c** with **10b** kinetically were not successful. At $[\mathbf{1c}]_0 = 9.92 \times 10^{-5}$ mol L^{-1} and $[\mathbf{10b}]_0 = 1.08 \times 10^{-2}$ mol L^{-1}, 50 % of **1c** were consumed after 3.5 h, but the decay of **1c** was not monoexponential.
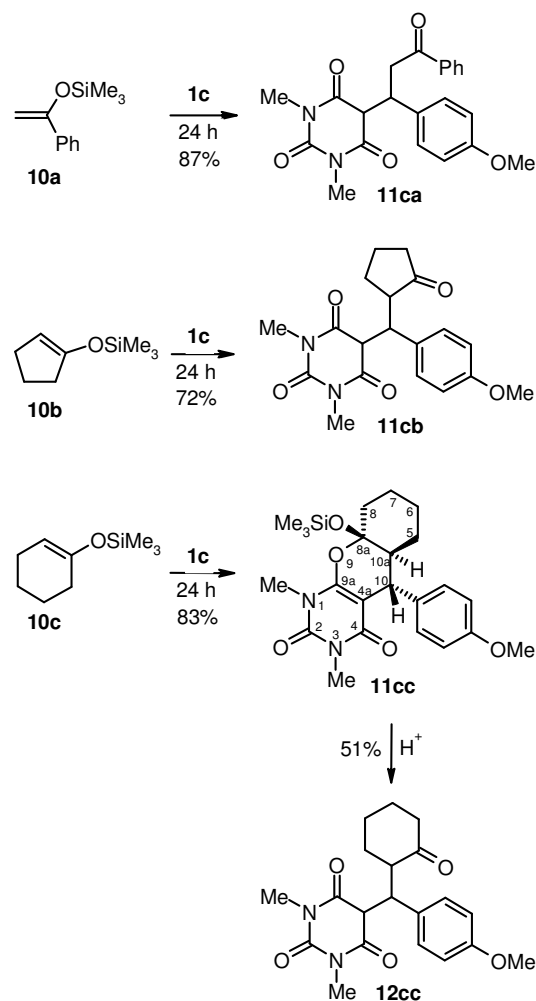
SCHEME 2.4: Reactions of **1c** with silyl enol ethers **10a-c** in DMSO at 20 °C.

The reaction of **1c** with 1-(trimethylsiloxy)cyclohexene (**10c**, $N = 5.21$, $s = 1.00$)[57] did not give the expected cyclohexanone **12cc**. When the solution of the reaction product in DMSO was diluted with water and extracted with ethyl acetate, the hetero Diels-Alder adduct **11cc** was isolated as the only product. X-ray analysis of **11cc** revealed the trans fusion of the cyclohexane and the tetrahydropyran ring with a pseudo equatorial position of the anisyl group and a pseudo axial orientation of the trimethylsiloxy group (Figure 2.7).
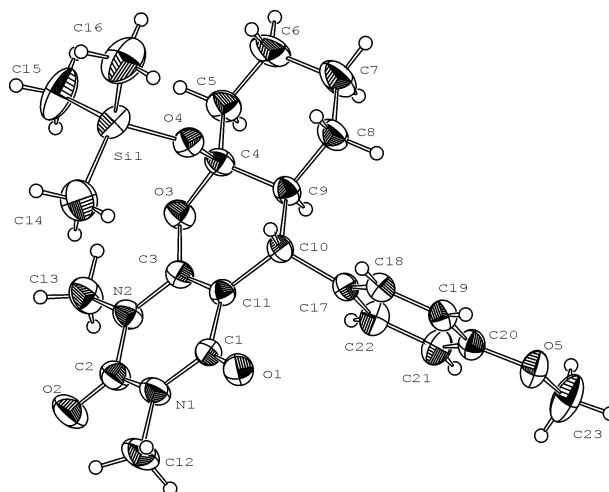
FIGURE 2.7: X-ray crystal structure (ORTEP projection) of **11cc**. Atom numbers refer to the x-ray analysis.

The trans diaxial coupling of the vicinal protons 10-H and 10a-H ($^3J_{10-10a}$ = 10.8 Hz) is in accord with this structure. The trans-fusion of the two rings of the chromene fragment excludes a concerted Diels-Alder reaction.[59] Because the product has not been exposed to acidic conditions, epimerization of the acetal center appears unlikely[60-62] and we assume a stepwise mechanism via a dipolar intermediate.[63]

Treatment of **11cc** with 1 M aqueous HCl cleaves the silylated acetal and yields the initially expected cyclohexanone **12cc** as a 7:1 mixture of two diastereomers.
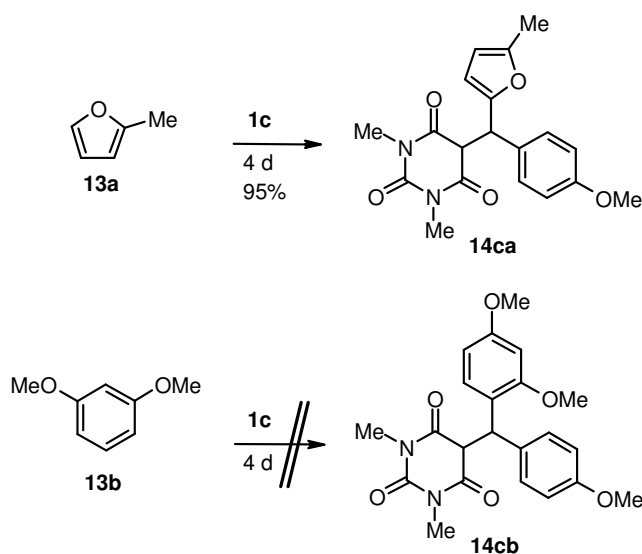
SCHEME 2.5: Reactions of **1c** with the electron rich arenes **13a** and **13b** in DMSO at 20 °C.

As predicted by equation 2.1, 1,3-dimethoxybenzene (**13b**, $N = 2.48$, $s = 1.09$)[57] does not react with **1c** ($E = -10.37$) in DMSO; after 4 days at room temperature we did not observe any conversion (Scheme 2.5). Analogously, equation 2.1 predicts a very slow reaction ($k_2 = 3.14 \times 10^{-8}$ L mol^{-1} s^{-1}) of **1c** with 2-methylfuran (**13a**, $N = 3.61$, $s = 1.11$).[34] While this rate constant refers to a half reaction time of 10 years for a 0.1 M solution in dichloromethane, the electrophilic substitution product **14ca** was obtained in 95 % yield after 4 days in DMSO. The kinetic investigation of this reaction yields a rate constant of $k_2 = 1.24 \times 10^{-4}$ L mol^{-1} s^{-1} (DMSO, 20 °C), i.e., almost four orders of magnitude faster than calculated by equation 2.1. Though reactions of neutral reactants via dipolar intermediates can be expected to show large dependence on solvent polarity,[64] we cannot explain at present why calculated and observed rate constant for the reaction of **1c** with **13a** differ so much. Possibly, secondary orbital interactions as indicated in transition state **15** account for the high reactivity of 2-methylfuran (**13a**).

15
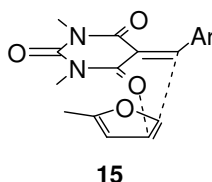
In order to check the applicability of the *E* parameters of the benzylidene(thio)barbituric acids **1a-e** listed in Table 2.3 for reactions with other types of nucleophiles, we have also studied the rates of the reactions of **1b** and **1c** with propyl amine and morpholine.
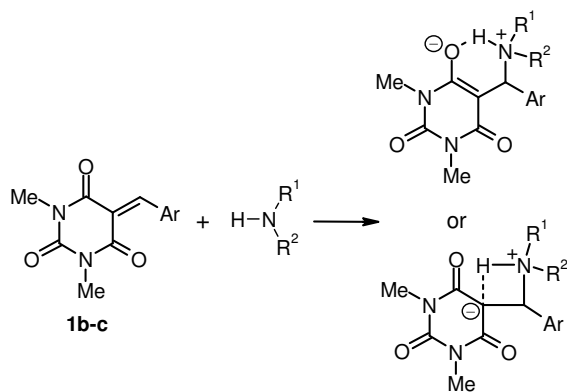
SCHEME 2.6: Reactions of **1b** and **1c** with amines in DMSO at 20 °C.

Because alkyl ammonium ions have higher pK_a values than 5-alkyl substituted barbituric acids,[65] the additions of primary and secondary amines to **1b** and **1c** yield zwitterionic adducts in DMSO as shown in Scheme 2.6. While the additions of propyl amine proceeded

quantitatively, the reactions with morpholine were incomplete and the absorbances of the electrophiles **1b** and **1c** did not disappear completely.

TABLE 2.4: Experimental and calculated (equation 2.1) second-order rate constants k_2 for the reactions of amines with **1b** and **1c** in comparison with literature data.

	nucleophile	N / s[a], [b]	exp. k_2[b] / L mol^{-1} s^{-1}	calc. k_2[b] / L mol^{-1} s^{-1}	k_2[c] / L mol^{-1} s^{-1}
1b	Propyl amine	15.70 / 0.64	2.12×10^3	7.61×10^1	-
	Morpholine	16.96 / 0.67	2.01×10^4	6.52×10^2	-
	Piperidine	17.19 / 0.71	-	1.40×10^3	2.9×10^4
1c	Propyl amine	15.70 / 0.64	3.13×10^4	2.58×10^3	-
	Morpholine	16.96 / 0.67	2.02×10^5	2.60×10^4	-
	Piperidine	17.19 / 0.71	-	6.95×10^4	3.2×10^5

[a] Ref.[66]. [b] DMSO, 20 °C. [c] MeCN, 25 °C, ref.[7]

Table 2.4 compares calculated and experimental rate constants for the additions of amines and shows that equation 2.1 predicts rate constants for the additions of propyl amine and morpholine to **1c** with an accuracy of one order of magnitude. The corresponding reactions of **1b** proceed 28 and 31 times faster than predicted.

The reported rate constants for the additions of piperidine to **1b** and **1c** in acetonitrile at 25 °C are 20 and 5 times greater than the calculated rate constants for these reactions in DMSO at 20 °C, again showing qualitative agreement. For the reactions of secondary amines with benzylidene Meldrum's acids in aqueous DMSO Bernasconi postulated an early development of hydrogen bonding on the reaction coordinate, which was supposed to be responsible for enhanced intrinsic rate constants k_0.[67, 68] Furthermore, Oh and Lee proposed that the additions of benzyl amines to dicarbonyl activated olefins in acetonitrile proceed through cyclic transition states with four-membered or six-membered rings, where the amine proton forms a hydrogen bond to C_α of the Michael acceptor or to a carbonyl oxygen.[69-72] As a consequence, it is possible that the constant higher reactivity of amines in reactions with benzylidenebarbituric acids is due to interactions of the N–H bonds with the developing negative charge on C_α or one of the carbonyl oxygens of the Michael acceptor.

However, because the deviation between calculated and experimental rate constants for the reactions of **1a-e** with amines is within the previously suggested confidence limit of equation 2.1 (one to two orders of magnitude)[73] these deviations shall not be overinterpreted.

2.4 Conclusion

The linear-free-energy-relationship $\log k_2(20\ °C) = s(N + E)$ (equation 2.1) was considered to be suitable for the calculation of the second-order rate constants of the reactions of the benzylidene(thio)barbituric acids **1a-e** with carbanions and amines from the E parameters of **1a-e** determined in this work and the nucleophile-specific parameters N and s reported earlier.[36, 37, 39, 40] The agreement between calculated and experimental data is within one order of magnitude for carbanions, while the few amines examined react 10-30 times faster than calculated. 2-Methylfuran (**13a**), the only π-nucleophile, which was kinetically investigated, reacted 4 orders of magnitude faster than predicted. It ought to be speculated if the stabilizing secondary orbital interactions are responsible for the failure of equation 2.1 to predict this rate constant.

2.5 Experimental section

2.5.1 General Comments

All reactions were performed under an atmosphere of dry nitrogen. ^{1}H- and ^{13}C-NMR chemical shifts are expressed in ppm and refer to the corresponding solvents (d_6-DMSO: $\delta_H = 2.50$, $\delta_C = 39.5$ and CDCl$_3$: $\delta_H = 7.26$, $\delta_C = 77.2$). DEPT and HSQC experiments were employed to assign the signals. d_6-DMSO for NMR was distilled over CaH$_2$ and stored under an argon atmosphere.

2.5.2 Synthesis of 5-Benzylidene-1,3-dimethyl(thio)barbituric Acids

Benzylidene(thio)barbituric acids **1a-e** were synthesized from the corresponding (thio)barbituric acids and *p*-substituted benzaldehydes according to ref. [74].

1,3-Dimethyl-5-(2,3,6,7-tetrahydro-1*H*,5*H*-pyrido[3,2,1-ij]quinolin-9-ylmethylene)-pyrimidine-2,4,6(1*H*,3*H*,5*H*)-trione (**1a**): Red crystals, 90 % yield, mp 197-198 °C (EtOH). ^{1}H-NMR (300 MHz, CDCl$_3$): δ 1.98 (quint, ^3J = 6.3 Hz, 4H, 2 × CH$_2$), 2.78 (t, ^3J = 6.0 Hz, 4H, 2 × CH$_2$), 3.35-3.39 (m, 10H, 2 × NCH$_3$ + 2 × CH$_2$), 8.07 (s, 2H, Ar), 8.30 (s, 1H, CH). ^{13}C-NMR (75.5 MHz, CDCl$_3$): δ 21.3 (CH$_2$), 27.8 (CH$_2$), 28.4 (NCH$_3$), 29.0 (NCH$_3$), 50.7 (CH$_2$), 107.9 (C(COR)$_2$), 120.6 (C$_{Ar}$-H), 120.7 (C$_{Ar}$), 137.6 (C$_{Ar}$), 149.4 (C$_{Ar}$-N), 152.2 (CO), 158.4 (CH), 162.0 (CO), 164.5 (CO). C$_{19}$H$_{21}$N$_3$O$_3$ (339.4): Calc. C 67.77, H 6.24, N 12.38; found C 67.26, H 6.21, N 12.38. HR-MS (EI) [M$^+$]: Calc. 339.1583; found 339.1556.

1,3-Dimethyl-5-(2,3,6,7-tetrahydro-1*H*,5*H*-pyrido[3,2,1-ij]quinolin-9-ylmethylene)-2-thioxo-dihydropyrimidine-4,6(1*H*,5*H*)-dione (**1d**): Red crystals, 99 % yield, mp 193-194 °C (EtOH). ^{1}H-NMR (300 MHz, CDCl$_3$): δ 1.99 (quint, ^3J = 6.3 Hz, 4H, 2 × CH$_2$), 2.79 (t, ^3J = 6.3 Hz, 4H, 2 × CH$_2$), 3.40 (t, ^3J = 5.7 Hz, 4H, 2 × CH$_2$), 3.81 (s, 6H, 2 × NCH$_3$), 8.09 (s, 2H, Ar), 8.30 (s, 1H, CH). ^{13}C-NMR (150.8 MHz, CDCl$_3$): δ 21.5 (CH$_2$), 27.9 (CH$_2$), 36.0 (NCH$_3$), 36.6 (NCH$_3$), 51.1 (CH$_2$), 108.3 (C(COR)$_2$), 121.1 (C$_{Ar}$-H), 121.7 (C$_{Ar}$), 138.4 (C$_{Ar}$), 150.5 (C$_{Ar}$-N), 159.7 (CH), 160.5 (CO), 163.6 (CO), 180.4 (CS). HR-MS (ESI) [MH$^+$]: Calc. 356.1433; found 356.1428.

2.5.3 Characterization of Potassium Salts *3* by NMR Spectroscopy

Under an argon atmosphere potassium salt **2** (0.090 mmol) and electrophile **1** (0.090 mmol) were dissolved in 0.7 mL of dry d_6-DMSO. The resulting mixture was investigated by NMR spectroscopy.

1,3-Dimethyl-2,4,6-trioxo-5-[1-(2,3,6,7-tetrahydro-1*H*,5*H*-pyrido[3,2,1-ij]quinoline-9-yl)-2,2'-dicyanoethyl]-hexahydropyrimidine-5-yl potassium (**3ah**): ^{1}H-NMR (400 MHz, d_6-DMSO): δ 1.85 (quint, ^3J = 5.7 Hz, 4H, 2 × CH$_2$), 2.61 (t, ^3J = 6.5 Hz, 4H, 2 × CH$_2$), 3.04 (t, ^3J = 5.7 Hz, 4H, 2 × CH$_2$), 3.06 (s, 6H, 2 × NCH$_3$), 4.43 (d, ^3J = 11.9 Hz, 1H, CH), 6.02 (d,

3ah
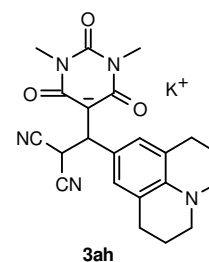
^3J = 11.9 Hz, 1H, CH), 6.85 (s, 2H, Ar). ^{13}C-NMR (100 MHz, d_6-DMSO): δ 21.6 (CH$_2$), 25.8 (CH(CN)$_2$), 26.5, 27.1, 43.2 (CH), 49.2 (CH$_2$), 83.7 (C-5), 115.0 (CN), 115.3 (CN), 120.0 (2 × C$_{Ar}$), 125.9 (2 × C$_{Ar}$-H), 128.7 (C$_{Ar}$), 141.3 (C$_{Ar}$-N), 152.5 (CO), 161.5 (2 × CO).

1,3-Dimethyl-2,4,6-trioxo-5-[1-(4-dimethylaminophenyl)-2,2'-dicyano-ethyl]-hexahydropyrimidine-5-yl potassium (**3bh**): ^{1}H-NMR (400 MHz, d_6-DMSO): δ 2.84 (s, 6H, N(CH$_3$)$_2$), 3.07 (s, 6H, 2 × NCH$_3$), 4.57 (d, ^3J = 11.9 Hz, 1H, CH), 6.08 (d, ^3J = 11.9 Hz, 1H, CH), 6.60 (d, ^3J = 8.8 Hz, 2H, Ar), 7.33 (d, ^3J = 8.8 Hz, 2H, Ar). ^{13}C-NMR (100 MHz, d_6-DMSO): δ 25.9 (CH(CN)$_2$), 26.5 (2 × NCH$_3$), 40.0 (N(CH$_3$)$_2$), 43.2 (CH), 83.6 (C-5), 111.9 (2 × C$_{Ar}$-H), 114.9 (CN), 115.1 (CN), 128.3 (2 × C$_{Ar}$-H), 129.7, 149.2 (C$_{Ar}$), 152.5 (CO), 161.6 (CO).
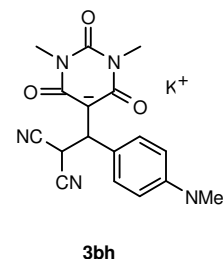
1,3-Dimethyl-2,4,6-trioxo-5-[1-(4,4'-dimethyl-2,6-dioxocyclohexyl)-1'-(4-methoxyphenyl)-methyl]-hexahydropyrimidine-5-yl potassium (**3cb**): ^{1}H-NMR (400 MHz, d_6-DMSO): δ 0.99 (s, 3H, CH$_3$), 1.04 (s, 3H, CH$_3$), 2.04–2.33 (m, CH$_2$, 4H), 3.00 (s, 3H, NCH$_3$), 3.08 (s, br, 3H, NCH$_3$), 3.67 (s, 3H, OCH$_3$), 6.08 (s, 1H, CH), 6.68 (d, ^3J = 8.8 Hz, 2H, Ar), 6.90 (d, ^3J = 8.8 Hz, 2H, Ar), 14.60 (s, 1H, OH). ^{13}C-NMR (75.5 MHz, d_6-DMSO): δ 26.5 (NCH$_3$), 27.0 (CH$_3$), 27.4 (NCH$_3$), 29.4 (CH$_3$), 31.0 (CH), 44.8 (CH$_2$), 50.6 (CH$_2$), 54.8 (OCH$_3$), 89.6 (C-5), 112.7 (C$_{Ar}$-H), 114.6, 116.1, 127.6 (C$_{Ar}$-H), 136.6, 152.1, 156.2, 163.2, 174.1, 196.2.
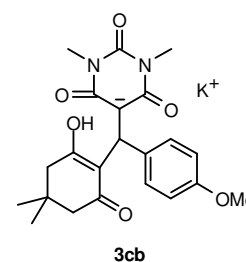
5-[2-Acetyl-1-(2,3,6,7-tetrahydro-1H,5H-pyrido[3,2,1-ij]quinoline-9-yl)-3-oxobutyl]-1,3-dimethyl-2-thioxodihydropyrimidine-4,6(1H,5H)-dione-5-yl potassium (**3de**): ^{1}H-NMR (300 MHz, d_6-DMSO): δ 1.82 (quint, ^3J = 5.4 Hz, 4H, 2 × CH$_2$), 1.96, 2.02 (2s, 6H, 2 × CH$_3$-CO), 2.57 (t, ^3J = 6.3 Hz, 4H, 2 × CH$_2$), 2.97 (t, ^3J = 5.1 Hz, 4H, CH$_2$), 3.46 (s, 6H, 2 × NCH$_3$), 4.67 (d, ^3J = 12.3 Hz, 1H, CH), 5.41 (d, ^3J = 12.3 Hz, 1H, CH), 6.73 (s, 2H, Ar). ^{13}C-NMR (100 MHz, d_6-DMSO): δ 22.0 (CH$_2$), 27.3 (CH$_2$), 28.4 (CH$_3$-CO), 30.6 (CH$_3$-CO), 34.5 (2 × NCH$_3$), 40.3 (CH), 49.5 (CH$_2$), 69.7 (CH(COCH$_3$)$_2$), 91.5 (C-5), 120.0 (2 × C$_{Ar}$), 126.2 (2 × C$_{Ar}$-H), 131.7 (C$_{Ar}$), 140.6 (C$_{Ar}$-N), 160.2 (2 × CO), 174.9 (CS), 203.9 (CO-CH$_3$), 204.6 (CO-CH$_3$).
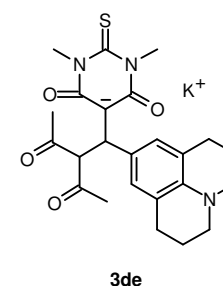
1,3-Dimethyl-5-[1-(2,3,6,7-tetrahydro-1H,5H-pyrido[3,2,1-ij]quinoline-9-yl)-2,2'-dicyano-ethyl]-2-thioxodihydropyrimidine-4,6(1H,5H)-dione-5-yl potassium (**3dh**): ^{1}H-NMR (300 Hz, d_6-DMSO): δ 1.83 (quint, [3]J = 5.4 Hz, 4H, 2 × CH$_2$), 2.60 (t, [3]J = 6.3 Hz, 4H, 2 × CH$_2$), 3.03 (t, [3]J = 5.4 Hz, 4H, 2 × CH$_2$), 3.51 (s, 6H, 2 × NCH$_3$), 4.43 (d, [3]J = 12.1 Hz, 1H, CH), 5.96 (d, [3]J = 12.1 Hz, 1H, CH), 6.82 (s, 2H, Ar). ^{13}C-NMR (75.5 MHz, d_6-DMSO): δ 21.7 (CH$_2$), 26.1 (CH(CN)$_2$), 27.3 (CH$_2$), 34.4 (2 × NCH$_3$), 43.2 (CH), 49.3 (CH$_2$), 88.9 (C-5), 115.0 (CN), 115.3 (CN), 120.3 (2 × C$_{Ar}$), 126.1 (2 × C$_{Ar}$-H), 127.8 (C$_{Ar}$), 141.7 (C$_{Ar}$-N), 160.4 (2 × CO), 175.6 (C=S).
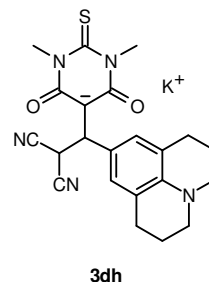
5-[2-Acetyl-1-(4-dimethylaminophenyl)-3-oxobutyl]-1,3-dimethyl-2-thioxodihydropyrimidine-4,6(1H,5H)-dione-5-yl potassium (**3ee**): ^{1}H-NMR (400 MHz, d_6-DMSO): δ 1.93, 2.05 (2s, 2 × 3H, 2 × CH$_3$-CO), 2.78 (s, 6H, N(CH$_3$)$_2$), 3.46 (s, 6H, 2 × NCH$_3$), 4.78 (d, [3]J = 12.5 Hz, 1H, CH), 5.47 (d, [3]J = 12.4 Hz, 1H, CH), 6.52 (d, [3]J = 8.7 Hz, 2H, Ar), 7.22 (d, [3]J = 8.6 Hz, 2H, Ar). ^{13}C-NMR (100 MHz, d_6-DMSO): δ 28.4 (CH$_3$-CO), 30.4 (CH$_3$-CO), 34.4 (NCH$_3$), 40.4 (N(CH$_3$)$_2$), 40.4 (CH), 69.8 (CH(COCH$_3$)$_2$), 91.4 (C-5), 112.0 (C$_{Ar}$-H), 128.3 (C$_{Ar}$-H), 132.6 (C$_{Ar}$-N), 148.5 (C$_{Ar}$), 160.3 (2 × CO), 174.9 (CS), 203.8 (CO-CH$_3$), 204.5 (CO-CH$_3$).
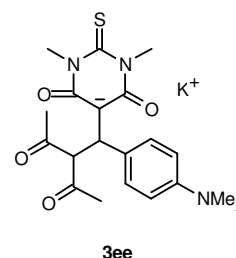
2.5.4 Synthesis of Products *5*

Under a nitrogen atmosphere potassium salt **2** (0.44 mmol) was added to a stirred solution of electrophile **1** (0.36 mmol) in dry DMSO (4 mL). Conc. HCl (0.1 mL) was added after 10 min, the resultant mixture was stirred for additional 2 h and then poured into water (30 mL). After extraction with ethyl acetate (3 × 20 mL) and removal of the solvent in vacuo, the solid residue was recrystallized from ethanol.

5-[1-(4-Dimethylaminophenyl)-2-nitropropyl]-1,3-dimethylpyrimidine-2,4,6-(1H,3H,5H)-trione (**5bm**): Colorless crystals, 74 % yield, isolated as mixture of diastereomers (10:1). Major diastereomer: ^{1}H-NMR (300 MHz, CDCl$_3$): δ 1.39, (d, [3]J = 6.9 Hz, 3H, CH$_3$), 2.92 (s, 6H, N(CH$_3$)$_2$), 3.05, 3.17 (2s, 6H, 2 × NCH$_3$), 3.68 (d, [3]J = 3.3 Hz, 1H, 5-H), 4.02 (dd, [3]J = 11.4 Hz, [3]J = 3.6 Hz, 1H, CH), 5.55 (m, 1H, CH), 6.55 (d, [3]J = 9.0 Hz, 2H, Ar), 6.82 (d,
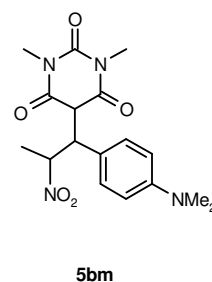
$^3J = 8.7$ Hz, 2H, Ar). ^{13}C-NMR (75.5 MHz, CDCl$_3$): δ 19.7 (CH$_3$), 28.4, 28.5 (NCH$_3$), 40.3, 51.2, 51.7, 83.5 (CH), 112.5 (C$_{Ar}$-H), 119.9, 129.0 (C$_{Ar}$-H), 150.7, 151.0, 167.2, 167.4. C$_{17}$H$_{22}$N$_4$O$_5$ (362.4): Calc. C 56.35, H 6.12, N 15.46; found C 56.17, H 6.14, N 15.16. HR-MS (EI) [M$^+$]: Calc. 362.1590; found 362.1565.

1,3-Dimethyl-5-[(4,4'-dimethyl-2,6-dioxocyclohexyl)(4-methoxy-phenyl)methyl]-pyrimidine-2,4,6(1H,3H,5H)-trione **(5cb)**: Colorless crystals, 93 % yield, mp 146 –147 °C (EtOH). ^{1}H-NMR (400 MHz, CDCl$_3$): δ 1.13 (s, 3H, CH$_3$), 1.26 (s, 3H, CH$_3$), 2.40 (m, 4H, CH$_2$), 3.35 (s, 3H, NCH$_3$), 3.44 (s, 3H, NCH$_3$), 3.78 (s, 3H, OCH$_3$), 5.51 (s, 1H, CH), 6.82 (d, $^3J = 8.8$ Hz, 2H, Ar), 7.02 (d, $^3J = 8.8$ Hz, 2H, Ar), 11.32 (br. s, 1H, OH), 12.82 (s, 1H, 6-OH). ^{13}C-NMR (75.5 MHz, CDCl$_3$): δ 27.3, 29.0, 29.4, 30.2, 31.4, 33.1, 46.2 (CH$_2$), 47.2 (CH$_2$), 55.4 (OCH$_3$), 92.8 (C-5), 113.9 (C$_{Ar}$-H), 116.8 (C-1), 127.8 (C$_{Ar}$-H), 129.1, 150.9, 158.1, 162.5, 164.3, 190.9, 191.4. IR (KBr): $\tilde{v} = 3428, 3055, 3001, 2959, 2839, 2632, 1702, 1609, 1510, 1466, 1421, 1389, 1305, 1264, 1249, 1178, 1154, 1117, 1095, 1031, 938$ cm^{-1}. C$_{22}$H$_{26}$N$_2$O$_6$ (414.4): Calc. C 63.77, H 6.32, N 6.76; found C 63.50, H 6.33, N 6.55.
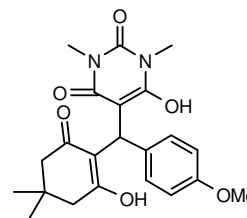
5-[2-Acetyl-1-(4-methoxyphenyl)-3-oxobutyl]-1,3-dimethylpyrimidine-2,4,6(1H,3H,5H)-trione **(5ce)**: Colorless crystals, 93 % yield, mp 116–118 °C (EtOH). ^{1}H-NMR (400 MHz, CDCl$_3$): δ 1.88 (s, 3H, CH$_3$), 2.36 (s, 3H, CH$_3$), 2.92 (s, 3H, NCH$_3$), 3.10 (s, 3H, NCH$_3$), 3.69 (s, 3H, OCH$_3$), 3.73 (d, $^3J = 4.4$ Hz, 1H, 5-H), 4.28 (dd, $^3J = 12.0$ Hz, $^4J = 4.4$ Hz, 1H, CH), 4.79 (d, $^3J = 12.4$ Hz, 1H, CH), 6.70, (d, $^3J = 8.8$ Hz, 2H, Ar), 6.85 (d, $^3J = 8.8$ Hz, 2H, Ar). ^{13}C-NMR (100 MHz, CDCl$_3$): δ 28.1 (NCH$_3$), 28.2 (NCH$_3$), 28.5 (CH$_3$), 30.6 (CH$_3$), 46.5 (CH), 51.1 (CH), 55.3 (OCH$_3$), 70.7 (CH), 114.4 (C$_{Ar}$-H), 126.5, 129.1 (C$_{Ar}$-H), 150.8, 158.8, 159.9, 167.6 (2 × CO), 201.4 ($\underline{C}$OCH$_3$), 202.4 ($\underline{C}$OCH$_3$). IR (KBr): $\tilde{v} = 3409, 2943, 2843, 1744, 1678, 1611, 1570, 1540, 1514, 1424, 1380, 1363, 1256, 1185, 1140, 1120, 1085, 1022, 994$ cm^{-1}. C$_{19}$H$_{22}$N$_2$O$_6$ (374.4): Calc. C 60.95, H 5.92, N 7.48; found C 60.90, H 5.86, N 7.57.
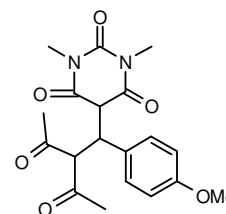
2.5.5 Kinetic Experiments

The temperature of the solutions during all kinetic studies was kept constant at (20 ± 0.1) °C by using a circulating bath thermostat. Dry DMSO for kinetics was purchased (< 50 ppm H_2O).

For the evaluation of kinetics the stopped-flow spectrophotometer systems Hi-Tech SF-61DX2 or Applied Photophysics SX.18MV-R stopped-flow reaction analyzer were used. Rate constants k_{obs} (s^{-1}) were obtained by fitting the single exponential $A_t = A_0\exp(-k_{obs}t) + C$ to the observed time-dependent electrophile absorbance (averaged from at least 4 kinetic runs for each nucleophile concentration). For the stopped-flow experiments 2 stock solutions were used: A solution of the electrophile in DMSO and a solution of the carbanion, which was either used as potassium salt or generated by the deprotonation of the CH acid with 1.05 equivalents of KO^tBu.

Reaction of **1a** with **2b** (DMSO, 20 °C, stopped flow, 487 nm)

[**1a**] / M	[**2b-K**] / M	k_{obs} / s^{-1}
2.18×10^{-5}	7.78×10^{-4}	1.24×10^{-1}
2.18×10^{-5}	1.56×10^{-3}	2.46×10^{-1}
2.18×10^{-5}	2.22×10^{-3}	3.53×10^{-1}
2.18×10^{-5}	3.00×10^{-3}	4.60×10^{-1}
2.18×10^{-5}	3.89×10^{-3}	5.89×10^{-1}

$$k_2 = (1.49 \pm 0.03) \times 10^2 \text{ M}^{-1}\text{s}^{-1}$$
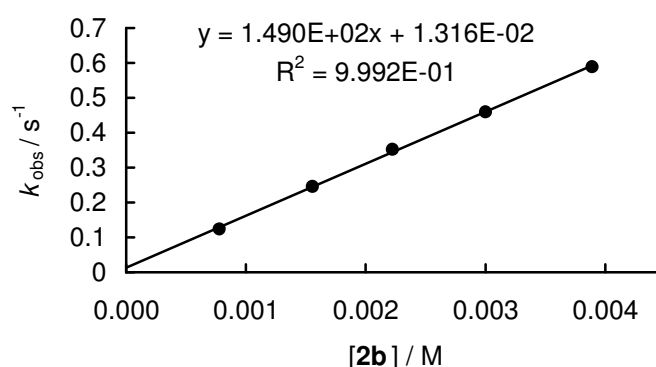
Reaction of **1a** with **2g** (DMSO, 20 °C, stopped flow, 500 nm)

[**1a**] / M	[**2g**] / M	k_{obs} / s^{-1}
2.90×10^{-5}	4.08×10^{-4}	1.48
2.90×10^{-5}	8.17×10^{-4}	2.99
2.90×10^{-5}	1.14×10^{-3}	4.33
2.90×10^{-5}	1.43×10^{-3}	5.29
2.90×10^{-5}	1.76×10^{-3}	6.58

$$k_2 = (3.78 \pm 0.05) \times 10^3 \text{ M}^{-1}\text{s}^{-1}$$

$y = 3.780E+03x - 6.515E-02$
$R^2 = 9.994E-01$
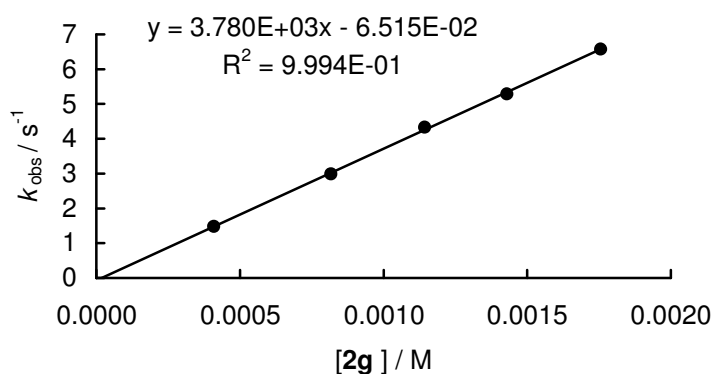
Reaction of **1a** with **2h** (DMSO, 20 °C, stopped flow, 487 nm)

[**1a**] / M	[**2h**] / M	k_{obs} / s^{-1}
2.18×10^{-5}	9.51×10^{-4}	1.14×10^1
2.18×10^{-5}	1.43×10^{-3}	1.75×10^1
2.18×10^{-5}	1.90×10^{-3}	2.31×10^1
2.18×10^{-5}	2.38×10^{-3}	2.92×10^1
2.18×10^{-5}	2.85×10^{-3}	3.52×10^1

$$k_2 = (1.27 \pm 0.04) \times 10^4 \text{ M}^{-1}\text{s}^{-1}$$

$y = 1.272E+04x - 6.637E-01$
$R^2 = 9.970E-01$
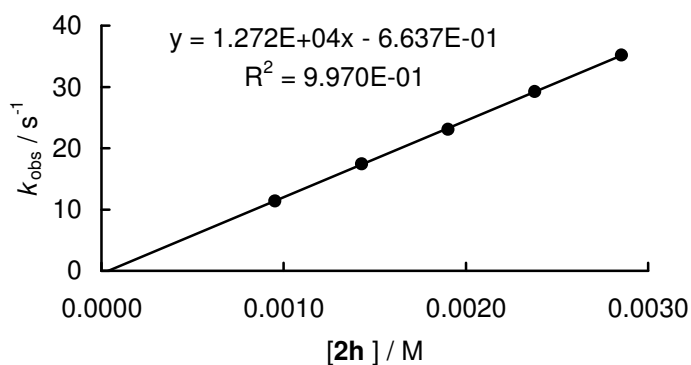
Reaction of **1a** with **2i** (DMSO, 20 °C, stopped flow, 500 nm)

[**1a**] / M	[**2i**] / M	k_{obs} / s^{-1}
2.90×10^{-5}	5.87×10^{-4}	4.36
2.90×10^{-5}	7.83×10^{-4}	5.75
2.90×10^{-5}	9.78×10^{-4}	7.35
2.90×10^{-5}	1.17×10^{-3}	8.82
2.90×10^{-5}	1.37×10^{-3}	1.00×10^{1}

$$k_2 = (7.34 \pm 0.20) \times 10^3 \text{ M}^{-1}\text{s}^{-1}$$
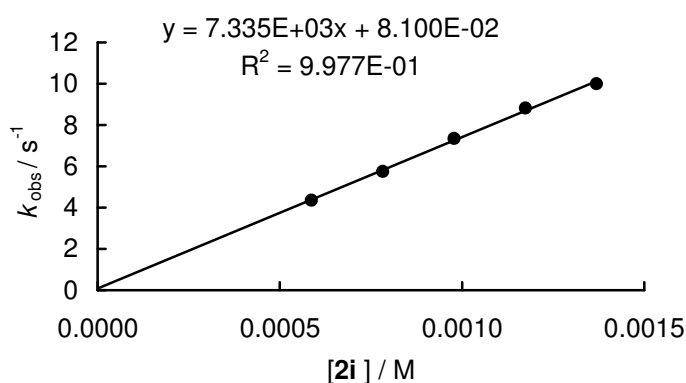
Reaction of **1a** with **2k** (DMSO, 20 °C, stopped flow, 500 nm)

[**1a**] / M	[**2k**] / M	k_{obs} / s^{-1}
2.63×10^{-5}	5.26×10^{-4}	3.84
2.63×10^{-5}	6.48×10^{-4}	4.87
2.63×10^{-5}	7.89×10^{-4}	5.90
2.63×10^{-5}	9.11×10^{-4}	6.81

$$k_2 = (7.66 \pm 0.17) \times 10^3 \text{ M}^{-1}\text{s}^{-1}$$
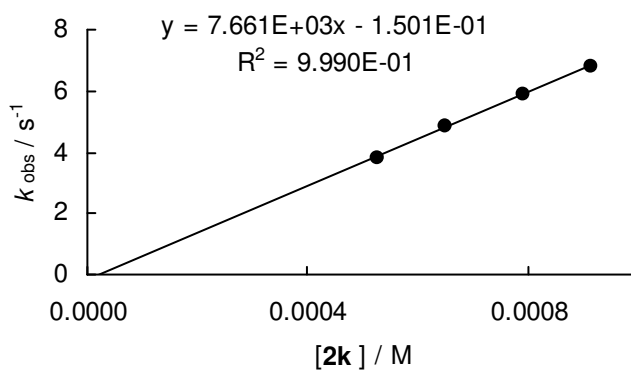
Reaction of **1b** with **2b** (DMSO, 20 °C, stopped flow, 487 nm)

[**1b**] / M	[**2b**] / M	k_{obs} / s^{-1}
3.80×10^{-5}	7.78×10^{-4}	8.24×10^{-1}
3.80×10^{-5}	1.56×10^{-3}	1.74
3.80×10^{-5}	2.22×10^{-3}	2.50
3.80×10^{-5}	3.00×10^{-3}	3.23
3.80×10^{-5}	3.89×10^{-3}	4.07

$$k_2 = (1.04 \pm 0.03) \times 10^3 \text{ M}^{-1}\text{s}^{-1}$$

$$y = 1.040\text{E}+03x + 9.233\text{E}-02$$
$$R^2 = 9.968\text{E}-01$$
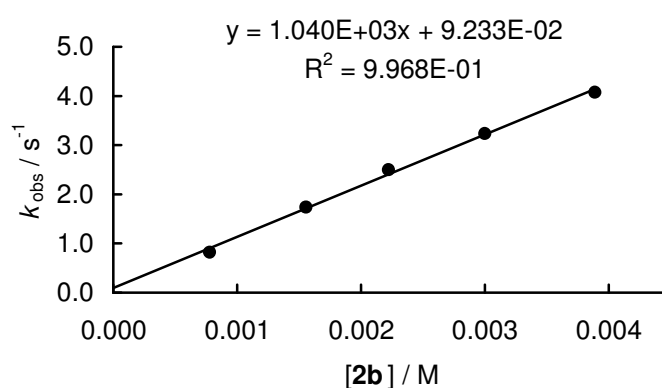
Reaction of **1b** with **2g** (DMSO, 20 °C, stopped flow, 500 nm)

[**1b**] / M	[**2g**] / M	k_{obs} / s^{-1}
2.85×10^{-5}	4.08×10^{-4}	8.47
2.85×10^{-5}	8.17×10^{-4}	1.77×10^{1}
2.85×10^{-5}	1.14×10^{-3}	2.41×10^{1}
2.85×10^{-5}	1.43×10^{-3}	2.97×10^{1}
2.85×10^{-5}	1.76×10^{-3}	3.59×10^{1}

$$k_2 = (2.03 \pm 0.04) \times 10^4 \text{ M}^{-1}\text{s}^{-1}$$

$$y = 2.026\text{E}+04x + 6.710\text{E}-01$$
$$R^2 = 9.986\text{E}-01$$

Reaction of **1b** with **2h** (DMSO, 20 °C, stopped flow, 487 nm)

[**1b**] / M	[**2h**] / M	k_{obs} / s^{-1}
3.80×10^{-5}	9.51×10^{-4}	5.65×10^{1}
3.80×10^{-5}	1.43×10^{-3}	8.68×10^{1}
3.80×10^{-5}	1.90×10^{-3}	1.14×10^{2}
3.80×10^{-5}	2.38×10^{-3}	1.39×10^{2}
3.80×10^{-5}	2.85×10^{-3}	1.70×10^{2}

$$k_2 = (5.88 \pm 0.12) \times 10^4 \; \text{M}^{-1}\text{s}^{-1}$$

Reaction of **1b** with **2i** (DMSO, 20 °C, stopped flow, 500 nm)

[**1b**] / M	[**2i**] / M	k_{obs} / s^{-1}
4.00×10^{-5}	5.87×10^{-4}	2.31×10^{1}
4.00×10^{-5}	7.83×10^{-4}	3.11×10^{1}
4.00×10^{-5}	9.78×10^{-4}	3.88×10^{1}
4.00×10^{-5}	1.17×10^{-3}	4.73×10^{1}
4.00×10^{-5}	1.37×10^{-3}	5.41×10^{1}

$$k_2 = (4.00 \pm 0.07) \times 10^4 \; \text{M}^{-1}\text{s}^{-1}$$
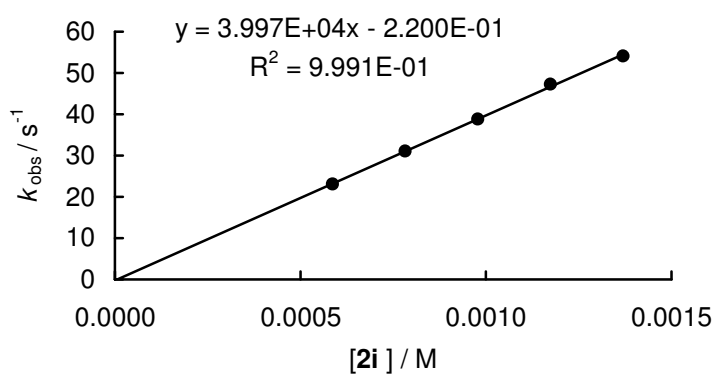
Reaction of **1b** with **2k** (DMSO, 20 °C, stopped flow, 500 nm)

[**1b**] / M	[**2k**] / M	k_{obs} / s^{-1}
3.03×10^{-5}	4.38×10^{-4}	1.65×10^{1}
3.03×10^{-5}	6.48×10^{-4}	2.41×10^{1}
3.03×10^{-5}	7.89×10^{-4}	2.87×10^{1}
3.03×10^{-5}	9.11×10^{-4}	3.31×10^{1}
	$k_2 = (3.49 \pm 0.05) \times 10^4$ M^{-1}s^{-1}	

$$y = 3.492E{+}04x + 1.271E{+}00$$
$$R^2 = 9.997E{-}01$$
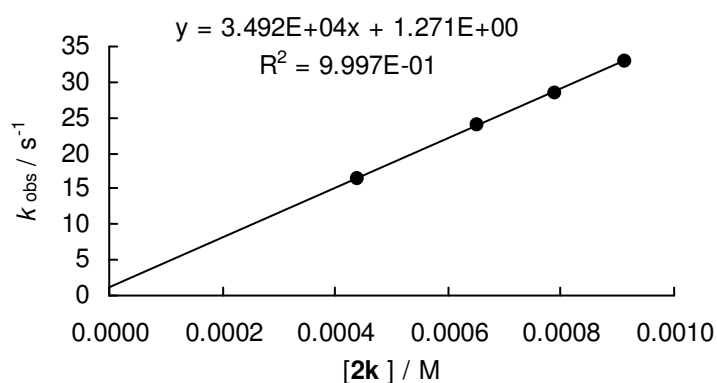
Reaction of **1b** with propyl amine (DMSO, 20 °C, stopped flow, 480 nm)

[**1b**] / M	[amine] / M	k_{obs} / s^{-1}
4.57×10^{-5}	6.00×10^{-3}	1.24×10^{1}
4.57×10^{-5}	9.01×10^{-3}	1.88×10^{1}
4.57×10^{-5}	1.20×10^{-2}	2.51×10^{1}
4.57×10^{-5}	1.50×10^{-2}	3.21×10^{1}
4.57×10^{-5}	1.80×10^{-2}	3.76×10^{1}
	$k_2 = (2.12 \pm 0.04) \times 10^3$ M^{-1}s^{-1}	

$$y = 2.124E{+}03x - 2.927E{-}01$$
$$R^2 = 9.990E{-}01$$
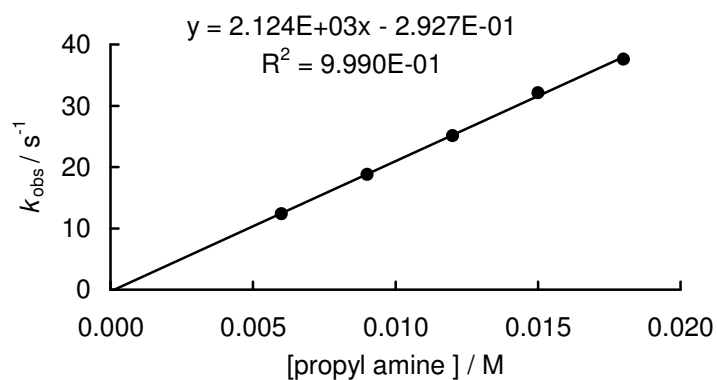
Reaction of **1b** with morpholine (DMSO, 20 °C, stopped flow, 480 nm)

[**1b**] / M	[amine] / M	k_{obs} / s^{-1}
2.51×10^{-5}	2.50×10^{-3}	1.43×10^{2}
2.51×10^{-5}	4.49×10^{-3}	1.78×10^{2}
2.51×10^{-5}	6.56×10^{-3}	2.20×10^{2}
2.51×10^{-5}	8.55×10^{-3}	2.58×10^{2}
2.51×10^{-5}	1.05×10^{-2}	3.05×10^{2}
$k_2 = (2.01 \pm 0.06) \times 10^{4}$ M^{-1}s^{-1}		

y = 2.013E+04x + 8.953E+01
R^2 = 9.972E-01
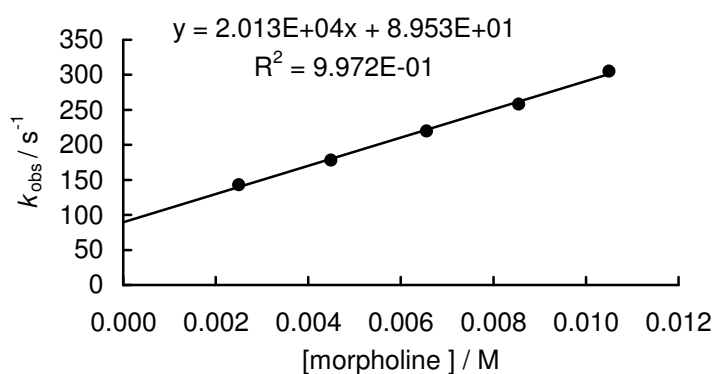
Reaction of **1c** with **2b** (DMSO, 20 °C, stopped flow, 364 nm)

[**1c**] / M	[**2b**] / M	k_{obs} / s^{-1}
1.82×10^{-5}	2.78×10^{-4}	1.27×10^{1}
1.82×10^{-5}	5.55×10^{-4}	2.64×10^{1}
1.82×10^{-5}	8.33×10^{-4}	3.99×10^{1}
1.82×10^{-5}	1.11×10^{-3}	5.43×10^{1}
1.82×10^{-5}	1.39×10^{-3}	6.59×10^{1}
$k_2 = (4.83 \pm 0.09) \times 10^{4}$ M^{-1}s^{-1}		

y = 4.834E+04x - 4.190E-01
R^2 = 9.990E-01
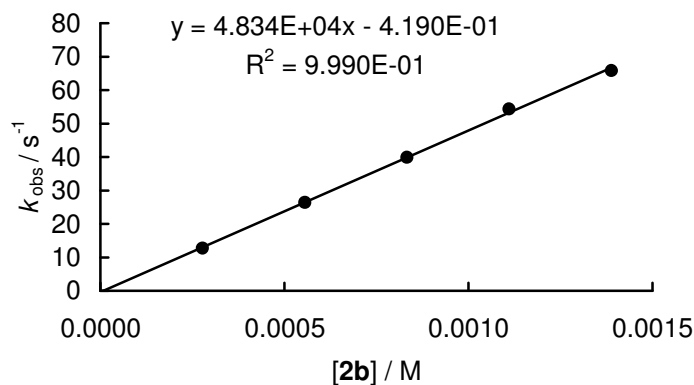
Reaction of **1c** with **2g** (DMSO, 20 °C, stopped flow, 375 nm)

[**1c**] / M	[**2g**] / M	k_{obs} / s^{-1}
2.81×10^{-5}	3.42×10^{-4}	3.52×10^2
2.81×10^{-5}	3.94×10^{-4}	4.31×10^2
2.81×10^{-5}	4.47×10^{-4}	4.74×10^2
2.81×10^{-5}	4.99×10^{-4}	5.27×10^2
	$k_2 = (1.08 \pm 0.09) \times 10^6$ M^{-1}s^{-1}	

$$y = 1.083\text{E}{+}06x - 9.458\text{E}{+}00$$
$$R^2 = 9.849\text{E}{-}01$$
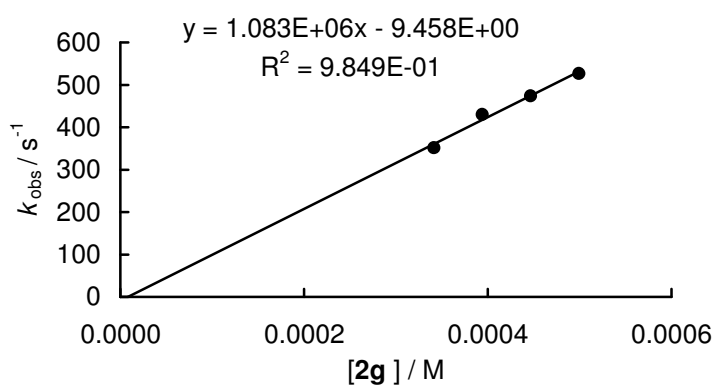
Reaction of **1c** with **2h** (DMSO, 20 °C, stopped flow, 375 nm)

[**1c**] / M	[**2h**] / M	k_{obs} / s^{-1}
2.92×10^{-5}	2.85×10^{-4}	5.06×10^2
2.92×10^{-5}	3.72×10^{-4}	7.00×10^2
2.92×10^{-5}	4.60×10^{-4}	8.30×10^2
2.92×10^{-5}	5.69×10^{-4}	1.03×10^3
2.92×10^{-5}	6.57×10^{-4}	1.19×10^3
	$k_2 = (1.80 \pm 0.05) \times 10^6$ M^{-1}s^{-1}	

$$y = 1.801\text{E}{+}06x + 7.623\text{E}{+}00$$
$$R^2 = 9.975\text{E}{-}01$$
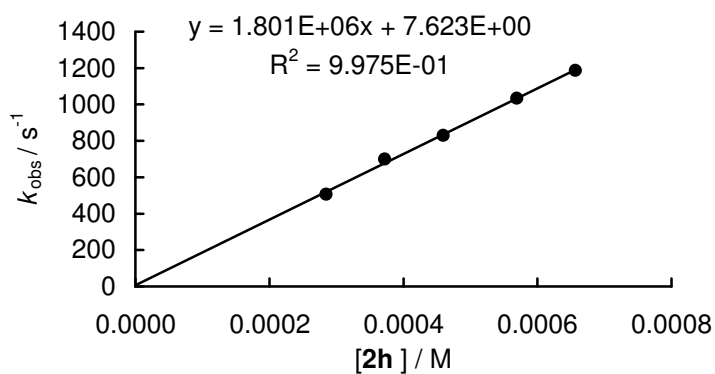
Reaction of **1c** with **2i** (DMSO, 20 °C, stopped flow, 375 nm)

[**1c**] / M	[**2i**] / M	k_{obs} / s^{-1}
2.81×10^{-5}	2.92×10^{-4}	4.35×10^2
2.81×10^{-5}	3.40×10^{-4}	5.04×10^2
2.81×10^{-5}	3.89×10^{-4}	5.74×10^2
2.81×10^{-5}	4.47×10^{-4}	6.73×10^2
2.81×10^{-5}	5.06×10^{-4}	7.49×10^2

$$k_2 = (1.49 \pm 0.03) \times 10^6 \text{ M}^{-1}\text{s}^{-1}$$

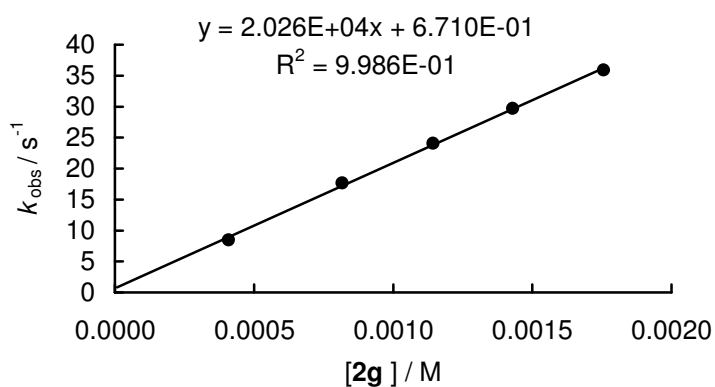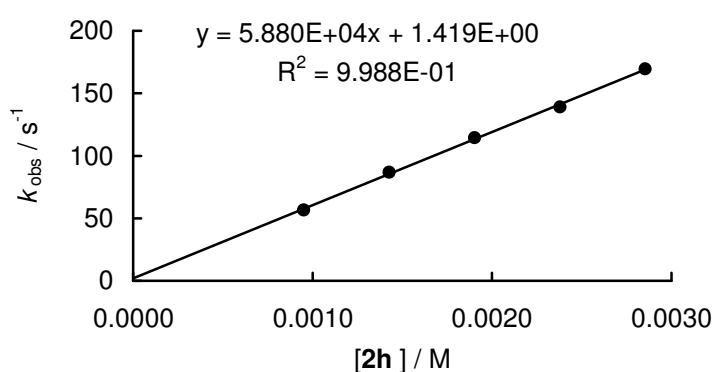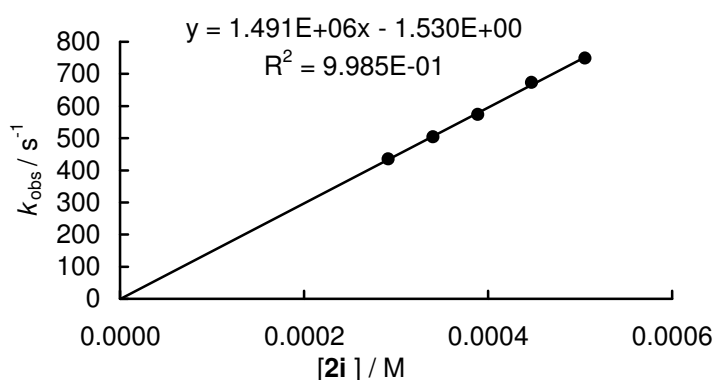Reaction of **1c** with **2k** (DMSO, 20 °C, stopped flow, 375 nm)

[**1c**] / M	[**2k**] / M	k_{obs} / s^{-1}
2.81×10^{-5}	2.85×10^{-4}	3.98×10^2
2.81×10^{-5}	3.40×10^{-4}	4.53×10^2
2.81×10^{-5}	3.96×10^{-4}	5.60×10^2
2.81×10^{-5}	4.51×10^{-4}	6.12×10^2
2.81×10^{-5}	5.07×10^{-4}	7.09×10^2

$$k_2 = (1.41 \pm 0.09) \times 10^6 \text{ M}^{-1}\text{s}^{-1}$$
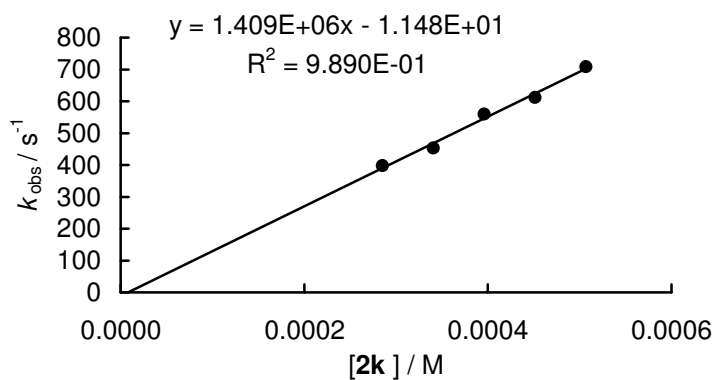
Reaction of **1c** with **10c** (DMSO, 20 °C, stopped flow, 375 nm)

[**1c**] / M	[**10c**] / M	k_{obs} / s^{-1}
1.23×10^{-4}	1.75×10^{-2}	1.66×10^{-6}
1.09×10^{-4}	3.26×10^{-2}	3.53×10^{-6}
	$k_2 = 1.24 \times 10^{-4}$ M^{-1}s^{-1}	
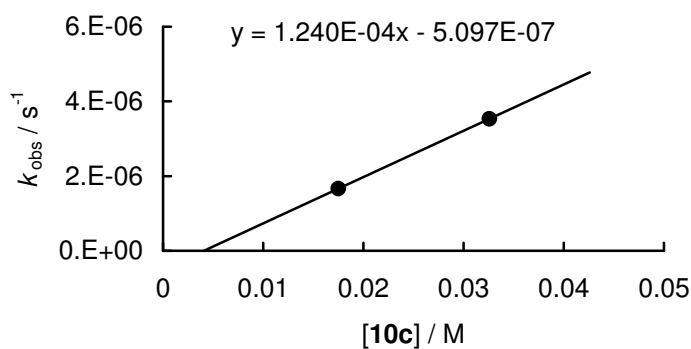
Reaction of **1c** with propyl amine (DMSO, 20 °C, stopped flow, 380 nm)

[**1c**] / M	[amine] / M	k_{obs} / s^{-1}
4.41×10^{-5}	5.77×10^{-3}	1.61×10^{2}
4.41×10^{-5}	8.84×10^{-3}	2.54×10^{2}
4.41×10^{-5}	1.19×10^{-2}	3.61×10^{2}
4.41×10^{-5}	1.41×10^{-2}	4.37×10^{2}
4.41×10^{-5}	1.77×10^{-2}	5.25×10^{2}
	$k_2 = (3.13 \pm 0.12) \times 10^{4}$ M^{-1}s^{-1}	

46
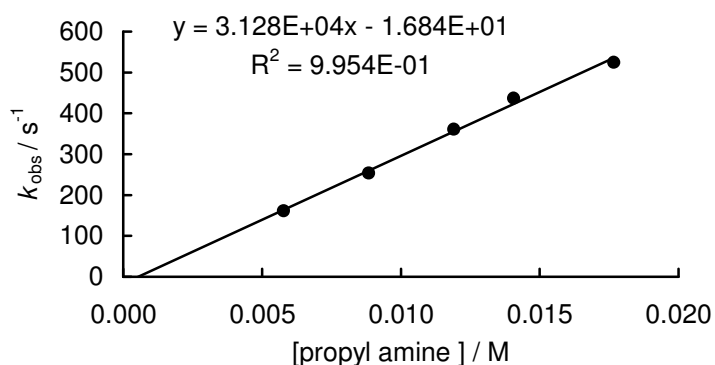
Reaction of **1c** with morpholine (DMSO, 20 °C, stopped flow, 380 nm)

[**1c**] / M	[amine] / M	k_{obs} / s^{-1}
5.04×10^{-5}	2.60×10^{-3}	5.83×10^2
5.04×10^{-5}	3.75×10^{-3}	8.71×10^2
5.04×10^{-5}	6.34×10^{-3}	1.38×10^3
5.04×10^{-5}	7.21×10^{-3}	1.52×10^3

$$k_2 = (2.02 \pm 0.09) \times 10^5 \text{ M}^{-1}\text{s}^{-1}$$
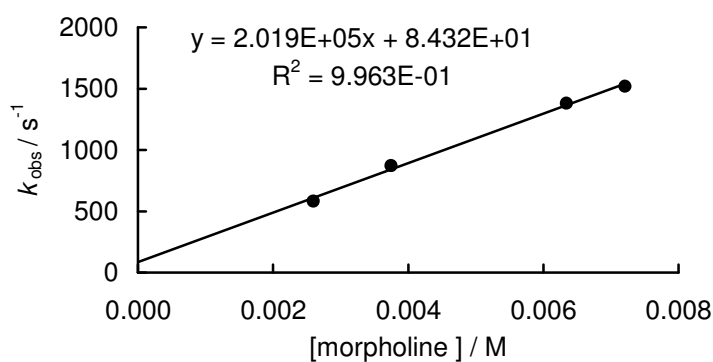
Reaction of **1d** with **2b** (DMSO, 20 °C, stopped flow, 500 nm)

[**1d**] / M	[**2b**] / M	k_{obs} / s^{-1}
2.30×10^{-5}	4.66×10^{-4}	1.95
2.30×10^{-5}	8.16×10^{-4}	3.46
2.30×10^{-5}	1.17×10^{-3}	4.97
2.30×10^{-5}	1.52×10^{-3}	6.54
2.30×10^{-5}	1.87×10^{-3}	8.04

$$k_2 = (4.36 \pm 0.02) \times 10^3 \text{ M}^{-1}\text{s}^{-1}$$
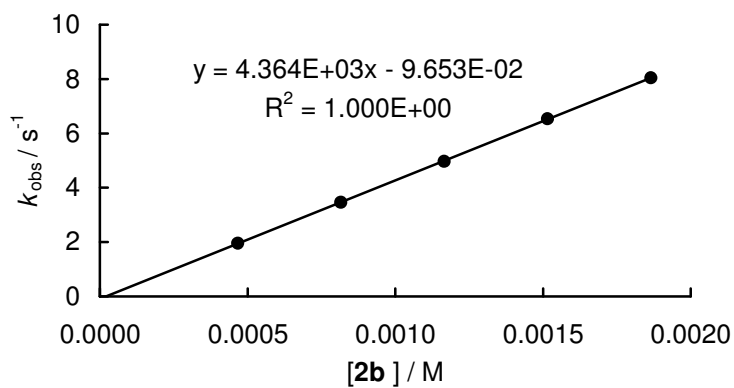
Reaction of **1d** with **2e** (DMSO, 20 °C, stopped flow, 500 nm)

[**1d**] / M	[**2e**] / M	k_{obs} / s^{-1}
2.43×10^{-5}	4.16×10^{-4}	4.59
2.43×10^{-5}	8.32×10^{-4}	8.94
2.43×10^{-5}	1.25×10^{-3}	1.42×10^{1}
2.43×10^{-5}	1.66×10^{-3}	1.93×10^{1}
2.43×10^{-5}	2.08×10^{-3}	2.38×10^{1}

$$k_2 = (1.17 \pm 0.02) \times 10^4 \text{ M}^{-1}\text{s}^{-1}$$

$y = 1.173\text{E}+04x - 4.680\text{E}-01$
$R^2 = 9.990\text{E}-01$
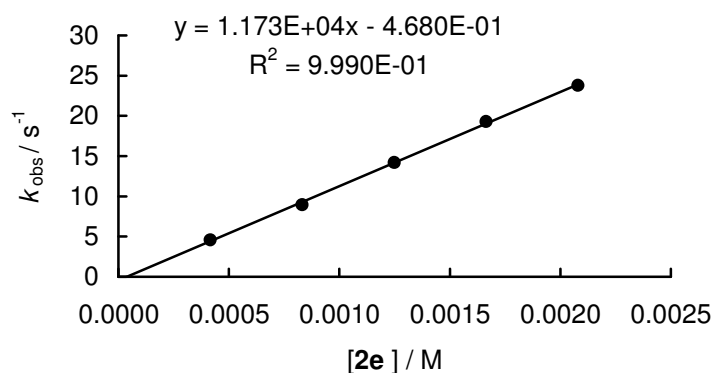
Reaction of **1d** with **2g** (DMSO, 20 °C, stopped flow, 500 nm)

[**1d**] / M	[**2g**] / M	k_{obs} / s^{-1}
4.25×10^{-5}	4.32×10^{-4}	3.21×10^{1}
4.25×10^{-5}	6.34×10^{-4}	4.81×10^{1}
4.25×10^{-5}	8.65×10^{-4}	6.45×10^{1}
4.25×10^{-5}	1.15×10^{-3}	8.65×10^{1}
4.25×10^{-5}	1.44×10^{-3}	1.07×10^{2}

$$k_2 = (7.41 \pm 0.07) \times 10^4 \text{ M}^{-1}\text{s}^{-1}$$

$y = 7.413\text{E}+04x + 5.354\text{E}-01$
$R^2 = 9.997\text{E}-01$
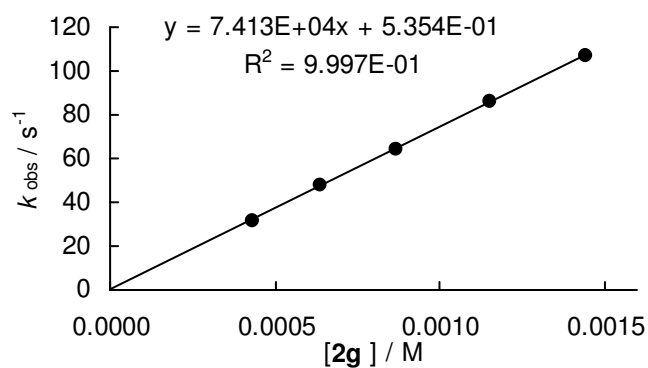
Reaction of **1d** with **2h** (DMSO, 20 °C, stopped flow, 500 nm)

[**1d**] / M	[**2h**] / M	k_{obs} / s^{-1}
5.06×10^{-5}	5.82×10^{-4}	8.64×10^{1}
5.06×10^{-5}	7.76×10^{-4}	1.16×10^{2}
5.06×10^{-5}	9.70×10^{-4}	1.44×10^{2}
5.06×10^{-5}	1.16×10^{-3}	1.83×10^{2}
5.06×10^{-5}	1.36×10^{-3}	2.12×10^{2}

$$k_2 = (1.64 \pm 0.05) \times 10^5 \ \text{M}^{-1}\text{s}^{-1}$$
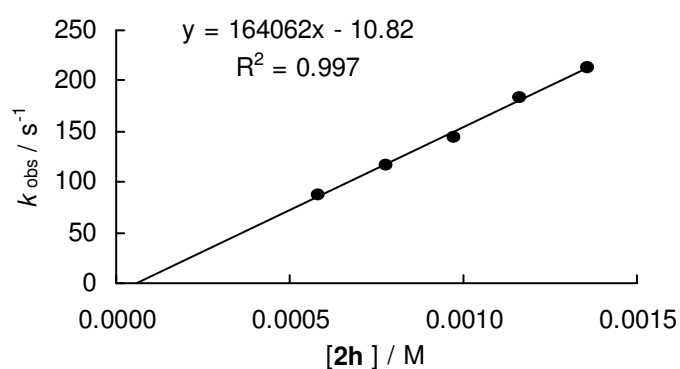
Reaction of **1d** with **2i** (DMSO, 20 °C, stopped flow, 500 nm)

[**1d**] / M	[**2i**] / M	k_{obs} / s^{-1}
4.25×10^{-5}	5.87×10^{-4}	6.04×10^{1}
4.25×10^{-5}	8.81×10^{-4}	9.37×10^{1}
4.25×10^{-5}	1.18×10^{-3}	1.24×10^{2}
4.25×10^{-5}	1.76×10^{-3}	1.86×10^{2}

$$k_2 = (1.06 \pm 0.01) \times 10^5 \ \text{M}^{-1}\text{s}^{-1}$$

49
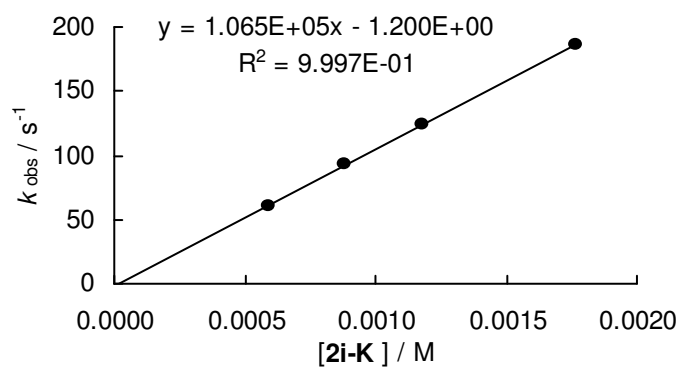
Reaction of **1d** with **2k** (DMSO, 20 °C, stopped flow, 500 nm)

[**1d**] / M	[**2k**] / M	k_{obs} / s^{-1}
2.59×10^{-5}	4.38×10^{-4}	4.95×10^{1}
2.59×10^{-5}	5.26×10^{-4}	5.80×10^{1}
2.59×10^{-5}	6.48×10^{-4}	7.27×10^{1}
2.59×10^{-5}	7.89×10^{-4}	8.99×10^{1}
2.59×10^{-5}	9.11×10^{-4}	1.02×10^{2}

$$k_2 = (1.13 \pm 0.03) \times 10^5 \ \text{M}^{-1}\text{s}^{-1}$$
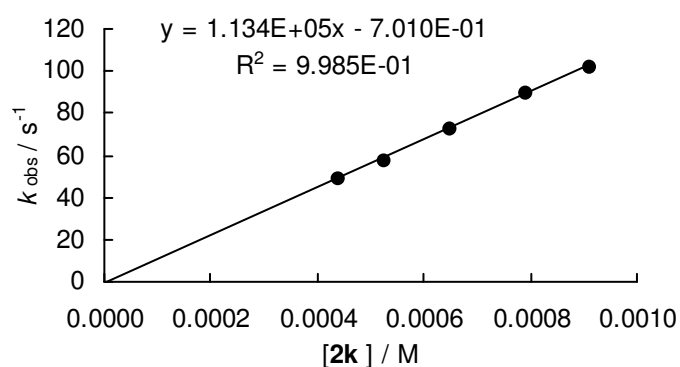
Reaction of **1e** with **2a** (DMSO, 20 °C, stopped flow, 500 nm)

[**1e**] / M	[**2a**] / M	k_{obs} / s^{-1}
3.01×10^{-5}	6.85×10^{-4}	3.26×10^{-1}
3.01×10^{-5}	1.20×10^{-3}	5.75×10^{-1}
3.01×10^{-5}	1.71×10^{-3}	8.29×10^{-1}
3.01×10^{-5}	2.23×10^{-3}	1.08
3.01×10^{-5}	2.74×10^{-3}	1.35

$$k_2 = (4.97 \pm 0.04) \times 10^2 \ \text{M}^{-1}\text{s}^{-1}$$
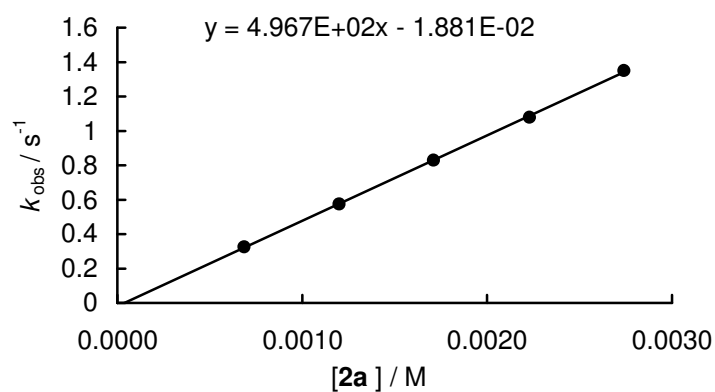
Reaction of **1e** with **2b** (DMSO, 20 °C, stopped flow, 500 nm)

[**1e**] / M	[**2b**] / M	k_{obs} / s^{-1}
2.31×10^{-5}	4.66×10^{-4}	1.42×10^{1}
2.31×10^{-5}	8.16×10^{-4}	2.71×10^{1}
2.31×10^{-5}	1.17×10^{-3}	4.05×10^{1}
2.31×10^{-5}	1.52×10^{-3}	5.31×10^{1}
2.31×10^{-5}	1.87×10^{-3}	6.62×10^{1}

$$k_2 = (3.72 \pm 0.02) \times 10^4 \text{ M}^{-1}\text{s}^{-1}$$

$y = 3.716E+04x - 3.122E+00$
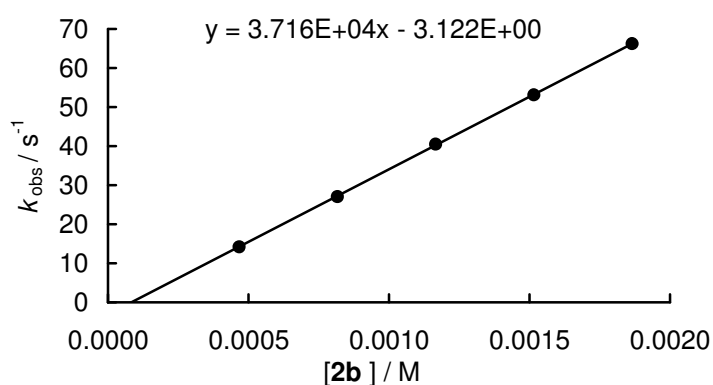
Reaction of **1e** with **2e** (DMSO, 20 °C, stopped flow, 500 nm)

[**1e**] / M	[**2e**] / M	k_{obs} / s^{-1}
2.31×10^{-5}	4.00×10^{-4}	3.88×10^{1}
2.31×10^{-5}	8.00×10^{-4}	7.86×10^{1}
2.31×10^{-5}	1.20×10^{-3}	1.19×10^{2}
2.31×10^{-5}	1.60×10^{-3}	1.62×10^{2}
2.31×10^{-5}	2.00×10^{-3}	2.04×10^{2}

$$k_2 = (1.03 \pm 0.01) \times 10^5 \text{ M}^{-1}\text{s}^{-1}$$

$y = 1.035E+05x - 3.690E+00$
$R^2 = 9.997E-01$
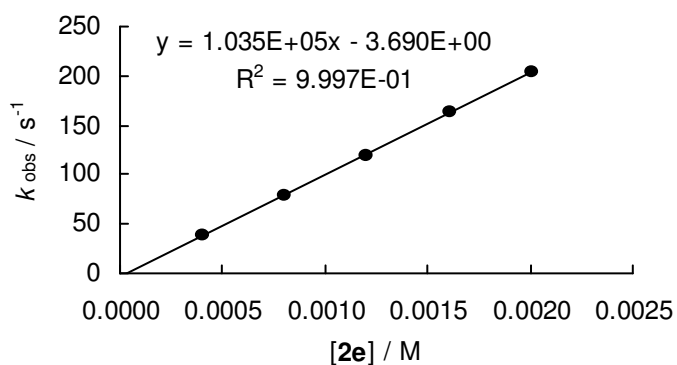
Reaction of **1e** with **2g** (DMSO, 20 °C, stopped flow, 500 nm)

[**1e**] / M	[**2g**] / M	k_{obs} / s^{-1}
2.85×10^{-5}	4.32×10^{-4}	2.04×10^{2}
2.85×10^{-5}	6.34×10^{-4}	3.25×10^{2}
2.85×10^{-5}	8.65×10^{-4}	4.13×10^{2}
2.85×10^{-5}	1.15×10^{-3}	5.56×10^{2}
2.85×10^{-5}	1.44×10^{-3}	7.09×10^{2}

$$k_2 = (4.89 \pm 0.15) \times 10^5 \text{ M}^{-1}\text{s}^{-1}$$

$$y = 4.892\text{E}+05x - 1.480\text{E}+00$$
$$R^2 = 9.971\text{E}-01$$
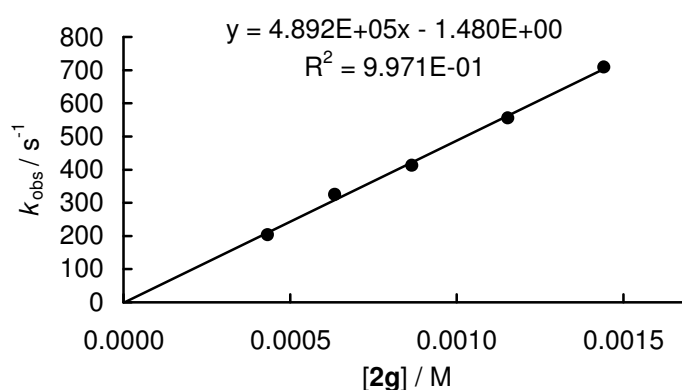
Reaction of **1e** with **2i** (DMSO, 20 °C, stopped flow, 500 nm)

[**1e**] / M	[**2i**] / M	k_{obs} / s^{-1}
2.85×10^{-5}	5.87×10^{-4}	3.63×10^{2}
2.85×10^{-5}	8.81×10^{-4}	5.78×10^{2}
2.85×10^{-5}	1.18×10^{-3}	8.19×10^{2}
2.85×10^{-5}	1.76×10^{-3}	1.23×10^{3}
2.85×10^{-5}	2.35×10^{-3}	1.60×10^{3}

$$k_2 = (7.05 \pm 0.18) \times 10^5 \text{ M}^{-1}\text{s}^{-1}$$

$$y = 7.049\text{E}+05x - 3.412\text{E}+01$$
$$R^2 = 9.980\text{E}-01$$
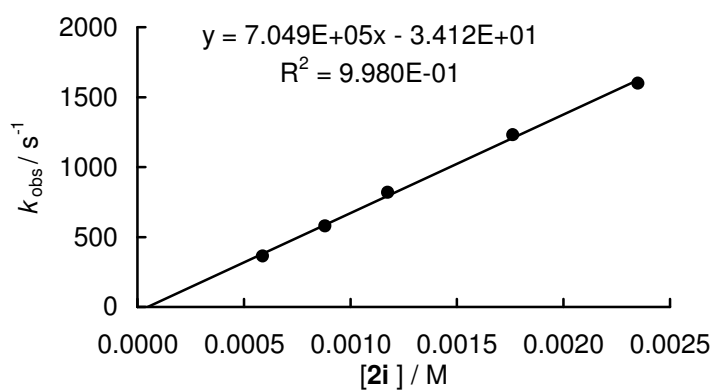
Reaction of **1e** with **2k** (DMSO, 20 °C, stopped flow, 500 nm)

[**1e**] / M	[**2k**] / M	k_{obs} / s^{-1}
3.03×10^{-5}	5.26×10^{-4}	3.39×10^{2}
3.03×10^{-5}	6.48×10^{-4}	4.15×10^{2}
3.03×10^{-5}	7.89×10^{-4}	5.00×10^{2}
3.03×10^{-5}	9.11×10^{-4}	6.01×10^{2}

$$k_2 = (6.71 \pm 0.35) \times 10^5 \text{ M}^{-1}\text{s}^{-1}$$

$$y = 6.709E{+}05x - 1.838E{+}01$$
$$R^2 = 9.947E{-}01$$
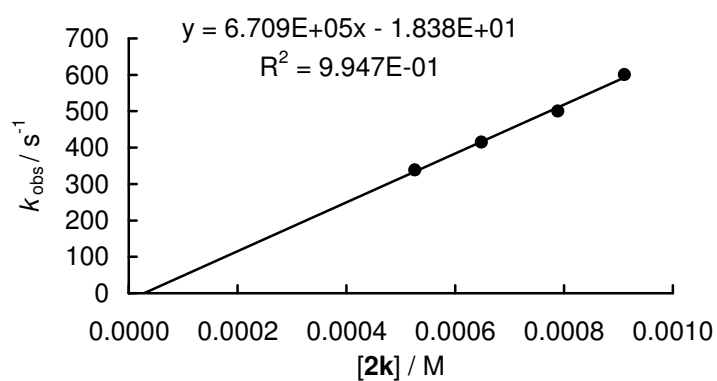
2.6 References

[1]   R. Bednar, O. E. Polansky, P. Wolschann, *Z. Naturforsch. B* **1975**, *30*, 582-586.

[2]   Review: J. T. Bojarski, J. L. Mokrosz, H. J. Barton, M. H. Paluchowska, *Adv. Heterocycl. Chem.* **1985**, *38*, 229-297.

[3]   P. Schuster, O. E. Polansky, F. Wessely, *Tetrahedron* **1966**, *Suppl. 8 (II)*, 463-483.

[4]   For a review of other electrically neutral organic Lewis acids, see: F. J. Kunz, P. Margaretha, O. E. Polansky, *Chimia* **1970**, *24*, 165-181.

[5]   For further nucleophilic reactions on aryl-substituted electrophilic olefins, see: Z. Rappoport, D. Ladkani, *Chem. Scri.* **1974**, *5*, 124-133.

[6]   R. Bednar, E. Haslinger, U. Herzig, O. E. Polansky, P. Wolschann, *Monatsh. Chem.* **1976**, *107*, 1115-1125.

[7]   B. Schreiber, H. Martinek, P. Wolschann, P. Schuster, *J. Am. Chem. Soc.* **1979**, *101*, 4708-4713.

[8]   A. N. Osman, A. A. El-Gendy, M. M. Kandeel, E. M. Ahmed, M. M. M. Hussein, *Bull. Fac. Pharm. (Cairo Univ.)* **2003**, *41*, 59-68 (*Chem. Abstr.* **2004**, *143*, 286367).

[9]   R. Cremlyn, J. P. Bassin, F. Ahmed, M. Hastings, I. Hunt, T. Mattu, *Phosphorus, Sulfur Silicon Relat. Elem.* **1992**, *73*, 161-172.

[10]   A. R. Katritzky, I. Ghiviriga, D. C. Oniciu, F. Soti, *J. Heterocyc. Chem.* **1996**, *33*, 1927-1934.

[11]   A. I. Dyachkov, B. A. Ivin, N. A. Smorygo, E. G. Sochilin, *J. Org. Chem. USSR* **1976**, *12*, 1124-1129; *Zh. Org. Khim.* **1976**, *12*, 1115-1122.

[12]   A. V. Moskvin, G. V. Kulpina, L. F. Strelkova, V. A. Gindin, B. A. Ivin, *J. Org. Chem. USSR* **1989**, *25*, 1995-2001; *Zh. Org. Khim.* **1989**, *25*, 2208-2216.

[13]   M. El Hashash, M. Mahmoud, H. El Fiky, *Rev. Roum. Chim.* **1979**, *24*, 1191-1202.

[14]   A. F. Fahmy, M. M. Mohamed, A. A. Afify, M. Y. El Kady, M. A. El Hashash, *Rev. Roum. Chim.* **1980**, *25*, 125-133.

[15]   J. D. Figueroa-Villar, C. L. Carneiro, E. R. Cruz, *Heterocycles* **1992**, *34*, 891-894.

[16]   F. M. Soliman, K. M. Khalil, *Phosphorus, Sulfur Silicon Relat. Elem.* **1987**, *29*, 165-167.

[17]   F. M. Soliman, M. M. Said, S. S. Maigali, *Heteroat. Chem.* **1997**, *8*, 157-164.

[18]   H. Allouchi, Y. Fellahi, C. Hebert, C. Courseille, Y. Frangin, *J. Heterocyclic Chem.* **2003**, *40*, 51-55.

[19]   Y. Frangin, C. Guimbal, F. Wissocq, H. Zamarlik, *Synthesis* **1986**, 1046-1050.

[20]   Y. Fellahi, P. Dubois, V. Agafonov, F. Moussa, J.-E. Ombetta-Goka, J. Guenzet, Y. Frangin, *Bull. Soc. Chim. Fr.* **1996**, *133*, 869-874.

[21]   B. S. Jursic, D. M. Neumann, *Tetrahedron Lett.* **2001**, *42*, 4103-4107.

[22]   B. S. Jursic, E. D. Stevens, *Tetrahedron Lett.* **2003**, *44*, 2203-2210.

[23]   J. W. G. Meisner, A. C. van der Laan, U. K. Pandit, *Tetrahedron Lett.* **1994**, *35*, 2757-2760.

[24]   K. Tanaka, X. Chen, T. Kimura, F. Yoneda, *Tetrahedron Lett.* **1987**, *28*, 4173-4176.

[25]   K. Tanaka, X. Chen, F. Yoneda, *Tetrahedron* **1988**, *44*, 3241-3249.

[26]   K. Tanaka, X. Chen, T. Kimura, F. Yoneda, *Chem. Pharm. Bull.* **1988**, *36*, 60-69.

[27]   K. Tanaka, X. Chen, T. Kimura, F. Yoneda, *Chem. Pharm. Bull.* **1986**, *34*, 3945-3948.

[28]   H. H. Zoorob, M. A. Elzahab, M. Abdel-Mogib, M. A. Ismail, M. Abdel-Hamid, *Arzneimittel-Forsch.* **1997**, *47(II)*, 958-962.

[29]   H. S. Thokchom, A. D. Nongmeikapam, W. S. Laitonjam, *Can. J. Chem.* **2005**, *83*, 1056-1062.

[30]   R. K. Robins, *J. Am. Chem. Soc.* **1956**, *78*, 784-790.

[31]   J. L. Scott, L. V. Foye, *Cancer Chemother. Rep.* **1962**, *20*, 73-80.

[32]   R. K. Robins, *J. Med. Chem.* **1964**, *7*, 186-199.

[33]   M. W. Sabaa, N. A. Mohamed, K. D. Khalil, A. A. Yassin, *Polym. Degrad. Stab.* **2000**, *70*, 121-133.

[34]   H. Mayr, T. Bug, M. F. Gotta, N. Hering, B. Irrgang, B. Janker, B. Kempf, R. Loos, A. R. Ofial, G. Remennikov, H. Schimmel, *J. Am. Chem. Soc.* **2001**, *123*, 9500-9512.

[35]   R. Lucius, H. Mayr, *Angew. Chem.* **2000**, *112*, 2086-2089; *Angew. Chem. Int. Ed.* **2000**, *39*, 1995-1997.

[36]   R. Lucius, R. Loos, H. Mayr, *Angew. Chem.* **2002**, *114*, 97-102; *Angew. Chem. Int. Ed.* **2002**, *41*, 91-95.

[37]   T. Lemek, H. Mayr, *J. Org. Chem.* **2003**, *68*, 6880-6886.

[38]   S. T. A. Berger, F. Seeliger, F. Hofbauer, H. Mayr, *Org. Biomol. Chem.* **2007**, *5*, 3020-3026.

[39]   S. T. A. Berger, A. R. Ofial, H. Mayr, *J. Am. Chem. Soc.* **2007**, *129*, 9753-9761.

[40]   T. Bug, T. Lemek, H. Mayr, *J. Org. Chem.* **2004**, *69*, 7565-7576.

[41]   C. F. Bernasconi, M. W. Stronach, *J. Am. Chem. Soc.* **1991**, *113*, 2222-2227.

[42]   C. F. Bernasconi, S. Fornarini, *J. Am. Chem. Soc.* **1980**, *102*, 5329-5336.

[43]   (a) C. F. Bernasconi, R. J. Ketner, *J. Org. Chem.* **1998**, *63*, 6266-6272. (b) See also: P. Margaretha, *Tetrahedron* **1972**, *28*, 83-87.

[44]   C. F. Bernasconi, *Tetrahedron* **1989**, *45*, 4017-4090 and references cited therein.

[45]   E. Haslinger, P. Wolschann, *Org. Magn. Reson.* **1977**, *9*, 1-7.

[46]   S. Patai, Z. Rappoport, *J. Chem. Soc.* **1962**, 377-382.

[47]   M. Incze, G. Dörnyei, M. Kajtar-Peredy, C. Szantay, *Synth. Commun.* **1995**, *25*, 3389-3393.

[48]   F. F. Abdel-Latif, *Ind. J. Chem. B* **1991**, *30*, 363-365.

[49]   I. Devi, B. S. D. Kumar, P. J. Bhuyan, *Tetrahedron Lett.* **2003**, *44*, 8307-8310.

[50]   A. Martinez-Grau, J. L. Marco, *Bioorg. Med. Chem. Lett.* **1997**, *7*, 3165-3170.

[51]   C. de los Rios, J. L. Marco, M. D. C. Carreiras, P. M. Chinchon, A. G. Garcia, M. Villarroya, *Bioorg. Med. Chem.* **2002**, *10*, 2077-2088.

[52]   W. K. Summers, L. V. Majovski, G. M. Marsh, K. Tachiki, A. Kling, *New Engl. J. Med.* **1986**, *315*, 1241-1245.

[53]   B. J. Sahakian, A. M. Owen, N. J. Morant, S. A. Eagger, S. Boddington, L. Crayton, H. A. Crockford, M. Crooks, K. Hill, R. Levy, *Psychopharmacology* **1993**, *110*, 395-401.

[54]   C. M. Lee, W. D. Kumler, *J. Org. Chem.* **1962**, *27*, 2052-2054.

[55]   A. Loewenstein, A. Melera, P. Rigny, W. Walter, *J. Phys. Chem.* **1964**, *68*, 1597-1598.

[56]   K. B. Wiberg, P. R. Rablen, *J. Am. Chem. Soc.* **1995**, *117*, 2201-2209.

[57]   H. Mayr, B. Kempf, A. R. Ofial, *Acc. Chem. Res.* **2003**, *36*, 66-77.

[58]   H. H. Zoorob, M. M. Abou El Zahab, M. Abdel-Mogib, M. A. Ismail, *Tetrahedron* **1996**, *52*, 10147-10158.

[59]   For an intramolecular hetero-Diels-Alder reaction of a benzylidenebarbituric acid derivative under high pressure, see: L. F. Tietze, C. Ott, K. Gerke, M. Buback, *Angew. Chem.* **1993**, *105*, 1536-1538; *Angew. Chem. Int. Ed.* **1993**, *32*, 1485-1486.

[60]   G. Dujardin, A. Martel, E. Brown, *Tetrahedron Lett.* **1998**, *39*, 8647-8650.

[61]   A. Martel, S. Leconte, G. Dujardin, E. Brown, V. Maisonneuve, R. Retoux, *Eur. J. Org. Chem.* **2002**, 514-525.

[62]   A. Palasz, *Org. Biomol. Chem.* **2005**, *3*, 3207-3212.

[63]   A. Sera, N. Ueda, K. Itoh, H. Yamada, *Heterocycles* **1996**, *43*, 2205-2214.

[64]   C. Reichardt, *Solvents and Solvent Effects in Organic Chemistry*, 3rd Ed. Wiley-VCH Weinheim, **2003**.

[65]   K. A. Krasnov, V. I. Slesarev, Z. L. Artemeva, *J. Org. Chem. USSR* **1989**, *25*, 1402-1405.

[66]   S. Minegishi, H. Mayr, *J. Am. Chem. Soc.* **2003**, *125*, 286-295.

[67]   C. F. Bernasconi, C. J. Murray, *J. Am. Chem. Soc.* **1986**, *108*, 5251-5257.

[68]   C. F. Bernasconi, M. Panda, *J. Org. Chem.* **1987**, *52*, 3042-3050.

[69]   H. K. Oh, T. S. Kim, H. W. Lee, I. Lee, *Bull. Korean Chem. Soc.* **2003**, *24*, 193-196.

[70]   H. K. Oh, I. K. Kim, D. D. Sung, I. Lee, *Org. Biomol. Chem.* **2004**, *2*, 1213-1216.

[71]   H. K. Oh, I. K. Kim, H. W. Lee, I. Lee, *J. Org. Chem.* **2004**, *69*, 3806-3810.

[72]   H. K. Oh, J. M. Lee, D. D. Sung, I. Lee, *J. Org. Chem.* **2005**, *70*, 3089-3093.

[73]   H. Mayr, A. R. Ofial, *Pure Appl. Chem.* **2005**, *77*, 1807-1821.

[74]   Y. Xu, W. R. Dolbier, *Tetrahedron* **1998**, *54*, 6319-6328.

Chapter 3

Electrophilicity Parameters for 2-Benzylidene-indan-1,3-diones – a systematic extension of the benzhydrylium based electrophilicity scale

S. T. A. Berger, F. H. Seeliger, F. Hofbauer, H. Mayr, *Org. Biomol. Chem.* **2007**, *5*, 3020-3026.

3.1 Introduction

Numerous kinetic investigations have shown that the rate constants for the reactions of carbocations with nucleophiles can be described by equation 3.1.[1-4]

$$\log k_2(20\ °C) = s(N + E) \tag{3.1}$$

Therein, k_2 corresponds to the second-order rate constant in L mol^{-1} s^{-1}, s to the nucleophile-specific slope parameter, N to the nucleophilicity parameter, and E to the electrophilicity parameter. By using diarylcarbenium ions and quinone methides as reference electrophiles,[5] it was subsequently possible to compare the reactivities of numerous σ-, n- and π-nucleophiles in a single scale.

For the characterization of many synthetically important nucleophiles, for example stabilized carbanions and amines, reference electrophiles with $-10 > E > -16$ were needed. Because this range is presently only covered by the quinone methides **1i** and **1j** (Figure 3.1), which are difficult to synthesize, we were looking for more readily accessible alternatives.

Lemek showed that equation 3.1 is also applicable to reactions of nucleophiles with ordinary Michael acceptors (e.g., benzylidenemalononitriles).[6] Therefore, we expected a similar behavior of the easily accessible 2-benzylidene-indan-1,3-diones **1a-d**, which have previously been investigated in medical and material chemistry.[7] Some derivatives show antibacterial

58

activities or nonlinear optical properties, some have been used as electroluminescent devices or as eye lens clarification agents.[7] The 2-benzylidene-indan-1,3-diones can be considered as organic Lewis acids.[8] Because of their low lying LUMOs they are reactive Michael acceptors and have been used as heterodienes in cycloaddition reactions.[9]
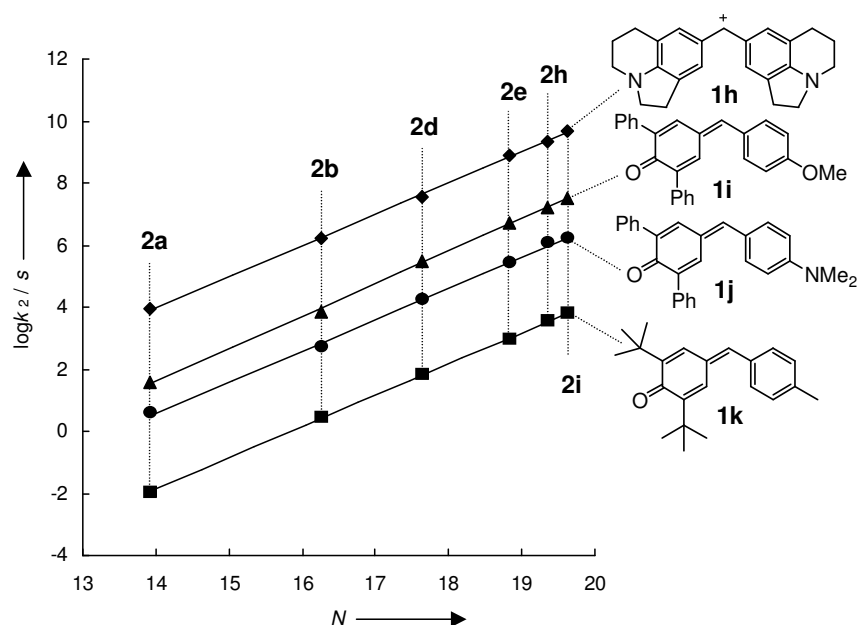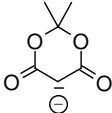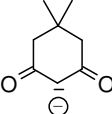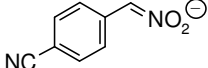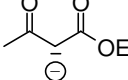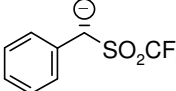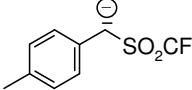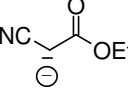
FIGURE 3.1: Correlation of (log k_2)/s with the nucleophilicity parameters N for the reactions of the diarylcarbenium ion **1h** and the quinone methides **1i-k** with carbanions **2** (DMSO, 20 °C, from ref. [5]). For structures of **2a-i** see Table 3.1.

Due to the fact that the double bonds of the 2-benzylidene-indan-1,3-diones are strongly polarized by the mesomeric electron-withdrawing effect of the carbonyl groups, the double bond is highly electrophilic and can be attacked by many nucleophiles. Zalukaevs and Anokhina showed that the reaction of 2-benzylidene-indan-1,3-dione with ethyl acetoacetate gives the corresponding Michael adduct.[10] In the reactions of 2-benzylidene-indan-1,3-diones with acetylacetone, ethyl acetoacetate, diethyl malonate, and phenylacetophenone, Michael adducts were obtained, which undergo consecutive reactions.[11] Additions of arylnitromethanes,[12] dimedone imines,[13] di- and trialkylphosphites,[14] and of phosphonium ylides[14b,c] have also been described. Recently, hydride transfer from the Hantzsch ester to a benzylidene-indan-1,3-dione derivative has been observed.[15]

We now report on the kinetics of the additions of the stabilized carbanions **2a-l** (Table 3.1) to the 2-benzylidene-indan-1,3-diones **1a-d** in DMSO and demonstrate that the second-order

rate constants k_2 can be described by equation 3.1. The results will then be compared with Bernasconi's rate constants for the reactions of 2-benzylidene-indan-1,3-dione **1d** with amines in DMSO/H$_2$O (50/50 v,v).[16]

TABLE 3.1: *N*- and *s*-parameters of the employed nucleophiles in DMSO.

nucleophile		*N*	*s*
	2a	13.91[a]	0.86[a]
	2b	16.27[a]	0.77[a]
	2c	16.96[b]	0.73[b]
	2d	17.64[a]	0.73[a]
	2e	18.82[a]	0.69[a]
	2f	18.67[c]	0.68[c]
	2g	19.35[a]	0.67[c]
	2h	19.36[a]	0.67[a]
	2i	19.62[a]	0.67[a]
	2j	20.61[b]	0.69[b]
	2k	20.71[b]	0.60[b]
	2l	21.54[b]	0.62[b]

[a] From ref. [5]. [b] From ref. [17]. [c] From ref. [18].

3.2 Results and Discussion

3.2.1 Preparation of the Electrophiles *1a-d*

The 2-benzylidene-indan-1,3-diones **1a-d** were synthesized by Knoevenagel condensation from indan-1,3-dione and substituted benzaldehydes in the presence of catalytic amounts of piperidine in boiling ethanol (Scheme 3.1).[19]
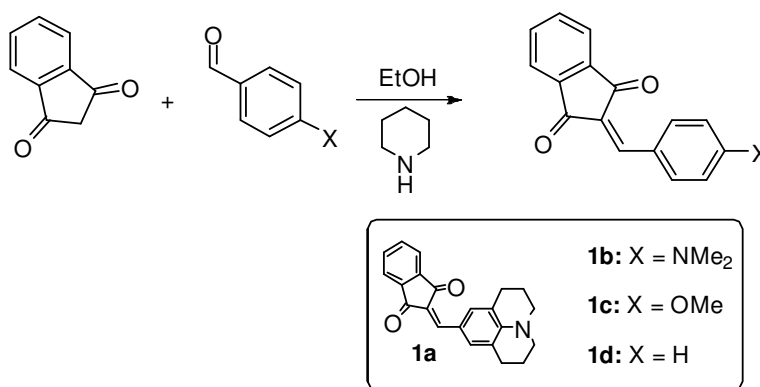
SCHEME 3.1: Preparation of the 2-benzylidene-indan-1,3-diones via Knoevenagel condensation.

3.2.2 Reaction Products

The anionic adducts **3⁻** obtained by mixing equimolar amounts of the Michael acceptors **1** and the potassium salts of the carbanions **2** in d_6-DMSO solutions were investigated by NMR spectroscopy. In few cases the products **3** obtained after protonation of **3⁻** were isolated and characterized (Scheme 3.2). Because other combinations of the electrophiles **1a-d** with the nucleophiles **2a-l** were expected to yield analogous reaction products, these have not been identified for all combinations, which were studied kinetically (Table 3.2).
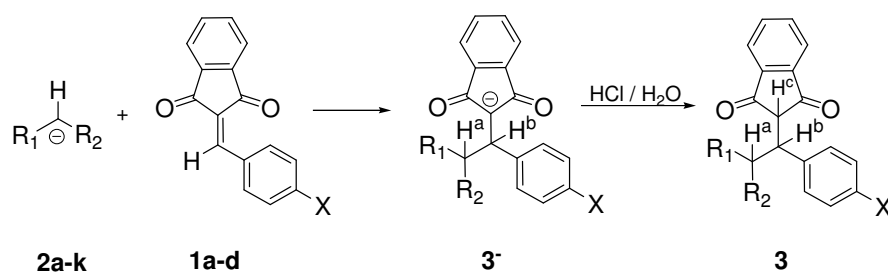
SCHEME 3.2: Reactions of the potassium salts of the carbanions **2a-k** with the 2-benzylidene-indan-1,3-diones **1a-d** in DMSO.

61

All Michael adducts 3^- and 3 show characteristic ^{1}H-NMR spectra with H^a and H^b as doublets from $\delta = 5.03-5.85$ ppm for H^a and $\delta = 3.98-4.40$ ppm for H^b. The double set of signals for product $3al$ indicates its existence as a pair of diastereomers (2:1).

TABLE 3.2: Characterized Michael adducts 3^- or 3 and some characteristic ^{1}H-NMR chemical shifts and coupling constants.

reactants		adducts	$\delta(H^a)$/ppm	$\delta(H^b)$/ppm	J / Hz
1a	2d	3ad$^-$	5.23	4.16	12.4
1a	2h	3ah$^-$	5.76	3.98	11.6
1a	2l	3al	ds[a]	ds[a]	ds[a]
1b	2h	3bh$^-$	5.81	4.17	11.3
1b	2k	3bk	5.03/5.31[b]	4.33[b]	[b]
1c	2d	3cd$^-$	5.28	4.34	12.3
1c	2h	3ch$^-$	5.85	4.24	11.4
1d	2d	3dd$^-$	5.35	4.40	12.3

[a] Diastereomers, double sets of signals in the ratio 2:1 have been found. [b] $\delta = 4.33$ (dt, $^3J = 7.7$ Hz, $^3J = 3.9$ Hz, 1H), 5.03 (dd, $^2J = 13.3$ Hz, $^3J = 7.4$ Hz, 1H), 5.31 (dd, $^2J = 13.3$ Hz, $^3J = 8.5$ Hz, 1H).

3.2.3 Kinetic Investigations in DMSO

The kinetic investigations were performed at 20 °C in DMSO by using the stopped-flow technique. All reactions reported in this chapter proceeded quantitatively, and the second-order rate constants k_2 (Table 3.3) were determined photometrically by monitoring the decrease of the absorbances of the colored electrophiles $1a$-d at their absorption maxima. The carbanions $2a$-l were either employed as potassium salts or were freshly generated by deprotonation of the corresponding CH acids with 1.05 equivalents of KO^{t}Bu. In general, the carbanions were applied in high excess over the electrophiles (10 to 100 equivalents), giving rise to almost constant carbanion concentrations (10^{-3} to 10^{-4} mol L^{-1}) during the kinetic measurements. In consequence, mono-exponential decays of the concentrations of the colored electrophiles were observed (equation 3.2). The first-order rate constants $k_{1\Psi}$ were obtained by least-squares fitting of the single-exponentials $A_t = A_0 \exp(-k_{1\Psi}t) + C$ to the time-dependent absorbances A of the electrophiles.

$$-\mathrm{d}[\mathbf{1}]/\mathrm{d}t = k_{1\Psi}[\mathbf{1}] \qquad (3.2)$$
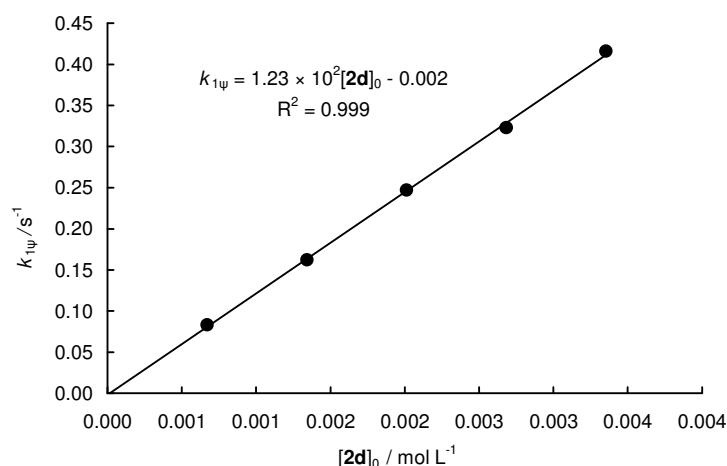
FIGURE 3.2: Determination of the second-order rate constant $k_2 = 123$ L mol^{-1}s^{-1} for the reaction of **1a** with the potassium salt of acetylacetone **2d** in DMSO at 20 °C.

Plots of $k_{1\Psi}$ versus the nucleophile concentrations $[2]_0$ give straight lines with the slopes k_2 as shown for one example in Figure 3.2 and for other kinetic experiments in the Experimental Section. In some cases the $k_{1\Psi}$ versus $[2]_0$ correlations do not go through the origin. Because all reactions proceed with quantitative formation of the adducts, we cannot presently explain this phenomenon. All second-order rate constants k_2 (L mol^{-1} s^{-1}) for the Michael additions are listed in Table 3.3.

TABLE 3.3: Second-order rate constants k_2 for the reactions of 2-benzylidene-indan-1,3-diones **1a**-**d** with stabilized carbanions **2a**-**l** in DMSO at 20 °C.
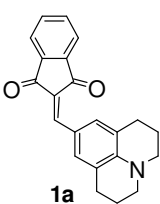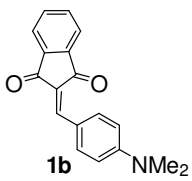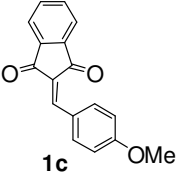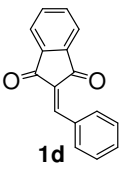
electrophile	C$^-$	base	k_2 / M^{-1}s^{-1}
	2b	-[a]	3.78×10^1
	2c	KO^{t}Bu	3.73×10^1
	2d	-[a]	1.23×10^2
	2e	-[a]	9.87×10^2
	2f	KO^{t}Bu	3.12×10^2
1a	**2h**	-[a]	1.27×10^3
	2i	KO^{t}Bu	1.86×10^3
$E = -14.68$[b]	**2j**	KO^{t}Bu	1.94×10^3
$\lambda_{max} = 523$ nm	**2k**	KO^{t}Bu	3.31×10^3
	2l	KO^{t}Bu	4.32×10^3

63

TABLE 3.3: Continued.

electrophile	C$^-$	base	k_2 / M^{-1}s^{-1}
	2b	-[a]	2.79×10^2
	2c	KO^{t}Bu	2.08×10^2
	2d	-[a]	8.86×10^2
1b	**2e**	-[a]	6.25×10^3
	2f	KO^{t}Bu	2.15×10^3
	2h	-[a]	8.17×10^3
$E = -13.56$[b]	**2i**	-[a]	1.00×10^4
$\lambda_{max} = 493$ nm	**2j**	KO^{t}Bu	6.86×10^3
	2k	KO^{t}Bu	1.32×10^4
	2b	-[a]	1.80×10^4
1c	**2d**	-[a]	3.87×10^4
	2f	KO^{t}Bu	5.69×10^4
	2g	KO^{t}Bu	1.18×10^5
$E = -11.32$[b]	**2h**	-[a]	2.07×10^5
$\lambda_{max} = 388$ nm			
	2a	-[a]	1.06×10^3
1d	**2b**	-[a]	1.06×10^5
	2d	-[a]	2.72×10^5
$E = -10.11$[b]			
$\lambda_{max} = 343$ nm[c]			

[a] Carbanion was employed as potassium salt. [b] Derived from equation 3.1. [c] λ_{max}(DMSO/H$_2$O 50/50, v/v) = 343 nm, from ref. [20].

3.2.4 Correlation Analysis

If equation 3.1 holds for the reactions of the 2-benzylidene-indan-1,3-diones **1a-d** with the carbanions **2a-l**, plots of (log k_2)/s vs. N should be linear with slopes of 1. Figure 3.3 shows that this is approximately the case. The correlation lines, drawn in Figure 3.3, result from a least-squares fit of calculated and experimental rate constants (minimization of $\Delta^2 = \Sigma(\log k_2 - s(N + E))^2$ with the nonlinear solver What's Best! by Lindo Systems Inc.) using the second-order rate constants k_2, given in Table 3.3, and the N and s parameters of **2a-l** listed in Table 3.1. Note that this procedure enforces slopes of 1 for plots of (log k_2)/s vs. N because equation 3.1 does not include an electrophile-specific slope parameter, in contrast

to a more general equation, which we have recently employed for S_N2 reactions.[21] The nitronate anions **2j** and **2l** strongly deviate from the correlations for the other nucleophiles and have not been included in the minimization process. According to equation 3.1, the intercepts on the *y*-axis, which equal the negative intercepts on the *x*-axis (because of the enforced unity slopes), correspond to the electrophilicity parameters *E*.
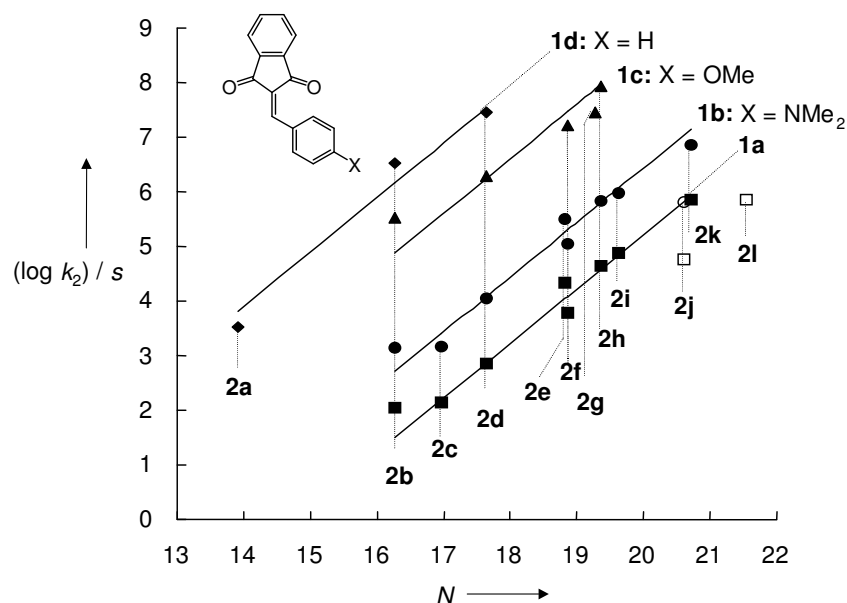
FIGURE 3.3: Correlation of (log k_2)/*s* versus the corresponding nucleophilicity parameters *N* of the carbanions **2a-l** for the reactions of 2-benzylidene-indan-1,3-diones **1a-d** with carbanions **2a-l** in DMSO at 20 °C. Open symbols were not included for the calculation of the correlation lines.

While the correlations in Figure 3.3 are only of moderate quality, one can see that the relative electrophilicities of the 2-benzylidene-indan-1,3-diones **1** are almost independent of the nature of the carbanionic reaction partner. However, there seem to be some regularities of the deviations concerning some of the carbanions. Thus, the 2-nitroisopropyl anion **2j** reacts approximately one order of magnitude more slowly with **1a** and **1b** than expected from its nucleophilicity parameters. Because **2j** is the only trisubstituted carbanion studied, this deviation may be a consequence of steric effects due to the fact that the 2-benzylidene-1,3-indandiones **1** are sterically more congested than the reference diarylcarbenium ions. On the other hand, the dimedone anion **2b** is generally 2-times more reactive than expected, and it cannot be due to a smaller steric demand of this carbanion, because the analogously shaped anion of Meldrum's acid **2a** deviates slightly in the other direction.
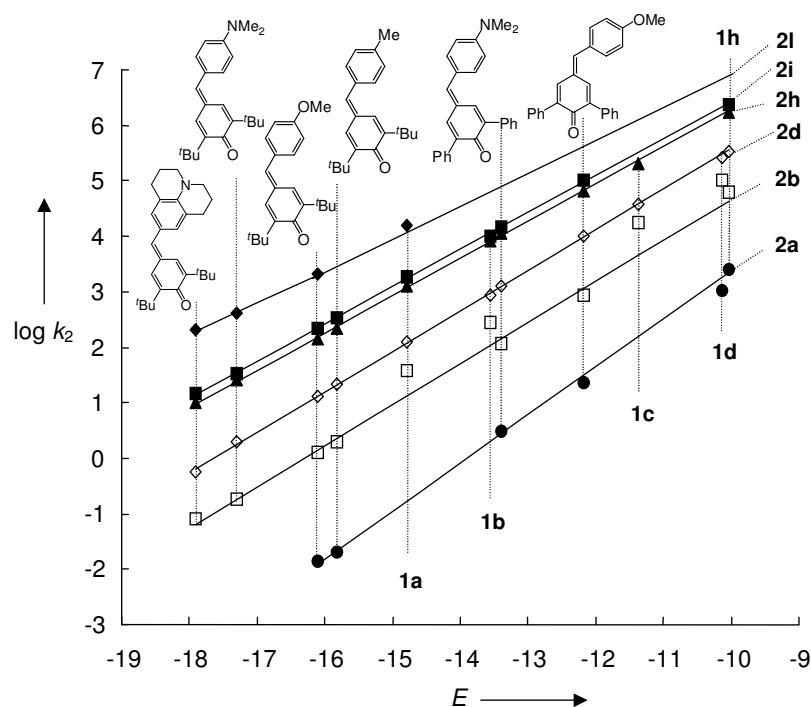
FIGURE 3.4: Rate constants for the reactions of carbanions with the 2-benzylidene-indan-1,3-diones **1a-d** and with reference electrophiles (quinone methides and diarylcarbenium ions) in DMSO at 20 °C. The rate constants of the reactions with **1a-d** were not used for the construction of the regression lines.

An alternative illustration of this behavior is shown in Figure 3.4. When the rate constants of the reactions of the carbanions **2** with electrophiles are plotted against the E parameters given in ref. [2e] and [5], all data points for the carbanions **2a**, **2d**, **2h**, **2i**, and **2l** follow good correlations. In contrast, the data points for the reactions of dimedone anion **2b** with Michael acceptors **1a-d** are located above the correlation line for the reference electrophiles, which are depicted in the upper part of Figure 3.4.
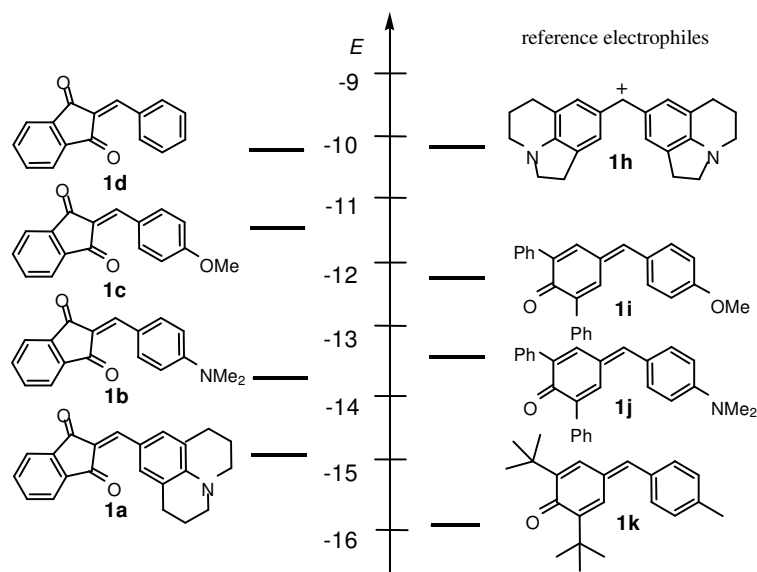
FIGURE 3.5: Comparison of the electrophilicity parameters E of 2-benzylidene-indan-1,3-diones **1a-d** with reference electrophiles **1h-k**.

According to Figure 3.5, the electrophilicities of the 2-benzylidene-indan-1,3-diones **1a-d** cover a range of more than four orders of magnitude and are located between **1h**, the least reactive representative of our series of reference diarylcarbenium ions and the most reactive representative of the series of di-*tert*-butyl substituted quinone methides (**1k**) that have been used as reference electrophiles.[5] Donor substituents on the phenyl ring lower the electrophilicity, as shown by the linear correlation with Hammett's σ_{p^+} constants (Figure 3.6).[2e], [22] For nucleophiles with $s = 0.7$, the slope corresponds to a Hammett reaction constant of $\rho = 1.6$. A comparison with the corresponding values for the structurally related benzylidenemalononitriles **1e-g** (**1e**: X = NMe$_2$; **1f**: X = OMe, **1g**: X = H) indicates that the electrophilicities of these two types of Michael acceptors are affected by para substituents X in a similar way.

67
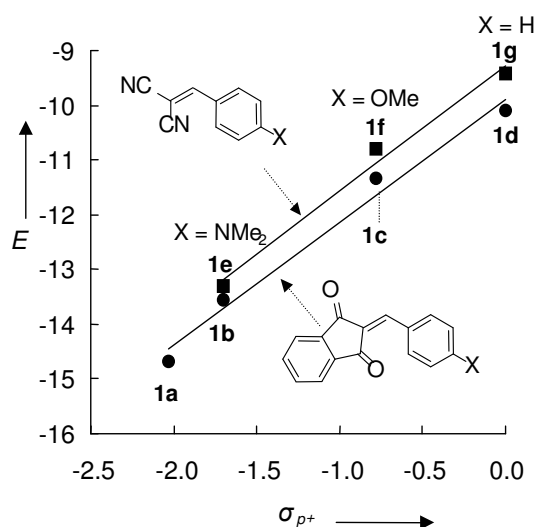
FIGURE 3.6: Correlation between the electrophilicity parameters E in DMSO of the benzylidene-indan-1,3-diones **1a-d** (circles, $E = 2.34\sigma_{p+} - 9.78$) and the benzylidene-malononitriles **1e-g** (squares, $E = 2.30\sigma_{p+} - 9.28$) with the Hammett σ_{p+} values for X. (σ_{p+} values taken from ref. [22]; σ_{p+} for **1a** taken from ref. [2e]).

However, the benzylidenemalononitriles **1e**-**g** are about 0.5 orders of magnitude more reactive than the analogously substituted 2-benzylidene-indan-1,3-diones **1b-d**. This reactivity order is surprising because indan-1,3-dione, (pK_a = 6.35−7.82 in DMSO/H$_2$O, v/v= 90/10 to 10/90)[23] is much more acidic than malononitrile ($pK_{a\ (DMSO)}$ = 11.1, $pK_{a\ (H2O)}$ = 11.2).[24], [25]

Assuming that the stabilization of the carbanions obtained by the addition of nucleophiles to 2-benzylidene-indan-1,3-diones **1a-d** and benzylidenemalononitriles **1e-g** corresponds to these pK_a values, one would expect that nucleophilic additions to **1a-d** have a higher thermodynamic driving force than the nucleophilic additions to the analogously substituted malononitriles **1e-g**. If ground-state effects are neglected, the higher reactivities of compounds **1e-g** compared to analogously substituted 2-benzylidene-indan-1,3-diones **1b-d** must, therefore, be due to lower intrinsic barriers for the additions to **1e-g**. This conclusion has previously been drawn by Bernasconi from a related series of experiments.[20b], [26]

In order to examine the applicability of the electrophilicity parameters E of the 2-benzylidene-indan-1,3-diones **1** for their reactions with other types of nucleophiles, we have compared experimental and calculated rate constants for the reactions of **1d** with amines (Table 3.4).

TABLE 3.4: Comparison of calculated and experimental second-order rate constants ($L\ mol^{-1}\ s^{-1}$, DMSO, 20 °C) for the additions of amines to 2-benzylidene-indan-1,3-dione **1d**.

	nucleophile	N/s [a]	$k_{2,calc}$ (eq. 3.1)	$k_{2,exp}$
1	piperidine	17.19/0.71	1.02×10^5	3.01×10^5 [b]
				2.10×10^5 [c]
2	morpholine	16.96/0.67	3.77×10^4	1.11×10^5 [b]
				6.30×10^4 [c]
3	n-propylamine	15.70/0.64	3.63×10^3	9.34×10^3 [c], [d]

[a] In DMSO, from ref. [4f]. [b] In DMSO, this work. [c] In DMSO/H_2O (50/50 v,v), from ref. [16]. [d] The experimental value $k_{2,exp}$ refers to the reaction of **1d** with n-butylamine.

Entries 1 and 2 in Table 3.4 indicate that the experimental second-order rate constants $k_{2,exp}$ for the addition of piperidine and morpholine to 2-benzylidene-indan-1,3-dione **1d** in DMSO are about three times larger than the corresponding second-order rate constants $k_{2,calc}$ calculated by equation 3.1. This agreement is within the previously postulated reliability of equation 3.1.

Because the experimental second-order rate constants $k_{2,exp}$ in DMSO are only about 1.5 to 2 times larger than the corresponding $k_{2,exp}$ in DMSO/H_2O (50/50 v,v, Table 3.4, right column), we can also compare the calculated second-order rate constants derived from the nucleophilicity parameters N and s of amines in DMSO with Bernasconi's experimental values in DMSO/H_2O (50/50 v,v).[16] Entry 3 in Table 3.4 confirms this conclusion and shows that the calculated rate constant for the addition of n-propylamine to **1d** agrees with the experimental rate constant for the addition of n-butylamine to **1d** in DMSO/H_2O (50/50 v,v) within a factor of 3.

On the other hand, the rates of the reactions of **1d** with amines in DMSO are similar to the rates in DMSO/H_2O (50/50 v,v). This is surprising because it is well known that amine nucleophilicities derived from reactions with diarylcarbenium ions are considerably lower in water than in DMSO (Table 3.5).

In line with previously reported rate constants for reactions of amines with diarylcarbenium ions in DMSO[4f] and water,[4a] we have now found that piperidine reacts 32−52 times faster

with diarylcarbenium ions **1h-n** (Scheme 3.3) in DMSO than in DMSO/H$_2$O (50/50 v,v) as shown in Table 3.5.
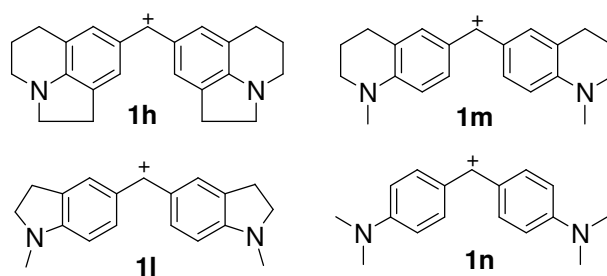
SCHEME 3.3: Diarylcarbenium ions used for the comparison of the nucleophilicities of piperidine in different solvents.

TABLE 3.5: Second-order rate constants k_2 for the reactions of piperidine with reference diarylcarbenium ions Ar$_2$CH$^+$ in DMSO, DMSO/water (50/50 v,v), and water at 20 °C.

Ar$_2$CH$^+$	E[a]	k_2 / L mol^{-1} s^{-1}		
		in DMSO[b]	in DMSO/H$_2$O (50/50)[c]	in H$_2$O[d]
1h	−10.04	1.13×10^5	2.92×10^3	3.05×10^3
1l	−8.76	6.67×10^5	2.06×10^4	9.01×10^3
1m	−8.22	2.51×10^6	4.78×10^4	2.64×10^4
1n	−7.02	-	3.15×10^5	6.09×10^4

[a] From ref. [2e]. [b] From ref. [4f]. [c] This work. [d] From ref. [4a].

Therefore, the question arises whether the similar rate of addition of piperidine and morpholine to the Michael acceptor **1d** in DMSO and DMSO/H$_2$O (50/50 v,v) is caused by an increase of the electrophilicity of **1d** in the presence of water.

In order to examine this question, we have compared the rates of addition of the malononitrile anion **2h** to **1a**, **1b**, and the diarylcarbenium ion **1h** in DMSO and in aqueous solvents. The carbanion **2h** has been selected for this purpose because its solvation has been reported to be of similar magnitude in DMSO and water.[5], [27] Table 3.6 shows that the reaction of **2h** with **1a** and **1b** is, indeed, 3−5 times faster in DMSO/H$_2$O (50/50 v,v) than in DMSO, whereas the reaction of this carbanion with the diarylcarbenium ion **1h** is 12-times slower in water than in pure DMSO.

TABLE 3.6: Comparison of the second-order rate constants of the reactions of malononitrile anion **2h** with Michael acceptors **1a** and **1b** and the diarylcarbenium ion **1h** in different solvents at 20°C.

electrophile	k_2 / L mol^{-1} s^{-1}		
	in DMSO	in DMSO/H$_2$O (50/50)	in H$_2$O
1a	1.27×10^3	6.39×10^3	-
1b	8.17×10^3	2.28×10^4	-
(lil)$_2$CH$^+$ (**1h**)	$1.76 \times 10^{6[a]}$	-	$1.50 \times 10^{5[b]}$

[a] From ref. [5]. [b] From ref. [27].

Thus, the presence of 50 % water in DMSO appears to increase the electrophilicities of the 2-benzylidene-1,3-indandiones **1a,b** (compared with diarylcarbenium ion **1h** as a reference) by approximately one order of magnitude. The observed similar reactivities of amines towards **1** in DMSO and DMSO/H$_2$O (50/50 v,v) can therefore be explained by a compensation effect, i.e., hydration of amines reduces their nucleophilicities by a similar amount as hydration increases the electrophilicities of the Michael acceptors **1**.
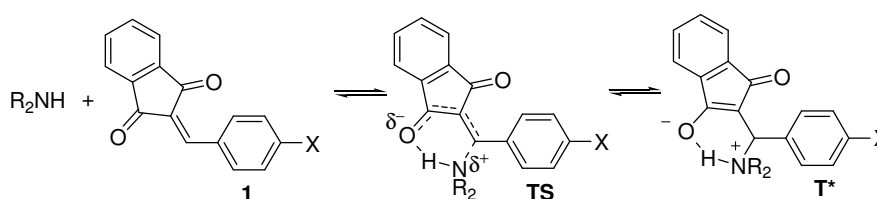
SCHEME 3.4: Addition of an amine nucleophile to 2-benzylidene-1,3-indandione 1 (TS: transition state, T*: zwitterionic intermediate).

A more quantitative analysis of these data appears problematic, because Bernasconi[16], [28] and Lee[29] have previously suggested that the transition states of the amine additions may also be stabilized by O-H interactions as depicted in Scheme 3.4. Because the additions of carbanions to **1a-d**, which are described in Table 3.3, cannot profit from such O-H interactions, the good agreement between calculated and experimental rate constants in Table 3.4 indicates that there is no large contribution of these interactions.

71

3.3 Conclusion

It was shown that the 2-benzylidene-indan-1,3-diones **1a-d** have electrophilicity parameters in the range of $-10 > E > -15$. With these data and the previously published nucleophilicity parameters of carbanions and amines,[30] it is now possible to calculate the rates of additions of these nucleophiles to 2-benzylidene-indan-1,3-diones **1a-d** with an accuracy even better than a factor of 3 in dimethyl sulfoxide solution. Because hydration appears to increase the electrophilicities of **1a-d** much more than it affects the electrophilicities of the previously used reference electrophiles (diarylcarbenium ions and quinone methides), we recommend to use the E parameters of 2-benzylidene-1-3-indandiones **1a-d** reported in this work only for predictions of rate constants in aprotic solvents.

3.4 Experimental Section

3.4.1 General Comments

DMSO with less than 50 ppm of H_2O was purchased. Stock solutions of KO^tBu were prepared by dissolving the corresponding alkoxide salt in DMSO under a nitrogen atmosphere. The 2-benzylidene-indan-1,3-diones **1a-d** were prepared according to a literature procedure:[19]

A solution of indan-1,3-dione (10 mmol) and the corresponding benzaldehyde (10 mmol) in absolute ethanol was treated with a few drops of piperidine and refluxed for 1 h, until the product precipitated. It was filtered off and after recrystallization from ethanol products **1a-d** were obtained with 80-90 % yield. ^{1}H- and ^{13}C-NMR data are in agreement with the literature values.

^{1}H- and ^{13}C-NMR spectra were recorded on a Bruker AMX 400 (400 MHz, 100 MHz) and on a Bruker ARX 300 (300 MHz, 75 MHz) and a Varian Mercury 200 (200 MHz). Chemical shifts are expressed in ppm and refer to d_6-DMSO (δ_H = 2.49 ppm, δ_C = 39.7 ppm) or to $CDCl_3$ (δ_H = 7.26 ppm, δ_C = 77.00 ppm).

3.4.2 Products of the Reactions of 2-Benzylidene-indan-1,3-dione (*1*) with Carbanions *2*

If nothing else is quoted, the reactions were performed as NMR-experiments at room temperature. Thus, 1 equiv. of the carbanion **2** (~ 0.1 mmol) was added to 1 equiv. of 2-benzylidene-indan-1,3-dione **1** (~ 0.1 mmol) in d_6-DMSO (0.7 mL). For a better intermixture of the compounds the NMR tube was put into an ultrasonic bath for 5 min. In all other cases the conditions for the reactions were not optimized for high yields. They are described subsequently.

The experiments were performed by me; the evaluations were done by Stefan Berger.

Reaction of **1a** with **2d**
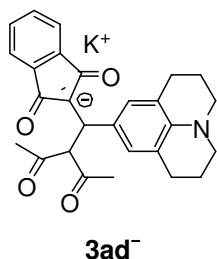
3ad: ^{1}H-NMR (d_6-DMSO, 200 MHz): δ = 1.80 (quint, ^3J = 5.0 Hz, 4H), 1.91 (s, 3H), 2.02 (s, 3H), 2.57 (t, ^3J = 6.4 Hz, 4H), 2.96 (t, ^3J = 5.2 Hz, 4H), 4.16 (d, ^3J = 12.4 Hz, 1H), 5.23 (d, ^3J = 12.4 Hz, 1H), 6.75 (s, 2H), 6.88 (dd, ^3J = 5.0 Hz, ^4J = 3.0 Hz, 2H), 7.08 (dd, ^3J = 5.0 Hz, ^4J = 3.0 Hz, 2H).

Reaction of **1a** with **2h**
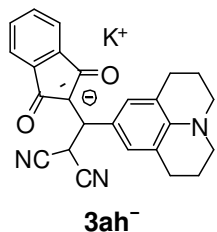
3ah: ^{1}H-NMR (d_6-DMSO, 200 MHz): δ = 1.82 (quint, ^3J = 5.2 Hz, 4H), 2.60 (t, ^3J = 6.4 Hz, 4H), 3.02 (t, ^3J = 5.4 Hz, 4H), 3.98 (d, ^3J = 11.6 Hz, 1H), 5.76 (d, ^3J = 11.6 Hz, 1H), 6.82 (s, 2H), 7.01 (dd, ^3J = 5.1 Hz, ^4J = 3.0 Hz, 2H), 7.18 (dd, ^3J = 5.1 Hz, ^4J = 3.0 Hz, 2H).

Reaction of **1a** with **2l**

At room temperature nitroethane **2l-H** (90 µL, 1.3 mmol) was added to a stirred solution of freshly sublimated KO^{t}Bu (137 mg, 1.22 mmol) in DMSO (5 mL). After stirring 2 min, **1a** was added (304 mg, 0.924 mmol) and a red clear solution was obtained. After 10 min HCl conc. (1.5 mL) was added, the mixture was poured into water (50 mL), and a purple precipitate was formed. The solvent was removed, and the crude product was dried in the vacuum. Recrystallization from ethanol gave **3al** (227 mg, 61 %), which was obtained as a mixture of diastereomers in the ratio 2:1.
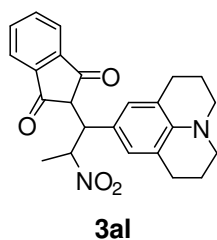
3al: ^{1}H-NMR (CDCl$_3$, 300 MHz): major product: δ = 1.72 − 1.86 (m, 7H), 2.39–2.62 (m, 4H), 2.92 (t, ^3J = 6.0 Hz, 4H), 3.34 (d, ^3J = 4.1 Hz, 1H), 3.88 (dd, ^3J = 11.4 Hz, ^4J = 4.1 Hz, 1H), 5.63–5.75 (m, 1H), 6.43 (s, 2H), 7.72–7.91 (m, 4H); minor product: δ = 1.39 (d, ^3J = 6.9 Hz, 3H), 1.72–1.86 (m, 4H), 2.39–2.62 (m, 4H), 3.01 (t, ^3J = 5.7 Hz, 4H), 3.20 (d, ^3J = 3.6 Hz, 1H), 3.79 (dd, ^3J = 11.4 Hz, ^4J = 3.6 Hz, 1H), 5.63−5.75 (m, 1H), 6.49 (s, 2H), 7.72–7.91 (m, 4H).

^{13}C-NMR (CDCl$_3$, 75 MHz): major product: δ = 19.1, 21.8, 27.4, 48.1, 49.7, 54.7, 85.3, 121.2, 121.5, 122.9, 123.2, 127.1, 135.4, 142.7, 198.1, 199.9. minor product: δ = 19.3, 21.6, 27.5, 47.9, 49.7, 55.6, 84.0, 121.5, 121.6, 122.8, 123.3, 127.6, 135.6, 142.3, 198.0, 199.4.

Reaction of **1b** with **2h**
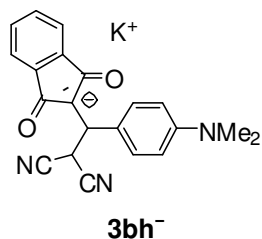
3bh: ^{1}H-NMR (d_6-DMSO, 400 MHz): δ = 2.85 (s, 6H), 4.17 (d, ^3J = 11.3 Hz, 1H), 5.81 (d, ^3J = 11.3 Hz, 1H), 6.62 (d, ^3J = 8.8 Hz, 2H), 7.05 (dd, ^3J = 5.0 Hz, ^4J = 3.0 Hz, 2H), 7.18 (dd, ^3J = 5.1 Hz, ^4J = 3.0 Hz, 2H), 7.35 (d, ^3J = 8.8 Hz, 2H). ^{13}C-NMR (d_6-DMSO, 100 MHz): δ = 26.4, 39.9, 42.2, 101.6, 111.9, 114.6, 116.3, 128.4, 128.5, 129.5, 140.1, 149.2, 187.6.

Reaction of **1b** with **2k**

At room temperature nitromethane **2k**-**H** (80 μL, 1.5 mmol) was added to a stirred solution of freshly sublimated KO^{t}Bu (167 mg, 1.49 mmol) in DMSO (5 mL). After addition of **1b** (336 mg, 1.21 mmol), the red solution was stirred for 10 min. The mixture was diluted with conc. HCl (1.5 mL) and water (50 mL). The yellow suspension was extracted with EtOAc (3 × 50 mL), and the organic layer was separated and dried over MgSO$_4$. The solvent was removed, and the crude orange product was dried in the vacuum. Recrystallization from ethanol yielded **3bk** (325 mg, 79 %) as an enantiomeric mixture.
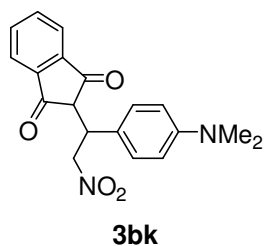
3bk: ^{1}H-NMR (CDCl$_3$, 300 MHz): δ = 2.81 (s, 6H), 3.39 (d, ^3J = 3.8 Hz, 1H), 4.33 (dt, ^3J = 7.7 Hz, ^3J = 3.9 Hz, 1H), 5.03 (dd, ^2J = 13.3 Hz, ^3J = 7.4 Hz, 1H), 5.31 (dd, ^2J = 13.3 Hz, ^3J = 8.5 Hz, 1H), 6.46 (d, ^3J = 9.0 Hz, 2H), 7.00 (d, ^3J = 9.0 Hz, 2H), 7.71–7.91 (m, 4H). ^{13}C-NMR (CDCl$_3$, 75 MHz): δ = 40.4, 41.7, 55.8, 77.0, 112.6, 122.6, 123.3, 123.5, 129.4, 135.9, 135.9, 142.7, 150.2, 198.1, 199.7.

Reaction of **1c** with **2d**
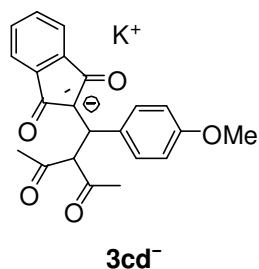
3cd: ^{1}H-NMR (d_6-DMSO, 200 MHz): δ = 1.87 (s, 3H), 2.07 (s, 3H), 3.66 (s, 3H), 4.34 (d, ^3J = 12.2 Hz, 1H), 5.28 (d, ^3J = 12.2 Hz, 1H), 6.71 (d, ^3J = 8.4 Hz, 2H), 6.92 (dd, ^3J = 4.8 Hz, ^4J = 3.0 Hz, 2H), 7.11 (dd, ^3J = 4.8 Hz, ^4J = 3.0 Hz, 2H), 7.37 (d, ^3J = 8.6 Hz, 2H).

Reaction of **1c** with **2h**
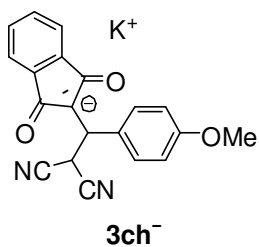
3ch: ^{1}H-NMR (d_6-DMSO, 400 MHz): δ = 3.72 (s, 3 H), 4.24 (d, ^3J = 11.6 Hz, 1H), 5.85 (d, ^3J = 11.2 Hz, 1H), 6.83 (d, ^3J = 8.8 Hz, 2H), 7.06 (dd, ^3J = 5.1 Hz, ^4J = 3.0 Hz, 2H), 7.19 (dd, ^3J = 5.1 Hz, ^4J = 3.0 Hz, 2H), 7.47 (d, ^3J = 8.8 Hz, 2H). ^{13}C-NMR (d_6-DMSO, 100 MHz): δ = 26.3, 42.1, 54.7, 101.2, 113.3, 114.5, 116.4, 128.6, 128.9, 133.9, 140.0, 157.9, 187.6.

Reaction of **1d** with **2d**
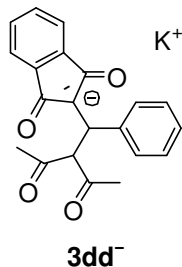
3dd: ^{1}H-NMR (d_6-DMSO, 200 MHz): δ = 1.88 (s, 3H), 2.08 (s, 3H), 4.40 (d, ^3J = 12.3 Hz, 1H), 5.35 (d, ^3J = 12.3 Hz, 1H), 6.91–7.46 (m, 9H). ^{13}C-NMR (d_6-DMSO, 100 MHz): δ = 28.3, 30.0, 40.8, 70.1, 104.2, 115.7, 124.6, 127.2, 127.8, 128.1, 140.5, 145.1, 187.5, 203.2, 204.1.

3.4.3 Kinetic Experiments

The temperature of the solutions during all kinetic studies was kept constant ($20 \pm 0.1°C$) by using a circulating bath thermostat. DMSO with a content of $H_2O < 50$ ppm was used for the kinetic experiments. For the evaluation of the kinetic experiments the stopped-flow spectrophotometer systems Hi-Tech SF-61DX2 or Applied Photophysics SX.18MV-R were used. Rate constants $k_{1\Psi}$ (s^{-1}) were obtained by fitting the single exponential $A = A_0\exp(-k_{1\Psi}t) + C$ to the observed time-dependent electrophile absorbance (averaged from at least 3 kinetic runs for each nucleophile concentration). For the stopped-flow experiments 2 stock solutions were used: A solution of the 2-benzylidene-indan-1,3-dione **1a-d** in DMSO and a solution of the carbanion **2** in DMSO, either generated by the deprotonation of the corresponding CH-acid with 1.05 equivalents of KO^{t}Bu or employed as potassium salt.

Reaction of **1a** with the potassium salt of ethyl acetylacetate (**2e**, stopped-flow, 500 nm)

$[E]_0$ / mol L^{-1}	$[C^-]_0$ / mol	$k_{1\Psi}$ / s^{-1}
2.93×10^{-5}	4.08×10^{-4}	4.10×10^{-1}
2.93×10^{-5}	8.17×10^{-4}	8.28×10^{-1}
2.93×10^{-5}	1.14×10^{-3}	1.15
2.93×10^{-5}	1.43×10^{-3}	1.43
2.93×10^{-5}	1.76×10^{-3}	1.74
$k_2 = 9.87 \times 10^2$ L mol^{-1}s^{-1}		
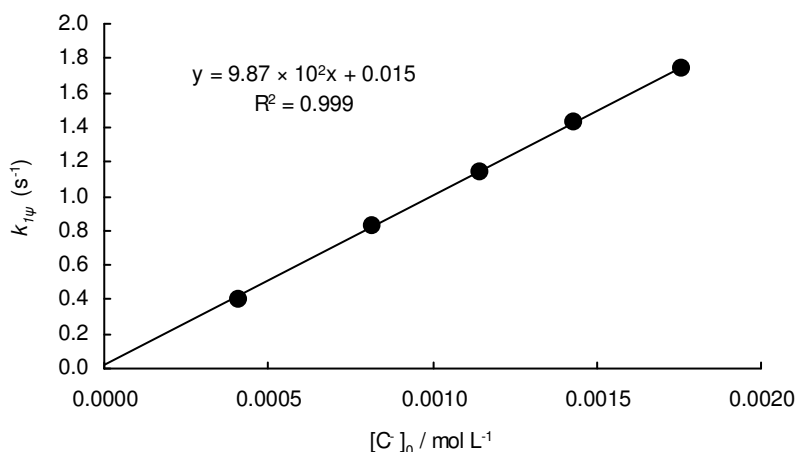
Reaction of **1a** with ethyl cyanoacetate (**2i**, stopped-flow, 500 nm)

$[E]_0$ / mol L^{-1}	$[C^-]_0$ / mol L^{-1}	$k_{1\Psi}$ / s^{-1}
2.93×10^{-5}	5.87×10^{-4}	1.08
2.93×10^{-5}	7.83×10^{-4}	1.45
2.93×10^{-5}	9.78×10^{-4}	1.80
2.93×10^{-5}	1.17×10^{-3}	2.19
2.93×10^{-5}	1.37×10^{-3}	2.53
$k_2 = 1.86 \times 10^3$ L mol^{-1}s^{-1}		

$y = 1.86 \times 10^3 x + 0.041$
$R^2 = 0.999$
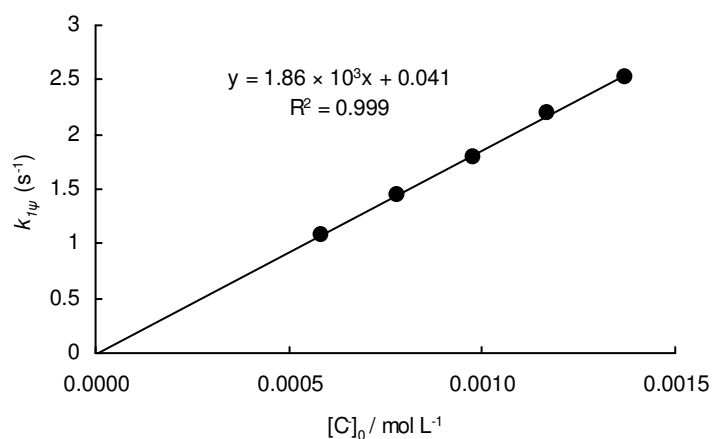
Reaction of **1b** with the potassium salt of dimedone (**2b**, stopped-flow, 490 nm)

$[E]_0$ / mol L^{-1}	$[C^-]_0$ / mol L^{-1}	$k_{1\Psi}$ / s^{-1}
1.80×10^{-5}	7.14×10^{-4}	2.01×10^{-1}
1.80×10^{-5}	1.02×10^{-3}	2.89×10^{-1}
1.80×10^{-5}	1.43×10^{-3}	4.02×10^{-1}
1.80×10^{-5}	1.79×10^{-3}	5.01×10^{-1}
$k_2 = 2.79 \times 10^2$ L mol^{-1}s^{-1}		

$y = 2.79 \times 10^2 x - 0.019$
$R^2 = 0.994$

77
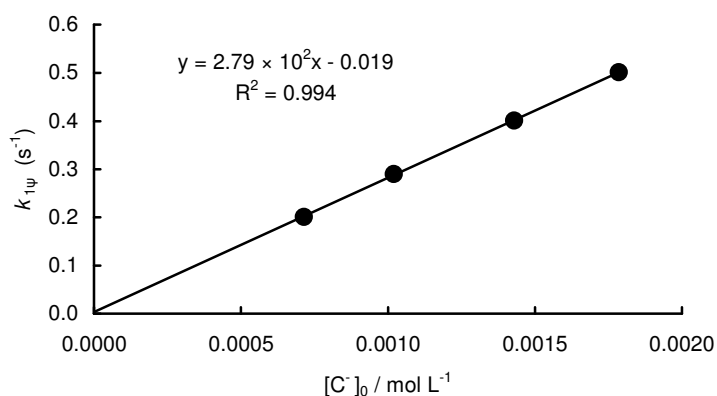
Reaction of **1b** with the potassium salt of acetylacetate (**2d**, stopped-flow, 500 nm)

$[E]_0 / \text{mol L}^{-1}$	$[C^-]_0 / \text{mol L}^{-1}$	$k_{1\Psi} / \text{s}^{-1}$
4.92×10^{-5}	6.71×10^{-4}	5.50×10^{-1}
4.92×10^{-5}	1.34×10^{-3}	1.15
4.92×10^{-5}	2.01×10^{-3}	1.80
4.92×10^{-5}	2.68×10^{-3}	2.33
4.92×10^{-5}	3.36×10^{-3}	2.94
$k_2 = 8.86 \times 10^2 \text{ L mol}^{-1}\text{s}^{-1}$		
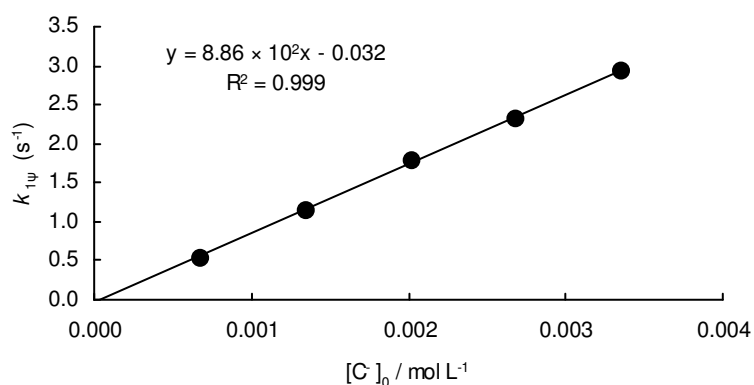
$y = 8.86 \times 10^2 x - 0.032$
$R^2 = 0.999$

Reaction of **1b** with the potassium salt of ethyl acetylacetate (**2e**, stopped-flow, 500 nm)

$[E]_0 / \text{mol}$	$[C^-]_0 / \text{mol}$	$k_{1\Psi} / \text{s}^{-1}$
2.92×10^{-5}	4.08×10^{-4}	2.36
2.92×10^{-5}	8.17×10^{-4}	5.02
2.92×10^{-5}	1.14×10^{-3}	6.98
2.92×10^{-5}	1.43×10^{-3}	9.02
2.92×10^{-5}	1.76×10^{-3}	10.7
$k_2 = 6.25 \times 10^3 \text{ L mol}^{-1}\text{s}^{-1}$		

$y = 6.25 \times 10^3 x - 0.131$
$R^2 = 0.998$
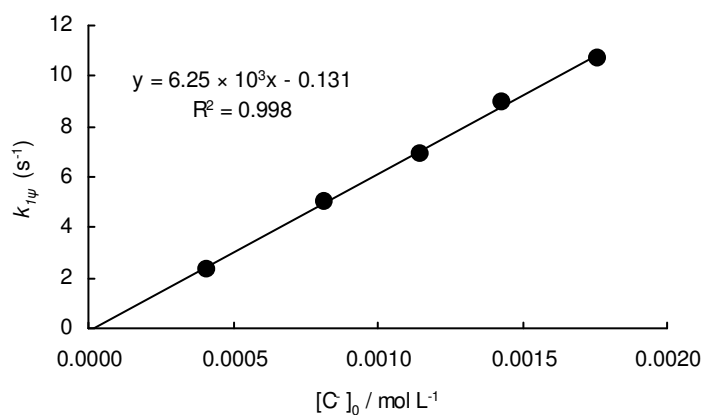
Reaction of **1b** with the potassium salt of malononitrile (**2h**, stopped-flow, 500 nm)

$[E]_0$ / mol L^{-1}	$[C^-]_0$ / mol L^{-1}	$k_{1\Psi}$ / s^{-1}
4.92×10^{-5}	6.60×10^{-4}	4.76
4.92×10^{-5}	1.32×10^{-3}	9.98
4.92×10^{-5}	1.98×10^{-3}	1.54×10^{1}
4.92×10^{-5}	2.64×10^{-3}	2.09×10^{1}
$k_2 = 8.17 \times 10^3$ L mol^{-1}s^{-1}		
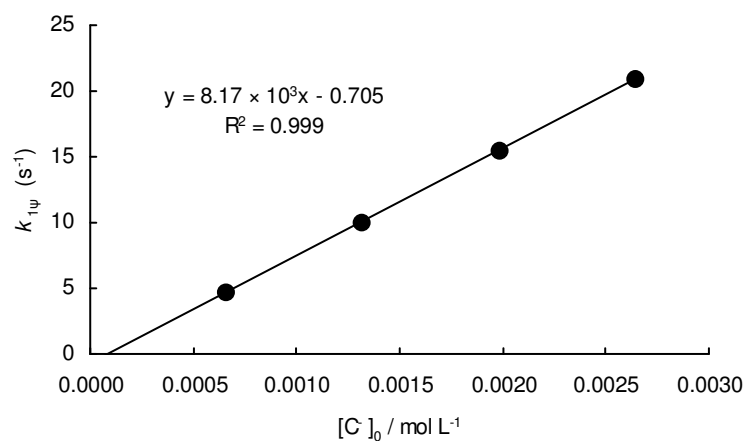
Reaction of **1b** with the potassium salt of ethyl cyanoacetate (**2i**, stopped-flow, 500 nm)

$[E]_0$ / mol	$[C^-]_0$ / mol	$k_{1\Psi}$ / s^{-1}
2.82×10^{-5}	5.87×10^{-4}	5.87
2.82×10^{-5}	7.83×10^{-4}	7.89
2.82×10^{-5}	9.78×10^{-4}	9.70
2.82×10^{-5}	1.17×10^{-3}	1.18×10^{1}
2.82×10^{-5}	1.37×10^{-3}	1.37×10^{1}
$k_2 = 1.00 \times 10^4$ L mol^{-1}s^{-1}		
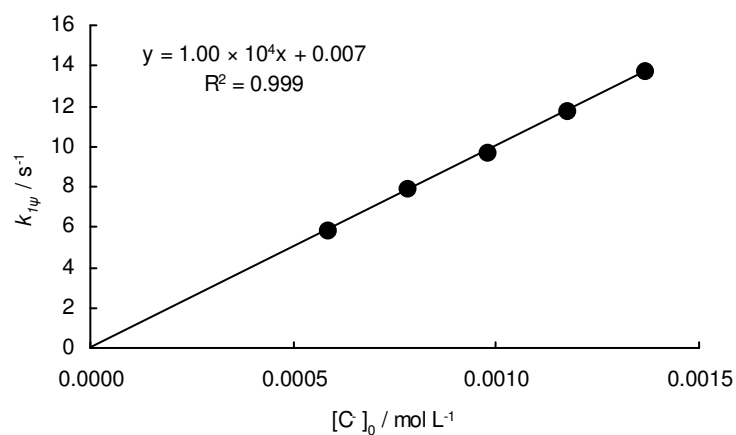
Reaction of **1d** with the potassium salt of Meldrum`s acid (**2a**, stopped-flow, 364 nm)

$[E]_0 / \text{mol L}^{-1}$	$[C^-]_0 / \text{mol L}^{-1}$	$k_{1\Psi} / \text{s}^{-1}$
2.13×10^{-5}	2.96×10^{-4}	2.79×10^{-1}
2.13×10^{-5}	5.93×10^{-4}	5.97×10^{-1}
2.13×10^{-5}	8.89×10^{-4}	9.15×10^{-1}
2.13×10^{-5}	1.19×10^{-3}	1.22
2.13×10^{-5}	1.48×10^{-3}	1.54

$$k_2 = 1.06 \times 10^3 \text{ L mol}^{-1}\text{s}^{-1}$$
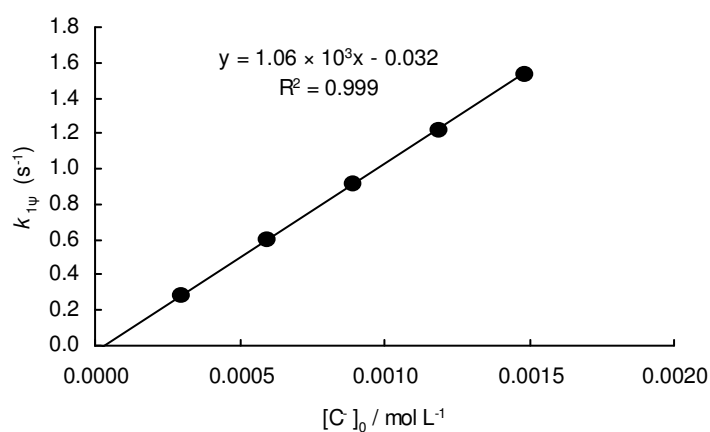
Reaction of **1d** with the potassium salt of dimedone (**2b**, stopped-flow, 390 nm)

$[E]_0 / \text{mol L}^{-1}$	$[C^-]_0 / \text{mol L}^{-1}$	$k_{1\Psi} / \text{s}^{-1}$
2.13×10^{-5}	2.78×10^{-4}	2.32×10^1
2.13×10^{-5}	5.55×10^{-4}	5.31×10^1
2.13×10^{-5}	8.33×10^{-4}	8.61×10^1
2.13×10^{-5}	1.11×10^{-3}	1.15×10^2
2.13×10^{-5}	1.39×10^{-3}	1.39×10^2

$$k_2 = 1.06 \times 10^5 \text{ L mol}^{-1}\text{s}^{-1}$$
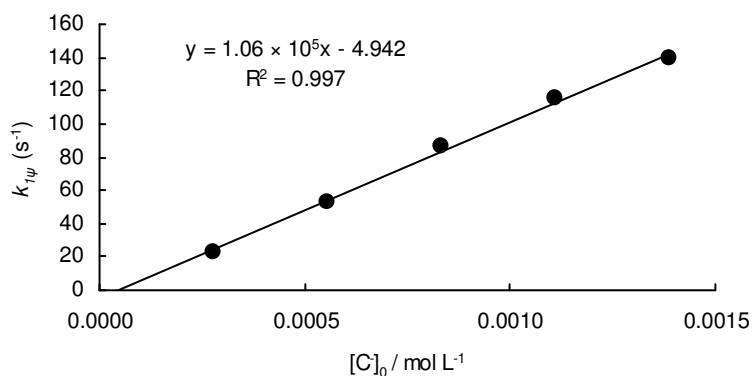
3.5 References

[1]   (a) H. Mayr, A. R. Ofial, *Pure Appl. Chem.* **2005**, *77*, 1807-1821. (b) H. Mayr, A. R. Ofial in *Carbocation Chemistry* (G. A. Olah, G. K. S. Prakash, Eds.), Wiley, Hoboken (N.J.), **2004**, Chapt. 13, p 331-358. (c) A. R. Ofial, H. Mayr, *Macromol. Symp.* **2004**, *215*, 353-367. (d) H. Mayr, B. Kempf, A. R. Ofial, *Acc. Chem. Res*. **2003**, *36*, 66-77. (e) H. Mayr, O. Kuhn, M. F. Gotta, M. Patz, *J. Phys. Org. Chem.* **1998**, *11*, 642-654. (f) H. Mayr, M. Patz, M. F. Gotta, A. R. Ofial, *Pure Appl. Chem.* **1998**, *70*, 1993-2000. (g) H. Mayr, M. Patz, *Angew. Chem.* **1994**, *106*, 990-1010; *Angew. Chem. Int. Ed. Engl.* **1994**, *33*, 938-957.

[2]   For reactions of carbocations with π–nucleophiles, see: (a) A. D. Dilman, H. Mayr, *Eur. J. Org. Chem.* **2005**, 1760-1764. (b) T. Tokuyasu, H. Mayr, *Eur. J. Org. Chem.* **2004**, 2791-2796. (c) B. Kempf, N. Hampel, A. R. Ofial, H. Mayr, *Chem. Eur. J.* **2003**, *9*, 2209-2218. (d) H. Mayr, T. Bug, M. F. Gotta, N. Hering, B. Irrgang, B. Janker, B. Kempf, R. Loos, A. R. Ofial, G. Remennikov, H. Schimmel, *J. Am. Chem. Soc.* **2001**, *123*, 9500-9512.

[3]   For reactions of carbocations with hydride donors, see: (a) H. Mayr, G. Lang, A. R. Ofial, *J. Am. Chem. Soc.* **2002**, *124*, 4076-4083. (b) M.-A. Funke, H. Mayr, *Chem. Eur. J.* **1997**, *3*, 1214-1222.

[4]   For reactions of carbocations with *n*-nucleophiles, see: (a) F. Brotzel, Y. C. Chu, H. Mayr, *J. Org. Chem*. **2007**, *72*, 3679-3688. (b) F. Brotzel, B. Kempf, T. Singer, H. Zipse, H. Mayr, *Chem. Eur. J.* **2007**, *13*, 336-345. (c) B. Kempf, H. Mayr, *Chem. Eur. J.* **2005**, *11*, 917-927. (d) T. B. Phan, H. Mayr, *Can. J. Chem.* **2005**, *83*, 1554-1560. (e) S. Minegishi, H. Mayr, *J. Am. Chem. Soc.* **2003**, *125*, 286-295.

[5]   R. Lucius, R. Loos and H. Mayr, *Angew. Chem.* **2002**, *114*, 97-102; *Angew. Chem. Int. Ed.* **2002**, *41*, 91-95.

[6]   T. Lemek, H. Mayr, *J. Org. Chem.* **2003**, *68*, 6880-6886.

[7]   See references 10–13 cited in: D. B. Ramachary, K. Anebouselvy, N. S. Chowdari, C. F. Barbas, *J. Org. Chem.* **2004**, *69*, 5838-5849.

[8]   (a) R. Cammi, C. Ghio, J. Tomasi, *Int. J. Quantum Chem.* **1986**, *29*, 527-539. (b) E. Liedl, P. Wolschann, *Monatsh. Chem.* **1982**, *113*, 1067-1071. (c) H. Goerner, J. Leitich, O. E. Polansky, W. Riemer, U. Ritter-Thomas, B. Schlamann, *Monatsh.*

Chem. **1980**, *111*, 309-329. (d) P. Margaretha, *Tetrahedron* **1972**, *28*, 83-87. (f) P. Margaretha, O. E. Polansky, *Monatsh. Chem.* **1969**, *100*, 576-583.

[9]   (a) J. Bloxham, C. P. Dell, *J. Chem. Soc.*, *Perkin Trans. 1* **1993**, *24*, 3055-3059. (b) N. F. Eweiss, *J. Heterocycl. Chem.* **1982**, *19*, 273-277. (c) P. P. Righetti, A. Gamba, G. Tacconi, G. Desimoni, *Tetrahedron* **1981**, *37*, 1779-1785. (d) J. Bitter, J. Leitich, H. Partale, O. E. Polansky, W. Riemer, U. Ritter-Thomas, B. Schlamann, B. Stilkerieg, *Chem. Ber.* **1980**, *113*, 1020-1032.

[10]   L. P. Zalukajevs, I. Anokhina, *Zh. Obshch. Khim.* **1964**, *34*, 840-843. Cited in ref. [14]

[11]   T. Zimaity, E. Afsah, M. Hammouda, *Indian J. Chem.* **1979**, *17b*, 578-580.

[12]   L. P. Zalukajevs, D. G. Vnenkovskaya, *Zh. Org. Khim.* **1966**, *2*, 672. Cited in ref. [14]

[13]   E. I. Stankevich, G. Vanags, *Zh. Obshch. Khim.* **1962**, *32*, 1146-1151. Cited in ref. [14]

[14]   (a) B. A. Arbuzov, T. D. Sorokina, N. P. Bogonostseva and V. S. Vinogradova, *Dokl. Akad. Nauk SSSR* **1966**, *171*, 605. (b) A. Mustafa, M. M. Sidky and F. M. Soliman, *Tetrahedron* **1967**, *23*, 99-105. (c) F. M. Soliman, M. M. Said and S. S. Maigali, *Heteroat. Chem.* **1997**, *8*, 157-164.

[15]   X.-Q. Zhu, H.-Y. Wang, J.-S. Wang, Y.-C. Liu, J. Org. Chem. **2001**, *66*, 344-347.

[16]   C. F. Bernasconi, M. W. Stronach, *J. Am. Chem. Soc.* **1991**, *113*, 2222-2227.

[17]   T. Bug, T. Lemek, H. Mayr, *J. Org. Chem.* **2004**, *69*, 7565-7576.

[18]   S. T. A. Berger, A. R. Ofial, H. Mayr, *J. Am. Chem. Soc.* **2007**, *129*, 9753-9761.

[19]   R. K. Behera, A. Nayak, *Indian J. Chem.* **1976**, *14b*, 223-224.

[20]   (a) C. F. Bernasconi, A. Laibelman and J. L. Zitomer, *J. Am. Chem. Soc.* **1985**, *107*, 6563–6570. (b) C. F. Bernasconi, A. Laibelman and J. L. Zitomer, *J. Am. Chem. Soc.* **1985**, *107*, 6570–6575.

[21]   T. B. Phan, M. Breugst, H. Mayr, *Angew. Chem.* **2006**, *118*, 3954-3959; *Angew. Chem. Int. Ed.* **2006**, *45*, 3869-3874.

[22]   C. Hansch, A. Leo, R. W. Taft, *Chem. Rev.* **1991**, *91,* 165-195.

[23]   C. F. Bernasconi, P. Paschalis, *J. Am. Chem. Soc.* **1986**, *108*, 2969-2977.

[24]   F. G. Bordwell, J. A. Harrelson Jr., A. V. Satish, *J. Org. Chem.* **1989**, *54*, 3101-3105.

[25]   A. Albert, E. P. Serjeant, *The Determination of Ionization Constants: A Laboratory Manual,* 3rd ed., Chapman and Hall, London **1984**, p. 137-160.

[26]   C. F. Bernasconi, R. B. Killion Jr., *J. Org. Chem.* **1989**, *54*, 2878-2885.

[27]   T. Bug, H. Mayr, *J. Am. Chem. Soc.* **2003**, *125*, 12980-12986.

[28]   (a) C. F. Bernasconi, *Acc. Chem. Res.* **1987**, *20*, 301-308. (b) C. F. Bernasconi, *Tetrahedron*, **1989**, *45*, 4017–4090.

[29]   H. K. Oh, J. H. Yang, H. W. Lee and I. Lee, *J. Org. Chem.*, **2000**, *65*, 5391-5395.

[30]   For a database of reactivity parameters *E*, *N*, and *s*, see: http://www.cup.uni-muenchen.de/oc/mayr/DBintro.html.

Chapter 4

Reactions of Nitro(hetero)arenes with Carbanions:

Bridging Aromatic, Heteroaromatic, and Vinylic Electrophilicity

4.1 Introduction

The concept of Vicarious Nucleophilic Substitution (VNS) of hydrogen in electron deficient arenes was developed three decades ago.[1, 2] Since then, this method has been thoroughly studied and has become a versatile tool for the introduction of a variety of substituents into aromatic or heteroaromatic nitro-compounds.[3-6]

In general, the reaction proceeds *via* fast and reversible addition of a carbanion, bearing a leaving group X (e.g., halogen) at the carbanion center, to a nitroarene followed by base induced β-elimination of H–X from the resultant σ_H-adduct. At least two equivalents of base are necessary for the reaction to proceed, one for the deprotonation of the CH-acid to form the carbanion, and the second for inducing the β-elimination of H–X. After final protonation the substituted nitroarene or -heteroarene is obtained (Scheme 4.1).[7-10]
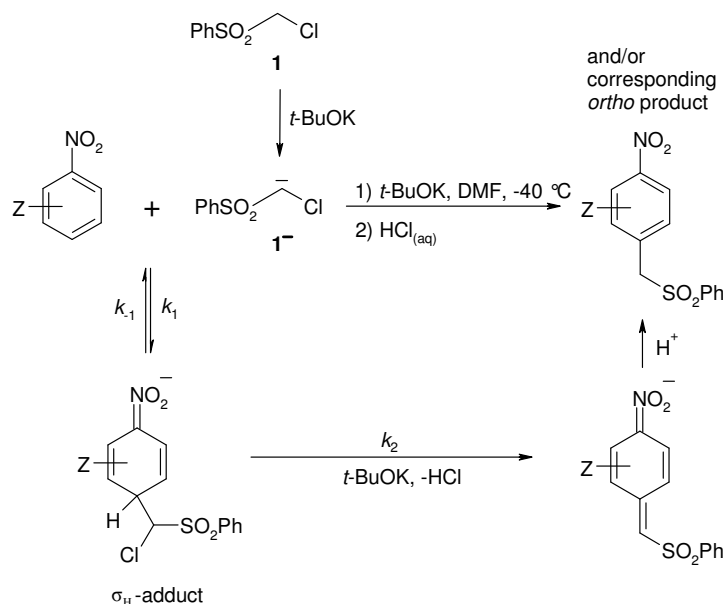
SCHEME 4.1: Mechanism of the Vicarious Nucleophilic Substitution in nitroarenes with the anion of chloromethyl phenyl sulfone (1^-).

It has been reported that the solvent, the nature and concentration of the base, and the steric demand of the carbanion have a considerable influence upon the ratio of isomeric products.[11] When there is a high excess of the base, H-X elimination is faster than the retroaddition of the σ_H-adduct, and the formation of the σ_H-adducts becomes irreversible.

Nitro-substituted heteroarenes, similar to their carbocyclic analogues, readily enter the VNS reaction giving products, which are important building blocks in organic synthesis.[12] Therefore, it is of interest to determine their electrophilic activity and compare it with that of typical aliphatic electrophiles.

Understanding and predicting the influence of substituents will help to control regioselectivity in nucleophilic aromatic displacement reactions. Analogous investigations of substituent effects on the electrophilic activities of nitro-substituted benzenoid arenes have already been studied earlier.[13, 14]

4.2 Results

4.2.1 Synthesis of the Reactants

Chloromethyl phenyl sulfone (**1**) was synthesized via S_N2-type reaction of sodium benzenesulfinate with bromo(chloro)methane in DMSO at 80 °C, according to ref. [15]. After crystallization from ethanol, the product precipitated in 59% yield (Scheme 4.2).

SCHEME 4.2: Synthesis of chloromethyl phenyl sulfone (**1**).[15]

In contrast to the nitropyridines **4a-d**, which are commercially available, all nitro-substituted five-membered heterocycles used in this work had to be synthesized or purified.

N-Methyl-nitropyrroles **5a** and **5b** were obtained by nitration of *N*-methyl-pyrrole with nitronium acetate as nitrating agent. In variation of the prescription in ref. [16], the temperature was lowered to −20 °C and precisely controlled during the reaction in order to decrease the amount of side products (Scheme 4.3). After neutralization, a mixture of the nitropyrroles was obtained by steam distillation. GC analysis showed that two regioisomers were formed, which were isolated by column chromatography (SiO$_2$, hexane/ethyl acetate 5:1).

SCHEME 4.3: Synthesis of 1-methyl-2-nitropyrrole (**5a**) and 1-methyl-3-nitropyrrole (**5b**).[16]

The methylation of 4-nitroimidazole can occur in two possible positions. When dimethyl sulfate in dioxane is employed as methylating reagent, the formation of 1-methyl-5-nitroimidazole (**6a**) takes place exclusively (Scheme 4.4).[17] Under basic conditions, using the non-toxic dimethyl carbonate as reagent, the formation of 1-methyl-4-nitroimidazole (**6b**) is

favored.[18] Although the isomer **6a** is also formed to about 15% in this reaction, compound **6b** can be purified by recrystallization from ethanol.
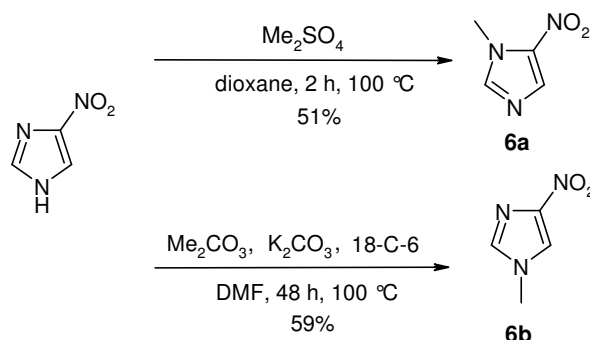
SCHEME 4.4: Synthesis of 1-methyl-5-nitroimidazole (**6a**) and 1-methyl-4-nitroimidazole (**6b**).[17, 18]

1-Methyl-4-nitropyrazole (**7**) was synthesized according to ref. [19] (Scheme 4.5) by condensation of 1,1,3,3-tetramethoxypropane with *N*-methyl-urea, followed by nitration with nitric acid in sulfuric acid. Aminolysis of the resultant nitropyrimidone in methanol yielded an azadienamine, which was converted into 2-nitro-3-propylamino-propenal by acid catalyzed hydrolysis. This nitro-enamine can be considered as a synthetic equivalent of nitromalonaldehyde and was condensed with *N*-methyl-hydrazine hydrochloride in the presence of triethylamine in methanol to yield nitropyrazole **7**.
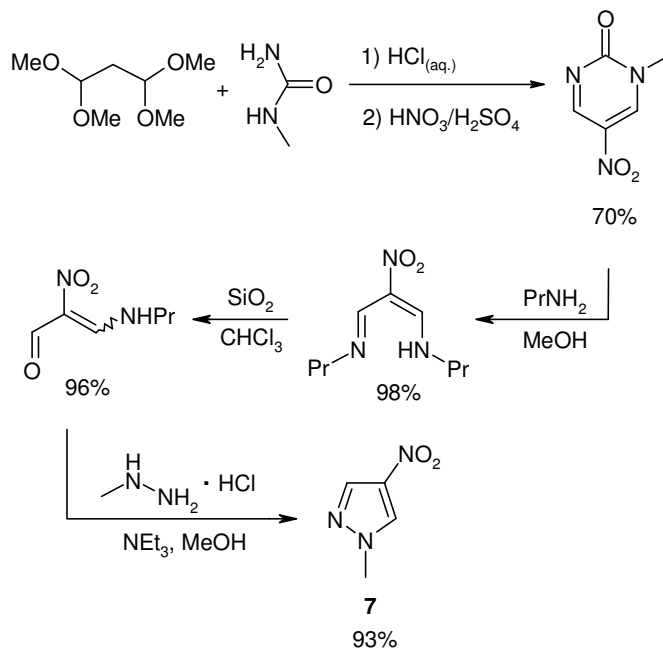
SCHEME 4.5: Synthesis of 1-methyl-4-nitropyrazole (**7**).[19]

Commercially available 2-nitrothiophene (**8**) always contains up to 15% of the 3-nitro isomer, which cannot be easily removed by distillation or column chromatography. For this purpose the mixture of isomers was treated with chlorosulfonic acid in chloroform at 40 °C according to ref. [20] and the course of the reaction was monitored by ^{1}H NMR spectroscopy. When 3-nitrothiophene − the more reactive of the two isomers − was completely consumed according to NMR, the reaction mixture was poured into ice-water. Extraction and recrystallization from hexane / diethyl ether yielded 51% 2-nitrothiophene (**8**) in high isomeric purity.

2-Bromo-5-nitrothiophene was synthesized via nitration of 2-bromo-thiophene with nitric acid in acetic acid anhydride (Scheme 4.6).[21] The crude product was purified by steam distillation and recrystallization from hexane/ethyl acetate.
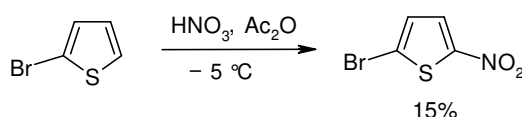
SCHEME 4.6: Synthesis of 2-bromo-5-nitrothiophene.[21]

In order to obtain 5-nitrothiazole, the commercially available 2-amino analogue was bromo-deaminated using the Sandmeyer protocol.[22] The subsequent debromination was achieved with copper powder and acetic acid in moderate yield (Scheme 4.7).[23]
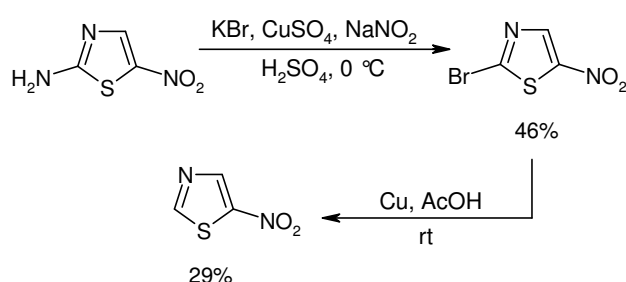
SCHEME 4.7: Synthesis of 2-bromo-5-nitrothiazole and 5-nitrothiazole.[22, 23]

4.2.2 Product Studies

As previously shown, the anion of chloromethyl phenyl sulfone (**1⁻**) undergoes VNS reactions with a broad variety of electron-deficient arenes[15, 24] and was used as a substrate in earlier mechanistic studies.[7-10, 13, 14] Accordingly, it was also chosen as the reference nucleophile in

this work. For the determination of relative electrophilic reactivities of various heteroarenes toward 1^- by competition experiments, it was necessary to have samples of all VNS products, which were synthesized as described in Schemes 4.8 and 4.9. Some of these products were described earlier, as specified in the Schemes.

(i) 1.) DMF, KO^{t}Bu, -40 °C, 5 min
    2.) HCl$_{(aq)}$
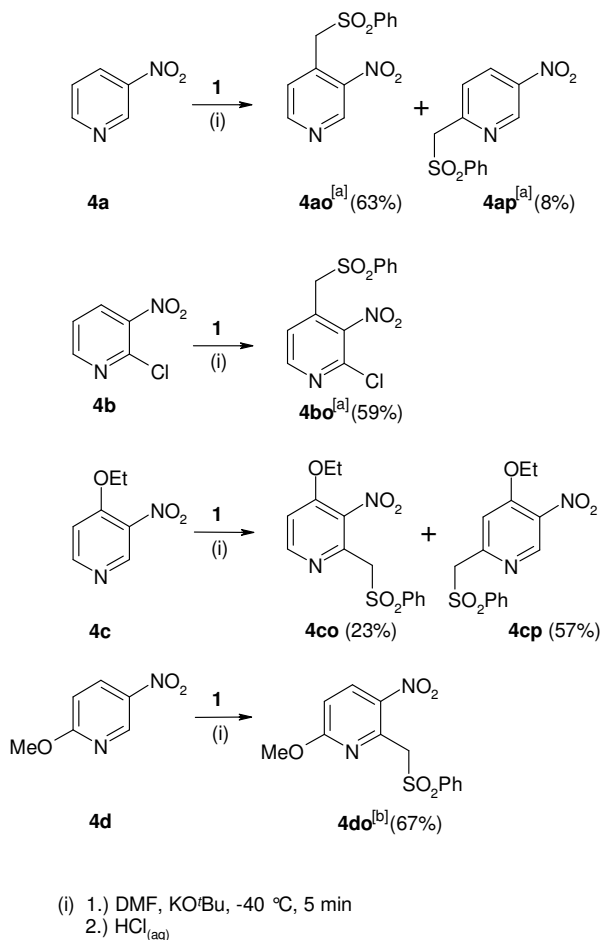
SCHEME 4.8: VNS reactions of 2-nitropyridines **4a**-**d** with the anion of chloromethyl phenyl sulfone (1^-).[25] – [a] Ref. [26]. [b] Ref. [27, 28].

The ratios of isomeric products obtained by VNS reactions of 3-nitropyridine (**4a**),[26] 2-chloro-3-nitropyridine (**4b**),[26] and 2-methoxy-5-nitropyridine (**4d**)[28] with the sulfonyl carbanion 1^- agree with those reported in the literature (Scheme 4.8). Compound **4c** is predominately attacked by 1^- at position 6 to yield **4cp** as the major product (Scheme 4.8) in accordance with the quantitative competition experiments discussed below. In contrast, the reaction of 1^- with 4-methoxy-3-nitropyridine was reported to yield only the corresponding 2-substitution product.[28]

In the presence of strong bases, 1-unsubstituted nitropyrroles, nitroimidazoles, and nitropyrazoles are converted into the corresponding anions, which do not react with nucleophiles. Therefore, we used the non-acidic 1-methylated derivatives **5**-**7** for our competition experiments.
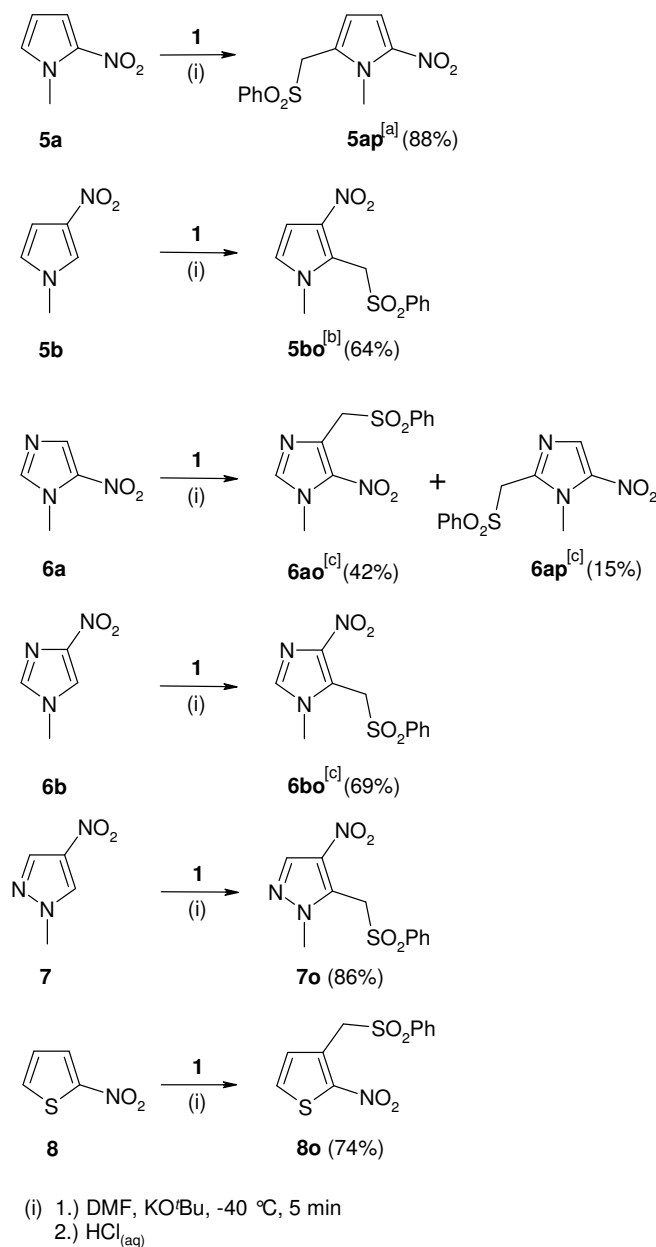
SCHEME 4.9: VNS reactions of 5-membered heterocycles **5-8** with the anion of chloromethyl phenyl sulfone (**1⁻**). – [a] Ref. [29]. [b] Ref. [30]. [c] Ref. [31].

The VNS reactions of **1⁻** with *N*-methyl-2-nitropyrrole (**5a**) and *N*-methyl-3-nitropyrrole (**5b**) gave only single regioisomers (Scheme 4.9).[29, 30]

While Crozet and co-workers[32-34] reported the exclusive formation of **6ao**, when **6a** was treated with **1** and potassium hydroxide in DMSO at room temperature, we isolated a mixture of 4-benzenesulfonylmethyl-1-methyl-5-nitroimidazole (**6ao**, 42%) and 15% of the corresponding 2-isomer (**6ap**, Scheme 4.9) in accordance with earlier reports.[31] Only one regioisomer was obtained in the reaction of 1-methyl-4-nitroimidazole (**6b**, Scheme 4.9) with **1⁻**.

N-Methyl-4-nitropyrazole (**7**) was exclusively attacked at position 5 to give *N*-methyl-4-nitro-5-(phenylsulfonylmethyl)-pyrazole (**7o**) in 86 % yield (Scheme 4.9), in analogy to previously reported reactions of **7** with other carbanions.[35, 36] In contrast to the regioselectivity of the reaction of **5a** with **1⁻** (see above), 2-nitrothiophene (**8**) is selectively attacked at the 3-position by **1⁻** (Scheme 4.9).[30, 37]

4.2.3 Competition Experiments

For the determination of the relative electrophilic reactivities of the electron deficient arenes **3-8**, a mixture of two nitro(hetero)arenes was treated with chloromethyl phenyl sulfone (**1**) and KO^{t}Bu. The products obtained after treatment of the reaction mixtures with diluted hydrochloric acid were extracted with chloroform and analyzed by GC and/or HPLC (Scheme 4.10).
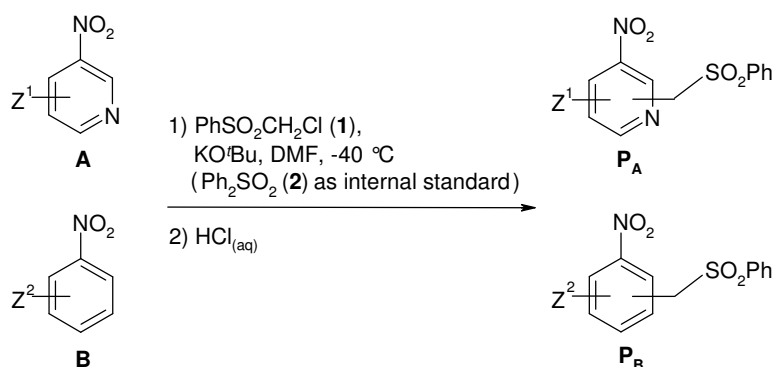
SCHEME 4.10: Competition experiment for determining the relative electrophilic reactivities of two nitro(hetero)arenes **A** and **B**.

A low reaction temperature (–40 °C) and a high concentration of potassium *tert*-butoxide (four equivalents) guaranteed the reaction to proceed under kinetic control with irreversible formation of the σ$_H$-adduct (Scheme 4.1). Because dehydrohalogenation of the σ$_H$-adducts is much faster than the reverse reaction (k_2[B] >> k_{-1})[13, 14] the ratio of the isolated products

reflects the ratio of the addition rate constants k_1. As competitors for the nitroheteroarenes we used the *para*-substituted nitrobenzenes **3b-d** (formula see Figure 4.1) and 1-nitronaphthalene (**3e**), which allowed us to combine the relative reactivities of this work with those of earlier studies.[13, 14] A summary of all relative reactivities determined in this investigation is shown in Table 4.1. If there is more than one reaction center in the nitroheteroarenes, the chromatographically determined product ratios are also given. The results obtained by HPLC analysis are in good agreement with those from GC measurements. While the results of the two methods differ by 25% for the first entry of Table 4.1, the deviation for all other systems is less than 10%. For further evaluation only the results obtained by GC are considered.

Equation 4.1 represents the logarithm of the competition constants $k_A/k_B = \kappa$. By expressing all available competition constants (GC) in this way, an overdetermined set of linear equations (equation 4.1) is obtained, which is solved by least squares minimization[38] to give the k_{rel} values listed in Figure 4.1. The activity of one *ortho*-position in nitrobenzene (**3a**) was defined as 1.0,[13] and the previously reported overall activities of 4-chloronitrobenzene (**3d**, $k_{rel} = 250$),[13] 4-methoxynitrobenzene (**3b**, $k_{rel} = 1.8$),[14] 4-fluoronitrobenzene (**3c**, $k_{rel} = 100$),[14] and 1-nitronaphthalene (**3e**, $k_{rel} = 4500$)[14] were treated as invariable.

$$\log k_A - \log k_B = \log \kappa \qquad (4.1)$$

TABLE 4.1: Reactivity ratios derived from competition experiments.

A	B	analysis	κ[a], [b]	regioselectivity
4a	**3e**	GC	17 ± 1	[**4ao**]:[**4ap**] = 12 ± 2
		HPLC[c]	13 ± 1	[**4ao**]:[**4ap**] = 12 ± 2
4b	**3e**	GC	19 ± 1	
		HPLC[c]	21 ± 0.1	
4c	**3d**	GC	4.5 ± 0.4	[**4cp**]:[**4co**] = 2.0 ± 0.1
		HPLC[c]	4.2 ± 0.3	[**4cp**]:[**4co**] = 2.6 ± 0.1
3e	**4c**	GC[d]	4.8 ± 0.1	
4d	**3e**	GC	3.7 ± 0.2	
		HPLC[c]	3.7 ± 0.5	
3b	**5a**	GC	2.2 ± 0.1	
5b	**5a**	GC	5.0 ± 0.3	
5b	**3b**	GC	2.8 ± 0.3	
		HPLC[c]	3.1 ± 0.4	

TABLE 4.1: Continued.

A	B	analysis	$\kappa^{[a],[b]}$	regioselectivity
6a	**3b**	GC	11 ± 1	[**6ao**]:[**6ap**] = 1.00 ± 0.03
		HPLC[e]	9.9 ± 1.4	[**6ao**]:[**6ap**] = 0.87 ± 0.11
3c	**6a**	GC	7.0 ± 0.3	[**6ao**]:[**6ap**] = 0.90 ± 0.04
6b	**3c**	GC	5.7 ± 0.4	
		HPLC[c]	6.2± 0.5	
6b	**3d**	GC	1.8 ± 0.1	
7	**3c**	GC	1.0 ± 0.1	
		HPLC[c]	1.1 ± 0.02	
3d	**7**	GC	2.7 ± 0.3	
8	**3e**	GC	3.9 ± 0.5	
		HPLC[c]	4.1 ± 0.7	

[a] $\kappa = k_A/k_B$ (ratio of the overall reactivity of A and B). [b] The indicated errors refer to the reproducibility of the chromatographic analysis, deviations between the results obtained by different methods show that the absolute errors are bigger. [c] Analysis at 264 nm. [d] Amount of *ortho*-product of **4c** is estimated on the basis of [**4cp**]:[**4co**] = 2.0 ± 0.04. [e] Analysis at 280 nm.

The reactions of 5-nitrofuran-2-carbonitrile, 2-bromo-5-nitrothiophene, and 5-nitrothiazole with **1**⁻ gave complex mixtures of products, which could not be analyzed quantitatively by GC and HPLC. Their electrophilic reactivities could, therefore, not be determined by analogous competition experiments. In line with these observations, nitrothiazoles have previously been reported to decompose in the presence of alkoxides.[39-41]
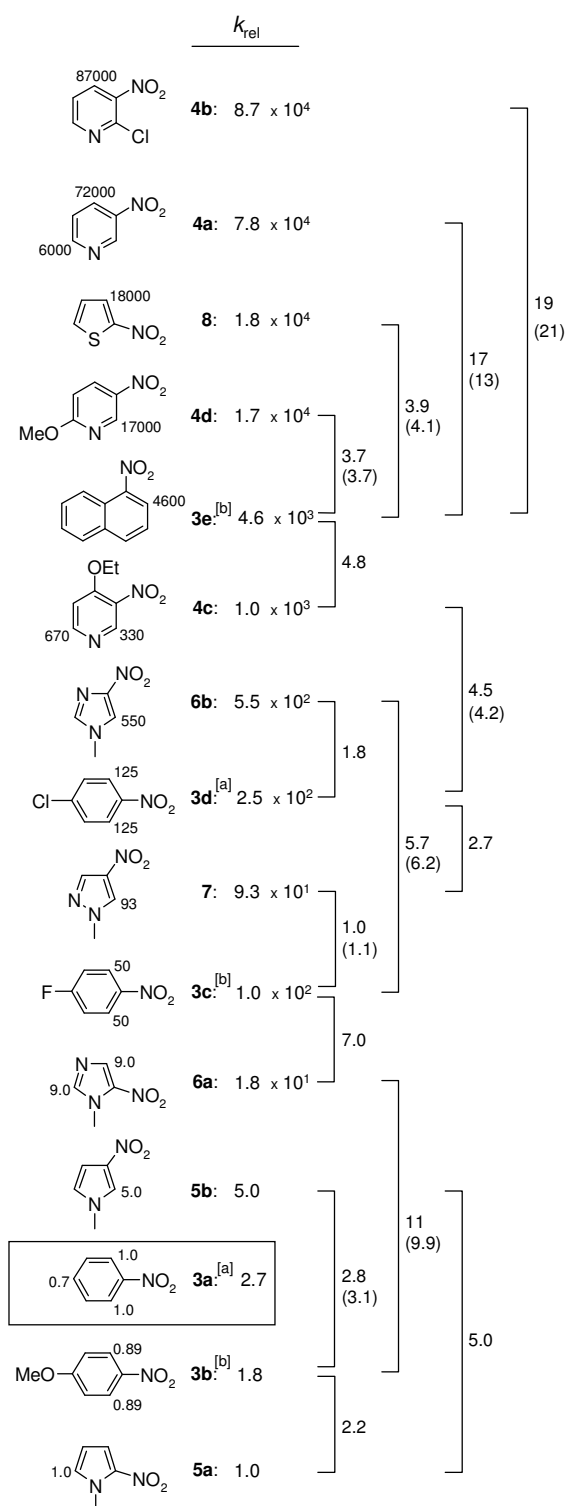
FIGURE 4.1: Overall relative reactivities k_{rel} (−40 °C) of nitro(hetero)arenes toward the anion of chloromethyl phenyl sulfone (**1⁻**) based on κ-values (Table 4.1) in relation to nitrobenzene (**3a,** k_{rel} = 2.7).[13] The numbers in the formula give the relative reactivities of the corresponding positions with respect to one *ortho*-position of nitrobenzene. The numbers in parentheses indicate HPLC results, all other numbers result from GC analysis. − [a] Ref. [13]. [b] Ref. [14].

4.2.4 Direct Rate Measurements

In 2003, Lemek showed that the reactions of α-halocarbanions with 4-methoxynitrobenzene (**3b**) yield persistent σ$_H$-adducts in DMF at −40 °C.[8] The second-order rate constants for these additions were determined by UV-Vis spectroscopy. Analogously, we determined the rate constants for the additions of **1⁻** to **3b**, **3d**, and 2,4-dichloro-nitrobenzene (**3f**, studied in refs. [13] and [14]) by following the absorbance of the σ$_H$-adduct at 425 nm (Table 4.2). In order to inhibit the elimination of HCl from the σ$_H$-adducts, chloromethyl phenyl sulfone **1** was used in slight excess over KO^{t}Bu. Entries 1/2 and 3/4 of Table 4.2 show that the second-order rate constants determined for these additions do not depend on the reaction conditions, i.e., which of the two reagents is used as the major component under pseudo-first-order conditions.

The ratio of the directly measured rate constants (k_{3d}/k_{3b} = 123, from Table 4.2) is in good agreement with the relative reactivities determined by competition experiments (k_{3d}/k_{3b} = 139, from Figure 4.1). Thus, the consistency of the two independent methods of reactivity studies is confirmed.

TABLE 4.2: Second-order rate constants k_2 of the reactions of carbanion **1⁻** with vinylic and aromatic electrophiles in DMF at −40 °C.

no.	A[a]	B	k_2 (−40 °C) / M⁻¹ s⁻¹ [b]
1[c]	**1⁻**	**3b**	**(2.26 ± 0.12) × 10⁻¹**
2[c]	**3b**	**1⁻**	(2.34 ± 0.17) × 10⁻¹
3[c]	**1⁻**	**3d**	(2.95 ± 0.11) × 10¹
4[c]	**3d**	**1⁻**	**(2.77 ± 0.08) × 10¹**
5[c]	**3f**[d]	**1⁻**	(1.95 ± 0.11) × 10²
6[e]	**1⁻**	**10a**	(1.01 ± 0.03) × 10¹
7[e]	**1⁻**	**10b**	4.65 ± 0.31[f]
8[e]	**1⁻**	**10c**	2.64 ± 0.12

[a] Compound used in excess to ensure pseudo-first-order kinetics. [b] Bold values are considered to be more reliable and are used for further calculations [c] Exponential increase of the σ$_H$-adduct (425 nm) is followed. [d] **3f**: 2,4-Dichloro-nitrobenzene. [e] Exponential decrease of the electrophile band is followed. [f] $\Delta H^‡$ = 28.3 ± 1.1 kJ mol⁻¹ and $\Delta S^‡$ = −111 ± 5 J mol⁻¹ K⁻¹.

In order to compare the reactivities of aliphatic and aromatic electrophiles, the kinetics of the additions of 1^- to diethyl benzylidenemalonates **10a-c** (Scheme 4.11) were studied analogously (Table 4.2, entries 6-8). The electrophiles **10a-c** show strong absorption bands in the UV-Vis spectra at $\lambda_{max} = 400 - 420$ nm. When treated with an excess of 1^-, complete decolorization of the solutions was observed, indicating quantitative reactions. From the exponential decay of the absorbances of **10a-c**, the pseudo-first-order rate constants were derived and plotted against the variable concentrations of 1^- to give the second-order rate constants listed in Table 4.2 (entries 6-8).[42]

The reaction course proposed in Scheme 4.11 was confirmed by the isolation of **11a**, the protonated addition product of 1^- to diethyl benzylidenemalonate **10a**.
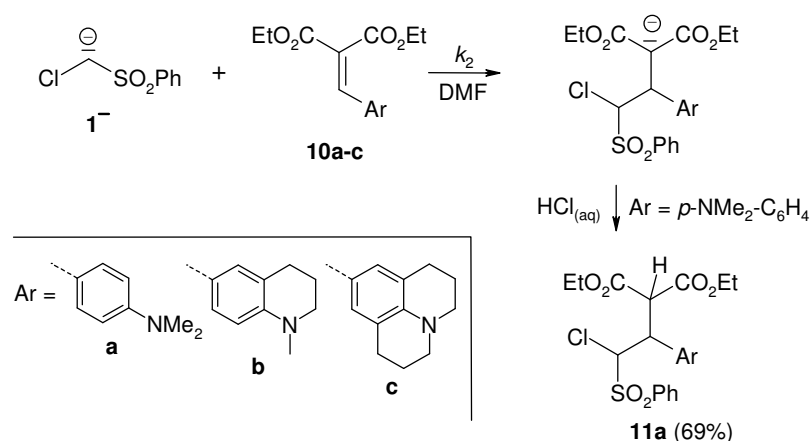
SCHEME 4.11: Reactions of carbanion 1^- with Michael acceptors **10a-c**.

Kinetic studies of the reaction of 1^- with diethyl benzylidenemalonate **10b** at various temperatures yielded the Eyring activation parameters $\Delta H^{\ddagger} = 28.3 \pm 1.1$ kJ mol^{-1} and $\Delta S^{\ddagger} = -111 \pm 5$ J mol^{-1} K^{-1}.

In order to link the kinetic data in Figure 4.1 and Table 4.2 to our comprehensive reactivity scales,[43] we also studied the kinetics of the additions of nitroethyl anion (9^-) to **10a-c** and the quinone methides **12a-c** in DMF (Scheme 4.12) at various temperatures. From the second-order rate constants the Eyring activation parameters and the second-order rate constants at -40 °C were derived (Table 4.3).
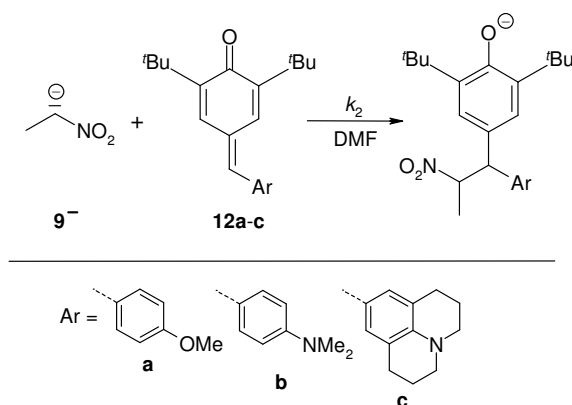
SCHEME 4.12: Reaction of the nitroethyl anion (**9⁻**) with the quinone methides **12a**-**c**.

TABLE 4.3: Second-order rate constants k_2 and Eyring activation parameters of the reactions of the nitroethyl anion (**9⁻**) with quinone methides **12a**-**c** and diethyl benzylidenemalonates **10a**-**c** in DMF. The exponential decrease of UV-Vis absorbances of the electrophile is followed.

	k_2 (20 °C) / M^{-1} s^{-1}	$\Delta H^{\ddagger}$ / kJ mol^{-1}	$\Delta S^{\ddagger}$ / J mol^{-1} K^{-1}	k_2 (−40 °C)[a] / M^{-1} s^{-1}
10a	$(4.52 \pm 0.18) \times 10^{-1}$	44.4 ± 1.7	-101 ± 6	$(3.01 \pm 0.57) \times 10^{-3}$
10b	$(2.46 \pm 0.02) \times 10^{-1}$	45.4 ± 0.8	-102 ± 3	$(1.56 \pm 0.15) \times 10^{-3}$
10c	1.76×10^{-1}	46.1 ± 0.4	-102 ± 1	$(1.01 \pm 0.05) \times 10^{-3}$
12a	$(1.15 \pm 0.04) \times 10^{3}$	33.3 ± 0.5	-73 ± 2	$(2.55 \pm 0.23) \times 10^{1}$
12b	$(1.94 \pm 0.10) \times 10^{2}$	30.2 ± 1.9	-98 ± 6	6.15 ± 1.52
12c	$(8.97 \pm 0.46) \times 10^{1}$	31.1 ± 1.5	-101 ± 5	2.62 ± 0.53

[a] Calculated from Eyring parameters.

4.3 Discussion

4.3.1 Relative Reactivities of Heteroarenes

As pyridine is well known to be π-electron deficient compared to benzene, it is not surprising that the nitropyridines **4a**-**d** are more electrophilic than analogously substituted nitrobenzenes. The introduction of a ring nitrogen into nitrobenzene (**3a**) and 4-methoxynitrobenzene (**3b**) increases the electrophilic reactivity by 4 orders of magnitude: 3-Nitropyridine (**4a**) is about 29000 times more reactive than nitrobenzene (**3a**, Figure 4.1), and the 2-position of **4d** is 19000 times more reactive than one of the corresponding positions of **3b**.

The overall reactivity of 4-ethoxy-3-nitropyridine (**4c**, $k_{rel} = 1000$) towards **1⁻** is approximately 17 times lower than the activity of 2-methoxy-5-nitropyridine (**4d**). Since it is known that the orientation of the VNS in 6-donor substituted 3-nitropyridines is controlled by the conjugation of NO_2 with these substituents,[28] the activating effect of a nitro group depends strongly on the orientation of such substituents. With the assumption that the electronic effects of methoxy and ethoxy are similar (Hammett σ), the comparison of compounds **4c** and **4d** shows that the activating effect of a nitro group is more reduced by alkoxy groups in *ortho*-position than by alkoxy groups in *para*-position. Similar effects were observed for 2- and 4-methoxynitrobenzenes.[14]

2-Chloro-3-nitropyridine (**4b**, $k_{rel} = 87000$) is only 1.1 times more reactive than 3-nitropyridine (**4a**), indicating a neglible activating effect by chlorine. On the other hand, chlorine has a noticeable activating effect in the benzene series, and 2-chloro-nitrobenzene is 6.4 times more reactive towards **1⁻** than nitrobenzene (**3a**).[13, 14] The preferred attack of **1⁻** at position 4 in 3-nitropyridine (**4a**) is in good agreement with the relative reactivities of different chloro-substituted 3-nitropyridines in nucleophilic aromatic substitutions of chloride.[44] 4-Chloro-3-nitropyridine reacts 16 times faster with pyridine than 2-chloro-5-nitropyridine and 31 times faster than 2-chloro-3-nitropyridine.

Pyrrole is around 10^{10} times more nucleophilic than benzene,[45] due to its higher π-electron density and lower aromaticity. Remarkably, in the case of Vicarious Nucleophilic Substitution the electrophilicities of the nitropyrroles **5a** and **5b** are comparable to that of nitrobenzene (**3a**), indicating that the increased electron density in pyrroles is compensated by the reduced aromaticity. Thereby, 1-methyl-3-nitropyrrole (**5b**, $k_{rel} = 5.0$) is 5 times more reactive than its 2-nitro isomer **5a** ($k_{rel} = 1.0$).

The same ranking of reactivity was found for the two isomers of *N*-methyl-nitroimidazole (**6a** and **6b**, Scheme 4.4). The 4-nitro compound **6b**, which is structurally related to **5b**, reacts 31 times faster with **1⁻** than *N*-methyl-5-nitroimidazole (**6a**, $k_{rel} = 18$).

Figure 4.2 illustrates that replacement of a CH-group by nitrogen generally increases the electrophilicity of the aromatic ring towards **1⁻**. Comparison with the relative reactivities of nitrobenzene (**3a**) and 3-nitropyridine (**4a**) shows that this effect is much larger in the six-membered than in the five-membered rings. Nitroimidazole **6a** is only activated by a factor of

18 in relation to nitropyrrole **5a**. The position, where the additional nitrogen atom is located in the ring is also important: *N*-Methyl-4-nitroimidazole (**6b**) is activated by a factor of 110, whereas the isomeric nitropyrazole **7** is only 19 times more reactive than **5b**.
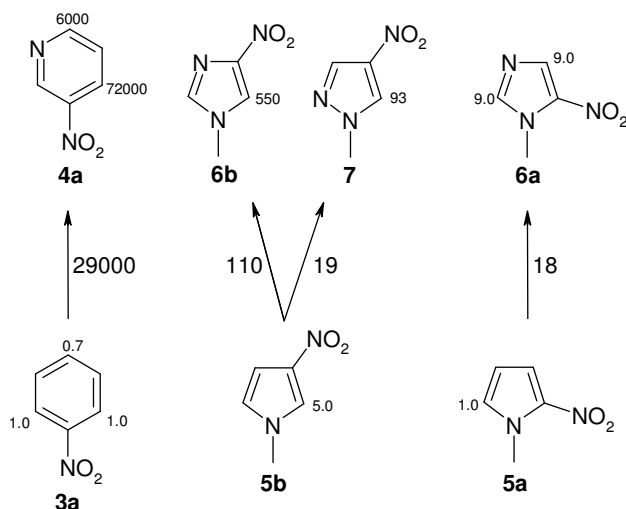
FIGURE 4.2: Effect of an additional nitrogen atom in the ring on the overall activity towards **1⁻**.

Although thiophene is considerably more nucleophilic than benzene, acceptor substituted thiophene derivatives are also known to be more active in S_NAr reactions than analogously substituted benzene derivatives.[46-48] The activity of 2-nitrothiophene (**8**) in the VNS reaction with **1⁻** follows this pattern. With $k_{rel} = 18000$, compound **8** is the most active five-membered heterocycle of Figure 4.1, comparable to the nitropyridines **4a-d**. Possibly the low aromaticity of thiophene and the ability of sulfur to expand its electron octet facilitates the accommodation of the negative charge in the σ_H-adduct and, therefore, enhances the activity in nucleophilic addition reactions.

4.3.2 Quantum Chemical Calculations

The nitro(hetero)arenes **3-8** and the corresponding methyl anion adducts have been calculated with Gaussian03.[49] Structures were optimized at the B3LYP level using the 6-31G(d) basis set. Single point energies have then been calculated at the B3LYP/6-311+G(d,p) level. Combination of these energies with thermochemical corrections derived from a harmonic vibrational frequency analysis at the B3LYP/6-31G(d) level yield the enthalpies H_{298} at 298 K. For detailed information, see the section 4.5.5.

A plot of the logarithms of the partial rate constants versus the calculated methyl anion affinities shows a moderate correlation (Figure 4.3). Multiplication of log k_{rel} with 2.303 RT converts the y-axis of Figure 4.3 into relative activation free energies $\Delta\Delta G^{\ddagger}$. The resulting slope $\Delta\Delta G^{\ddagger}$ / $\Delta\Delta H_{rxn}(CH_3^-)$ = 0.29 indicates that approximately 30% of the calculated differences in gas phase methyl anion affinities are reflected by the relative activation energies in solution. A quantitative interpretation of this ratio is problematic, because it is well-known that the differences of ion stabilization in the gas phase are generally attenuated in solution.[50]

From the small size of this ratio and the significant scatter shown in Figure 4.3 one can conclude, however, that the electrophilicities of the nitroarenes depend on the relative stabilities of the σ-adducts but that other, transition state specific, properties contribute.
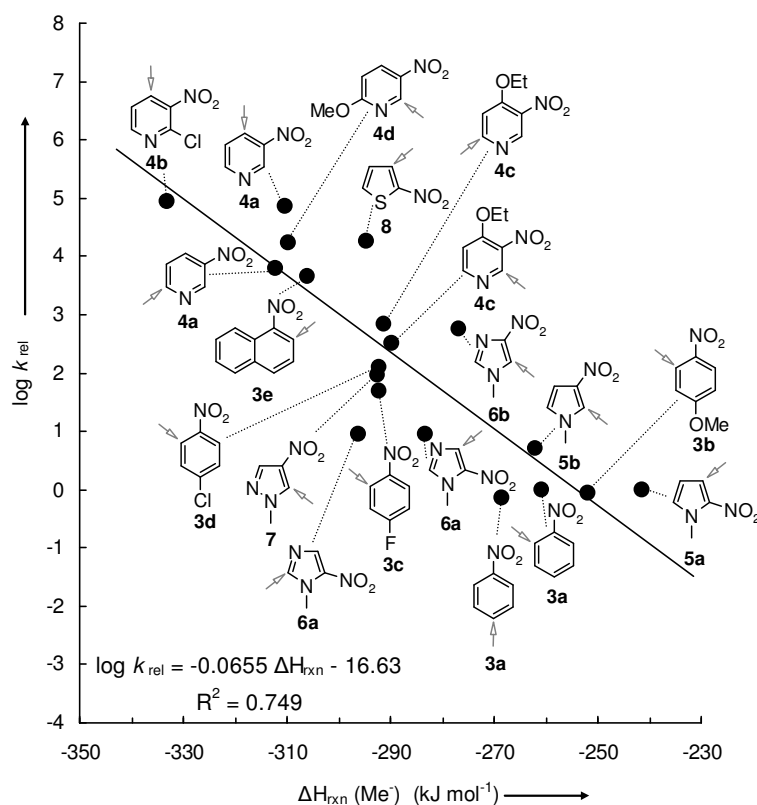
FIGURE 4.3: Correlation of logarithmic relative partial reactivities (−40 °C) of nitro(hetero)arenes versus its methyl anion affinities (B3LYP/6-311+G(d,p)//B3LYP/6-31G(d)).

The correlation between the relative reactivities and the LUMO energies of the nitroarenes is even worse (R^2 = 0.31, Figure 4.4). Nitrobenzene (**3a**) − one of the least reactive electrophiles

− and 2-methoxy-5-nitropyridine (**4d**) − one of the most reactive electrophiles − almost have the same LUMO energies. Thus, LUMO energies by themselves are also not suitable for predicting the relative reactivities of nitro(hetero)arenes. Despite the poor correlations, one observation might be significant: Systems, which strongly deviate in a positive or negative direction from the correlation in Figure 4.3 usually deviate in the same direction in the (log k_{rel})/E_{LUMO} correlation (Figure 4.4). Therefore, one might argue that systems where the $\Delta G°$ and frontier orbital term enforce each other, give rise to the deviations in one or the other direction. We hesitate to interpret these data more quantitatively because neither the relative stabilities of the adducts (Figure 4.3) nor the relative magnitudes of the LUMO coefficients (see Experimental section) can correctly predict the regioselectivity of the nucleophilic attack at compounds **3a**, **4a**, **4b**, and **6a**. A special effect directing into the *ortho*-position of the nitro group seems to be operating. Though one might consider the positive counter ions being responsible for this orientation, the rate constants are independent of the nature of the counter ion.
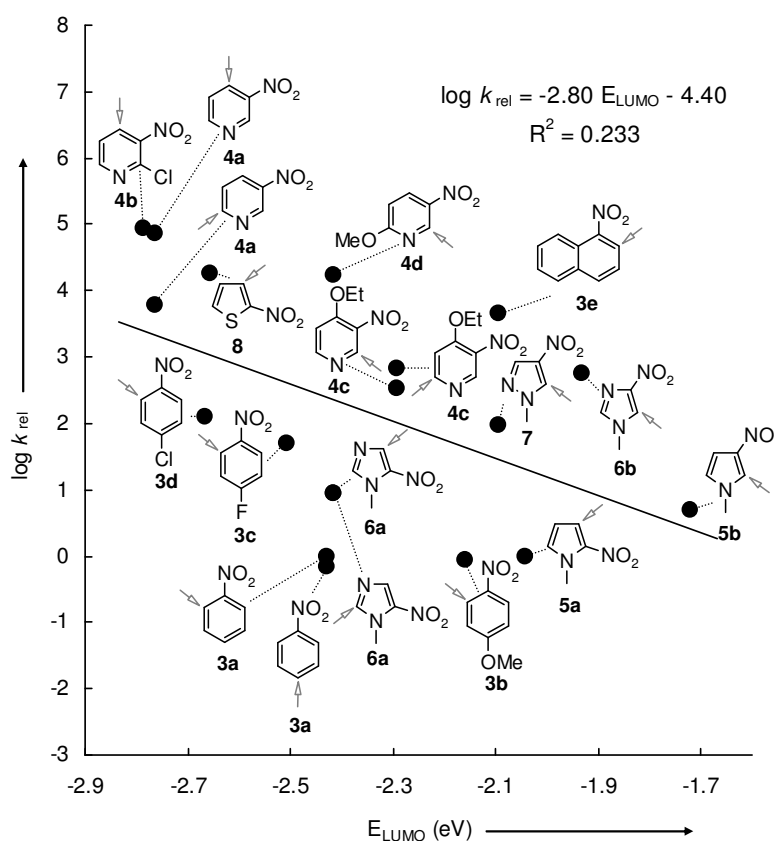
FIGURE 4.4: Correlation of logarithmic relative partial reactivities (−40 °C) of nitro(hetero)arenes versus the corresponding LUMO energy (B3LYP/6-31G(d)).

4.3.3 Comparison of Aromatic and Aliphatic Electrophiles

From the second-order rate constants k_2 of the reactions of 1^- with **10a-c** and **3b,d** at $-40\,°C$ in DMF (Table 4.2), one can derive that the electrophilicities of the benzylidenemalonates **10a-c** are in between those of **3b** and **3d** (Figure 4.5).
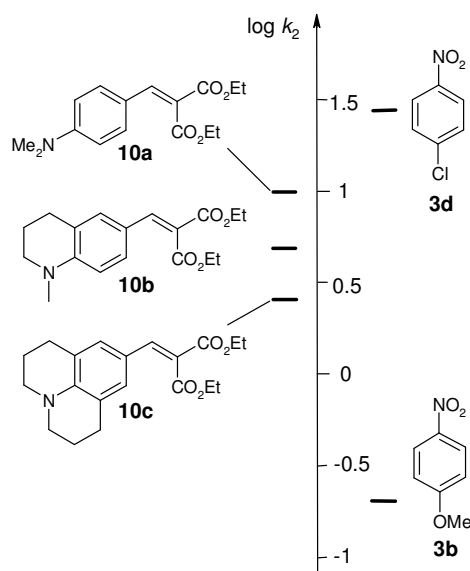
FIGURE 4.5: Second-order rate constants $(L\,mol^{-1}\,s^{-1})$ for the additions of 1^- to aromatic and vinylic electrophiles (DMF, $-40\,°C$).

Because electrophilicity parameters E for compounds **10a-c** have recently been determined,[51] we can now include the nitroarenes **3-8** (Figure 4.1) into the comprehensive electrophilicity scale based on the correlation equation 4.2.[43]

$$\log k_2\,(20\,°C) = s\,(N + E) \tag{4.2}$$

s = nucleophile-specific slope parameter, N = nucleophilicity parameter, E = electrophilicity parameter.

For that purpose, the relative rate constants at $-40\,°C$ given in Figure 4.1 have to be converted into second-order rate constants $(L\,mol^{-1}\,s^{-1})$ at $20\,°C$. From the ratio k_2 (Table 2) / k_{rel} (Figure 4.1) for the reaction of 1^- with **3b** (0.126) and **3d** (0.111) one can derive that multiplication of k_{rel} from Figure 4.1 with the average value 0.119 yields the second-order rate constants $(-40\,°C,\,DMF)$ for the reactions of 1^- with the nitroarenes **3-8**. From the temperature dependence of the reaction of 1^- with **10b** in DMF an activation entropy of

$\Delta S^{\ddagger} = -111 \text{ J mol}^{-1} \text{ K}^{-1}$ was determined (see footnote [f] of Table 4.2). As expected, this value is of the same order of magnitude as those for other combinations of carbanions with neutral electrophiles in DMF (Table 4.3) and was, therefore, used to transform the second-order rate constants at $-40\,°C$ into values at $20\,°C$ according to equation 4.3.

$$k_{T_2} = e^{\left\{\ln T_2 + \ln\left(\frac{k_b}{h}\right) + \frac{\Delta S^{\neq}}{R} - \left[\frac{T_1}{T_2}\left(\ln\frac{T_1}{k_{T_1}} + \ln\frac{k_b}{h} + \frac{\Delta S^{\neq}}{R}\right)\right]\right\}} \tag{4.3}$$

k_{T_2}	second-order rate constant at temperature T_2
k_{T_1}	second-order rate constant at temperature T_1
R	gas constant

k_b	Boltzman's constant
h	Planck's constant
$\Delta S^{\ddagger}$	Eyring activation entropy

TABLE 4.4: Calculation of second-order rate constants k_2 (DMF, 20 °C) for the reactions of **1⁻** with the nitroarenes **3-8** from the corresponding relative rate constants at −40 °C.

	k_{rel} (−40 °C)[a]	k_2 (−40 °C)[b]	$k_{2,\text{calc}}$ (−40 °C)[c]	$k_{2,\text{calc}}$ (20 °C)[d]
	/ M^{-1} s^{-1}	/ M^{-1} s^{-1}	/ M^{-1} s^{-1}	/ M^{-1} s^{-1}
4b	8.7×10^4	-	1.0×10^4	5×10^4
4a	7.8×10^4	-	9.3×10^3	5×10^4
8	1.8×10^4	-	2.1×10^3	1×10^4
4d	1.7×10^4	-	2.0×10^3	1×10^4
3e	4.6×10^3	-	5.5×10^2	5×10^3
3f	-	1.95×10^2	2.0×10^2	2×10^3
4c	1.0×10^3	-	1.2×10^2	2×10^3
6b	5.5×10^2	-	6.6×10^1	9×10^2
3d	2.5×10^2	2.77×10^1	3.0×10^1	5×10^2
3c	1.0×10^2	-	1.2×10^1	2×10^2
7	9.3×10^1	-	1.1×10^1	2×10^2
10a	-	10.1	1.0×10^1	2×10^2
10b	-	4.65	4.7	1×10^2
10c	-	2.64	2.6	7×10^1
6a	1.8×10^1	-	2.1	6×10^1
5b	5.0	-	6.0×10^{-1}	2×10^1
3a	2.7	-	3.2×10^{-1}	1×10^1
3b	1.8	2.26×10^{-1}	2.1×10^{-1}	1×10^1
5a	1.0	-	1.2×10^{-1}	6

[a] From competition experiments (Figure 1). [b] From direct rate measurements (Table 2). [c] Calculated by multiplication of k_{rel} with the average factor 0.119. [d] Calculated with $\Delta S^{\ddagger} = -111 \text{ J mol}^{-1} \text{ K}^{-1}$ (for details see the Experimental Section).

Figure 4.6 shows a linear correlation between the rate constants ($\log k_2$) of the reactions of $\mathbf{1}^-$ with $\mathbf{10a\text{-}c}$ at 20 °C (from Table 4.4, last column) versus the E-parameters of these electrophiles. According to equation 4.2, the slope yields $s = 0.64$ and the intercept on the abscissa gives $N = 26.64$ for the carbanion $\mathbf{1}^-$ in DMF.
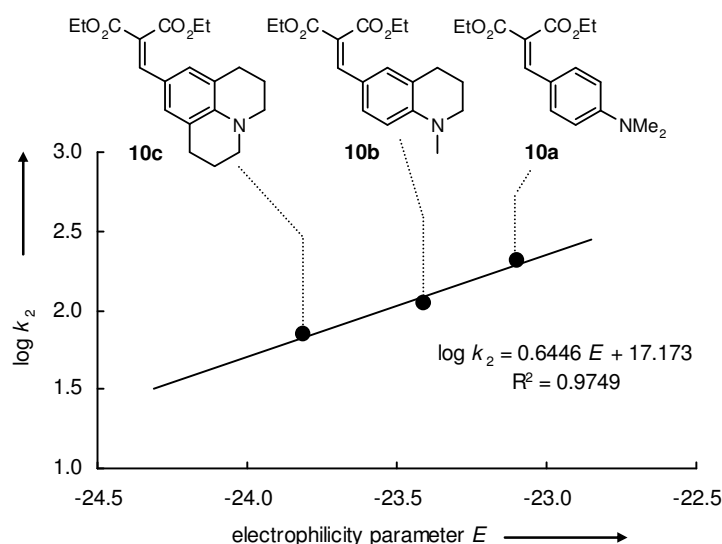
FIGURE 4.6: Plot of $\log k_2$ for the reactions of $\mathbf{1}^-$ with $\mathbf{10a\text{-}c}$ (20 °C, DMF, Table 4.4) versus the electrophilicity parameters E of the benzylidenemalonates $\mathbf{10a\text{-}c}$.

Substitution of N and s for $\mathbf{1}^-$ and the value of $\log k_{2,\text{ calc}}$ (20 °C) from Table 4.4 into equation 4.2 allows to calculate the electrophilicity parameters E for the nitroheteroarenes $\mathbf{3\text{-}8}$, which are depicted in Figure 4.7 along with several previously characterized electrophiles.

It should be noted that the slope parameter s for the carbanion $\mathbf{1}^-$ was derived from only three rate constants with electrophiles in a relatively narrow range of reactivity. For that reason, the E-values for electrophiles, which differ by several orders of magnitude from those of compounds $\mathbf{10a\text{-}c}$, should be treated with caution.
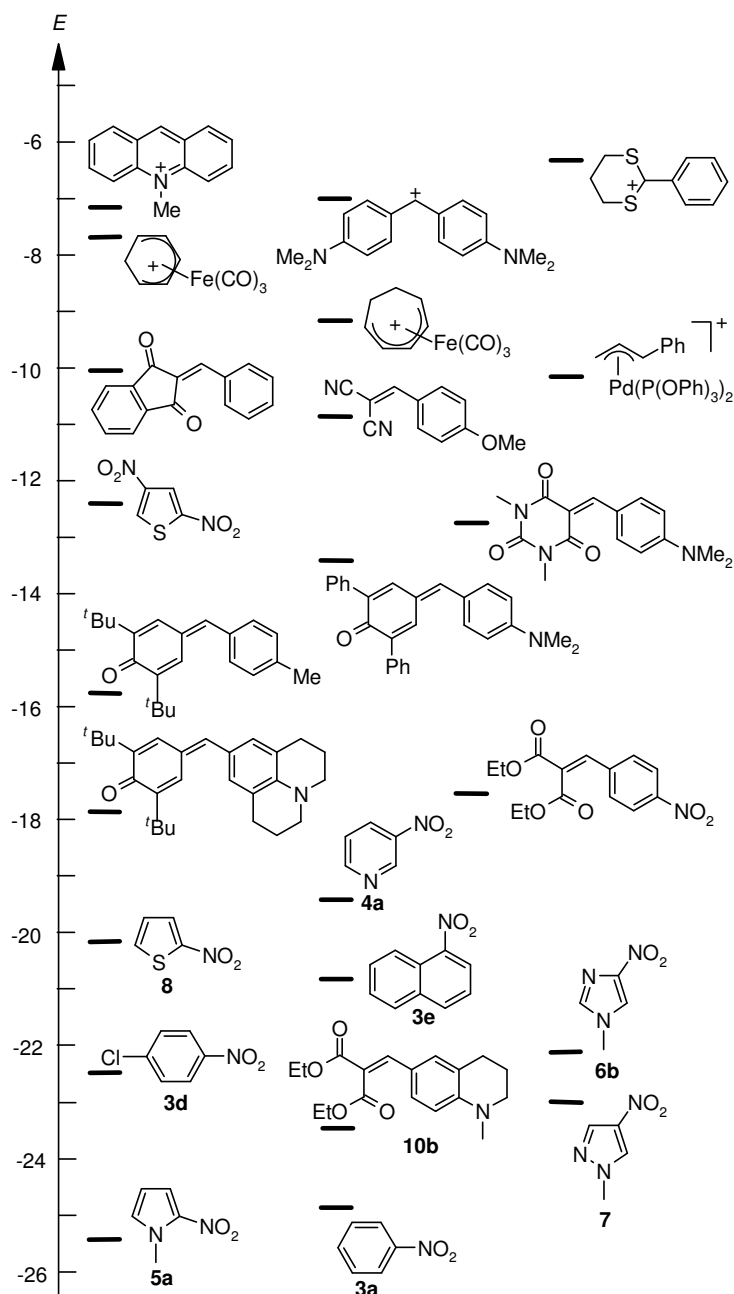
Figure 4.7: Electrophilicity scale according to equation 4.2.

4.4 Conclusion

The UV-Vis spectroscopically determined second-order rate constants for the reactions of the sulfonyl-stabilized carbanion **1⁻** with the aromatic (**3b**, **3d**) and nonaromatic electrophiles (**10a-c**) can be used to link the manifold of relative electrophilic reactivities of nitroheteroarenes in VNS reactions − determined by competition experiments − with the comprehensive electrophilicity scale based on equation 4.2. Because of the uncertainty in the

nucleophilicity parameters N and s for carbanion 1^- in DMF, the E-parameters given in Figure 4.7 should be considered preliminary. However, the comparison of aromatic and nonaromatic electrophiles shown in Figure 4.7 provides a reliable orientation, which can be used to guide synthetic studies until more reliable electrophilicity parameters E for these compounds become available.

4.5 Experimental Section

4.5.1 General Comments

^{1}H and ^{13}C NMR chemical shifts are expressed in ppm and refer to TMS. DEPT and HSQC experiments were employed to assign the signals. Syringes used to transfer reagents were purged with nitrogen prior to use. All competitive and preparative VNS reactions were carried out with magnetic stirring in flame dried glassware under an atmosphere of dry nitrogen. Dry DMF was purchased (< 50 ppm H_2O). Cooling of the reaction vessels was performed by using a cryostat unit. The yields of the products in competitive experiments were determined either by gas chromatography or HPLC using diphenyl sulfone as an internal standard. GC was performed with nitrogen as mobile phase and FID detector on Thermo Electron Focus apparatus equipped with MN 25 m × 0.25 mm stainless column packed with fused-silica and automatic injection unit (temperature gradient: 150 °C[2 min] − 8 °C/min − 280°C [10 min]). For HPLC a CC 250/4 Nucleosil® 120−3 normal phase column and n-heptane and ethyl acetate as mobile phase were used (gradient: 0−100% ethyl acetate or 0−50% ethyl acetate in 45 min, detector: UV-Vis).

4.5.2 Synthesis

4.5.2.1 General Procedure for Preparative VNS Reactions

To a solution of **1** (307 mg, 1.61 mmol) in DMF (5 mL) cooled to –40 °C a solution of KO^{t}Bu (452 mg, 2.50 mmol) in DMF (6 mL) was added and the mixture was stirred for 30 s. Then, a solution of the appropriate arene or heteroarene in DMF (2 mL) was added and the mixture was stirred for further 5 min at –40 °C followed by the addition of 1 M HCl (15 mL). The mixture was then extracted with CH_2Cl_2 (3 × 40 mL). The combined organic layers were

dried over $MgSO_4$ and the solvent was evaporated. The pure products were isolated by column chromatography over silica gel or recrystallization from EtOH.

2-Benzenesulfonylmethyl-4-ethoxy-3-nitropyridine (4co). Colorless crystals, 23% yield, mp 146−147 °C (EtOH). ^{1}H NMR (400 MHz, $CDCl_3$): δ 1.45 (t, ^3J = 7.2 Hz, 3 H, $CH_2C\underline{H}_3$), 4.21 (q, ^3J = 7.2 Hz, 2 H, $C\underline{H}_2CH_3$), 4.73 (s, 2 H, CH_2), 6.96 (d, ^3J = 5.7 Hz, 1 H, 5-H), 7.52−7.80 (m, 5 H, C_6H_5), 8.42 (d, ^3J = 5.9 Hz, 1 H, 6-H). ^{13}C NMR (100.6 MHz, $CDCl_3$): δ 14.1 (CH_3), 60.2 (CH_2-S), 66.0 ($\underline{C}H_2CH_3$), 108.9 (C-5), 128.4 (C_{Ar}-H), 129.2 (C_{Ar}-H), 134.1 (C_{Ar}-H), 138.5 (C_{Ar}), 139.5 (C_{Ar}), 142.5 (C_{Ar}), 151.9 (C6), 157.5 (C_{Ar}). MS (ESI): 667.4 [2M+Na]$^+$, 345.3 [M+Na]$^+$, 323.3 [MH]$^+$. MS (EI) m/z (%) = 323 (3) [MH]$^+$, 257 (11), 241 (23), 213 (21), 171 (10), 165 (30), 154 (12), 153 (32), 141 (11), 125 (12), 110 (17), 107 (11), 95 (32), 83 (20), 77 (100), 55 (18), 54 (11), 52 (18), 51 (37). $C_{14}H_{14}N_2O_5S$ (322.3): Calc. C 52.17, H 4.38, N 8.69, S 9.95; found C 52.08, H 4.40, N 8.68, S 10.14.

6-Benzenesulfonylmethyl-4-ethoxy-3-nitropyridine (4cp). Pale yellow crystals, 57% yield, mp 150−151 °C (EtOH). ^{1}H NMR (400 MHz, $CDCl_3$): δ 1.53 (t, ^3J = 7.2 Hz, 3 H, $CH_2C\underline{H}_3$), 4.30 (q, ^3J = 7.0 Hz, 2 H, $C\underline{H}_2CH_3$), 4.57 (s, 2 H, CH_2-S), 7.23 (s, 1 H, 2-H), 7.53−7.74 (m, 5 H, C_6H_5), 8.74 (s, 1 H, 5-H). ^{13}C NMR (100.6 MHz, $CDCl_3$): δ 14.1 (CH_3), 64.3 (CH_2-S), 66.2 ($\underline{C}H_2CH_3$), 111.1 (C-5), 128.3 (C_{Ar}-H), 129.3 (C_{Ar}-H), 134.2 (C_{Ar}-H), 136.1 (C_{Ar}), 137.9 (C_{Ar}), 146.5 (C-2), 154.6 (C_{Ar}), 158.5 (C_{Ar}). MS (ESI): 667.4 [2M+Na]$^+$, 345.3 [M+Na]$^+$, 323.4 [MH]$^+$. MS (EI) m/z (%) = 258 (52), 257 (100), 230(11), 229 (63), 183 (16), 107 (17), 78 (11), 77 (66), 51 (29), 39 (14). $C_{14}H_{14}N_2O_5S$ (322.3): Calc. C 52.17, H 4.38, N 8.69, S 9.95; found C 52.04, H 4.41, N 8.79, S 10.03.

5-Benzenesulfonylmethyl-4-nitroimidazole (7o). Pale green crystals, 86% yield, mp 193−195 °C (EtOH). ^{1}H NMR (300 MHz, $CDCl_3$): δ 4.10 (s, 3 H, CH_3), 4.95 (s, 2 H, CH_2), 7.49−7.72 (m, 5 H, C_{Ar}-H), 8.01 (s, 1 H, 3-H). ^{13}C NMR (75.5 MHz, $CDCl_3$): δ 38.8 (CH_3), 51.4 (CH_2), 128.5 (2 C_{Ar}-H), 129.4 (2 C_{Ar}-H), 129.7 (2 C_{Ar}), 134.9 (C_{Ar}-H), 136.0 (C_{Ar}-H), 136.9 (C_{Ar}). Calc. C 46.97, H 3.94, N 14.94, S 11.40; found C 47.04, H 3.95, N 14.92, S 11.76.

2-[2-Benzenesulfonyl-2-chloro-1-(4-dimethylamino-phenyl)-ethyl]-malonic acid diethyl ester (10a): A 0.52 M solution of KO^{t}Bu in DMF (0.96 mL, 0.50 mmol) was added slowly to a solution of **1** (0.50 mmol) in DMF (5 mL) at −40 °C. The mixture was stirred for 2 min before

a solution of **9a** (0.50 mmol) in DMF (2.5 mL) was added dropwise within 1 min. After 20 min the mixture was allowed to warm up to 0 °C, poured into cooled 3% aqueous HCl (100 mL), and then extracted with ethyl acetate (3 × 20 mL). After drying over MgSO$_4$ and removal of the solvent in vacuo at room temperature, purification of the residue by column chromatography (SiO$_2$, hexane / ethyl acetate 3:1) yielded 69% of a yellow oil. ^{1}H NMR (300 MHz, CDCl$_3$): δ 1.04 (t, ^3J = 7.2 Hz, 3 H, CH$_2$CH$_3$), 1.24 (t, ^3J = 7.2 Hz, 3 H, CH$_2$CH$_3$), 2.91 (s, 6 H, N(CH$_3$)$_2$), 3.97 (q, ^3J = 7.2 Hz, 2 H, CH$_2$CH$_3$), 4.18 (q, ^3J = 7.2 Hz, 2 H, CH$_2$CH$_3$), 4.20 (dd, ^3J = 9.2 Hz, ^3J = 6.2 Hz, 1 H, CH), 4.53 (d, ^3J = 9.0 Hz, 1 H, CH), 5.59 (d, ^3J = 6.3 Hz, 1 H, CH), 6.56 (d, ^3J = 8.7 Hz, 2 H, C$_{Ar}$H), 7.24 (d, ^3J = 9.0 Hz, 2 H, C$_{Ar}$H), 7.43–7.60 (m, 3 H, C$_{Ar}$-H), 7.74–7.77 (m, 2 H, C$_{Ar}$H). ^{13}C NMR (75.5 MHz, CDCl$_3$): δ 13.9 (CH$_2$CH$_3$), 14.1 (CH$_2$CH$_3$), 40.5 (N(CH$_3$)$_2$), 47.3 (CH), 55.4 (CH(CO$_2$Et)$_2$), 61.6 (CH$_2$), 62.0 (CH$_2$), 76.0 (CHCl), 112.0 (2 × C$_{Ar}$-H), 121.9 (C$_{Ar}$), 129.1(C$_{Ar}$-H), 129.3 (C$_{Ar}$-H), 131.0 (2 × C$_{Ar}$-H), 134.1 (C$_{Ar}$-H), 137.9 (C$_{Ar}$-S), 150.4 (C$_{Ar}$-N), 167.6 (CO$_2$Et), 168.2 (CO$_2$Et). MS (EI) m/z (%) = 481.1 (22) [M$^+$], 341.1 (21), 340.1 (17), 339.1 (77), 293.2 (16), 292.2 (100), 219.1 (28), 183.1 (25), 182.1 (14), 181.1 (97), 180.1 (20), 174.1 (31), 158.1 (25), 146.1 (12), 145.1 (18), 144.1 (15), 77.0 (15). HR-MS (EI): calc: 481.1326, found: 481.1313.

4.5.3 Competition Experiments

4.5.3.1 General Procedure for Competitive VNS Reactions

Chloromethylphenyl sulfone (**1**, 95.3 mg, 0.500 mmol), diphenyl sulfone (**2**, 43.7 mg, 0.200 mmol) and the appropriate competing arenes/heteroarenes were dissolved in DMF (4 mL) in a 10 mL round-bottomed *Schlenk* flask. 1 mL of this mixture was transferred to another 10 mL round-bottomed *Schlenk* flask and cooled to –40 °C. Then, 0.84 mL (0.50 mmol) of a 0.6 M KO^{t}Bu solution in THF was added and the mixture was stirred for 15 s at – 40 °C. After that 1 M HCl (5 mL) and water (5 mL) were added and the mixture was extracted with 4 mL CH$_2$Cl$_2$. The organic layer was dried over MgSO$_4$ and then subjected to GC (injection volume: 1 μL) or HPLC (injection volume: 10 μL). The reaction was repeated three times for every pair.

The product mixtures were analyzed by gas chromatography and high performance liquid chromatography. The product ratios were determined relative to diphenyl sulfone (**2**) as an internal standard. To guarantee the reproducibility of the obtained results, all examined VNS-

products were first isolated on a preparative scale and characterized. Figure 4.8 and Figure 4.9 show typical GC and HPLC chromatograms obtained for a VNS experiment, where 4-methoxy-nitrobenzene (**3b**) was competing with *N*-methyl-3-nitropyrrole (**5b**) for **1⁻**.
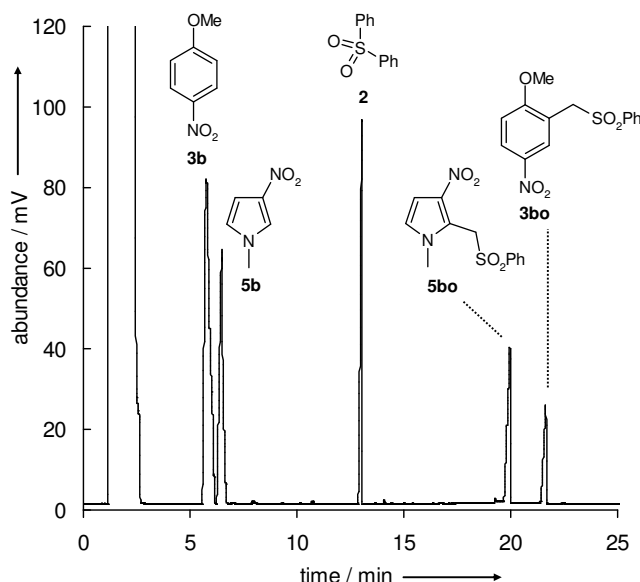
FIGURE 4.8: GC analysis of the product mixture obtained from an experiment in which 4-methoxy-nitrobenzene (**3b**) and 1-methyl-3-nitropyrrole (**5b**) competed for **1⁻** (diphenylsulfone (**2**) as internal standard).
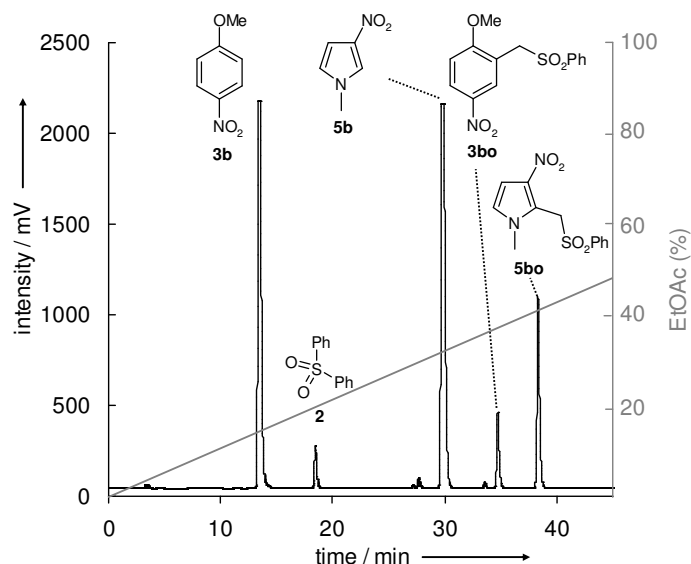
FIGURE 4.9: HPLC analysis of the product mixture obtained from an experiment in which 4-methoxy-nitrobenzene (**3b**) and 1-methyl-3-nitropyrrole (**5b**) competed for **1⁻** (diphenylsulfone (**2**) as internal standard).

The relative activities determined for particular pairs of nitro(hetero)arenes were calculated from the observed product ratios with equation 4.4.

$$\frac{k_A}{k_B} = \frac{\ln\left(\dfrac{[A]_0 - \sum[P_A]}{[A]_0}\right)}{\ln\left(\dfrac{[B]_0 - \sum[P_B]}{[B]_0}\right)} \qquad (4.4)$$

$[A]_0$ and $[B]_0$ are starting concentrations of the nitro(hetero)arenes; $[P_A]$ and $[P_B]$ are the concentrations of reaction products of nitroarenes A and B, respectively.

4.5.3.2 Calibration Factors for GC/HPLC Analysis

GC and HPLC calibration factors $f_{GC/HPLC}$ for the VNS products of nitro(hetero)arenes were determined according to the following procedure: Approximately $n = 4 \times 10^{-2}$ mmol of a VNS product of a nitro(hetero)arene (P_x^y) and the same amount of diphenylsulfone (**2**) were dissolved in CHCl$_3$ (3 mL), and the resultant solution was injected three times on the GC. In case of HPLC the experiments were only performed once. The integrated peak areas a were evaluated according to equation 4.5:

$$f(P_x^y) = \frac{a(\mathbf{2}) \cdot n(P_x^y)}{a(P_x^y) \cdot n(\mathbf{2})} \qquad (4.5)$$

The calibration factors of the individual injections were averaged (last column of Table 4.5).

TABLE 4.5: GC calibration factors.

X	n / mmol	$a(X)$[a]			f_{GC}[b]			f_{GC}[c]
		I	II	III	I	II	III	
3bo	9.11×10^{-3}	3.50×10^6	3.37×10^6	3.53×10^6	1.50	1.49	1.50	1.49
2	4.40×10^{-2}	2.53×10^7	2.42×10^7	2.55×10^7				
3co	3.89×10^{-2}	1.09×10^7	1.08×10^7	1.01×10^7	1.18	1.14	1.15	1.15
2	5.22×10^{-2}	1.72×10^7	1.65×10^7	1.55×10^7				

TABLE 4.5: Continued.

X	n / mmol	$a(X)$[a] I	II	III	f_{GC}[b] I	II	III	f_{GC}[c]
3do	2.66×10^{-2}	6.95×10^6	7.51×10^6	7.35×10^6	1.33	1.31	1.32	1.32
2	4.49×10^{-2}	1.56×10^7	1.67×10^6	1.64×10^6				
3eo	2.14×10^{-2}	1.02×10^7	5.95×10^6	5.17×10^6	1.93	1.90	1.92	1.92
2	3.48×10^{-2}	3.21×10^7	1.84×10^7	1.62×10^7				
4ao	2.37×10^{-2}	9.58×10^6	1.02×10^7	9.80×10^6	1.32	1.32	1.34	1.33
2	3.39×10^{-2}	1.81×10^7	1.92×10^7	1.88×10^7				
4ap	2.26×10^{-2}	6.95×10^6	6.75×10^6	6.97×10^6	1.78	1.86	1.84	1.83
2	3.99×10^{-2}	2.18×10^7	2.21×10^7	2.26×10^7				
4bo	3.84×10^{-2}	8.25×10^6	8.11×10^6	6.62×10^6	1.48	1.52	1.46	1.49
2	5.04×10^{-2}	1.61×10^7	1.62×10^7	1.27×10^7				
4co	3.32×10^{-2}	3.64×10^6	3.49×10^6	3.73×10^6	3.40	3.30	3.34	3.35
2	4.58×10^{-2}	1.71×10^7	1.59×10^7	1.72×10^6				
4cp	2.30×10^{-2}	4.20×10^6	3.50×10^6	3.59×10^6	2.01	2.05	2.02	2.03
2	3.48×10^{-2}	1.28×10^7	1.09×10^7	1.10×10^7				
4do	1.91×10^{-2}	6.82×10^6	6.90×10^6	7.20×10^6	1.61	1.64	1.60	1.61
2	2.79×10^{-2}	1.60×10^7	1.65×10^7	1.68×10^7				
5ap	3.03×10^{-2}	4.01×10^6	4.23×10^6	4.03×10^6	4.74	4.65	4.84	4.74
2	3.34×10^{-2}	2.10×10^7	2.17×10^7	2.15×10^7				
5bo	2.46×10^{-2}	1.04×10^7	9.77×10^6	9.63×10^6	1.64	1.69	1.74	1.69
2	2.52×10^{-2}	1.75×10^7	1.69×10^7	1.72×10^7				
6ao	4.83×10^{-2}	3.97×10^6	3.98×10^6	3.98×10^6	3.87	3.93	3.92	3.91
2	5.13×10^{-2}	1.63×10^7	1.66×10^7	1.66×10^7				
6ap	3.16×10^{-2}	9.38×10^5	8.37×10^5	9.02×10^5	14.2	15.3	14.4	14.6
2	3.34×10^{-2}	1.41×10^7	1.35×10^7	1.37×10^7				

TABLE 4.5: Continued.

X	n / mmol	$a(X)$[a]			f_{GC}[b]			f_{GC}[c]
		I	II	III	I	II	III	
6bo	2.45×10^{-2}	1.86×10^{6}	1.78×10^{6}	1.58×10^{6}	6.44	6.42	6.47	6.44
2	3.25×10^{-2}	1.44×10^{7}	1.37×10^{7}	1.22×10^{7}				
7o	2.84×10^{-2}	1.07×10^{7}	1.06×10^{7}	1.10×10^{7}	1.59	1.59	1.59	1.59
2	5.31×10^{-2}	3.18×10^{7}	3.16×10^{7}	3.28×10^{7}				
8o	2.61×10^{-2}	4.72×10^{6}	4.90×10^{6}	4.77×10^{6}	2.92	2.88	2.89	2.89
2	4.86×10^{-2}	2.56×10^{7}	2.62×10^{7}	2.56×10^{7}				

[a] Integrated peak area. [b] Calibration factor. [c] Averaged calibration factor.

TABLE 4.6: HPLC calibration factors.

X	n / mmol	$a(X)$[a]	$f_{HPLC}(X)$[b]
3bo[c]	3.29×10^{-2}	1.30×10^{7}	6.63×10^{-2}
2[c]	5.04×10^{-2}	1.32×10^{6}	
3co	3.89×10^{-2}	9.32×10^{6}	2.63×10^{-1}
2	5.22×10^{-2}	3.28×10^{6}	
3do	3.85×10^{-2}	9.28×10^{6}	1.92×10^{-1}
2	5.27×10^{-2}	2.44×10^{6}	
3eo	2.14×10^{-2}	1.65×10^{7}	2.04×10^{-1}
2	3.48×10^{-2}	5.49×10^{6}	
4ao	2.37×10^{-2}	2.15×10^{7}	2.92×10^{-1}
2	3.39×10^{-2}	8.98×10^{6}	
4ap	2.26×10^{-3}	3.96×10^{7}	1.54×10^{-1}
2	3.99×10^{-2}	1.07×10^{7}	
4bo	3.84×10^{-2}	5.51×10^{6}	4.92×10^{-1}
2	5.04×10^{-2}	3.56×10^{6}	
4co	3.94×10^{-2}	2.97×10^{6}	6.77×10^{-1}
2	5.27×10^{-2}	2.69×10^{6}	

TABLE 4.6: Continued.

X	n / mmol	$a(X)^{[a]}$	$f_{HPLC}(X)^{[b]}$
4cp	3.66×10^{-2}	8.17×10^6	2.49×10^{-1}
2	5.04×10^{-2}	2.80×10^6	
4do	4.02×10^{-2}	1.41×10^7	2.21×10^{-1}
2	5.04×10^{-2}	3.92×10^6	
5bo	4.03×10^{-2}	1.46×10^7	2.75×10^{-1}
2	5.27×10^{-2}	5.23×10^6	
6ao[c]	4.83×10^{-2}	4.74×10^6	1.00×10^{-1}
2[c]	5.13×10^{-2}	5.06×10^5	
6ap[c]	4.66×10^{-2}	1.23×10^7	1.00×10^{-1}
2[c]	5.13×10^{-2}	1.36×10^6	
6bo	3.70×10^{-2}	5.41×10^6	4.61×10^{-1}
2	5.18×10^{-2}	3.49×10^6	
7o	2.52×10^{-2}	2.15×10^7	1.73×10^{-1}
2	5.41×10^{-2}	7.96×10^6	
8o	4.45×10^{-2}	1.32×10^7	3.40×10^{-1}
2	5.27×10^{-2}	5.31×10^6	

[a] Integrated peak area. [b] Calibration factor. [c] Evaluation at 280 nm.

4.5.3.3 Competition Experiments with Nitropyridines *4a*-*d*
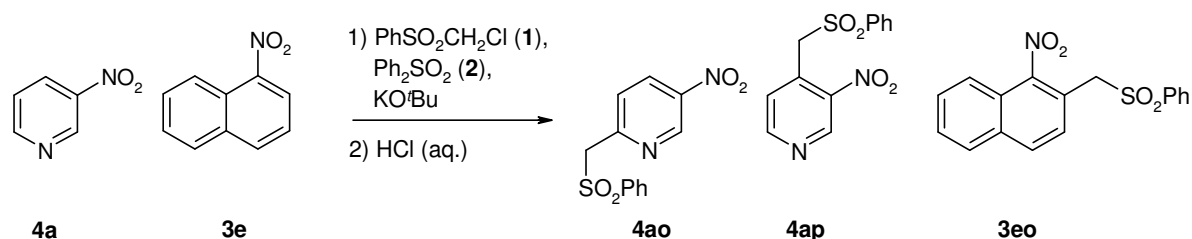
$n(\mathbf{1}) = 0.125$ mmol, $n(\mathbf{2}) = 0.056$ mmol, $n(\mathbf{4a}) = 0.176$ mmol, $n(\mathbf{3e}) = 0.527$ mmol, $n(\mathrm{KO}^t\mathrm{Bu}) = 0.500$ mmol

no.	$a(\mathbf{1})^{[a]}$	$a(\mathbf{2})^{[a]}$	$a(\mathbf{4ao})^{[a]}$	$a(\mathbf{4ap})^{[a]}$	$a(\mathbf{3eo})^{[a]}$	$\dfrac{k(\mathbf{4a})}{k(\mathbf{3e})}$	$\dfrac{k(\mathbf{4a}^o)}{k(\mathbf{4a}^p)}$
$1_{(GC)}$	0	1.15×10^7	7.94×10^6	5.86×10^5	1.28×10^6	1.7×10^1	9.8
	0	1.32×10^7	9.70×10^6	7.23×10^5	1.51×10^6	1.8×10^1	9.7
	0	1.29×10^7	9.20×10^6	6.86×10^5	1.45×10^6	1.7×10^1	9.7
$2_{(GC)}$	0	1.16×10^7	7.55×10^6	4.10×10^5	1.25×10^6	1.6×10^1	1.3×10^1
	0	1.14×10^7	7.53×10^6	4.11×10^5	1.26×10^6	1.6×10^1	1.3×10^1
	0	1.13×10^7	6.80×10^6	3.66×10^5	1.09×10^6	1.6×10^1	1.4×10^1
$3_{(GC)}$	0	1.09×10^7	7.22×10^6	4.63×10^5	1.14×10^6	1.7×10^1	1.1×10^1
	0	1.17×10^7	8.29×10^6	5.22×10^5	1.42×10^6	1.6×10^1	1.2×10^1

[a] Integrated peak area.

$k(\mathbf{4a})/k(\mathbf{3e}) = (1.7 \pm 0.1) \times 10^1$, $k(\mathbf{4a}^o)/k(\mathbf{4a}^p) = (1.2 \pm 0.2) \times 10^1$

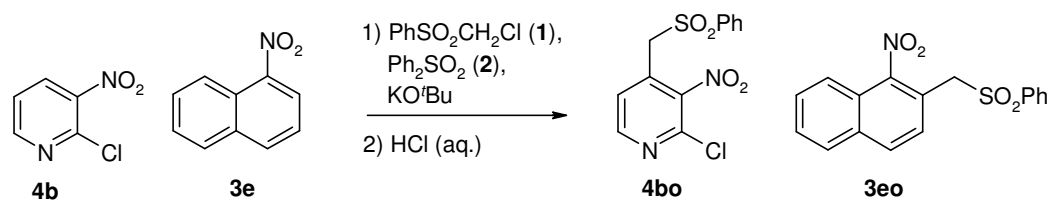| no.	$a(\mathbf{1})^{[a]}$	$a(\mathbf{2})^{[a]}$	$a(\mathbf{4ao})^{[a]}$	$a(\mathbf{4ap})^{[a]}$	$a(\mathbf{3eo})^{[a]}$	$\dfrac{k(\mathbf{4a})}{k(\mathbf{3e})}$	$\dfrac{k(\mathbf{4a}^o)}{k(\mathbf{4a}^p)}$
$1_{(HPLC)}$	0	5.80×10^6	2.63×10^7	4.07×10^6	1.23×10^7	1.3×10^1	1.2×10^1
$2_{(HPLC)}$	0	6.15×10^6	2.79×10^7	4.97×10^6	1.35×10^7	1.3×10^1	1.1×10^1
$3_{(HPLC)}$	0	5.32×10^6	2.33×10^7	3.02×10^6	1.16×10^7	1.2×10^1	1.5×10^1

[a] Integrated peak area.

$k(\mathbf{4a})/k(\mathbf{3e}) = (1.3 \pm 0.1) \times 10^1$, $k(\mathbf{4a}^o)/k(\mathbf{4a}^p) = (1.2 \pm 0.2) \times 10^1$

$n(\mathbf{1}) = 0.125$ mmol, $n(\mathbf{2}) = 0.050$ mmol, $n(\mathbf{4b}) = 0.150$ mmol, $n(\mathbf{3e}) = 0.600$ mmol, $n(\text{KO}^t\text{Bu}) = 0.500$ mmol

no.	$a(\mathbf{1})$[a]	$a(\mathbf{2})$[a]	$a(\mathbf{4bo})$[a]	$a(\mathbf{3eo})$[a]	$\dfrac{k(\mathbf{4b})}{k(\mathbf{3e})}$
$1_{(GC)}$	0	3.75×10^6	1.72×10^6	3.12×10^5	1.9×10^1
	0	3.88×10^6	1.70×10^6	2.92×10^5	2.0×10^1
	0	3.71×10^6	1.70×10^6	3.13×10^5	1.9×10^1
$2_{(GC)}$	0	4.89×10^6	2.83×10^6	5.56×10^5	1.8×10^1
	0	5.03×10^6	2.99×10^6	6.06×10^5	1.8×10^1
	0	5.04×10^6	3.08×10^6	6.55×10^5	1.7×10^1
$3_{(GC)}$	0	3.86×10^6	2.22×10^6	4.53×10^5	1.8×10^1
	0	3.53×10^6	1.80×10^6	3.07×10^5	2.1×10^1
	0	3.77×10^6	2.23×10^6	4.79×10^5	1.9×10^1

[a] Integrated peak area.

$k(\mathbf{4b})/k(\mathbf{3e}) = (1.9 \pm 0.1) \times 10^1$

no.	$a(\mathbf{1})$[a]	a $(\mathbf{2})$[a]	$a(\mathbf{4bo})$[a]	$a(\mathbf{3eo})$[a]	$\dfrac{k(\mathbf{4b})}{k(\mathbf{3e})}$
$1_{(HPLC)}$	0	9.01×10^5	1.50×10^6	8.04×10^5	2.1×10^1
$2_{(HPLC)}$	0	1.77×10^6	4.03×10^6	2.33×10^6	2.1×10^1
$3_{(HPLC)}$	0	1.08×10^6	2.32×10^6	1.32×10^6	2.1×10^1

[a] Integrated peak area.

$k(\mathbf{4b})/k(\mathbf{3e}) = (2.1 \pm 0.01) \times 10^1$
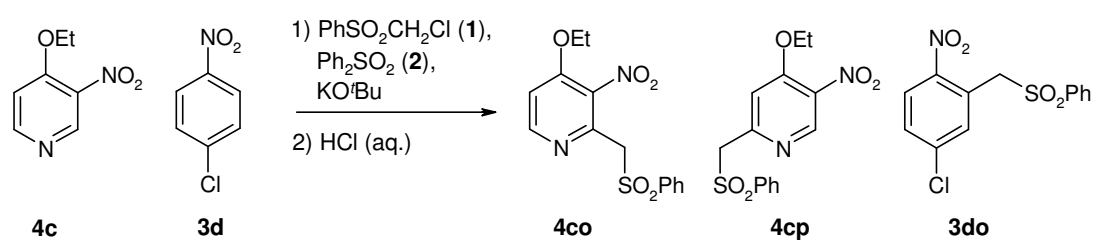
$n(\mathbf{1}) = 0.126$ mmol, $n(\mathbf{2}) = 0.050$ mmol, $n(\mathbf{4c}) = 0.362$ mmol, $n(\mathbf{3d}) = 0.303$ mmol, $n(\mathrm{KO}^t\mathrm{Bu}) = 0.504$ mmol

| no.	$a(\mathbf{1})^{[a]}$	$a(\mathbf{2})^{[a]}$	$a(\mathbf{4co})^{[a]}$	$a(\mathbf{4cp})^{[a]}$	$a(\mathbf{3do})^{[a]}$	$\dfrac{k(\mathbf{4c})}{k(\mathbf{3d})}$	$\dfrac{k(\mathbf{4c}^p)}{k(\mathbf{4c}^o)}$
$1_{(GC)}$	0	5.27×10^6	7.63×10^5	2.37×10^6	9.73×10^5	5.2	1.9
	0	5.74×10^6	7.86×10^5	2.43×10^6	1.02×10^6	5.1	1.9
	0	5.59×10^6	7.20×10^5	2.29×10^6	9.97×10^5	4.8	1.9
$2_{(GC)}$	0	5.05×10^6	7.16×10^5	2.32×10^6	1.16×10^6	4.2	2.0
	0	5.00×10^6	6.83×10^5	2.21×10^6	1.07×10^6	4.3	2.0
	0	4.83×10^6	6.09×10^5	1.97×10^6	9.86×10^5	4.2	2.0
$3_{(GC)}$	0	5.98×10^6	8.62×10^5	2.83×10^6	1.40×10^6	4.2	2.0
	0	6.75×10^6	8.91×10^5	2.96×10^6	1.53×10^6	4.0	2.0
	0	6.41×10^6	8.53×10^5	2.78×10^6	1.39×10^6	4.2	2.0

[a] Integrated peak area.

$k(\mathbf{4c})/k(\mathbf{3d}) = 4.5 \pm 0.4$, $k(\mathbf{4c}^p)/k(\mathbf{4c}^o) = 2.0 \pm 0.04$

no.	$a(\mathbf{1})^{[a]}$	$a(\mathbf{2})^{[a]}$	$a(\mathbf{4co})^{[a]}$	$a(\mathbf{4cp})^{[a]}$	$a(\mathbf{3do})^{[a]}$	$\dfrac{k(\mathbf{4c})}{k(\mathbf{3d})}$	$\dfrac{k(\mathbf{4c}^p)}{k(\mathbf{4c}^o)}$
$1_{(HPLC)}$	0	1.43×10^6	7.81×10^5	5.52×10^6	1.96×10^6	4.6	2.6
$2_{(HPLC)}$	0	8.95×10^5	5.20×10^5	3.73×10^6	1.52×10^6	4.0	2.6
$3_{(HPLC)}$	0	1.74×10^6	1.01×10^6	7.34×10^6	3.02×10^6	3.9	2.7

[a] Integrated peak area.

$k(\mathbf{4c})/k(\mathbf{3d}) = 4.2 \pm 0.3$, $k(\mathbf{4c}^p)/k(\mathbf{4c}^o) = 2.6 \pm 0.03$
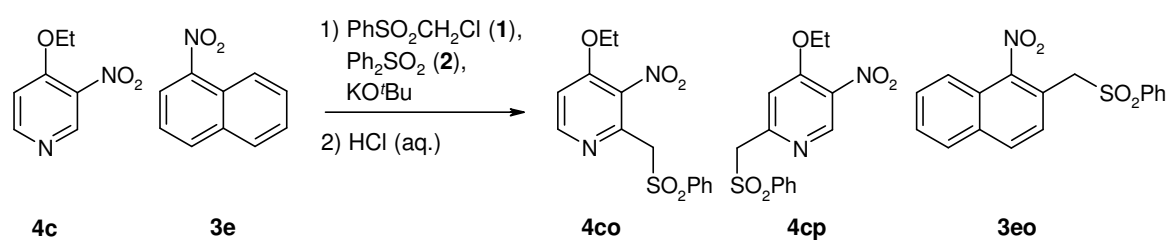
$n(\mathbf{1}) = 0.126$ mmol, $n(\mathbf{2}) = 0.055$ mmol, $n(\mathbf{4c}) = 0.653$ mmol, $n(\mathbf{3e}) = 0.246$ mmol, $n(\mathrm{KO}^t\mathrm{Bu}) = 0.504$ mmol

no.	$a(\mathbf{1})^{[a]}$	$a(\mathbf{2})^{[a]}$	$a(\mathbf{4co})^{[a], [b]}$	$a(\mathbf{4cp})^{[a]}$	$a(\mathbf{3eo})^{[a]}$	$\dfrac{k(\mathbf{3e})}{k(\mathbf{4c})}$
$1_{(GC)}$	0	8.35×10^6		8.20×10^5	2.10×10^6	4.5
	0	7.70×10^6		8.01×10^5	2.15×10^6	4.7
	0	8.42×10^6		9.61×10^5	2.62×10^6	4.8
$2_{(GC)}$	0	6.69×10^6		7.70×10^5	2.12×10^6	4.9
	0	6.88×10^6		7.76×10^5	2.12×10^6	4.8
	0	7.10×10^6		8.07×10^5	2.25×10^6	4.9
$3_{(GC)}$	0	1.03×10^7		8.98×10^5	2.43×10^6	4.7
	0	1.10×10^7		8.53×10^5	2.30×10^6	4.7
	0	1.10×10^7		9.65×10^5	2.62×10^6	4.7

[a] Integrated peak area. [b] Peak in chromatogram is too small and not separated completely from **3eo** so that evaluation is not possible. Thus, the molarity of **4co** in the product mixture is calculated by the known ratio $k(\mathbf{4c}^p)/k(\mathbf{4c}^o) = 2.0 \pm 0.04$.

$k(\mathbf{3e})/k(\mathbf{4c}) = 4.8 \pm 0.1$
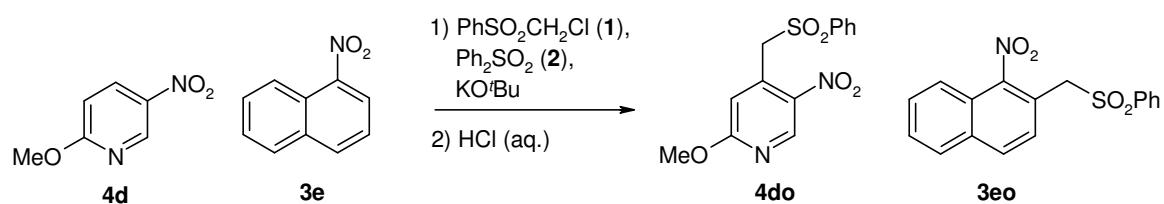
$n(\mathbf{1}) = 0.125$ mmol, $n(\mathbf{2}) = 0.050$ mmol, $n(\mathbf{4d}) = 0.300$ mmol, $n(\mathbf{3e}) = 0.300$ mmol, $n(\mathrm{KO}^t\mathrm{Bu}) = 0.500$ mmol

| no.	$a(\mathbf{1})$[a]	$a(\mathbf{2})$[a]	$a(\mathbf{4do})$[a]	$a(\mathbf{3eo})$[a]	$\dfrac{k(\mathbf{4d})}{k(\mathbf{3e})}$
$1_{(GC)}$	0	3.63×10^6	1.92×10^6	4.55×10^5	3.8
	0	3.62×10^6	2.03×10^6	4.89×10^5	3.7
	0	3.87×10^6	2.03×10^6	4.68×10^5	3.9
$2_{(GC)}$	0	3.63×10^6	1.92×10^6	4.55×10^5	3.8
	0	3.62×10^6	2.03×10^6	4.89×10^5	3.7
	0	3.87×10^6	2.03×10^6	4.68×10^5	3.9
$3_{(GC)}$	0	2.68×10^6	1.24×10^6	3.14×10^5	3.5
	0	2.72×10^6	1.31×10^6	3.42×10^5	3.4
	0	2.75×10^6	1.36×10^6	3.46×10^5	3.5

[a] Integrated peak area.

$k(\mathbf{4d})/k(\mathbf{3e}) = 3.7 \pm 0.2$

no.	$a(\mathbf{1})$[a]	a $(\mathbf{2})$[a]	$a(\mathbf{4do})$[a]	$a(\mathbf{3eo})$[a]	$\dfrac{k(\mathbf{4d})}{k(\mathbf{3e})}$
$1_{(HPLC)}$	0	1.45×10^6	5.64×10^6	2.17×10^6	3.0
$2_{(HPLC)}$	0	1.13×10^6	4.57×10^6	1.25×10^6	4.2
$3_{(HPLC)}$	0	8.92×10^5	3.02×10^6	8.65×10^5	4.0

[a] Integrated peak area.

$k(\mathbf{4d})/k(\mathbf{3e}) = 3.7 \pm 0.5$

4.5.3.4 Competition Experiments with Nitropyrroles **5a**-**b**
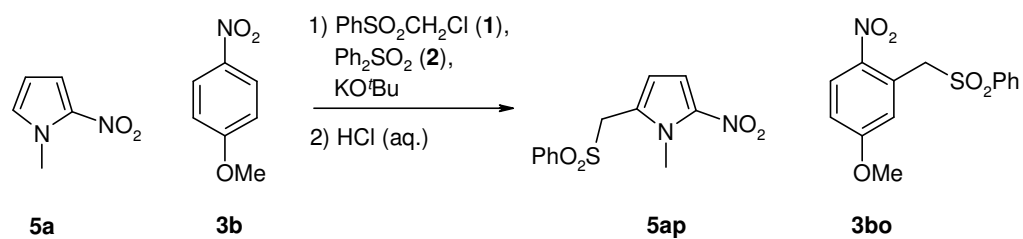
$n(\mathbf{1}) = 0.125$ mmol, $n(\mathbf{2}) = 0.049$ mmol, $n(\mathbf{5a}) = 0.302$ mmol, $n(\mathbf{3b}) = 0.300$ mmol, $n(\mathrm{KO}^{t}\mathrm{Bu}) = 0.500$ mmol

no.	$a(\mathbf{1})$[a]	$a(\mathbf{2})$[a]	$a(\mathbf{5ap})$[a]	$a(\mathbf{3bo})$[a]	$\dfrac{k(\mathbf{3b})}{k(\mathbf{5a})}$
1 (GC)	0	5.31×10^6	3.49×10^5	2.34×10^6	2.2
	0	5.36×10^6	3.28×10^5	2.25×10^6	2.2
	0	5.49×10^6	3.66×10^5	2.52×10^6	2.3
2 (GC)	0	7.01×10^6	5.91×10^5	3.64×10^6	2.0
	0	7.43×10^6	6.08×10^5	3.79×10^6	2.0
	0	7.59×10^6	6.13×10^5	3.86×10^6	2.1
3 (GC)	0	4.98×10^6	3.23×10^5	2.22×10^6	2.2
	0	5.02×10^6	3.26×10^5	2.24×10^6	2.3
	0	5.02×10^6	3.07×10^5	2.09×10^6	2.2

[a] Integrated peak area.

$k(\mathbf{3b})/k(\mathbf{5a}) = 2.2 \pm 0.1$
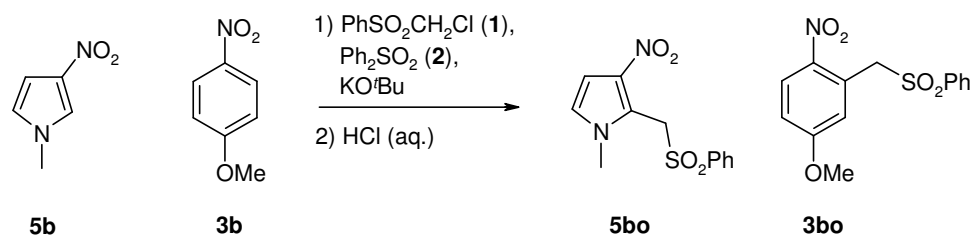
$n(\mathbf{1}) = 0.125$ mmol, $n(\mathbf{2}) = 0.050$ mmol, $n(\mathbf{5b}) = 0.199$ mmol, $n(\mathbf{3b}) = 0.299$ mmol, $n(\mathrm{KO}^t\mathrm{Bu}) = 0.500$ mmol

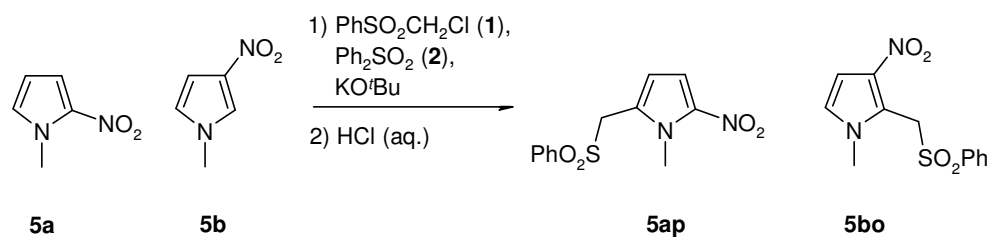| no.	$a(\mathbf{1})^{[a]}$	$a(\mathbf{2})^{[a]}$	$a(\mathbf{5bo})^{[a]}$	$a(\mathbf{3bo})^{[a]}$	$\dfrac{k(\mathbf{5b})}{k(\mathbf{3b})}$
$1_{(GC)}$	0	5.10×10^6	3.21×10^6	1.87×10^6	3.2
	0	5.20×10^6	3.43×10^6	1.99×10^6	3.3
	0	5.57×10^6	3.43×10^6	2.00×10^6	3.2
$2_{(GC)}$	0	6.25×10^6	3.61×10^6	2.60×10^6	2.6
	0	6.69×10^6	3.83×10^6	2.74×10^6	2.6
	0	6.76×10^6	4.06×10^6	2.93×10^6	2.6
$3_{(GC)}$	0	7.72×10^6	4.30×10^6	3.12×10^6	2.5
	0	1.30×10^7	6.36×10^6	4.59×10^6	2.5
	0	1.30×10^7	6.21×10^6	4.48×10^6	2.5

[a] Integrated peak area.

$k(\mathbf{5b})/k(\mathbf{3b}) = 2.8 \pm 0.3$

| no.	$a(\mathbf{1})^{[a]}$	$a(\mathbf{2})^{[a]}$	$a(\mathbf{5bo})^{[a]}$	$a(\mathbf{3bo})^{[a]}$	$\dfrac{k(\mathbf{5b})}{k(\mathbf{3b})}$
$1_{(HPLC)}$	0	3.24×10^6	1.65×10^7	6.00×10^6	3.6
$2_{(HPLC)}$	0	3.25×10^6	1.65×10^7	7.60×10^6	2.8
$3_{(HPLC)}$	0	5.59×10^6	2.95×10^7	1.34×10^7	2.9

[a] Integrated peak area.

$k(\mathbf{5b})/k(\mathbf{3b}) = 3.1 \pm 0.4$

$n(\mathbf{1}) = 0.125$ mmol, $n(\mathbf{2}) = 0.050$ mmol, $n(\mathbf{5a}) = 0.174$ mmol, $n(\mathbf{5b}) = 0.050$ mmol, $n(\text{KO}^t\text{Bu}) = 0.500$ mmol

no.	$a(\mathbf{1})$[a]	$a(\mathbf{2})$[a]	$a(\mathbf{5ap})$[a]	$a(\mathbf{5bo})$[a]	$\dfrac{k(\mathbf{5b})}{k(\mathbf{5a})}$
$1_{(GC)}$	0	1.12×10^7	9.15×10^5	2.96×10^6	5.0
	0	1.08×10^7	8.81×10^5	2.83×10^6	5.0
	0	1.06×10^7	8.59×10^5	2.76×10^6	5.0
$2_{(GC)}$	0	8.42×10^6	1.04×10^6	2.89×10^6	4.7
	0	8.81×10^6	1.04×10^6	2.95×10^6	4.8
	0	8.23×10^6	9.99×10^5	2.80×10^6	4.7
$3_{(GC)}$	0	1.00×10^7	9.04×10^5	3.01×10^6	5.4
	0	9.75×10^6	9.40×10^5	3.11×10^6	5.5
	0	9.21×10^6	9.07×10^5	2.94×10^6	5.4

[a] Integrated peak area.

$k(\mathbf{5b})/k(\mathbf{5a}) = 5.0 \pm 0.3$

4.5.3.5 Competition Experiments with Nitroimidazoles 6a-b
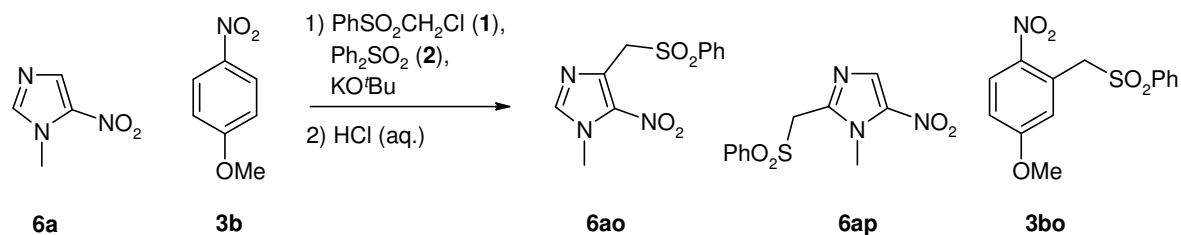
$n(1) = 0.125$ mmol, $n(2) = 0.050$ mmol, $n(6a) = 0.300$ mmol, $n(3b) = 0.300$ mmol, $n(KO^tBu) = 0.500$ mmol

no.	$a(1)^{[a]}$	$a(2)^{[a]}$	$a(6ao)^{[a]}$	$a(6ap)^{[a]}$	$a(3bo)^{[a]}$	$\dfrac{k(6a)}{k(3b)}$	$\dfrac{k(6a^o)}{k(6a^p)}$
$1_{(GC)}$	7.45×10^5	5.43×10^6	6.21×10^5	1.73×10^5	2.80×10^5	1.3×10^1	9.6×10^{-1}
	8.87×10^5	6.56×10^6	7.55×10^5	1.95×10^5	3.44×10^5	1.2×10^1	1.0
	8.90×10^5	8.39×10^6	6.91×10^5	1.93×10^5	3.70×10^5	1.1×10^1	9.6×10^{-1}
$2_{(GC)}$	8.81×10^5	8.51×10^6	7.04×10^5	2.02×10^5	3.75×10^5	1.1×10^1	9.3×10^{-1}
	8.92×10^5	8.40×10^6	7.45×10^5	2.10×10^5	3.99×10^5	1.1×10^1	9.5×10^{-1}
	1.01×10^6	8.28×10^6	7.17×10^5	2.02×10^5	4.40×10^5	9.2	9.5×10^{-1}
$3_{(GC)}$	9.45×10^5	7.76×10^6	5.92×10^5	1.72×10^5	3.56×10^5	9.5	9.2×10^{-1}
	9.81×10^5	8.09×10^6	6.83×10^5	1.97×10^5	4.16×10^5	9.4	9.3×10^{-1}

[a] Integrated peak area.

$k(6a)/k(3b) = (1.1 \pm 0.1) \times 10^1$, $k(6a^o)/k(6a^p) = 1.0 \pm 0.03$

no.	$a(1)^{[a]}$	$a(2)^{[a]}$	$a(6ao)^{[a]}$	$a(6ap)^{[a]}$	$a(3bo)^{[a]}$	$\dfrac{k(6a)}{k(3b)}$	$\dfrac{k(6a^o)}{k(6a^p)}$
$1_{(HPLC)}$	0	4.10×10^6	1.87×10^6	1.81×10^6	5.10×10^5	1.2×10^1	1.0
$2_{(HPLC)}$	0	4.24×10^6	1.59×10^6	2.00×10^6	6.20×10^5	9.4	8.0×10^{-1}
$3_{(HPLC)}$	0	3.53×10^6	1.20×10^6	1.52×10^6	5.17×10^5	8.5	7.9×10^{-1}

[a] Integrated peak area at 280 nm.

$k(6a)/k(3b) = 9.9 \pm 1.4$, $k(6a^o)/k(6a^p) = (8.7 \pm 1.1) \times 10^{-1}$
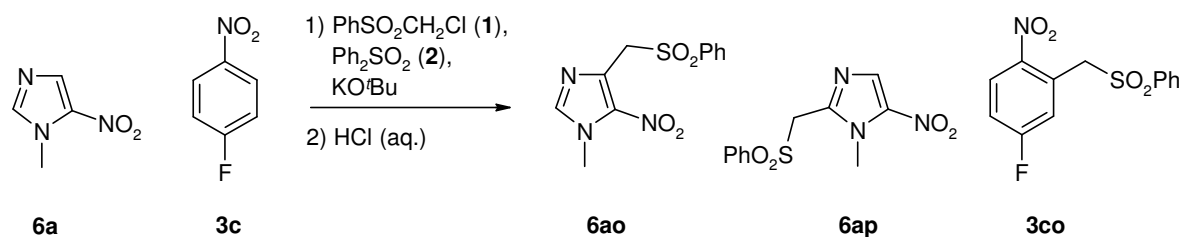
$n(\mathbf{1}) = 0.123$ mmol, $n(\mathbf{2}) = 0.047$ mmol, $n(\mathbf{6a}) = 0.529$ mmol, $n(\mathbf{3c}) = 0.176$ mmol, $n(\mathrm{KO}^t\mathrm{Bu}) = 0.492$ mmol

no.	$a(\mathbf{1})^{[a]}$	$a(\mathbf{2})^{[a]}$	$a(\mathbf{6ao})^{[a]}$	$a(\mathbf{6ap})^{[a]}$	$a(\mathbf{3co})^{[a]}$	$\dfrac{k(\mathbf{3c})}{k(\mathbf{6a})}$	$\dfrac{k(\mathbf{6a}^\circ)}{k(\mathbf{6a}^p)}$
$1_{(GC)}$	0	6.46×10^6	1.74×10^5	5.28×10^4	2.62×10^6	6.6	8.8×10^{-1}
	0	6.71×10^6	1.83×10^5	5.75×10^4	2.86×10^6	6.8	8.5×10^{-1}
	0	6.52×10^6	1.71×10^5	4.77×10^4	2.81×10^6	7.6	9.6×10^{-1}
$2_{(GC)}$	0	4.98×10^6	1.36×10^5	3.95×10^4	2.18×10^6	7.3	9.2×10^{-1}
	0	5.33×10^6	1.51×10^5	4.32×10^4	2.38×10^6	7.2	9.4×10^{-1}
	0	7.61×10^6	2.29×10^5	7.14×10^4	3.45×10^6	6.6	8.6×10^{-1}
$3_{(GC)}$	0	7.47×10^6	2.16×10^5	6.44×10^4	3.34×10^6	6.9	9.0×10^{-1}
	0	7.75×10^6	2.27×10^5	6.77×10^4	3.49×10^6	6.9	9.0×10^{-1}

[a] Integrated peak area.

$k(\mathbf{3c})/k(\mathbf{6a}) = 7.0 \pm 0.3$, $k(\mathbf{6a}^\circ)/k(\mathbf{6a}^p) = (9.0 \pm 0.4) \times 10^{-1}$
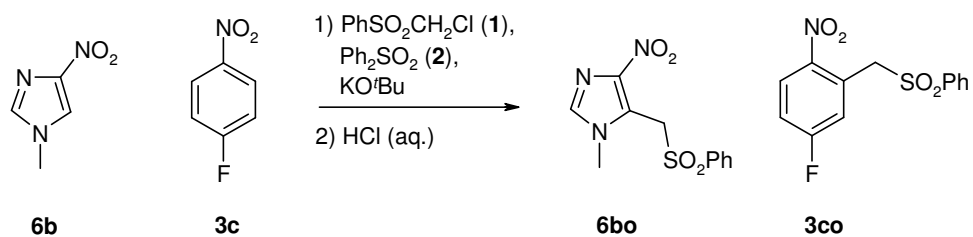
$n(\mathbf{1}) = 0.125$ mmol, $n(\mathbf{2}) = 0.050$ mmol, $n(\mathbf{6b}) = 0.300$ mmol, $n(\mathbf{3c}) = 0.299$ mmol, $n(KO^tBu) = 0.500$ mmol

| no.	$a(\mathbf{1})^{[a]}$	$a(\mathbf{2})^{[a]}$	$a(\mathbf{6bo})^{[a]}$	$a(\mathbf{3co})^{[a]}$	$\dfrac{k(\mathbf{6b})}{k(\mathbf{3c})}$
$1_{(GC)}$	0	6.57×10^6	2.05×10^6	2.18×10^6	6.1
	0	6.44×10^6	1.89×10^6	2.13×10^6	5.7
	0	6.22×10^6	1.73×10^6	2.02×10^6	5.5
$2_{(GC)}$	0	8.42×10^6	2.18×10^6	2.30×10^6	6.0
	0	9.71×10^6	2.14×10^6	2.50×10^6	5.3
	0	9.56×10^6	2.68×10^6	3.13×10^6	5.5
$3_{(GC)}$	0	9.44×10^6	2.52×10^6	2.80×10^6	5.7
	0	8.13×10^6	2.59×10^6	2.60×10^6	6.6
	0	1.01×10^7	2.39×10^6	2.84×10^6	5.2

[a] Integrated peak area.

$k(\mathbf{6b})/k(\mathbf{3c}) = 5.7 \pm 0.4$

no.	$a(\mathbf{1})^{[a]}$	$a(\mathbf{2})^{[a]}$	$a(\mathbf{6bo})^{[a]}$	$a(\mathbf{3co})^{[a]}$	$\dfrac{k(\mathbf{6b})}{k(\mathbf{3c})}$
$1_{(HPLC)}$	0	3.04×10^6	1.43×10^7	5.34×10^6	5.6
$2_{(HPLC)}$	0	3.54×10^6	1.76×10^7	5.98×10^6	6.2
$3_{(HPLC)}$	0	5.93×10^6	3.06×10^7	9.71×10^6	6.8

[a] Integrated peak area.

$k(\mathbf{6b})/k(\mathbf{3c}) = 6.2 \pm 0.5$
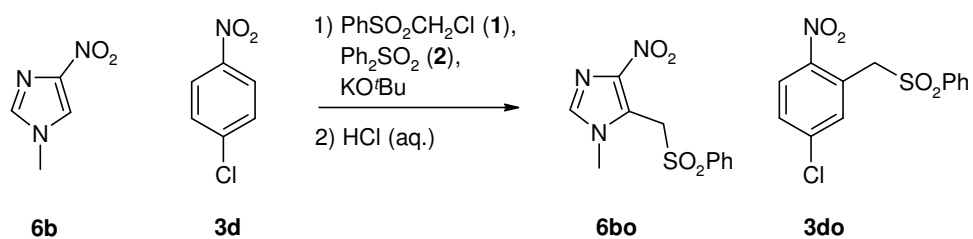
$n(\mathbf{1}) = 0.071$ mmol, $n(\mathbf{2}) = 0.027$ mmol, $n(\mathbf{6b}) = 0.133$ mmol, $n(\mathbf{3d}) = 0.268$ mmol, $n(\text{KO}^t\text{Bu}) = 0.284$ mmol

no.	$a(\mathbf{1})$[a]	$a(\mathbf{2})$[a]	$a(\mathbf{6bo})$[a]	$a(\mathbf{3do})$[a]	$\dfrac{k(\mathbf{6b})}{k(\mathbf{3d})}$
1(GC)	0	7.68×10^6	9.16×10^5	5.35×10^6	1.7
	0	7.28×10^6	8.89×10^5	4.92×10^6	1.8
	0	7.05×10^6	7.17×10^5	4.11×10^6	1.8
2(GC)	0	6.23×10^6	7.51×10^5	3.96×10^6	1.9
	0	6.53×10^6	7.64×10^5	4.07×10^6	1.9
	0	6.53×10^6	8.08×10^5	4.11×10^6	2.0
3(GC)	0	6.68×10^6	7.52×10^5	4.30×10^6	1.8
	0	6.52×10^6	7.18×10^5	4.16×10^6	1.8
	0	6.58×10^7	6.63×10^5	4.08×10^6	1.6

[a] Integrated peak area.

$k(\mathbf{6b})/k(\mathbf{3d}) = 1.8 \pm 0.1$

4.5.3.6 Competition Experiments with Nitropyrazole *7*
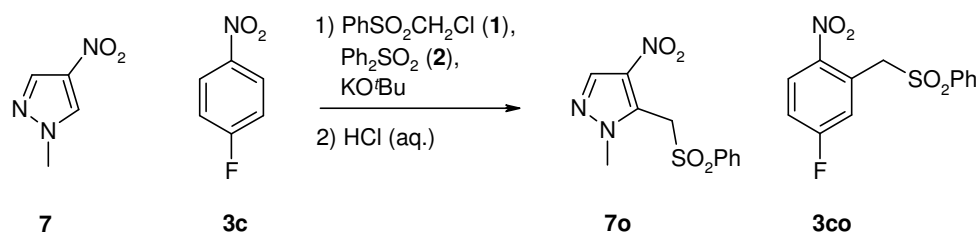
$n(\mathbf{1}) = 0.126$ mmol, $n(\mathbf{2}) = 0.053$ mmol, $n(\mathbf{7}) = 0.186$ mmol, $n(\mathbf{3c}) = 0.292$ mmol, $n(\mathrm{KO}^t\mathrm{Bu}) = 0.504$ mmol

no.	$a(\mathbf{1})^{[a]}$	$a(\mathbf{2})^{[a]}$	$a(\mathbf{7o})^{[a]}$	$a(\mathbf{3co})^{[a]}$	$\dfrac{k(\mathbf{7})}{k(\mathbf{3c})}$
$1_{(GC)}$	0	1.05×10^7	3.90×10^6	8.27×10^6	1.0
	0	1.05×10^7	3.86×10^6	8.23×10^6	1.0
	0	1.11×10^7	3.96×10^6	7.86×10^6	1.1
$2_{(GC)}$	0	1.32×10^7	3.76×10^6	8.21×10^6	9.9×10^{-1}
	0	1.56×10^7	4.58×10^6	1.04×10^7	9.5×10^{-1}
	0	1.50×10^7	4.39×10^6	9.66×10^6	9.8×10^{-1}
$3_{(GC)}$	0	1.12×10^7	3.74×10^6	7.97×10^6	1.0
	0	1.07×10^7	3.81×10^6	7.58×10^6	1.1
	0	1.11×10^7	3.87×10^6	7.85×10^6	1.1

[a] Integrated peak area.

$k(\mathbf{7})/k(\mathbf{3c}) = 1.0 \pm 0.1$

no.	$a(\mathbf{1})^{[a]}$	$a(\mathbf{2})^{[a]}$	$a(\mathbf{7o})^{[a]}$	$a(\mathbf{3co})^{[a]}$	$\dfrac{k(\mathbf{7})}{k(\mathbf{3c})}$
$1_{(HPLC)}$	0	2.21×10^6	9.95×10^6	9.46×10^6	1.1
$2_{(HPLC)}$	0	4.91×10^6	1.97×10^7	1.80×10^7	1.1
$3_{(HPLC)}$	0	7.54×10^6	3.11×10^7	2.97×10^7	1.1

[a] Integrated peak area.

$k(\mathbf{7})/k(\mathbf{3c}) = 1.1 \pm 0.02$
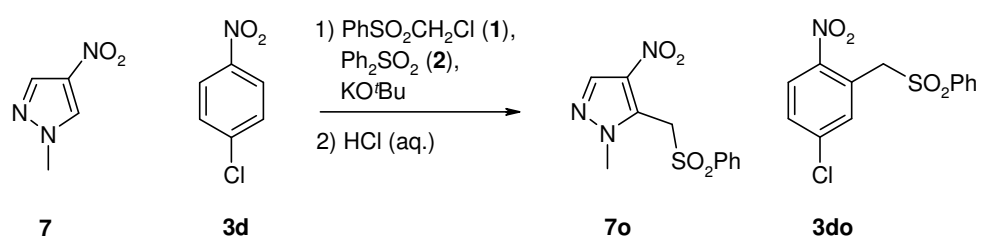
$n(\mathbf{1}) = 0.099$ mmol, $n(\mathbf{2}) = 0.042$ mmol, $n(\mathbf{7}) = 0.479$ mmol, $n(\mathbf{3d}) = 0.151$ mmol, $n(KO^tBu) = 0.396$ mmol

no.	$a(\mathbf{1})$[a]	$a(\mathbf{2})$[a]	$a(\mathbf{7o})$[a]	$a(\mathbf{3do})$[a]	$\dfrac{k(\mathbf{3d})}{k(\mathbf{7})}$
1(GC)	0	1.03×10^7	2.96×10^6	3.20×10^6	3.0
	0	1.02×10^7	2.73×10^6	2.97×10^6	3.0
	0	1.03×10^7	3.14×10^6	3.40×10^6	3.0
2(GC)	0	9.96×10^6	2.75×10^6	2.74×10^6	2.7
	0	9.59×10^6	2.73×10^6	2.70×10^6	2.7
	0	9.47×10^6	2.45×10^6	2.42×10^6	2.7
3(GC)	0	1.06×10^7	2.88×10^6	2.45×10^6	2.3
	0	1.10×10^7	3.10×10^6	2.65×10^6	2.3
	0	1.01×10^7	2.69×10^6	2.26×10^6	2.3

[a] Integrated peak area.

$k(\mathbf{3d})/k(\mathbf{7}) = 2.7 \pm 0.3$

127

4.5.3.7 Competition Experiments with Nitrothiophene 8
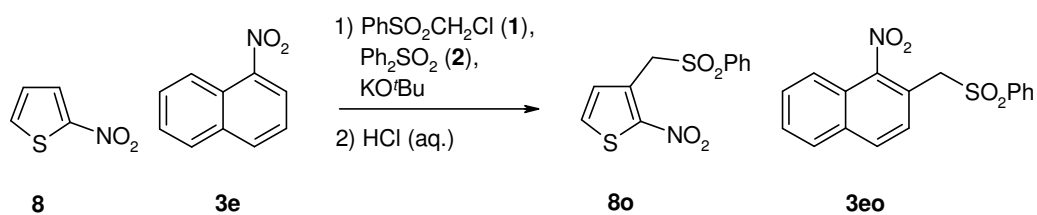
$n(\mathbf{1}) = 0.125$ mmol, $n(\mathbf{2}) = 0.050$ mmol, $n(\mathbf{8}) = 0.201$ mmol, $n(\mathbf{3e}) = 0.500$ mmol, $n(\mathrm{KO}^t\mathrm{Bu}) = 0.500$ mmol

no.	$a(\mathbf{1})$[a]	$a(\mathbf{2})$[a]	$a(\mathbf{8o})$[a]	$a(\mathbf{3eo})$[a]	$\dfrac{k(\mathbf{8})}{k(\mathbf{3e})}$
1$_{(GC)}$	0	2.53×10^6	6.86×10^5	6.10×10^5	4.6
	0	2.60×10^6	7.14×10^5	6.41×10^5	4.5
	0	2.55×10^6	7.08×10^5	6.35×10^5	4.6
2$_{(GC)}$	0	5.13×10^6	1.06×10^6	1.23×10^6	3.4
	0	4.61×10^6	8.42×10^5	8.28×10^5	4.0
	0	4.47×10^6	8.51×10^5	8.51×10^5	4.0
3$_{(GC)}$	0	3.66×10^6	6.86×10^5	7.84×10^5	3.5
	0	3.83×10^6	7.39×10^5	8.67×10^5	3.4
	0	3.70×10^6	7.09×10^5	8.04×10^5	3.5

[a] Integrated peak area.

$k(\mathbf{8})/k(\mathbf{3e}) = 3.9 \pm 0.5$

no.	$a(\mathbf{1})$[a]	$a(\mathbf{2})$[a]	$a(\mathbf{8o})$[a]	$a(\mathbf{3eo})$[a]	$\dfrac{k(\mathbf{8})}{k(\mathbf{3e})}$
1$_{(HPLC)}$	0	9.89×10^5	2.59×10^6	2.37×10^6	5.0
2$_{(HPLC)}$	0	2.37×10^6	5.21×10^6	6.21×10^6	3.8
3$_{(HPLC)}$	0	1.87×10^6	3.25×10^6	4.13×10^6	3.5

[a] Integrated peak area.

$k(\mathbf{8})/k(\mathbf{3e}) = 4.1 \pm 0.7$

4.5.4 Kinetic Experiments

The temperature of the solutions during all kinetic studies was kept constant (-40 ± 0.1°C) by using a bath thermostat. Dry DMF for kinetics was purchased (< 50 ppm H_2O). Rate constants k_{obs} (s^{-1}) were obtained by fitting the single exponential $A_t = A_0 \exp(-k_{obs}t) + C$ to the observed time-dependent absorbance of the minor component.

4.5.4.1 Reactions of **1⁻** with Michael Acceptors

Reaction of **1⁻** with **10b** (DMF, -40 °C, 400 nm)

[**10b**] / M	[**1⁻**] / M	k_{obs} / s^{-1}
7.64×10^{-5}	1.58×10^{-3}	5.31×10^{-3}
7.89×10^{-5}	2.36×10^{-3}	9.57×10^{-3}
7.90×10^{-5}	3.08×10^{-3}	1.21×10^{-2}
8.07×10^{-5}	3.85×10^{-3}	1.51×10^{-2}
8.11×10^{-5}	4.47×10^{-3}	1.95×10^{-2}
$k_2 = 4.65 \pm 0.31$ M^{-1} s^{-1}		

$y = 4.649\text{E}{+}00x - 1.770\text{E}{-}03$
$R^2 = 9.869\text{E}{-}01$
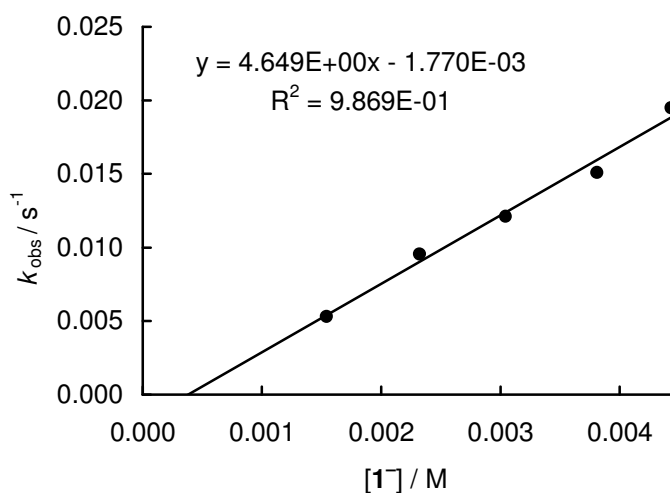
Reaction of **1**$^-$ with **10b** (DMF, various temperatures, 400 nm)

[**10b**] / M	[**1**$^-$] / M	T / K	k_{obs} / s^{-1}	k_2 / M^{-1} s^{-1}
7.87×10^{-5}	3.07×10^{-3}	219.2	4.19×10^{-3}	1.38
8.01×10^{-5}	3.13×10^{-3}	226.2	7.58×10^{-3}	2.46
7.90×10^{-5}	3.08×10^{-3}	233.2	1.21×10^{-2}	3.98
7.95×10^{-5}	3.10×10^{-3}	241.2	1.83×10^{-2}	5.97
7.85×10^{-5}	3.06×10^{-3}	248.2	3.07×10^{-2}	1.02×10^1

Eyring: $y = -3398.4x + 10.469$, $R^2 = 0.9953$

Arrhenius: $y = -3631.5x + 16.921$, $R^2 = 0.9959$
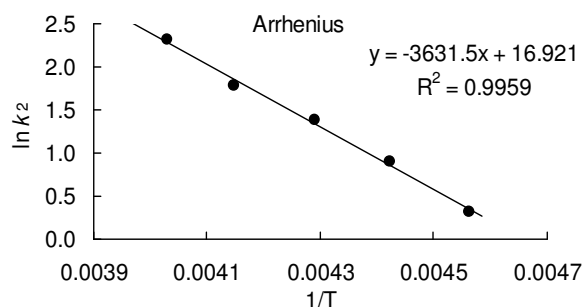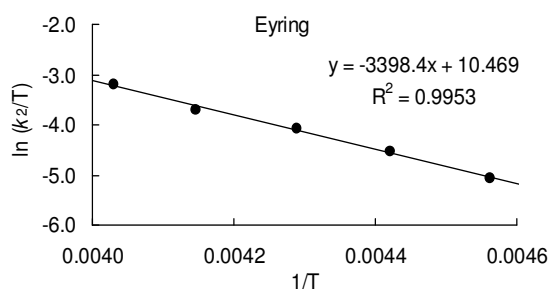
$\Delta H^{\ddagger} = (2.83 \pm 0.11) \times 10^1$ kJ mol^{-1}

$\Delta S^{\ddagger} = (-1.11 \pm 0.05) \times 10^2$ J mol^{-1} K^{-1}

k_2 (20 °C) $= 9.31 \times 10^1$ m^{-1} s^{-1}

$E_A = (3.02 \pm 0.11) \times 10^1$ kJ mol^{-1}

$\ln(A) = (1.69 \pm 0.06) \times 10^1$

Reaction of **1**$^-$ with **10a** (DMF, –40 °C, 400 nm)

[**10a**] / M	[**1**$^-$] / M	k_{obs} / s^{-1}
8.73×10^{-5}	1.34×10^{-3}	7.66×10^{-3}
8.52×10^{-5}	2.24×10^{-3}	1.58×10^{-2}
8.21×10^{-5}	3.23×10^{-3}	2.46×10^{-2}
8.17×10^{-5}	4.29×10^{-3}	3.68×10^{-2}
8.09×10^{-5}	4.95×10^{-3}	4.39×10^{-2}
	$k_2 = (1.01 \pm 0.03) \times 10^1$ M^{-1} s^{-1}	

$y = 1.005E{+}01x - 6.079E{-}03$

$R^2 = 9.966E{-}01$
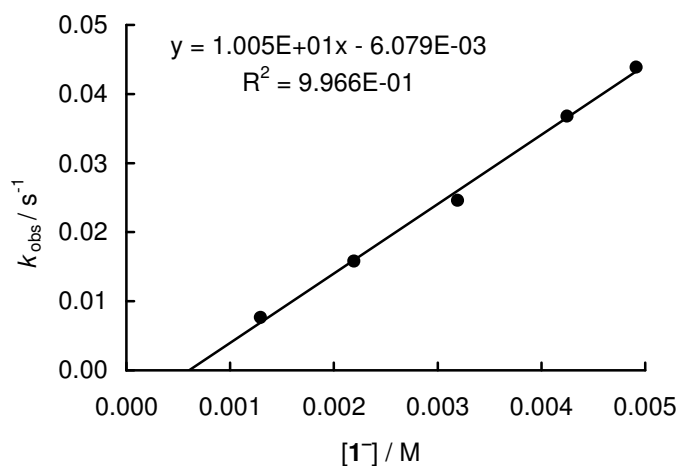
Reaction of **1⁻** with **10c** (DMF, –40 °C, 420 nm)

[**10c**] / M	[**1⁻**] / M	k_{obs} / s⁻¹
7.43×10^{-5}	1.04×10^{-3}	1.66×10^{-3}
7.45×10^{-5}	2.09×10^{-3}	4.00×10^{-3}
7.16×10^{-5}	3.27×10^{-3}	6.84×10^{-3}
7.11×10^{-5}	4.24×10^{-3}	9.46×10^{-3}
7.12×10^{-5}	5.49×10^{-3}	1.35×10^{-2}
	$k_2 = 2.64 \pm 0.12$ M⁻¹ s⁻¹	

$y = 2.639E+00x - 1.330E-03$
$R^2 = 9.939E-01$
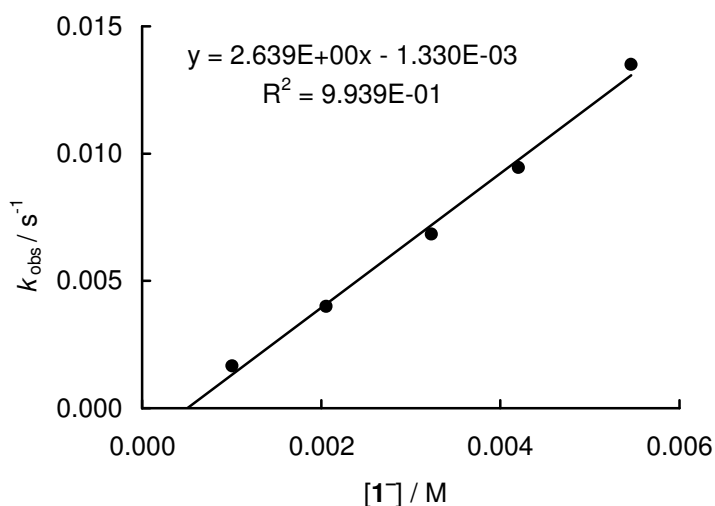
4.5.4.2 Reactions of **9⁻** with Michael Acceptors

Reaction of **9⁻** with **10a** (DMF, 20 °C, 380 nm)

[**10a**] / M	[**9⁻**] / M	k_{obs} / s⁻¹
5.82×10^{-5}	1.78×10^{-3}	6.98×10^{-4}
5.64×10^{-5}	3.37×10^{-3}	1.54×10^{-3}
5.58×10^{-5}	5.04×10^{-3}	2.22×10^{-3}
5.46×10^{-5}	6.53×10^{-3}	2.87×10^{-3}
	$k_2 = (4.52 \pm 0.18) \times 10^{-1}$ M⁻¹ s⁻¹	

$y = 4.520E-01x - 4.533E-05$
$R^2 = 9.968E-01$

131
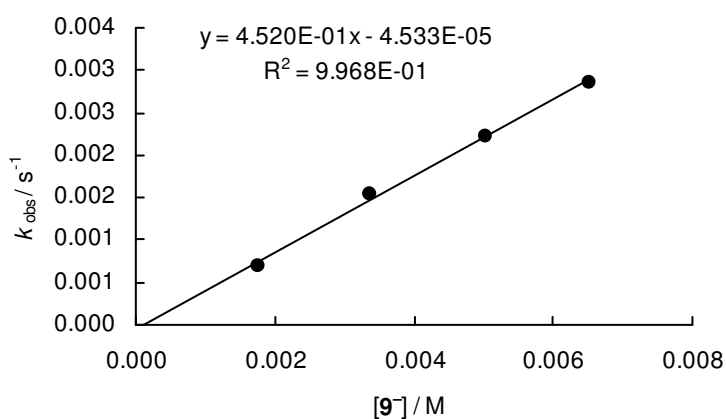
Reaction of **9⁻** with **10a** (DMF, various temperatures, 380 nm)

[**10a**] / M	[**9⁻**] / M	T / K	k_{obs} / s^{-1}	k_2 / M^{-1} s^{-1}
5.54×10^{-5}	5.01×10^{-3}	273.2	4.79×10^{-4}	9.62×10^{-2}
5.57×10^{-5}	5.03×10^{-3}	293.2	2.22×10^{-3}	4.44×10^{-1}
5.51×10^{-5}	6.58×10^{-3}	303.2	5.24×10^{-3}	7.99×10^{-1}
5.59×10^{-5}	5.05×10^{-3}	318.2	8.87×10^{-3}	1.77

Eyring: $y = -5343.5x + 11.659$, $R^2 = 0.997$

Arrhenius: $y = -5637.3x + 18.343$, $R^2 = 0.9974$
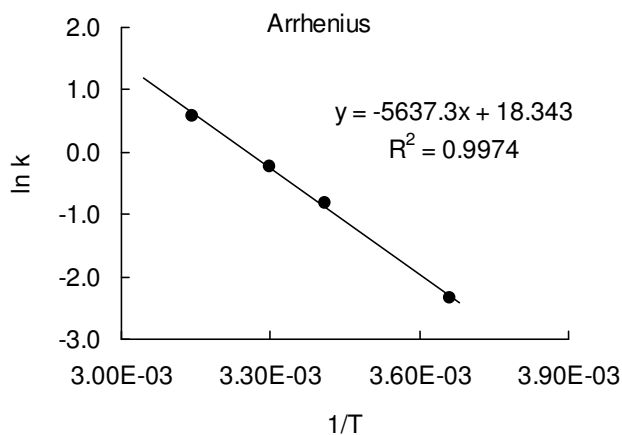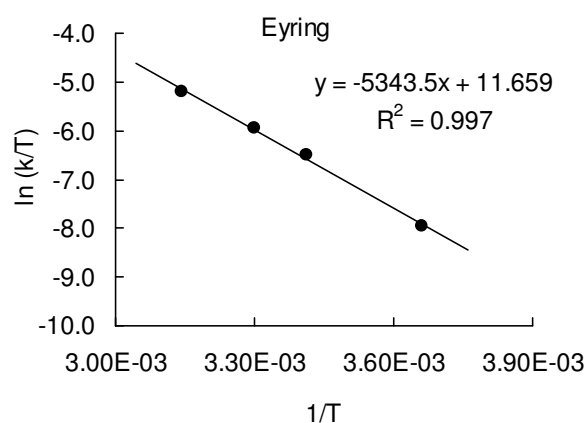
$\Delta H^{\ddagger} = (4.44 \pm 0.17) \times 10^1$ kJ mol^{-1}

$\Delta S^{\ddagger} = (-1.01 \pm 0.06) \times 10^2$ J mol^{-1} K^{-1}

$k_2 \, (-40 \, °C) = (3.01 \pm 0.57) \times 10^{-3}$ M^{-1} s^{-1}

$E_A = (4.69 \pm 0.17) \times 10^1$ kJ mol^{-1}

$\ln(A) = (1.83 \pm 0.07) \times 10^1$

Reaction of **9⁻** with **10b** (DMF, 20 °C, 390 nm)

[**10b**] / M	[**9⁻**] / M	k_{obs} / s^{-1}
6.97×10^{-5}	4.23×10^{-3}	1.02×10^{-4}
6.71×10^{-5}	5.30×10^{-3}	1.29×10^{-3}
6.49×10^{-5}	7.89×10^{-3}	1.92×10^{-3}
$k_2 = (2.46 \pm 0.02) \times 10^{-1}$ M^{-1} s^{-1}		

$y = 2.459E-01x - 1.811E-05$, $R^2 = 9.999E-01$
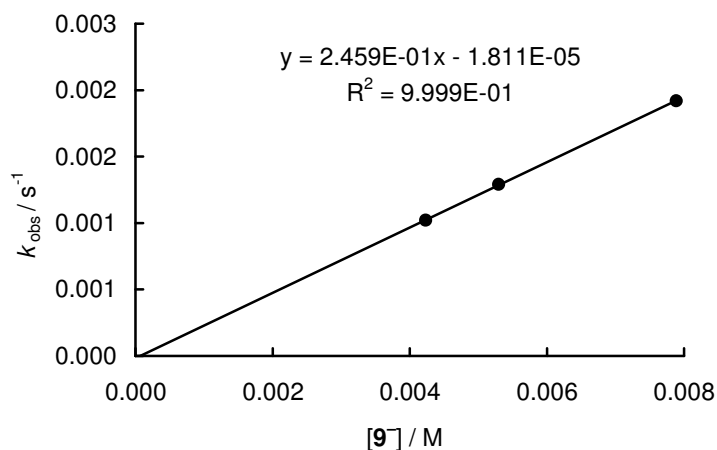
Reaction of **9⁻** with **10b** (DMF, various temperatures, 390 nm)

[**10b**] / M	[**9⁻**] / M	T / K	k_{obs} / s⁻¹	k_2 / M⁻¹ s⁻¹
6.53×10^{-5}	7.94×10^{-3}	273.2	4.43×10^{-4}	5.60×10^{-2}
6.80×10^{-5}	8.26×10^{-3}	293.2	1.92×10^{-3}	2.34×10^{-1}
6.59×10^{-5}	8.01×10^{-3}	313.2	7.03×10^{-3}	8.81×10^{-1}
6.56×10^{-5}	7.97×10^{-3}	338.2	1.94×10^{-2}	2.44

Eyring
y = -5465.5x + 11.524
R^2 = 0.9994

Arrhenius
y = -5766.3x + 18.233
R^2 = 0.9995
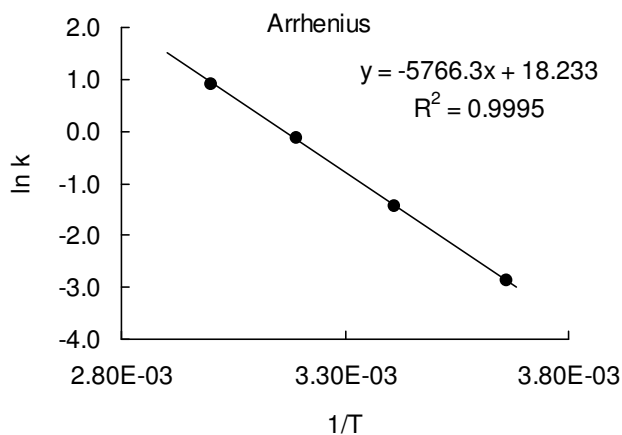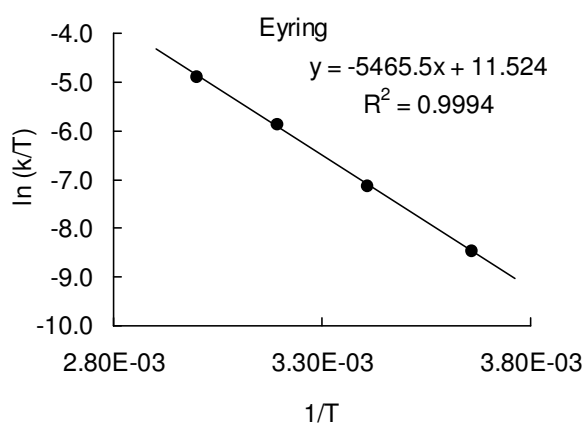
$\Delta H^{\ddagger} = (4.54 \pm 0.08) \times 10^1 \text{ kJ mol}^{-1}$

$\Delta S^{\ddagger} = (-1.02 \pm 0.03) \times 10^2 \text{ J mol}^{-1} \text{ K}^{-1}$

$k_2 (-40\ °C) = (1.56 \pm 0.15) \times 10^{-3} \text{ M}^{-1} \text{ s}^{-1}$

$E_A = (4.79 \pm 0.08) \times 10^1 \text{ kJ mol}^{-1}$
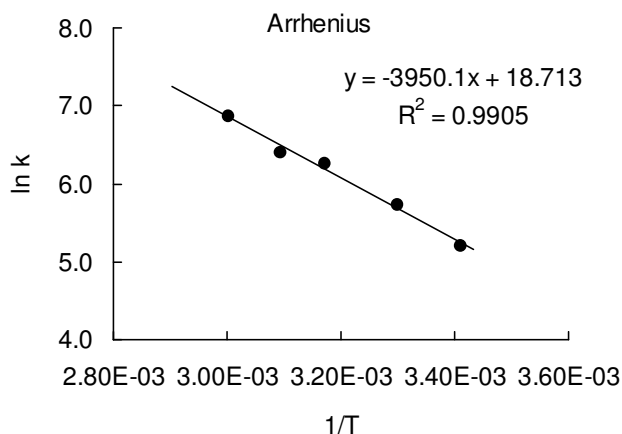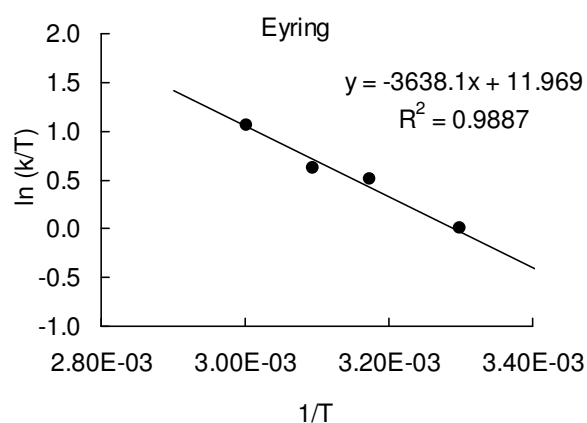
$\ln(A) = (1.82 \pm 0.03) \times 10^1$

Reaction of **9⁻** with **10c** (DMF, 20 °C, 380 nm)

[**10c**] / M	[**9⁻**] / M	k_{obs} / s⁻¹
5.57×10^{-5}	4.48×10^{-3}	7.37×10^{-4}
5.66×10^{-5}	5.66×10^{-3}	9.44×10^{-4}
5.53×10^{-5}	6.60×10^{-3}	1.11×10^{-3}
	$k_2 = (1.76 \pm 0.004) \times 10^{-1} \text{ M}^{-1} \text{ s}^{-1}$	

y = 1.756E-01x - 4.449E-05
R^2 = 1.000E+00
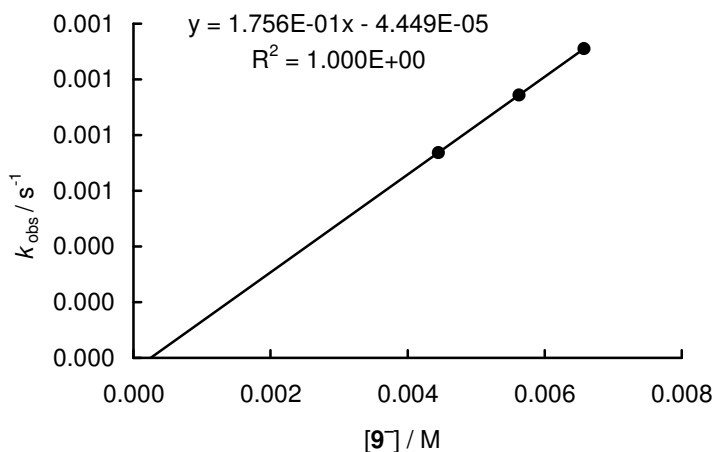
Reaction of **9⁻** with **10c** (DMF, various temperatures, 380 nm)

[**10c**] / M	[**9⁻**] / M	T / K	k_{obs} / s^{-1}	k_2 / M^{-1} s^{-1}
5.58×10^{-5}	6.66×10^{-3}	273.2	2.52×10^{-4}	3.80×10^{-2}
5.53×10^{-5}	6.60×10^{-3}	293.2	1.11×10^{-3}	1.69×10^{-1}
5.53×10^{-5}	6.60×10^{-3}	313.2	3.97×10^{-3}	6.04×10^{-1}
5.51×10^{-5}	6.57×10^{-3}	333.2	1.17×10^{-2}	1.79

Eyring plot: $y = -5544.3x + 11.435$, $R^2 = 0.9998$

Arrhenius plot: $y = -5845.1x + 18.144$, $R^2 = 0.9999$
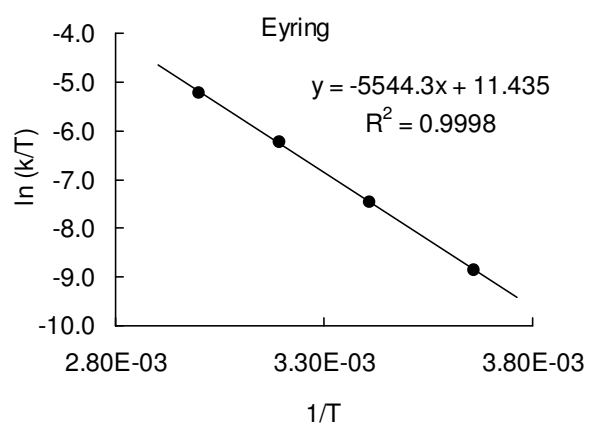
$\Delta H^{\ddagger} = (4.61 \pm 0.04) \times 10^1$ kJ mol^{-1}

$\Delta S^{\ddagger} = (-1.02 \pm 0.01) \times 10^2$ J mol^{-1} K^{-1}

$k_2 (-40\ °C) = (1.01 \pm 0.05) \times 10^{-3}$ M^{-1} s^{-1}
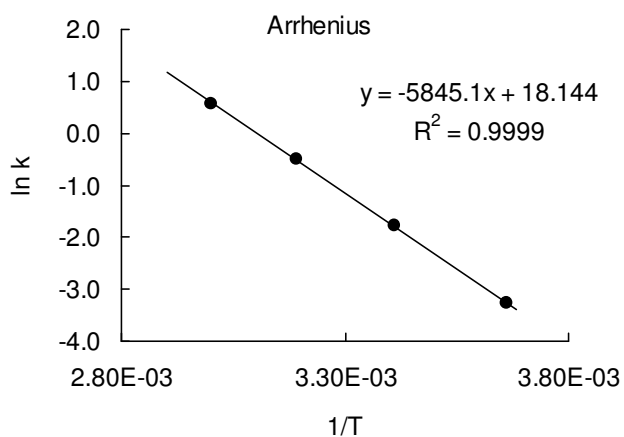
$E_A = (4.86 \pm 0.04) \times 10^1$ kJ mol^{-1}

$\ln(A) = (1.82 \pm 0.02) \times 10^1$

4.5.4.3 Reactions of 9⁻ with Quinone Methides

Reaction of **9⁻** with **12a** (DMF, 20 °C, stopped flow, 400 nm)

[**12a**] / M	[**9⁻**] / M	k_{obs} / s^{-1}
4.25×10^{-5}	8.03×10^{-4}	8.48×10^{-1}
4.25×10^{-5}	1.53×10^{-3}	1.73
4.25×10^{-5}	2.25×10^{-3}	2.41
4.25×10^{-5}	2.81×10^{-3}	3.22
4.25×10^{-5}	3.21×10^{-3}	3.62

$$k_2 = (1.15 \pm 0.04) \times 10^3 \ \text{M}^{-1} \ \text{s}^{-1}$$
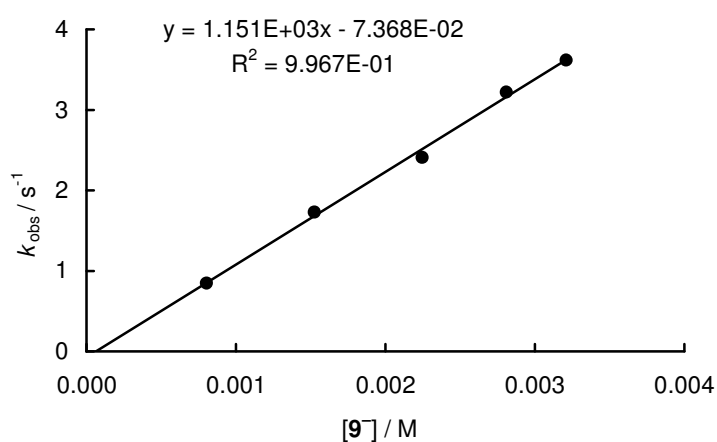
Reaction of **9⁻** with **12a** (DMF, various temperatures, stopped flow and J&M, 400 nm)

[**12a**] / M	[**9⁻**] / M	T / K	k_{obs} / s^{-1}	k_2 / M^{-1} s^{-1}
2.06×10^{-5}	2.08×10^{-4}	223.2	2.20×10^{-3}	1.11×10^{1}
2.06×10^{-5}	2.09×10^{-4}	233.2	4.44×10^{-3}	2.24×10^{1}
2.09×10^{-5}	2.11×10^{-4}	243.2	1.12×10^{-2}	5.58×10^{1}
2.06×10^{-5}	2.08×10^{-4}	263.2	4.80×10^{-2}	2.42×10^{2}
4.25×10^{-5}	2.25×10^{-3}	293.2	2.41	1.07×10^{3}
4.25×10^{-5}	2.25×10^{-3}	303.2	4.16	1.85×10^{3}
4.25×10^{-5}	2.25×10^{-3}	313.2	6.15	2.74×10^{3}
4.25×10^{-5}	2.25×10^{-3}	323.2	9.10	4.05×10^{3}
4.25×10^{-5}	2.25×10^{-3}	333.2	1.31×10^{1}	5.85×10^{3}

Eyring

$$y = -4003.7x + 14.958$$
$$R^2 = 0.9985$$

Arrhenius

$$y = -4274.5x + 21.569$$
$$R^2 = 0.9988$$
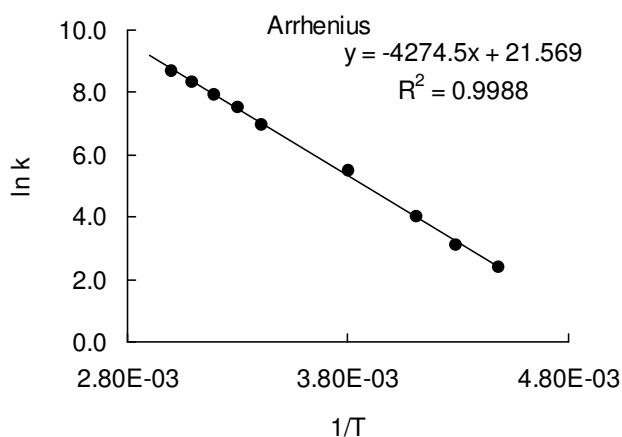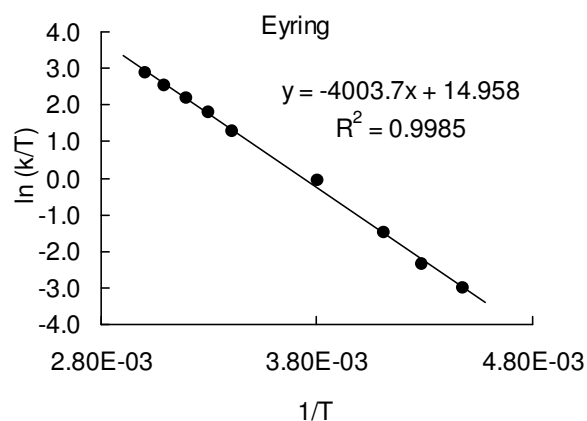
$\Delta H^{\ddagger} = (3.33 \pm 0.05) \times 10^1 \text{ kJ mol}^{-1}$

$\Delta S^{\ddagger} = (-7.32 \pm 0.18) \times 10^1 \text{ J mol}^{-1} \text{ K}^{-1}$

$k_2 (-40 \text{ °C}) = (2.55 \pm 0.23) \times 10^1 \text{ M}^{-1} \text{ s}^{-1}$

$E_A = (3.55 \pm 0.05) \times 10^1 \text{ kJ mol}^{-1}$

$\ln(A) = (2.16 \pm 0.02) \times 10^1$

Reaction of **9⁻** with **12b** (DMF, 20 °C, stopped flow, 500 nm)

[**12b**] / M	[**9⁻**] / M	k_{obs} / s^{-1}
2.48×10^{-5}	1.84×10^{-3}	3.21×10^{-1}
2.48×10^{-5}	2.34×10^{-3}	4.10×10^{-1}
2.48×10^{-5}	2.84×10^{-3}	5.16×10^{-1}
$k_2 = (1.94 \pm 0.10) \times 10^2 \text{ M}^{-1} \text{ s}^{-1}$		

$$y = 1.942E+02x - 3.933E-02$$
$$R^2 = 9.975E-01$$

136
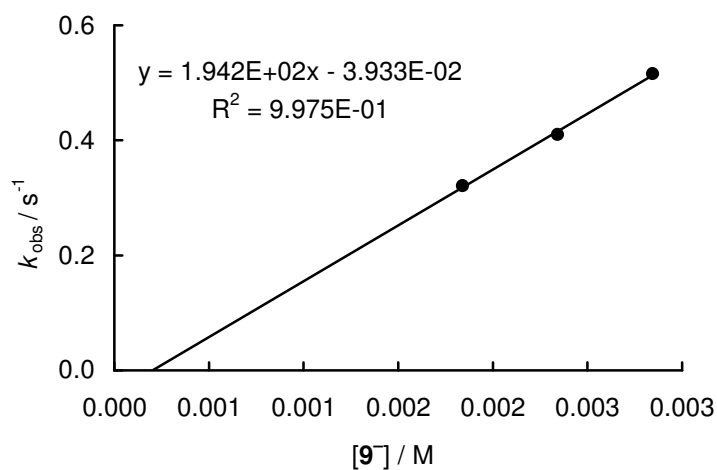
Reaction of **9⁻** with **12b** (DMF, various temperatures, stopped flow, 500 nm)

[**12b**] / M	[**9⁻**] / M	T / K	k_{obs} / s^{-1}	k_2 / M^{-1} s^{-1}
2.48×10^{-5}	2.84×10^{-3}	293.2	5.16×10^{-1}	1.81×10^{2}
2.48×10^{-5}	2.84×10^{-3}	303.2	8.68×10^{-1}	3.05×10^{2}
2.48×10^{-5}	2.84×10^{-3}	315.2	1.48	5.20×10^{2}
2.48×10^{-5}	2.84×10^{-3}	323.2	1.72	6.05×10^{2}
2.48×10^{-5}	2.84×10^{-3}	333.2	2.73	9.60×10^{2}

Eyring

y = -3638.1x + 11.969
R^2 = 0.9887

Arrhenius

y = -3950.1x + 18.713
R^2 = 0.9905

$\Delta H^{\ddagger} = (3.02 \pm 0.19) \times 10^1$ kJ mol^{-1}

$\Delta S^{\ddagger} = (-9.80 \pm 0.60) \times 10^1$ J mol^{-1} K^{-1}

k_2 (−40 °C) = 6.15 ± 1.52 M^{-1} s^{-1}

$E_A = (3.28 \pm 0.19) \times 10^1$ kJ mol^{-1}

$\ln(A) = (1.87 \pm 0.07) \times 10^1$

Reaction of **9⁻** with **12c** (DMF, 20 °C, stopped flow, 500 nm)

[**12c**] / M	[**9⁻**] / M	k_{obs} / s^{-1}
2.46×10^{-5}	1.84×10^{-3}	1.15×10^{-1}
2.46×10^{-5}	2.34×10^{-3}	1.92×10^{-1}
2.46×10^{-5}	2.84×10^{-3}	2.41×10^{-1}

$k_2 = (8.97 \pm 0.46) \times 10^1$ M^{-1} s^{-1}

y = 8.965E+01x - 1.533E-02
R^2 = 9.974E-01
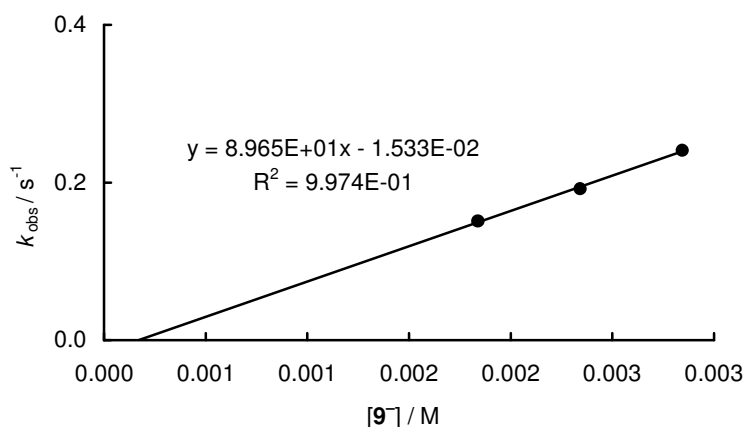
Reaction of **9⁻** with **12c** (DMF, various temperatures, stopped flow, 500 nm)

[**12c**] / M	[**9⁻**] / M	T / K	k_{obs} / s^{-1}	k_2 / M^{-1} s^{-1}
2.46×10^{-5}	2.84×10^{-3}	293.2	2.41×10^{-1}	8.47×10^{1}
2.46×10^{-5}	2.84×10^{-3}	303.2	3.95×10^{-1}	1.39×10^{2}
2.46×10^{-5}	2.84×10^{-3}	313.2	6.61×10^{-1}	2.32×10^{2}
2.46×10^{-5}	2.84×10^{-3}	323.2	8.78×10^{-1}	3.09×10^{2}
2.46×10^{-5}	2.84×10^{-3}	333.2	1.28	4.50×10^{2}

Eyring
y = -3741.5x + 11.559
R^2 = 0.9927

Arrhenius
y = -4053.7x + 18.304
R^2 = 0.994
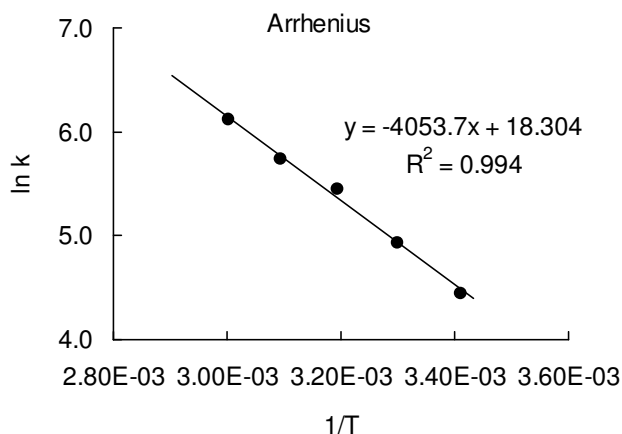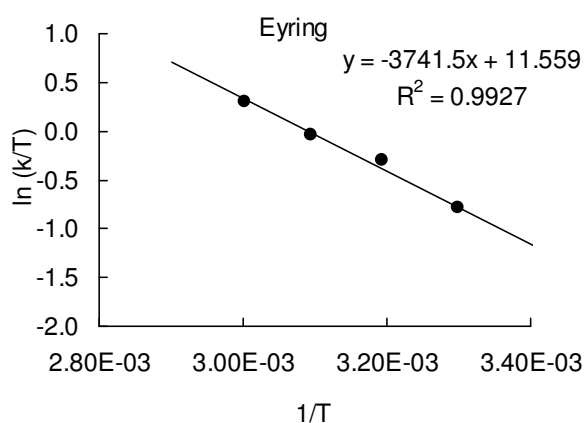
$\Delta H^{\ddagger} = (3.11 \pm 0.15) \times 10^{1}$ kJ mol^{-1}
$\Delta S^{\ddagger} = (-1.01 \pm 0.05) \times 10^{2}$ J mol^{-1} K^{-1}
k_2 (−40 °C) = 2.62 ± 0.53 M^{-1} s^{-1}

$E_A = (3.37 \pm 0.15) \times 10^{1}$ kJ mol^{-1}
$\ln(A) = (1.83 \pm 0.06) \times 10^{1}$

4.5.5 Quantum Chemical Calculations

nitrobenzene (**3a**)

3a   **3a_a2**   **3a_a3**   **3a_a4**

	B3LYP/6-31G(d)		B3LYP/6-311+G(d,p)// B3LYP/6-31G(d)				
	E_{tot}	H_{298}	E_{tot}	"H_{298}"	H_{rxn}	/ kcal mol^{-1}	/ kJ mol^{-1}
3a	-436.7505850	-436.639283	-436.8744693	-436.7631673			
methyl anion	-39.7902953	-39.758609	-39.8524446	-39.8207583			
3a_a4	-476.6780191	-476.528437	-476.8357953	-476.6862132	-0.1023	-64.2	-268.6
3a_a2	-476.6752506	-476.525670	-476.8328866	-476.6833060	-0.0994	-62.4	-260.9
3a_a3	-476.6392896	-476.491290	-476.7982246	-476.6502250	-0.0663	-41.6	-174.1

1-methoxy-4-nitrobenzene (**3b**)
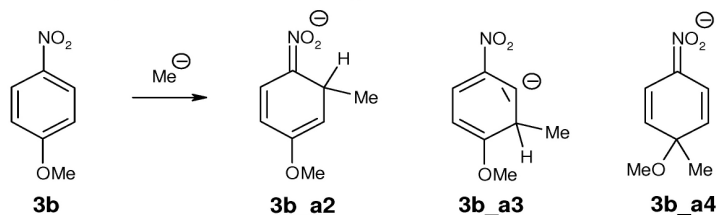
	B3LYP/6-31G(d)		B3LYP/6-311+G(d,p)//B3LYP/6-31G(d)				
	E_{tot}	H_{298}	E_{tot}	"H_{298}"	H_{rxn}	/ kcal mol^{-1}	/ kJ mol^{-1}
3b	-551.2758602	-551.129185	-551.4335495	-551.2868743			
methyl anion	-39.7902953	-39.758609	-39.8524446	-39.8207583			
3b_a4	-591.2093414	-591.024865	-591.4012137	-591.2167373	-0.1091	-68.5	-286.5
3b_a2	-591.1973919	-591.012627	-591.3883925	-591.2036276	-0.0960	-60.2	-252.0
3b_a3	-591.1618228	-590.978314	-591.3530839	-591.1695751	-0.0619	-38.9	-162.6

1-fluoro-4-nitrobenzene (**3c**)
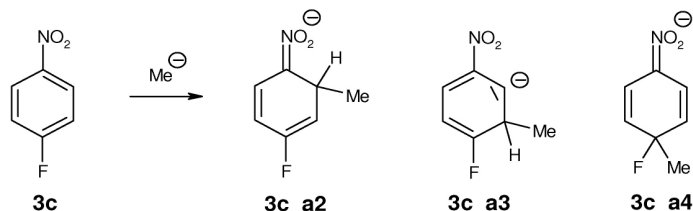
	B3LYP/6-31G(d)		B3LYP/6-311+G(d,p)//B3LYP/6-31G(d)				
	E_{tot}	H_{298}	E_{tot}	"H_{298}"	H_{rxn}	/ kcal mol^{-1}	/ kJ mol^{-1}
3c	-535.9833544	-535.879511	-536.1420483	-536.0382049			
methyl anion	-39.7902953	-39.758609	-39.8524446	-39.8207583			
3c_a4	-575.9307597	-575.788397	-576.1282417	-575.9858790	-0.1269	-79.6	-333.2
3c_a2	-575.9166114	-575.774192	-576.1102320	-575.9678126	-0.1088	-68.3	-285.8
3c_a3	-575.8779723	-575.736954	-576.0721326	-575.9311143	-0.0722	-45.3	-189.4

1-chloro-4-nitrobenzene (**3d**)
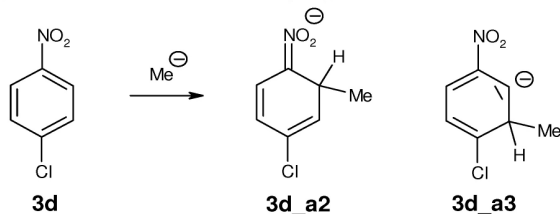
	B3LYP/6-31G(d)		B3LYP/6-311+G(d,p)//B3LYP/6-31G(d)				
	E_{tot}	H_{298}	E_{tot}	"H_{298}"	H_{rxn}	/ kcal mol^{-1}	/ kJ mol^{-1}
3d	-896.3448212	-896.242048	-896.4956875	-896.3929143			
methyl anion	-39.7902953	-39.758609	-39.8524446	-39.8207583			
3d_a2	-936.2837216	-936.142337	-936.4663983	-936.3250137	-0.1113	-69.9	-292.3
3d_a3	-936.2512143	-936.110835	-936.4333917	-936.2930124	-0.0793	-49.8	-208.3

1-nitronaphthaline (**3e**)
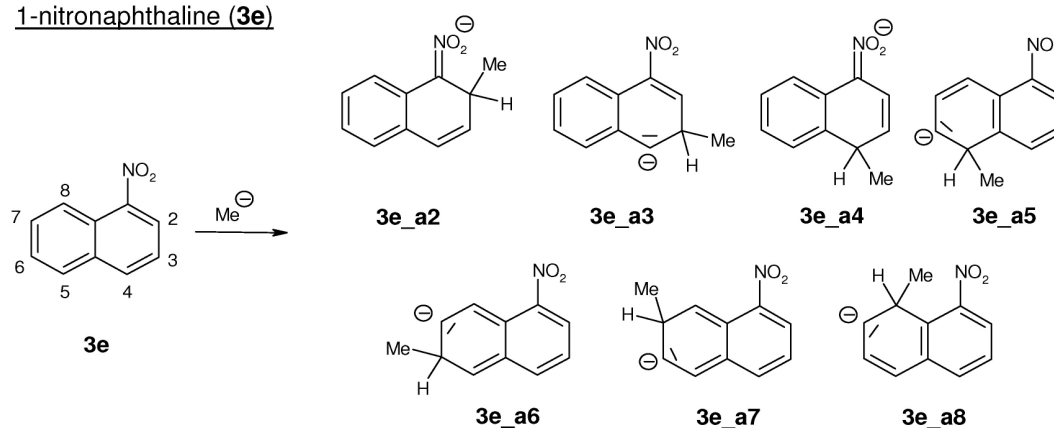
3e_a2   3e_a3   3e_a4   3e_a5

3e_a6   3e_a7   3e_a8

	B3LYP/6-31G(d)		B3LYP/6-311+G(d,p)// B3LYP/6-31G(d)				
	E_{tot}	H_{298}	E_{tot}	"H_{298}"	H_{rxn}	/ kcal mol^{-1}	/ kJ mol^{-1}
3e	-590.3881395	-590.227291	-590.5457952	-590.3849467			
methyl anion	-39.7902953	-39.758609	-39.8524446	-39.8207583			
3e_a4	-630.3353855	-630.135917	-630.5246592	-630.3251907	-0.1195	-75.0	-313.7
3e_a2	-630.3329354	-630.133479	-630.5216696	-630.3222132	-0.1165	-73.1	-305.9
3e_a5	-630.3129034	-630.114089	-630.5027969	-630.3039825	-0.0983	-61.7	-258.0
3e_a7	-630.3116741	-630.112933	-630.5012907	-630.3025496	-0.0968	-60.8	-254.3
3e_a8	-630.2918261	-630.093796	-630.4825192	-630.2844891	-0.0788	-49.4	-206.8
3e_a3	-630.2888651	-630.091001	-630.4783248	-630.2804607	-0.0748	-46.9	-196.3
3e_a6	-630.2891149	-630.091322	-630.4776634	-630.2798705	-0.0742	-46.5	-194.7

3-nitropyridine (**4a**)
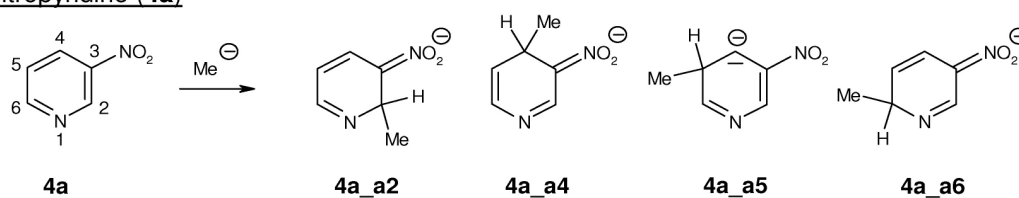
4a   4a_a2   4a_a4   4a_a5   4a_a6

	B3LYP/6-31G(d)		B3LYP/6-311+G(d,p)// B3LYP/6-31G(d)				
	E_{tot}	H_{298}	E_{tot}	"H_{298}"	H_{rxn}	/ kcal mol^{-1}	/ kJ mol^{-1}
4a	-452.7826697	-452.683381	-452.9102153	-452.8109266			
methyl anion	-39.7902953	-39.758609	-39.8524446	-39.8207583			
4a_a6	-492.7283198	-492.590062	-492.8888725	-492.7506147	-0.1189	-74.6	-312.2
4a_a4	-492.7285464	-492.590152	-492.8882535	-492.7498591	-0.1182	-74.2	-310.3
4a_a2	-492.7261678	-492.587916	-492.8866351	-492.7483833	-0.1167	-73.2	-306.4
4a_a5	-492.6879627	-492.551463	-492.8495676	-492.7130679	-0.0814	-51.1	-213.7
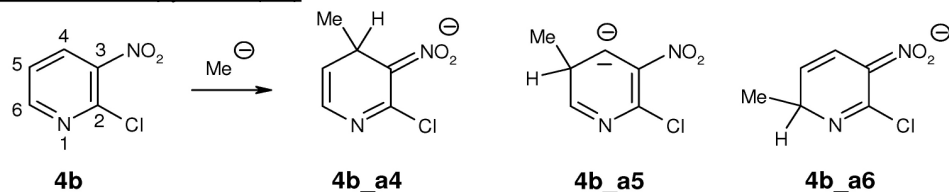
140

2-chloro-3-nitropyridine (**4b**)

	B3LYP/6-31G(d)		B3LYP/6-311+G(d,p)// B3LYP/6-31G(d)				
	E_{tot}	H_{298}	E_{tot}	"H_{298}"	H_{rxn}	/ kcal mol^{-1}	/ kJ mol^{-1}
4b	-912.3674805	-912.276998	-912.5229645	-912.4324820			
methyl anion	-39.7902953	-39.758609	-39.8524446	-39.8207583			
4b_a6	-952.3250659	-952.195437	-952.5113186	-952.3816897	-0.1284	-80.6	-337.2
4b_a4	-952.3242535	-952.194509	-952.5098222	-952.3800777	-0.1268	-79.6	-333.0
4b_a5	-952.2856604	-952.157463	-952.4720496	-952.3438522	-0.0906	-56.9	-237.9

4-ethoxy-3-nitropyridine (**4c**)
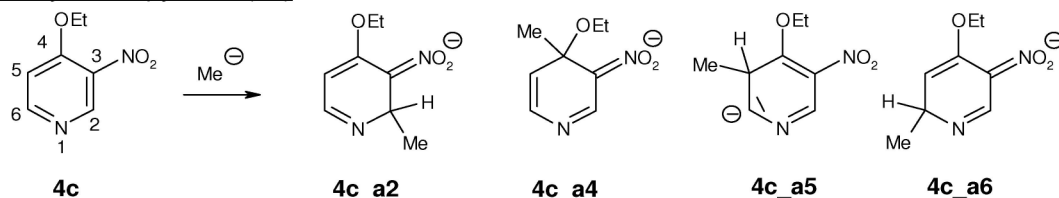
	B3LYP/6-31G(d)		B3LYP/6-311+G(d,p)// B3LYP/6-31G(d)				
	E_{tot}	H_{298}	E_{tot}	"H_{298}"	H_{rxn}	/ kcal mol^{-1}	/ kJ mol^{-1}
4c	-606.6198547	-606.455337	-606.7920359	-606.6275182			
methyl anion	-39.7902953	-39.758609	-39.8524446	-39.8207583			
4c_a4	-646.5625743	-646.359844	-646.7662182	-646.5634879	-0.1152	-72.3	-302.5
4c_a6	-646.5591281	-646.355790	-646.7625061	-646.5591680	-0.1109	-69.6	-291.1
4c_a2	-646.5583348	-646.355008	-646.7619948	-646.5586680	-0.1104	-69.3	-289.8
4c_a5	-646.5236215	-646.321842	-646.7266179	-646.5248384	-0.0766	-48.0	-201.0
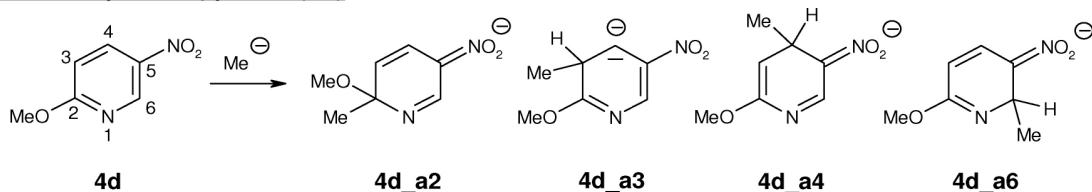
141

2-methoxy-5-nitropyridine (**4d**)

	B3LYP/6-31G(d)		B3LYP/6-311+G(d,p)// B3LYP/6-31G(d)				
	E_{tot}	H_{298}	E_{tot}	"H_{298}"	H_{rxn}	/ kcal mol^{-1}	/ kJ mol^{-1}
4d	-567.3213298	-567.186503	-567.4830699	-567.3482431			
methyl anion	-39.7902953	-39.758609	-39.8524446	-39.8207583			
4d_a6	-607.2663195	-607.092510	-607.4607799	-607.2869704	-0.1180	-74.0	-309.7
4d_a2	-607.2607941	-607.087778	-607.4555084	-607.2824923	-0.1135	-71.2	-298.0
4d_a4	-607.2595314	-607.085905	-607.4521583	-607.2785319	-0.1095	-68.7	-287.6
4d_a3	-607.2213838	-607.049318	-607.4163813	-607.2443155	-0.0753	-47.3	-197.7

1-methyl-2-nitropyrrole (**5a**)
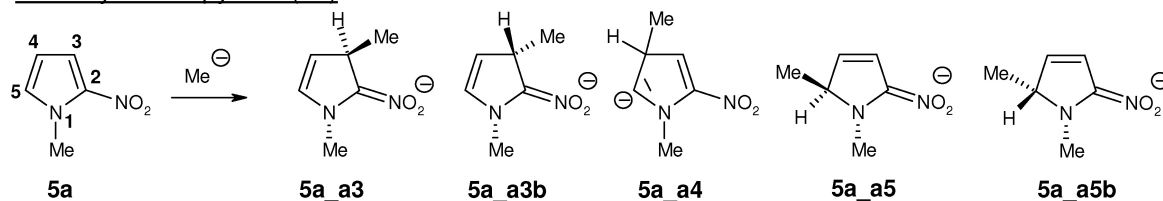
	B3LYP/6-31G(d)		B3LYP/6-311+G(d,p)// B3LYP/6-31G(d)				
	E_{tot}	H_{298}	E_{tot}	"H_{298}"	H_{rxn}	/ kcal mol^{-1}	/ kJ mol^{-1}
2no2pyr_1	-453.9817612	-453.858886	-454.1128507	-453.9899755			
methyl anion	-39.7902953	-39.758609	-39.8524446	-39.8207583			
5a_a5	-493.9019402	-493.741420	-494.0686996	-493.9081794	-0.0974	-61.1	-255.8
5a_a3b	-493.8959986	-493.735209	-494.0634580	-493.9026684	-0.0919	-57.7	-241.4
5a_a5b	-493.8963622	-493.735858	-494.0625848	-493.9020806	-0.0913	-57.3	-239.8
5a_a3	-493.8939805	-493.733189	-494.0609018	-493.9001103	-0.0894	-56.1	-234.7
5a_a4	-493.8325631	-493.674382	-494.0029282	-493.8447471	-0.0340	-21.3	-89.3

142
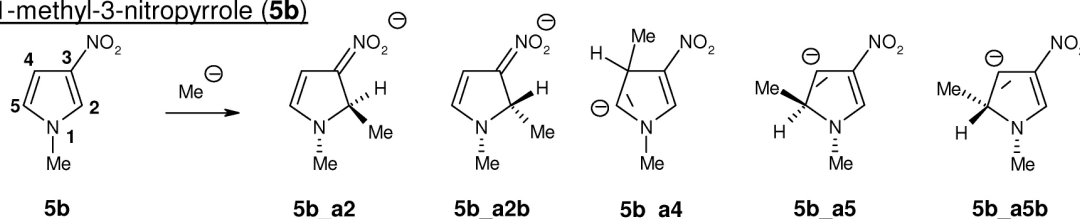
1-methyl-3-nitropyrrole (**5b**)

| | | | 5b_a2 | 5b_a2b | 5b_a4 | 5b_a5 | 5b_a5b |

	B3LYP/6-31G(d)		B3LYP/6-311+G(d,p)// B3LYP/6-31G(d)				
	E_{tot}	H_{298}	E_{tot}	"H_{298}"	H_{rxn}	/ kcal mol^{-1}	/ kJ mol^{-1}
5b	-453.9836782	-453.860911	-454.1160379	-453.9932707			
methyl anion	-39.7902953	-39.758609	-39.8524446	-39.8207583			
5b_a2	-493.9065635	-493.745874	-494.0745059	-493.9138164	-0.0998	-62.6	-262.0
5b_a2b	-493.9028691	-493.742154	-494.0704834	-493.9097683	-0.0957	-60.1	-251.4
5b_a4	-493.8625540	-493.702615	-494.0323023	-493.8723633	-0.0583	-36.6	-153.2
5b_a5	-493.8557752	-493.697120	-494.0251767	-493.8665215	-0.0525	-32.9	-137.8
5b_a5b	-493.8513463	-493.692734	-494.0197237	-493.8611114	-0.0471	-29.5	-123.6

1-methyl-5-nitroimidazole (**6a**)
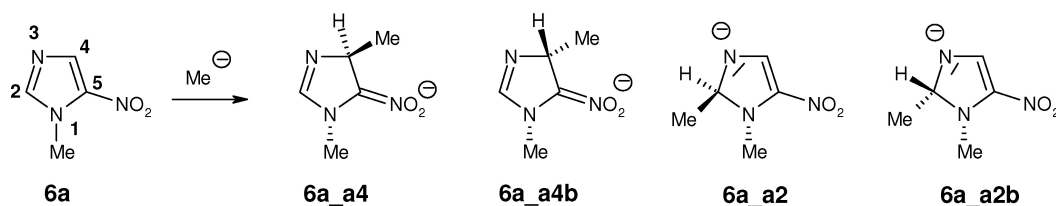
| | | | 6a_a4 | 6a_a4b | 6a_a2 | 6a_a2b |

	B3LYP/6-31G(d)		B3LYP/6-311+G(d,p)// B3LYP/6-31G(d)				
	E_{tot}	H_{298}	E_{tot}	"H_{298}"	H_{rxn}	/ kcal mol^{-1}	/ kJ mol^{-1}
6a	-470.0262963	-469.915070	-470.1611650	-470.0499387			
methyl anion	-39.7902953	-39.758609	-39.8524446	-39.8207583			
6a_a2	-509.9642525	-509.814673	-510.1330922	-509.9835127	-0.1128	-70.8	-296.2
6a_a4b	-509.9577280	-509.807962	-510.1283838	-509.9786178	-0.1079	-67.7	-283.3
6a_a2b	-509.9585186	-509.808864	-510.1269098	-509.9772552	-0.1066	-66.9	-279.8
6a_a4	-509.9552280	-509.805514	-510.1255408	-509.9758268	-0.1051	-66.0	-276.0

143
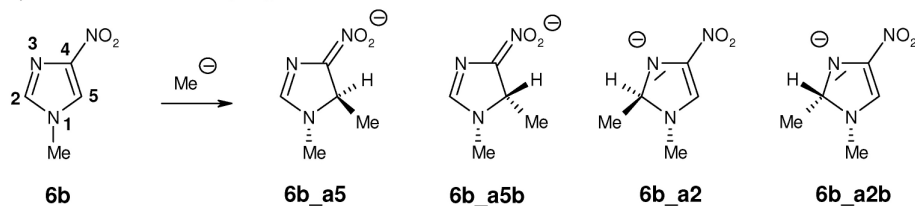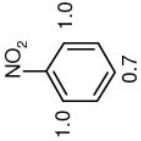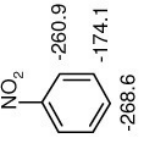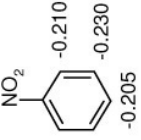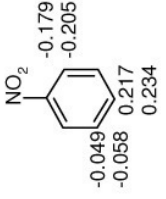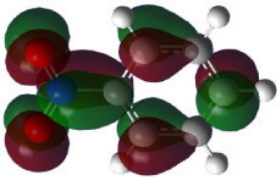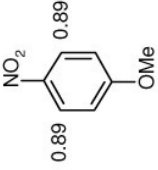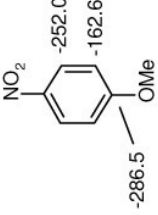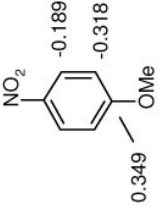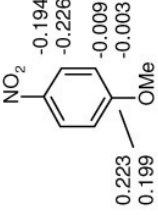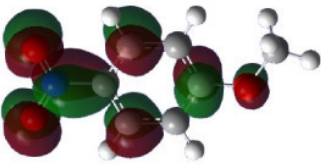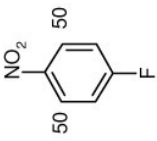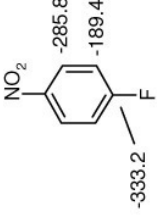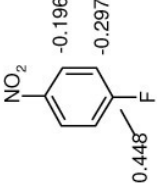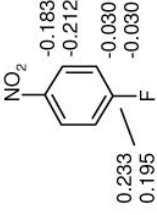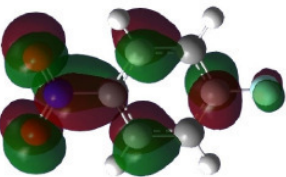
1-methyl-4-nitroimidazole (**6b**)

	B3LYP/6-31G(d)		B3LYP/6-311+G(d,p)// B3LYP/6-31G(d)				
	E_{tot}	H_{298}	E_{tot}	"H_{298}"	H_{rxn}	/ kcal mol^{-1}	/ kJ mol^{-1}
6b	-470.0274563	-469.916497	-470.1636808	-470.0527215			
methyl anion	-39.7902953	-39.758609	-39.8524446	-39.8207583			
6b_a5	-509.9575732	-509.808599	-510.1278684	-509.9788942	-0.1054	-66.1	-276.8
6b_a5b	-509.9549223	-509.805836	-510.1249210	-509.9758347	-0.1024	-64.2	-268.7
6b_a2	-509.9249401	-509.777450	-510.0963146	-509.9488245	-0.0753	-47.3	-197.8
6b_a2b	-509.9201896	-509.772690	-510.0907757	-509.9432761	-0.0698	-43.8	-183.3
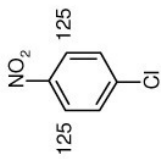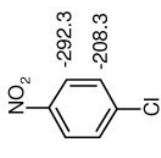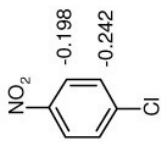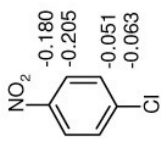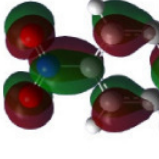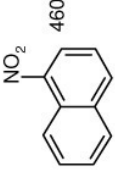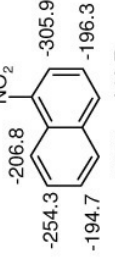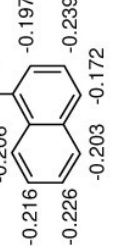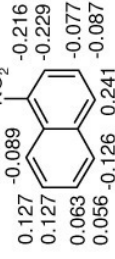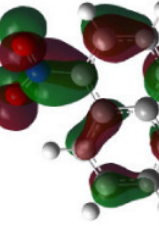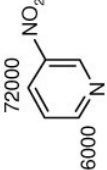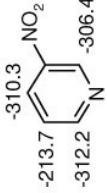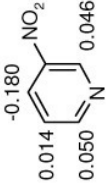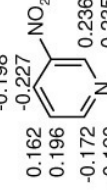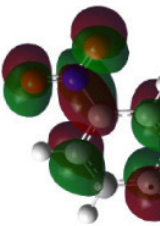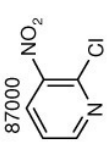
1-methyl-4-nitropyrazole (**7**)
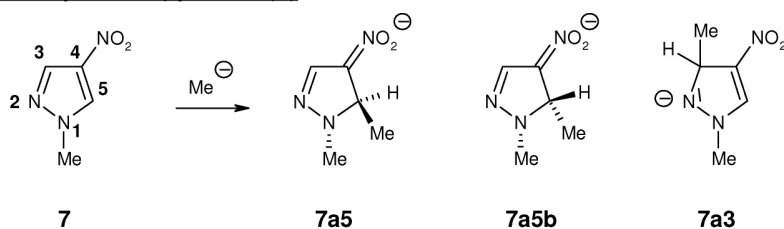
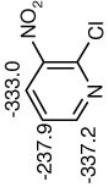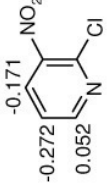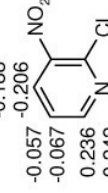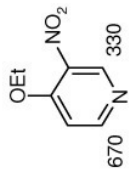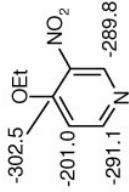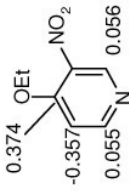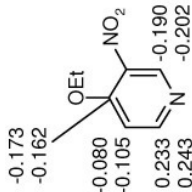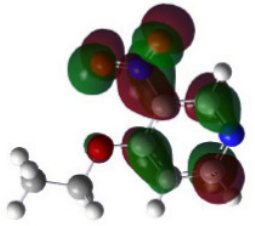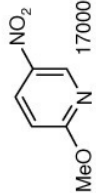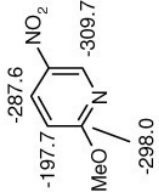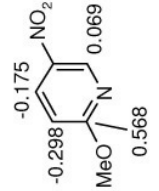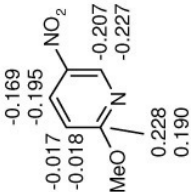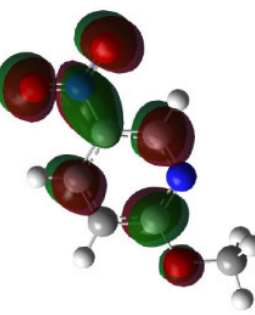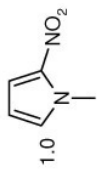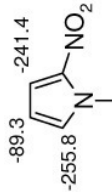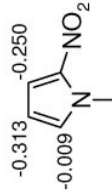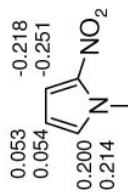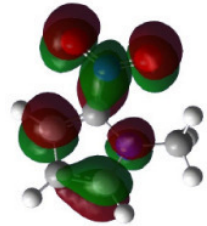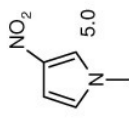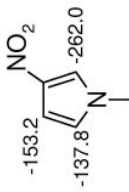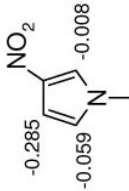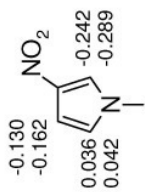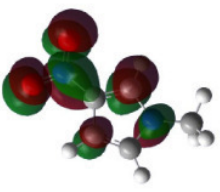|	B3LYP/6-31G(d)		B3LYP/6-311+G(d,p)// B3LYP/6-31G(d)				
	E_{tot}	H_{298}	E_{tot}	"H_{298}"	H_{rxn}	/ kcal mol^{-1}	/ kJ mol^{-1}
7	-470.0135178	-469.902460	-470.1492359	-470.0381781			
methyl anion	-39.7902953	-39.758609	-39.8524446	-39.8207583			
7_a5	-509.9513237	-509.801980	-510.1196309	-509.9702872	-0.1114	-69.9	-292.4
7_a5b	-509.9474427	-509.797985	-510.1154747	-509.9660170	-0.1071	-67.2	-281.1
7_a3	-509.9123397	-509.763616	-510.0846098	-509.9358861	-0.0769	-48.3	-202.0
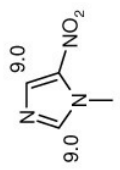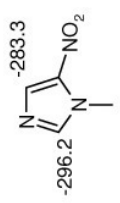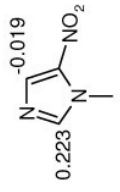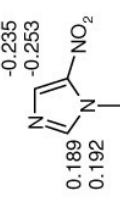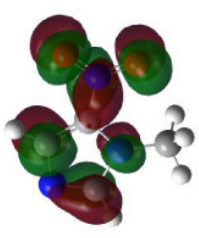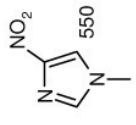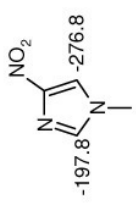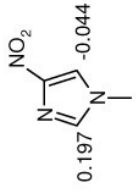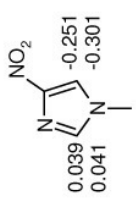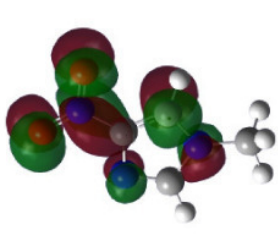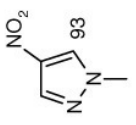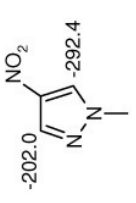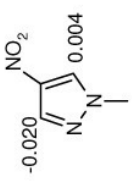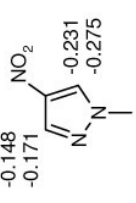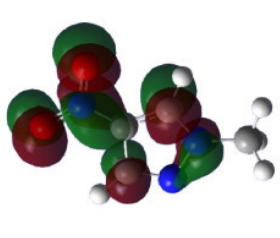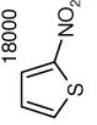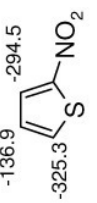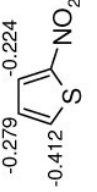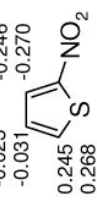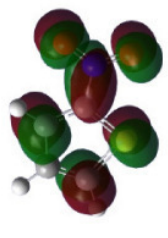
2-nitrothiophene (**8**)
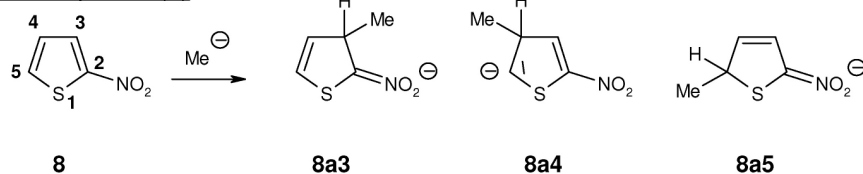
	B3LYP/6-31G(d)		B3LYP/6-311+G(d,p)// B3LYP/6-31G(d)			627.509	4.184
	E_{tot}	H_{298}	E_{tot}	"H_{298}"	H_{rxn}	/ kcal mol^{-1}	/ kJ mol^{-1}
8	-757.4989054	-757.421717	-757.6308831	-757.5536947			
methyl anion	-39.7902953	-39.758609	-39.8524446	-39.8207583			
8_a5	-797.4500601	-797.333612	-797.6147879	-797.4983398	-0.1239	-77.7	-325.3
8_a3	-797.4377288	-797.321360	-797.6029970	-797.4866282	-0.1122	-70.4	-294.5
8_a4	-797.3747228	-797.260456	-797.5408517	-797.4265849	-0.0521	-32.7	-136.9

144

no.	partial reactivities (experimental)	methyl anion affinities / kJ mol^{-1}	charges (NPA)	E(LUMO) / eV	LUMO coefficients 2p$_z$ 3p$_z$	LUMO
3a (NO$_2$)	1.0, 1.0, 0.7	−260.9, −174.1, −268.6	−0.210, −0.230, −0.205	−2.43	−0.179 / −0.205, 0.217 / 0.234, −0.049 / −0.058	
3b (NO$_2$, OMe)	0.89, 0.89	−252.0, −162.6, −286.5	−0.189, −0.318, 0.349	−2.16	−0.194 / −0.226, −0.009 / −0.003, 0.223 / 0.199	
3c (NO$_2$, F)	50, 50	−285.8, −189.4, −333.2	−0.196, −0.297, 0.448	−2.51	−0.183 / −0.212, −0.030 / −0.030, 0.233 / 0.195	

no.	partial reactivities (experimental)	methyl anion affinities / kJ mol^{-1}	charges (NPA)	E(LUMO) / eV	LUMO coefficients 2p$_z$ 3p$_z$	LUMO
3d	125, 125 (NO$_2$–C$_6$H$_4$–Cl)	−292.3, −208.3	−0.198, −0.242	−2.67	−0.180 / −0.205; −0.051 / −0.063	
3e	4600 (1-nitronaphthalene)	−305.9, −196.3, −313.7, −206.8, −254.3, −194.7, −258.0	−0.197, −0.239, −0.172, −0.206, −0.216, −0.226, −0.203	−2.47	−0.216 / −0.229; −0.077 / −0.087; −0.087 / −0.089; 0.127 / 0.127; 0.241 / 0.256; 0.063 / 0.056; −0.126 / −0.120	
4a	72000, 6000 (3-nitropyridine)	−310.3, −306.4, −213.7, −312.2	−0.180, 0.046, 0.014, 0.050	−2.76	−0.198 / −0.227; 0.236 / 0.235; 0.162 / 0.196; −0.172 / −0.190	
4b	87000, 6000 (3-nitro-2-chloropyridine)	−333.0, −237.9, −337.2	−0.171, −0.272, 0.052	−2.78	−0.188 / −0.206; 0.236 / 0.242; −0.057 / −0.067	

no.	partial reactivities (experimental)	methyl anion affinities / kJ mol^{-1}	charges (NPA)	E(LUMO) / eV	LUMO coefficients 2p$_z$ 3p$_z$	LUMO
4c	670 / 330 (OEt, NO$_2$ pyridine)	−302.5; −201.0; −291.1; −289.8 (OEt, NO$_2$ pyridine)	0.374; −0.357; 0.055; 0.056; −0.175 (OEt, NO$_2$ pyridine)	−2.29	−0.173 / −0.162; −0.080 / −0.105; 0.233 / 0.243; −0.190 / −0.202	
4d	17000 (NO$_2$, MeO pyridine)	−287.6; −197.7; −298.0; −309.7 (NO$_2$, MeO pyridine)	−0.298; 0.568; 0.069; −0.175 (NO$_2$, MeO pyridine)	−2.42	−0.169 / −0.195; −0.017 / −0.018; 0.228 / 0.190; −0.207 / −0.227	
5a	1.0 (NO$_2$ pyrrole)	−89.3; −255.8; −241.4 (NO$_2$ pyrrole)	−0.313; −0.009; −0.250 (NO$_2$ pyrrole)	−2.04	0.053 / 0.054; 0.200 / 0.214; −0.218 / −0.251	
5b	5.0 (NO$_2$ pyrrole)	−153.2; −137.8; −262.0 (NO$_2$ pyrrole)	−0.285; −0.059; −0.008 (NO$_2$ pyrrole)	−1.72	−0.130 / −0.162; 0.036 / 0.042; −0.242 / −0.289	

no.	partial reactivities (experimental)	methyl anion affinities / kJ mol^{-1}	charges (NPA)	E(LUMO) / eV	LUMO coefficients 2p$_z$ 3p$_z$	LUMO
6a	9.0 / 9.0	−283.3 / −296.2	−0.019 / 0.223	−2.42	−0.235 / −0.253 ; 0.189 / 0.192	
6b	550	−276.8 / −197.8	−0.044 / 0.197	−1.93	−0.251 / −0.301 ; 0.039 / 0.041	
7	93	−292.4 / −202.0	0.004 / −0.020	−2.09	−0.231 / −0.275 ; −0.148 / −0.171	
8	18000	−294.5 / −136.9 / −325.3	−0.224 / −0.279 / −0.412	−2.66	−0.246 / −0.270 ; −0.023 / −0.031 ; 0.245 / 0.268	

4.6 References

[1]   J. Golinski, M. Makosza, *Tetrahedron Lett.* **1978**, 3495-3498.

[2]   M. Makosza, J. Winiarski, *Acc. Chem. Res.* **1987**, *20*, 282-289.

[3]   O. N. Chupakhin, V. N. Charushin, H. C. v. d. Plas, *Nucleophilic Aromatic Substitution of Hydrogen*, Academic Press, San Diego, **1994**.

[4]   F. Terrier, *Nucleophilic Aromatic Displacement: The influence of the Nitro group*, VCH, New York, **1991**.

[5]   M. Makosza, K. Wojciechowski, *Liebigs Ann. Recl.* **1997**, 1805-1816.

[6]   M. Makosza, K. Wojciechowski, *Chem. Rev.* **2004**, *104*, 2631-2666.

[7]   M. Makosza, T. Glinka, *J. Org. Chem.* **1983**, *48*, 3860-3861.

[8]   T. Lemek, M. Makosza, D. S. Stephenson, H. Mayr, *Angew. Chem.* **2003**, *115*, 2899-2901; *Angew. Chem. Int. Ed.* **2003**, *42*, 2793-2795.

[9]   M. Makosza, A. Kwast, *J. Phys. Org. Chem.* **1998**, *11*, 341-349.

[10]   M. Makosza, T. Lemek, A. Kwast, F. Terrier, *J. Org. Chem.* **2002**, *67*, 394-400.

[11]   M. Makosza, T. Glinka, A. Kinowski, *Tetrahedron* **1984**, *40*, 1863-1868.

[12]   M. Makosza, *Synthesis* **1991**, 103-111.

[13]   M. Makosza, O. Lobanova, A. Kwast, *Tetrahedron* **2004**, *60*, 2577-2581.

[14]   (a) S. Blazej, *Dissertation* **2007**, Institute of Organic Chemistry, Polish Academy of Sciences, Warsaw. (b) S. Blazej, M. Makosza, in preparation.

[15]   M. Makosza, J. Golinski, J. Baran, *J. Org. Chem.* **1984**, *49*, 1488-1494.

[16]   H. J. Anderson, *Can. J. Chem.* **1957**, *35*, 21-27.

[17]   C. E. Hazeldine, F. L. Pyman, J. Winchester, *J. Chem. Soc.* **1924**, *125*, 1431-1441.

[18]   M. Lissel, *Liebigs Ann. Chem.* **1987**, 77-79.

[19]   N. Nishiwaki, T. Ogihara, T. Takami, M. Tamura, M. Ariga, *J. Org. Chem.* **2004**, *69*, 8382-8386.

[20]   B. Östman, *Acta Chem. Scand.* **1968**, *22*, 1687-1689.

[21]   V. S. Babasinian, *J. Am. Chem. Soc.* **1935**, *57*, 1763-1764.

[22]   H. v. Babo, B. Prijs, *Helv. Chim. Acta* **1950**, *33*, 306-313.

[23]   G. Klein, B. Prijs, H. Erlenmeyer, *Helv. Chim. Acta* **1955**, *38*, 1412-1414.

[24]   M. Makosza, S. Ludwiczak, *J. Org. Chem.* **1984**, *49*, 4562-4563.

[25]   Following notations are used throughout this paper: **3a**, **3b**, **3c**, ..., **4a**, **4b**, ..., **7**, etc. denote the nitro(hetero)arene. The additional letter (o = *ortho*, p = *para* or *pseudo-para*) indicates the position of CH_2SO_2Ph substituent in relation to the nitro group.

[26]   M. Makosza, B. Chylinska, B. Mudryk, *Liebigs Ann. Chem.* **1984**, 8-14.

[27]   M. Makosza, A. Tyrala, *Synthesis* **1987**, 1142-1144.

[28]   M. Makosza, S. Ludwiczak, *Pol. J. Chem.* **1998**, *72*, 1168-1172.

[29]   E. Kwast, M. Makosza, *Tetrahedron Lett.* **1990**, *31*, 121-122.

[30]   M. Makosza, E. Slomka, *Bull. Pol. Acad. Sci., Chem.* **1984**, *32*, 69-74.

[31]   M. Makosza, E. Kwast, *Bull. Pol. Acad. Sci., Chem.* **1987**, *35*, 287-292.

[32]   M. D. Crozet, V. Remusat, C. Curti, P. Vanelle, *Synth. Commun.* **2006**, *36*, 3639-3646.

[33]   M. D. Crozet, P. Perfetti, M. Kaafarani, M. P. Crozet, P. Vanelle, *Lett. Org. Chem.* **2004**, *1*, 326-330.

[34]   M. D. Crozet, P. Perfetti, M. Kaafarani, P. Vanelle, M. P. Crozet, *Tetrahedron Lett.* **2002**, *43*, 4127-4129.

[35]   M. K. Bernard, M. Makosza, B. Szafran, U. Wrzeciono, *Liebigs Ann. Chem.* **1989**, 545-549.

[36]   M. K. Bernard, *Tetrahedron* **2000**, *56*, 7273-7284.

[37]   M. Makosza, E. Kwast, *Tetrahedron* **1995**, *51*, 8339-8354.

[38]   Calculated with What`sBest! 7.0 nonlinear solver.

[39]   G. Bartoli, O. Sciacovelli, M. Bosco, L. Forlani, P. E. Todesco, *J. Org. Chem.* **1975**, *40*, 1275-1278.

[40]   G. Bartoli, M. Fiorentino, F. Ciminale, P. E. Todesco, *J. Chem. Soc., Chem. Commun.* **1974**, 732.

[41]   J. Liebschev, *"Methoden der organischen Chemie" Hetarene III/Teil 2*, Houben-Weyl, Stuttgart, **1994**.

[42]   For further details on kinetics of carbanions with Michael acceptors see: S. T. A. Berger, F. H. Seeliger, F. Hofbauer, H. Mayr *Org. Biomol. Chem.* **2007**, *5*, 3020-3026 and F. Seeliger, S. T. A. Berger, G. Y. Remennikov, K. Polborn, H. Mayr *J. Org. Chem.* **2007**, *72*, 9170-9180.

[43]   H. Mayr, A. R. Ofial, *Pure Appl. Chem.* **2005**, *77*, 1807-1821.

[44]   R. R. Bishop, E. A. S. Cavell, N. B. Chapman, *J. Chem. Soc.* **1952**, 437-446.

[45]   H. Mayr, T. Bug, M. F. Gotta, N. Hering, B. Irrgang, B. Janker, B. Kempf, R. Loos, A. R. Ofial, G. Remennikov, H. Schimmel, *J. Am. Chem. Soc.* **2001**, *123*, 9500-9512.

[46]   D. Spinelli, G. Consiglio, R. Noto, V. Frenna, *J. Org. Chem.* **1976**, *41*, 968-971.

[47]   D. Spinelli, G. Consiglio, *J. Chem. Soc., Perkin Trans. 2* **1975**, 1388-1391.

[48]   G. Doddi, G. Illuminati, P. Mencarelli, F. Stegel, *J. Org. Chem.* **1976**, *41*, 2824-2826.

[49]   Gaussian 03, Revision D.03, M. J. Frisch, G. W. Trucks, H. B. Schlegel, G. E. Scuseria, M. A. Robb, J. R. Cheeseman, J. A. Montgomery, Jr., T. Vreven, K. N. Kudin, J. C. Burant, J. M. Millam, S. S. Iyengar, J. Tomasi, V. Barone, B. Mennucci, M. Cossi, G. Scalmani, N. Rega, G. A. Petersson, H. Nakatsuji, M. Hada, M. Ehara, K. Toyota, R. Fukuda, J. Hasegawa, M. Ishida, T. Nakajima, Y. Honda, O. Kitao, H. Nakai, M. Klene, X. Li, J. E. Knox, H. P. Hratchian, J. B. Cross, V. Bakken, C. Adamo, J. Jaramillo, R. Gomperts, R. E. Stratmann, O. Yazyev, A. J. Austin, R. Cammi, C. Pomelli, J. W. Ochterski, P. Y. Ayala, K. Morokuma, G. A. Voth, P. Salvador, J. J. Dannenberg, V. G. Zakrzewski, S. Dapprich, A. D. Daniels, M. C. Strain, O. Farkas, D. K. Malick, A. D. Rabuck, K. Raghavachari, J. B. Foresman, J. V. Ortiz, Q. Cui, A. G. Baboul, S. Clifford, J. Cioslowski, B. B. Stefanov, G. Liu, A. Liashenko, P. Piskorz, I. Komaromi, R. L. Martin, D. J. Fox, T. Keith, M. A. Al-Laham, C. Y. Peng, A. Nanayakkara, M. Challacombe, P. M. W. Gill, B. Johnson, W. Chen, M. W. Wong, C. Gonzalez, and J. A. Pople, Gaussian, Inc., Wallingford CT, **2004**.

[50]   C. Schindele, K. N. Houk, H. Mayr, *J. Am. Chem. Soc.* **2002**, *124*, 11208-11214.

[51]   O. Kaumanns, H. Mayr, **2008**, manuscript in preparation.

Chapter 5

Nucleophilic Behavior of Sulfonyl-stabilized Carbanions

F. Seeliger and H. Mayr, *Org. Biomol. Chem.* **2008**, *submitted.*

5.1 Introduction

The relative inertness of the sulfone group to nucleophilic attack and its ability to enable deprotonation in *α*-position of attached alkyl groups have elevated the sulfone moiety to a premier position amongst carbanion-stabilizing groups.[1-4] Sulfonyl-stabilized carbanions can efficiently be alkylated and acylated, and therefore, are important reagents for the formation of C-C bonds.[5] Deprotonation of sulfones with bases and subsequent reaction with carbonyl compounds yields *β*-hydroxysulfones,[6] which can easily be reduced to give C=C bonds (Julia olefination).[7-10])

The pKa values of sulfones have systematically been investigated by Bordwell, who also studied the rate constants for the S$_N$2 reactions of a family of sulfonyl-stabilized carbanions with *n*-butyl chloride and *n*-butyl bromide in DMSO solution.[11] He reported that in contrast to the predictions of the reactivity-selectivity-principle, *n*-butyl bromide is generally $(3\text{-}4) \times 10^2$ times more reactive than *n*-butyl chloride, independent of the nucleophilicity of the carbanion. This work set out to compare the nucleophilic reactivities of sulfonyl-stabilized carbanions with those of related species.

The linear-free-energy-relationship 5.1, introduced in 1994,[12] is a versatile and powerful tool to organize polar organic reactivity. The reactions of carbocations with various types of nucleophiles as well as the reactions of carbanions with quinone methides and Michael acceptors are described by equation 5.1[13]

$$\log k_2(20\ °C) = s(N + E) \tag{5.1}$$

Electrophiles are characterized by the electrophilicity parameter E and nucleophiles are characterized by a nucleophilicity parameter N and a nucleophile-specific slope-parameter s.

X	pK_a [a]
1a: m-Cl	21.6
1b: p-CF$_3$	20.2
1c: p-CN	18.5
1d: p-NO$_2$	15.8

[a] DMSO, ref. [14]
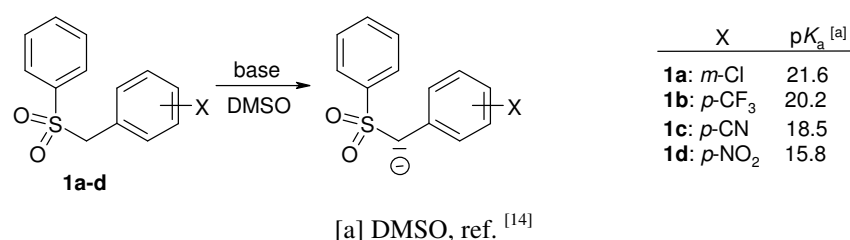
SCHEME 5.1: Sulfones **1a-d** studied in this work.

In order to investigate whether equation 5.1 can also be used to describe the nucleophilic reactivities of sulfonyl-stabilized carbanions, we have now investigated the addition reactions of four sulfonyl-stabilized carbanions (**1a-d**)⁻ (Scheme 5.1) to quinone methides (**2a-e**, Scheme 5.2), diarylcarbenium ions (**3a-b**, Scheme 5.2), and Michael acceptors (**4a-6d**, Scheme 5.2) in DMSO. The reactions of nucleophiles with Michael acceptors **4** (benzylidene Meldrum's acids), **5** (benzylidenebarbituric acids), and **6** (2-benzylidene-indan-1,3-diones) have only recently been demonstrated to follow equation 5.1[15-17] though with lower precision.

	R	Ar		Ar		Ar		Ar		Ar
2a:	^{t}Bu	julolidyl [a]	**3a**: julolidyl [a]	**4a**: julolidyl [a]	**5a**: julolidyl [a]	**6a**: julolidyl [a]
2b:	^{t}Bu	C$_6$H$_4$-p-NMe$_2$	**3b**: lilolidyl [a]		**5b**: C$_6$H$_4$-p-NMe$_2$	**6b**: C$_6$H$_4$-p-NMe$_2$
2c:	^{t}Bu	C$_6$H$_4$-p-OMe			**5c**: C$_6$H$_4$-p-OMe	**6c**: C$_6$H$_4$-p-OMe
2d:	^{t}Bu	C$_6$H$_4$-p-Me				**6d**: Ph
2e:	Ph	C$_6$H$_4$-p-NMe$_2$				

n = 1: lilolidyl
n = 2: julolidyl
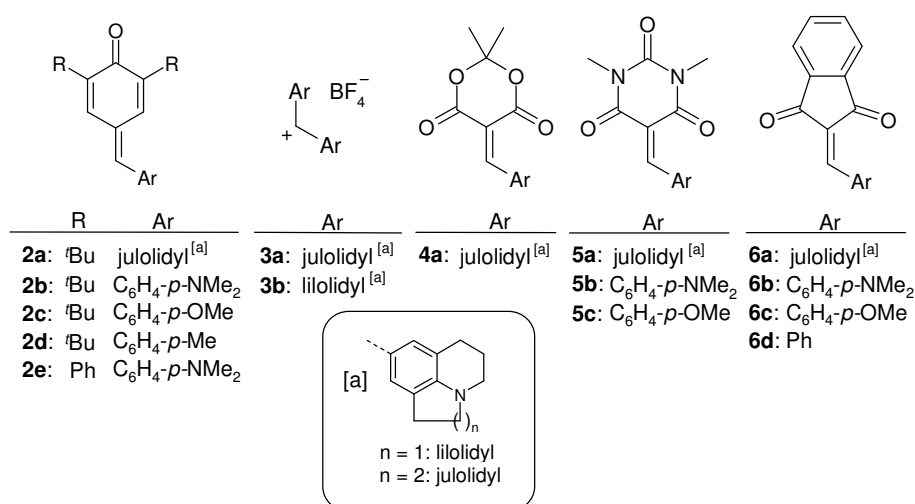
SCHEME 5.2: Electrophiles **2-6** employed for the determination of the nucleophilicities of sulfonyl-stabilized carbanions (**1a-d**)⁻.

5.2 Results

5.2.1 Product Studies

The attack of the sulfonyl-stabilized carbanions **1**⁻ to Michael acceptors has previously been described in literature.[18, 19] In order to prove the postulated reaction course, we synthesized some of the reaction products. Therefore, the sulfones **1b** and **1c** were combined with 1.05 equivalents of potassium *tert*-butoxide in dry THF solution and then treated with equimolar amounts of **5b** or **6b**. (Scheme 5.3). The resultant anionic adducts were then precipitated as potassium salts *via* slow addition of dry Et$_2$O. ^{1}H- and ^{13}C-NMR analyses in d_6-DMSO showed that despite drying for 10 hours at 10^{-2} mbar, the isolated crystalline products contain 0.2–0.5 equivalents of tetrahydrofuran.
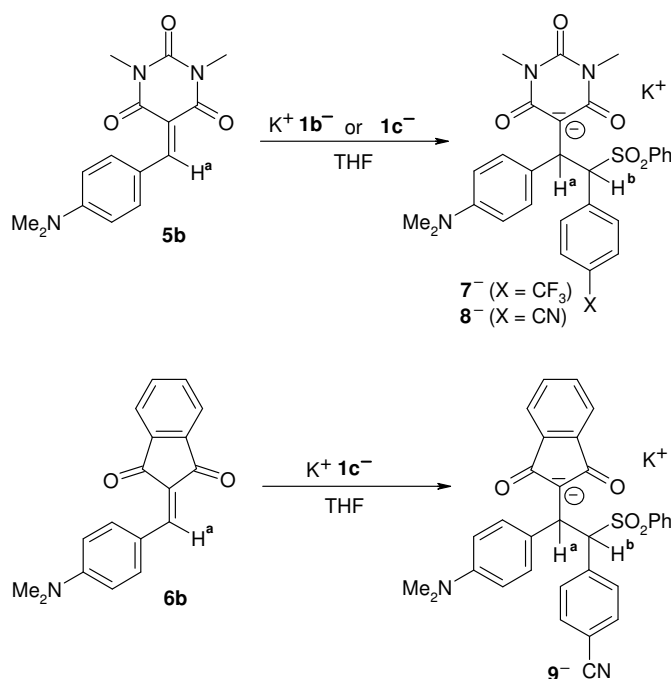
SCHEME 5.3: Michael additions of the sulfonyl-stabilized carbanions **1b**⁻ and **1c**⁻ to the benzylidenebarbituric acid **5b** and 2-benzylidene-indan-1,3-dione **6b**.

The observation of two sets of signals in the ^{1}H-NMR spectra of the anionic adducts (**7-9**)⁻ indicates the formation of two diastereomers (**7**⁻: 3:2, **8**⁻: 5:4, **9**⁻: 7:3). Protons H^a and H^b, which absorb as doublets between δ 4.51–5.08 ppm (H^a) and δ 5.95–6.57 ppm (H^b) with vicinal coupling constants of approximately 12 Hz, are characteristic for compounds **7-9**. The high upfield shifts of the ^{1}H-NMR signals of the vinylic protons H^a in compounds **5b** (δ 8.41 ppm)[20] and **6b** (δ 7.58 ppm)[21] to δ 4.51–5.08 ppm in products (**7-9**)⁻ indicate the nucleophilic attack in β-position of the Michael acceptor.[22]

154

The adducts of the carbanions (**1a-c**)⁻ to quinone methides **2a** and **2b** were synthesized analogously and treated with saturated ammonium chloride solution to yield the diastereomeric mixtures of the corresponding phenols **10-13** (Scheme 5.4), from which one diastereomer was separated by column chromatography.[23] In compounds **10-13** protons Hᵃ and Hᵇ absorb as doublets between δ 4.56–4.82 ppm (Hᵃ) and δ 4.86–4.96 ppm (Hᵇ) with ^3J coupling constants of (10.4 ± 0.4) Hz.
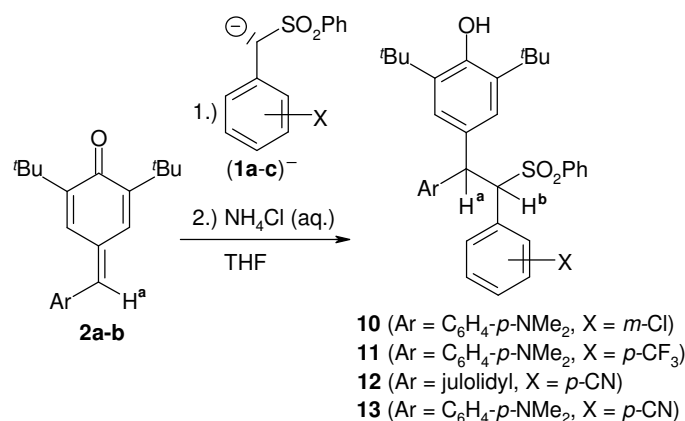
SCHEME 5.4: Additions of the sulfonyl-stabilized carbanions (**1a-c**)⁻ to the quinone methides **2a-b**.

Because analogous reaction products can be expected for other combinations of (**1a-d**)⁻ with **2-6**, product studies have not been performed for all reactions which have been studied kinetically.

5.2.2 Kinetics

The electrophiles **2-6** show strong absorption bands in the UV-Vis spectra at λ_{max} = 375–525 nm. By attack of the nucleophiles at the electrophilic double bond, the chromophore is interrupted, and the reaction can be followed by the decrease of the absorbances of the electrophiles. All reactions proceeded quantitatively, as indicated by the complete decolorization of the solutions. The kinetic experiments were performed under first-order conditions using a high excess of the nucleophiles. From the exponential decays of the UV-Vis absorbances of the electrophiles, the first-order rate constants $k_{1\Psi}$ were obtained. Plots of $k_{1\Psi}$ versus [**1**⁻] were linear, and their slopes yielded the second-order rate constants k_2 (Table 5.1).
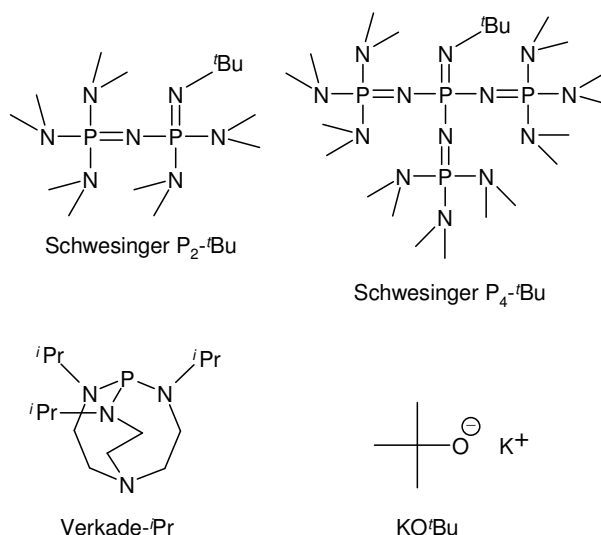
SCHEME 5.5: Sterically hindered bases used for the deprotonation of sulfones **1a-d**.

The carbanions were generated in DMSO solution by treatment of the sulfones **1a-d** with 1.05 equivalents of a strong hindered base, e.g., potassium *tert*-butoxide, Schwesinger's P_2- or P_4-phosphazene base, Verkade's football-shaped proazaphosphatrane base (Scheme 5.5). The large difference between the pK_a values of the sulfones **1** (pK_a = 15.8 – 21.6)[14] and Schwesinger's P_4-^{t}Bu base (pK_{BH^+} = 30.2),[24] potassium *tert*-butoxide (pK_{BH^+} = 29.4),[25] and Verkade's base (pK_{BH^+} ~ 27)[26, 27] warrant the quantitative formation of the carbanions under these conditions. Complete deprotonation of the sulfones **1b** and **1c** by 1.05 equivalents of Schwesinger's P_2-^{t}Bu base (pK_{BH^+} = 21.5)[24] was indicated by the observation that the UV-Vis absorbances of the solutions of the carbanions **1b⁻** and **1c⁻** at λ_{max} = 350 nm and λ_{max} = 375 nm, respectively, could not be increased by adding more of the P_2-^{t}Bu base.[23]

As demonstrated for the addition of the sulfonyl-stabilized carbanion **1c⁻** to the Michael acceptor **5a**, the rate of the reaction is not affected by the nature of the base used for the deprotonation of the sulfone **1**. Thus, a second-order rate constant of 1.48×10^4 M^{-1} s^{-1} was observed with Verkade's base, and $k_2 = 1.51 \times 10^4$ M^{-1} s^{-1} was observed, when KO^{t}Bu was used for the deprotonation (Table 5.1). The addition of equimolar amounts of 18-crown-6 as complexing agent for potassium ions does not influence the rate either, as shown for the reaction of **1c** with **6a** (Table 5.1). Therefore, the carbanions **1⁻** are not paired under the conditions used for the kinetic experiments.

Due to the yellow color of the carbanions (**1a-c**)⁻ in DMSO solution, electrophiles with UV-Vis maxima > 475 nm (i.e., **2a-b**, **2e**, **4a**, **5a-b**, **6a-b**) had to be employed for kinetic investigations. On the other side, the *p*-nitro-substituted carbanion **1d**⁻ absorbs at λ_{max} = 540 nm and electrophiles with UV-Vis maxima at λ = 375 − 475 nm (e.g. the yellow compounds **2c-d**, **5c**, **6c-d**) were used to study the reactivity of this carbanion.

TABLE 5.1: Second-order rate constants k_2 (DMSO, 20 °C) of the reactions of sulfonyl-stabilized carbanions **1a-d** with reference electrophiles **2-3** and Michael acceptors **4-6**.

sulfone	base	elec.	k_2 (L mol^{-1} s^{-1})
1a	P$_4$-^{t}Bu	**2a**	1.01×10^4
	P$_4$-^{t}Bu	**2b**	2.31×10^4
	KO^{t}Bu	**6a**	6.24×10^4
	KO^{t}Bu	**4a**	6.76×10^4
	KO^{t}Bu	**5a**	1.54×10^5
	KO^{t}Bu	**6b**	4.13×10^5
	KO^{t}Bu	**5b**	7.45×10^5
1b	P$_2$-^{t}Bu	**2a**	1.98×10^3
	P$_2$-^{t}Bu	**2b**	3.72×10^3
	Verkade	**6a**	1.34×10^4
	Verkade	**4a**	1.86×10^4
	Verkade	**5a**	3.85×10^4
	Verkade	**6b**	6.08×10^4
	Verkade	**5b**	1.66×10^5
	Verkade	**2e**	3.87×10^5
1c	P$_2$-^{t}Bu	**2a**	4.89×10^2
	P$_2$-^{t}Bu	**2b**	1.04×10^3
	KO^{t}Bu[a]	**6a**	5.61×10^3
	KO^{t}Bu	**6a**	5.77×10^3
	KO^{t}Bu	**4a**	1.04×10^4
	Verkade	**5a**	1.48×10^4
	KO^{t}Bu	**5a**	1.51×10^4
	Verkade	**6b**	2.53×10^4
	Verkade	**5b**	5.97×10^4

TABLE 5.1: Continued.

sulfone	base	elec.	k_2 (L mol^{-1} s^{-1})
1c	KO^{t}Bu	**2e**	1.84×10^5
1d	Verkade	**2c**	6.74×10^1
	Verkade	**2d**	1.10×10^2
	Verkade	**6c**	2.34×10^4
	Verkade	**5c**	5.53×10^4
	Verkade	**6d**	9.28×10^4
	Verkade	**3b**	2.85×10^6
	Verkade	**3a**	6.58×10^6

[a] addition of equimolar amounts of crown ether 18-C-6.

5.3 Discussion

In order to determine the nucleophilicity parameters N and s of the sulfonyl-stabilized carbanions (**1a-d**)$^-$, the logarithmic second-order rate constants log k_2 were plotted versus the electrophilicity parameters E of the corresponding electrophiles. As expected, the plots for the reactions of sulfonyl-stabilized carbanions (**1a-d**)$^-$ with the reference electrophiles **2** and **3** yield straight correlations. However, systematic deviations are found for the rate constants of the corresponding additions to the Michael acceptors **4-6** (Figures 5.1-5.3). The rate constants of these reactions are about one order of magnitude smaller than expected on the basis of the correlation with the reference electrophiles **2** and **3**.
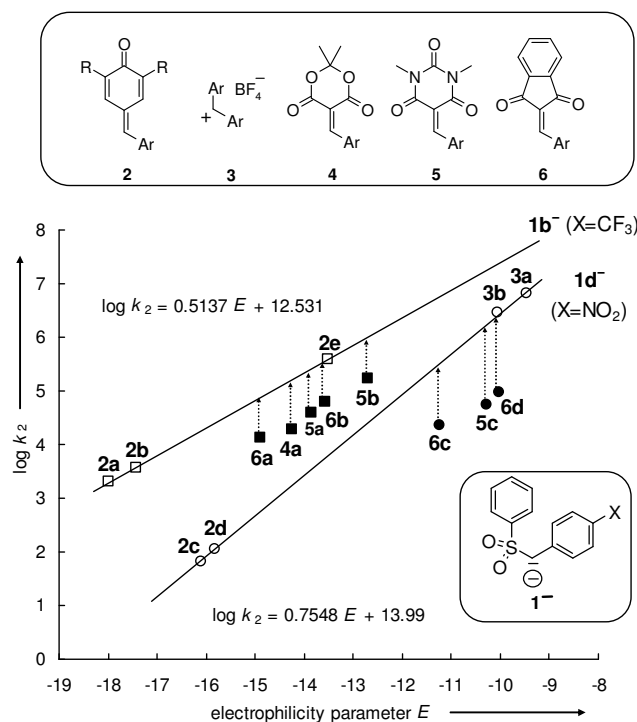
FIGURE 5.1: Plot of log k_2 (DMSO) versus electrophilicity parameters E for the reactions of carbanions **1b⁻** and **1d⁻** with the reference electrophiles **2**, **3** and Michael acceptors **4**-**6**.

Due to the high nucleophilicity of carbanion **1a⁻**, only the quinone methides **2a** and **2b** were available as reference systems to characterize this nucleophile. Thus, the deviations indicated by the arrows in Figure 5.2 are only estimates, due to the uncertainty of the correlation's slope.
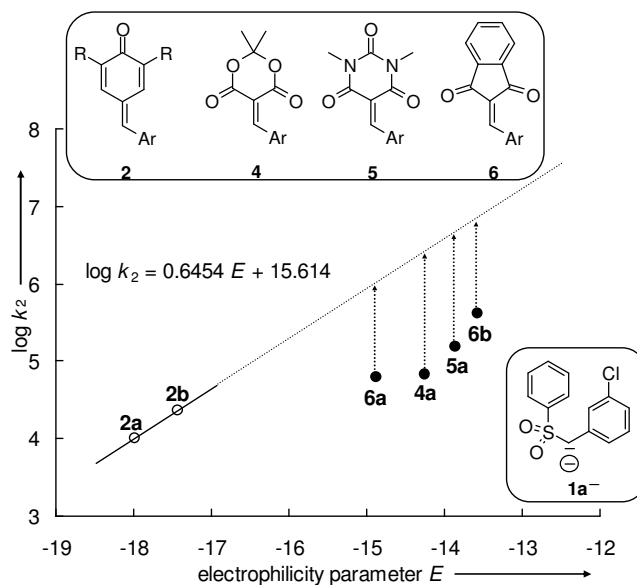
FIGURE 5.2: Plot of log k_2 (DMSO) versus electrophilicity parameters E for the reactions of carbanion **1a⁻** with the quinone methides **2** and Michael acceptors **4**-**6**.
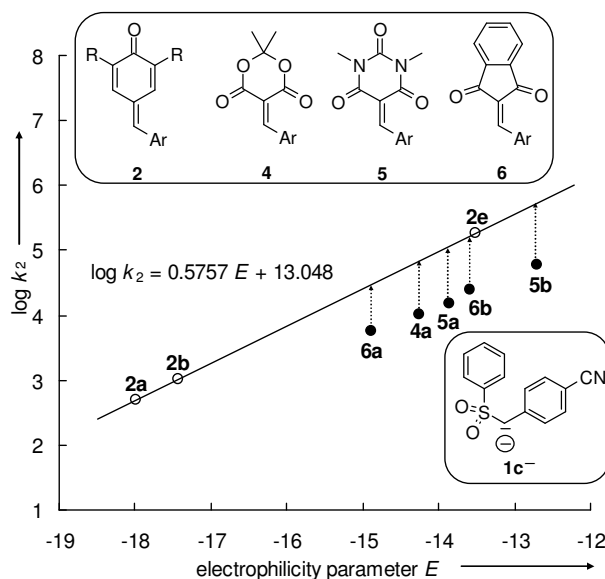
159

FIGURE 5.3: Plot of log k_2 (DMSO) versus electrophilicity parameters E for the reactions of carbanion **1c**⁻ with the quinone methides **2** and Michael acceptors **4**-**6**.

From the correlations drawn in Figures 5.1 and 5.3, which are based on the reactions of the carbanions (**1b-d**)⁻ with the reference electrophiles **2a-e**, we have derived the nucleophile-specific parameters N and s, listed in Table 5.2. As the reactivity of the carbanion **1a**⁻ was only investigated towards two reference compounds of comparable electrophilicity, the corresponding N and s values have not been calculated.

TABLE 5.2: Derived N and s parameters for sulfonyl-stabilized carbanions (**1b-d**)⁻.

carbanion	N	s
1b⁻	24.39	0.51
1c⁻	22.66	0.58
1d⁻	18.53	0.75

According to Figure 5.4, the phenylsulfonyl-stabilized benzyl anions (**1b-d**)⁻ are considerably more nucleophilic than their trifluoromethanesulfonyl-stabilized analogues (4 to 7 units in N) and the corresponding α-nitrobenzyl anions. To include the carbanion **1a**⁻, detailed structure-reactivity correlations shall, therefore, be based on individual rate constants.
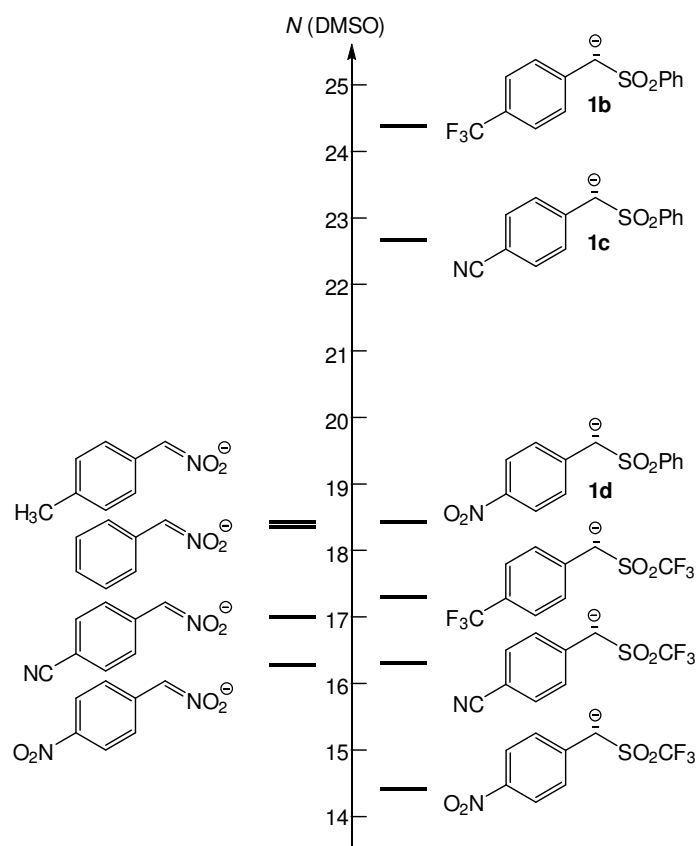
FIGURE 5.4: Comparison of the nucleophilicities of differently substituted benzyl anions in DMSO.

Second-order rate constants for the reactions of the quinone methide **2b** have been determined with all sulfonyl-stabilized carbanions **1⁻** except **1d⁻**. Because the electrophilicity of **2b** is only slightly smaller than that of **2c** and **2d**, the rate constant for the reaction of **1d⁻** with **2b** can reliably be calculated from the lower correlation line of Figure 5.1 as $k_2 = 8.70$ M^{-1} s^{-1}.

Figure 5.5 shows that the rate constants for the reactions of the carbanions (**1a-d**)⁻ with the quinone methide **2b** correlate only moderately with Hammett's σ^- parameters. The correlation with σ_p is even worse, and because of the deviation of p-CN and p-NO$_2$ in the opposite sense, a Yukawa-Tsuno treatment[28] would not improve this correlation.
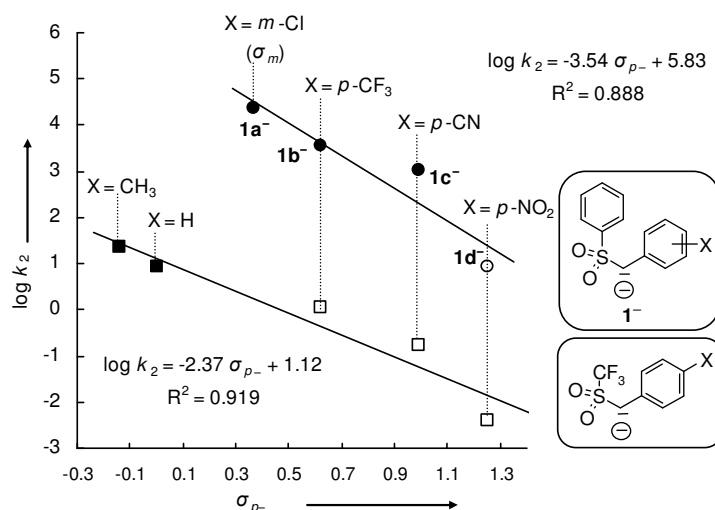
FIGURE 5.5: Correlations of the logarithmic second-order rate constants of the reactions of quinone methide **2b** with carbanions (**1a-d**)⁻ and with trifluoromethanesulfonyl-stabilized carbanions (DMSO) with the Hammett σ_{p-} values. Filled symbols: experimental rate constants; open symbols: calculated (equation 5.1) rate constants.

In agreement with a higher negative charge density at the benzylic carbon of carbanions (**1a-d**)⁻, the Hammett reaction constant ρ is more negative than for the analogous reactions of the corresponding trifluoromethtanesulfonyl-stabilized anions (Figure 5.5, lower graph). It should be noted, however, that in both correlations the cyano- and nitro-substituted compounds deviate in the same opposite directions.
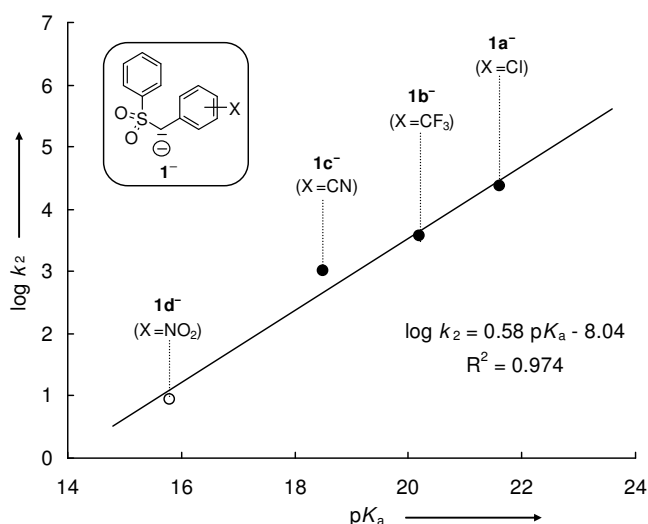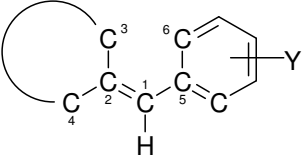
FIGURE 5.6: Brønsted plot for the reactions of sulfonyl-stabilized carbanions (**1a-d**)⁻ with the quinone methide **2b** (DMSO). Filled symbols: experimental rate constants; open symbol: calculated (equation 5.1) rate constant.

162

In contrast, the Brønsted correlation shown in Figure 5.6 is of high quality with a typical slope. Like in the Hammett correlation, the *p*-cyano substituted compound appears to be exceptionally nucleophilic.

The systematic deviations of the Michael acceptors **4-6** from the correlation with the reference electrophiles **2-3** (Figures 5.1-5.3) are not unprecedented. Similar deviations have previously been reported for the reactions of the anions of dimedone and diethyl malonate with the Michael acceptors **4-6**.[17] Combinations of **4-6** with the anion of dimedone were found to be slightly faster, combinations with the anion of diethyl malonate were slightly slower than expected. In order to reveal the origin of these deviations, quantum chemical calculations have been performed.

The structures of various conformers of the electrophiles **2-6** were calculated with Gaussian03[29] at the B3LYP level using the 6-31G(d,p) basis set.

TABLE 5.3: Calculated bond lengths (Å), angles (deg), and dihedral angles (deg) of quinone methides **2a-e** and Michael acceptors **4a-6d** (B3LYP/6-31(d,p)).

	C^1C^2	C^1C^5	$C^2C^1C^5$	$C^2C^1C^5C^6$	$C^5C^1C^2C^3$
2a[a]	1.3785	1.4470	131.6	24.9	8.9
2b	1.3774	1.4482	131.5	26.0	8.6
2c	1.3738	1.4550	130.9	29.2	8.0
2d	1.3721	1.4586	130.6	31.5	7.3
2e[a]	1.3798	1.4455	131.4	24.9	8.8
5a[a]	1.3818	1.4342	138.6	0.14	0.28
5b	1.3790	1.4374	138.6	0	0
5c	1.3739	1.4454	138.6	0	0
6a[a]	1.3704	1.4353	134.7	0.33	0.03
6b	1.3689	1.4370	134.6	0	0
6c	1.3646	1.4442	134.6	0	0
6d	1.3606	1.4524	134.6	0	0

[a] Geometry of the most stable conformer.

Table 5.3 summarizes some geometric parameters, e.g., bond lengths, bond angles, and dihedral angles around the electrophilic center of compounds **2-6**. The bond lengths C^1C^2 and C^1C^5 of quinone methides **2a-d**, benzylidenebarbituric acids **5a-c**, and 2-benzylidene-indan-1,3-diones **6a-d** depend on the substituent Y of the arylidene moiety and show similar trends in each class of the electrophiles. The stronger the electron-donating power of Y, the shorter is C^1C^5 and the longer is C^1C^2, indicating increasing importance of the resonance structure B in Scheme 5.6. Increasing weight of resonance structure B is also evident from a lowering of the dihedral angle $C^2C^1C^5C^6$ and a slight increase of the dihedral angle $C^5C^1C^2C^3$.
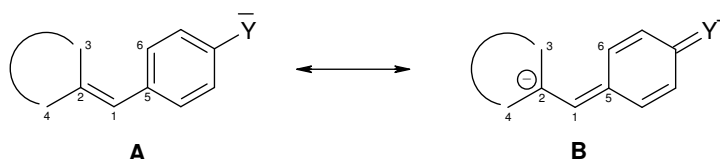
SCHEME 5.6: Resonance structures A and B of electrophiles **2-6**.

In contrast, the Michael acceptors **5-6** are practically planar. In the structures **5a-c** and **6a-d** the angle $C^2C^1C^5$ remains constant at 138.6 ° and 134.6 °, respectively, independent of the substituent Y. The slight increase of this angle from 130.6° (**2d**) to 131.6° (**2a**) can again be attributed to the higher planarity of compound **2a**.

The thermodynamics of the reactions of uncharged electrophiles **2**, **5**, and **6** with the methyl anion in the gas phase were calculated according to equation 5.2.

$$(\textbf{2-6}) \; + \; \text{Me}^{\ominus} \; \longrightarrow \; \left[(\textbf{2-6}) - \text{Me}\right]^{\ominus} \tag{5.2}$$
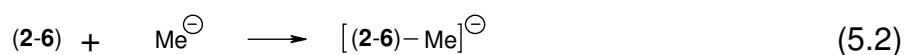
For that purpose, the methyl anion adducts of the electrophiles **2-6** were optimized at the B3LYP level using the 6-31G(d,p) basis set. Single point energies have then been calculated for (**2-6**) and [(**2-6**)−Me]⁻ at the B3LYP/6-311+G(d,p) level. Combination of these energies with thermochemical corrections derived from a harmonic vibrational frequency analysis at the B3LYP/6-31G(d,p) level yield the enthalpies H_{298} at 298 K.

Instead of using a Boltzmann distribution of different conformers, the energies (E_{tot}) of the most stable conformers of reactants and products were used to calculate the reaction enthalpies ΔH_R (i.e., methyl anion affinities) of the additions of Me⁻ to the quinone methides **2** and Michael acceptors **5-6** (Table 5.4).

TABLE 5.4: Enthalpies H_{298} at 298 K of the most stable conformer of quinone methides **2a**-**e**, Michael acceptors **5a**-**6d**, and of the corresponding methyl anion adducts (B3LYP/6-311+G(d,p)//B3LYP/6-31G(d,p)).

	H_{298} (**2-6**) / a.u.	H_{298} [(**2-6**)−Me]$^-$ / a.u.	ΔH_R(equation 5.2)[a] / kJ mol^{-1}
2a	−1179.652167	−1219.607306	−353.1
2b	−1024.832054	−1064.788299	−356.1
2c	−1005.425211	−1045.386170	−368.4
2d	−930.2016374	−970.1637763	−371.5
2e	−1172.526329	−1212.494423	−387.2
5a	−1126.5608446	−1166.5259801	−379.4
5b	−971.7403723	−1011.7070244	−383.4
5c	−952.3315878	−992.3053329	−402.0
6a	−1054.8948049	−1094.8507426	−355.3
6b	−900.0743254	−940.0316812	−359.0
6c	−880.6663918	−920.6301479	−375.8
6d	−766.1416161	−806.1102475	−388.6

[a] H_{298} (Me)$^-$ = −39.85227966 a.u.
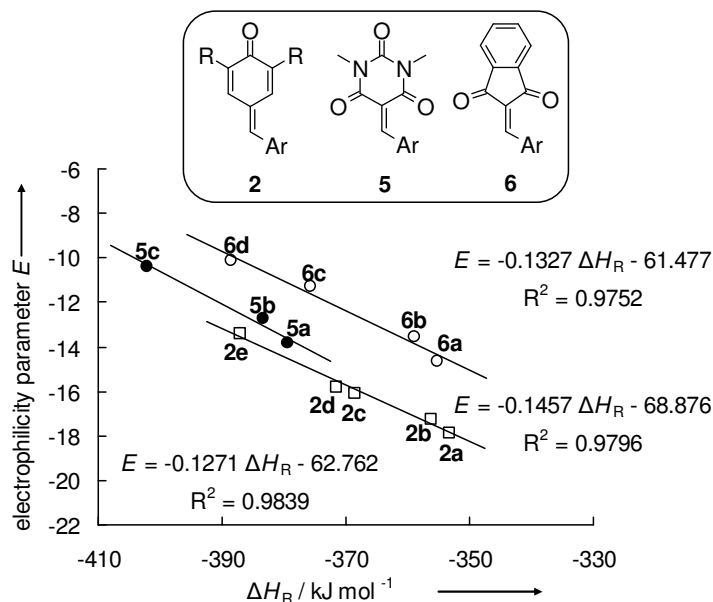
FIGURE 5.7: Plot of the electrophilicity parameters E versus the methyl anion affinities ΔH_R / kJ mol^{-1} (equation 5.2) of quinone methides **2** and Michael acceptors **5**-**6**.

When plotting the known *E*-parameters of the quinone methides **2a-e**, benzylidenebarbituric acids **5a-c**, and 2-benzylidene-indan-1,3-diones **6a-d** versus the calculated methyl anion affinities (from Table 5.4), one obtains separate linear correlations for each class of electrophiles (Figure 5.7). For a given methyl anion affinity ΔH_R the quinone methides **2a-e** possess the lowest, whereas the 2-benzylidene-indan-1,3-diones **6a-d** possess the highest electrophilicities. In other words, the reaction of the methyl anion with electrophiles of approximately the same *E*-parameters, e.g., **2e**, **5a**, and **6b**, is most exothermic for the quinone methides **2**.

Rate-equilibrium-relationships in solution

As the equilibrium constants *K* of the reactions of 4-dimethylaminopyridine (DMAP) with benzylidenebarbituric acid **5c** ($E = -10.37$)[15] and with the diarylcarbenium ion **3b** ($E = -10.04$)[30] have recently been determined,[31, 32] it is now possible to compare relative electrophilicities with relative Lewis-acidities in solution. With $K = 2.65 \times 10^2$ M^{-1} (DMAP + **5c**) and $K = 2.44 \times 10^4$ M^{-1} (DMAP + **3b**) one calculates that the diarylcarbenium ion **3b** is 92 times more Lewis-acidic than the benzylidenebarbituric acid **5c**, despite similar electrophilicities of the two compounds. That means, the Michael acceptors **5** are considerably more electrophilic than the diarylcarbenium ions **3** of the same Lewis-acidity.

Due to the of the large solvation energies of ions, the comparison of calculated methyl anion affinities of charged and neutral Lewis acids in the gas phase is not relevant for the situation in solution. However, if one considers that the quinone methides **2** are non-charged analogues of the diarylcarbenium ions **3**, the higher electrophilicities of the Michael acceptors **5** compared with Michael acceptors **2** (Figure 5.7) reflect the same phenomenon.

Steric approach

Recently, Crampton studied the reactions of trifluoromethanesulfonyl-stabilized carbanions with nitrobenzofurazan derivatives and concluded that the large steric requirement of the trifluoromethanesulfonyl-stabilized benzylic anions is responsible for their low reactivity towards these electrophiles.[33] Furthermore, the reactions of these carbanions with Michael acceptors **5**-**6** were found to be slightly slower than expected on the basis of their nucleophilicity parameters *N* and *s*, which have been derived from their reactions with diarylcarbenium ions **3**.[15, 16] For that reason one might speculate, whether the unexpected low reactivities of the structurally related sulfonyl-stabilized carbanions **1a-d** with Michael

acceptors **4-6** observed in this work are also caused by unfavorable steric interactions of these electrophile-nucleophile combinations.

In order to estimate the steric demand of the benzylidenebarbituric acids **5** and 2-benzylidene-indan-1,3-diones **6** in comparison with the quinone methides **2**, we calculated the energies of the adducts from the methanesulfonylethyl anion (**1e⁻**) and the electrophiles **2d**, **5c**, and **6d** (Scheme 5.7).
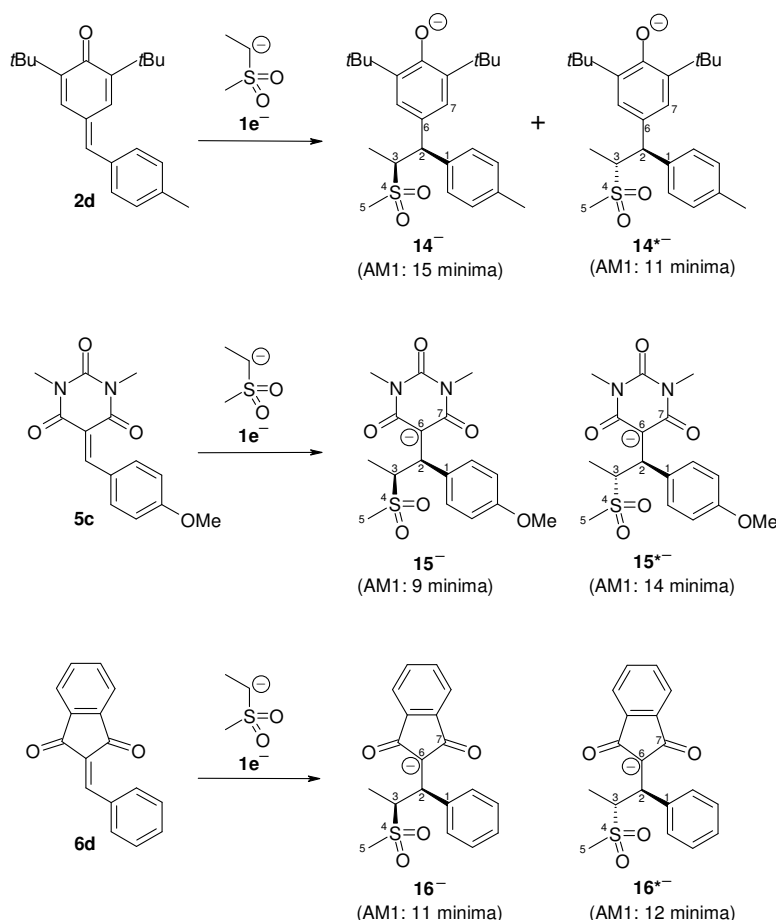
SCHEME 5.7: Quantum chemical calculations (AM1, DFT, see text) of the anionic addition products (**14-16**)⁻ from the methanesulfonyl-ethyl anion (**1e⁻**) and the electrophile **2d**, **5c**, and **6d**.

Therefore, the AM1 potential energy surfaces of the anionic adducts (**14-16**)⁻ and their diastereomers (**14-16**)*⁻ were scanned by varying systematically the three dihedral angles $C^1C^2C^3S^4$, $C^2C^3S^4C^5$, and $C^1C^2C^6C^7$ (illustrated in Scheme 5.7) by steps of 60°. The AM1 stationary points were then optimized at the B3LYP level using the 6-31G(d,p) basis set to yield E_{tot} for the various conformers (Experimental Section). For reasons of simplification only the most stable conformers of the more stable diastereomer were used (Table 5.5) for the

calculation of the reaction enthalpies ΔH_R of the isodesmic reactions depicted in Schemes 5.8-5.9.

TABLE 5.5: Total Energies E_{tot} of methyl anion adducts $(\mathbf{X\text{-}Me})^-$ and of the most stable conformers of methanesulfonyl-ethyl anion adducts $(\mathbf{X\text{-}1e})^-$ and $(\mathbf{X\text{-}1e})^{*-}$ (B3LYP/6-31G(d,p)).

	E_{tot} / a.u.
$(\mathbf{2d\text{-}Me})^-$	−970.4513386
$(\mathbf{5c\text{-}Me})^-$	−992.3656122
$(\mathbf{6d\text{-}Me})^-$	−806.1704239
$\mathbf{14}^{-\,[a]}$	−1597.6683061
$\mathbf{14}^{*-\,[a]}$	−1597.6665345
$\mathbf{15}^{-\,[a]}$	−1619.5856444
$\mathbf{15}^{*-\,[a]}$	−1619.5839903
$\mathbf{16}^{-\,[a]}$	−1433.3901603
$\mathbf{16}^{*-\,[a]}$	−1433.3902228

[a] The most stable conformer.
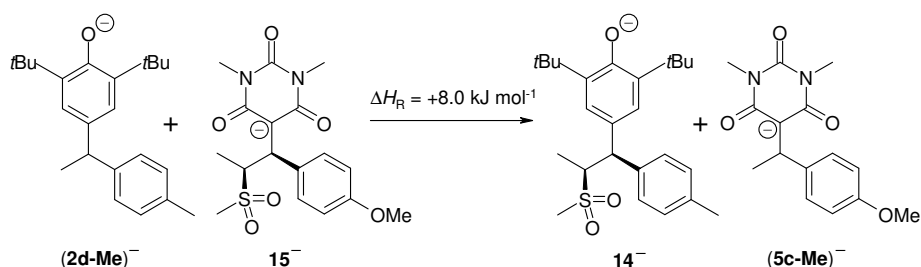
SCHEME 5.8: Isodesmic reaction of the methyl anion adduct of quinone methide $(\mathbf{2d\text{-}Me})^-$ with the methanesulfonyl-ethyl anion adduct of benzylidenebarbituric acid $\mathbf{15}^-$.
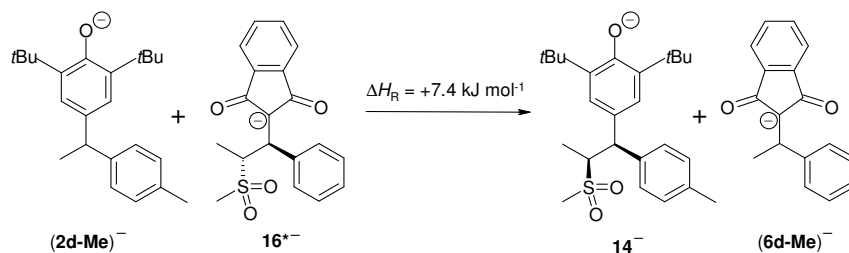
SCHEME 5.9: Isodesmic reaction of the methyl anion adduct of quinone methide $(\mathbf{2d}\text{-}\mathbf{Me})^-$ with the methanesulfonyl-ethyl anion adduct of benzylidene-indan-1,3-dione $\mathbf{16}^{*-}$.

The positive reaction enthalpies for the reactions in Schemes 5.8 and 5.9 prove that even less steric strain is created when the sterically more demanding sulfonyl-substituted carbanions are added to the Michael acceptors **5** and **6** than to the reference electrophiles **2**. So it has to be concluded that steric effects are not the reason for the unexpected slow reactions of sulfonyl-stabilized carbanions (**1a-d**)¯ with the Michael acceptors **4-6**. Therefore, a transition state-specific electronic effect must be responsible.

Inner sphere electron transfer

Though it has previously been demonstrated that reactions of ordinary carbanions with diarylcarbenium ions **3** and quinone methides **2** do not proceed via SET processes,[34] partial electron transfer (inner-sphere electron transfer) may contribute to the relative activation energies. Figure 5.5 shows a plot of the *E*-parameters of various electrophiles versus their one-electron reduction potentials E°_{red} in DMSO solution.[35] The reference electrophiles, diarylcarbenium ions **3** and quinone methides **2**, as well as the 2-benzylidene-indan-1,3-diones **6** and benzylidenebarbituric acids **5** show linear, but separate correlations (Figure 5.8). Thus, if compounds of comparable *E*-parameters are considered, the reference electrophiles **2** and **3** have higher reduction potentials E°_{red} and, therefore, are more easily reduced than the corresponding Michael acceptors **5** and **6**.
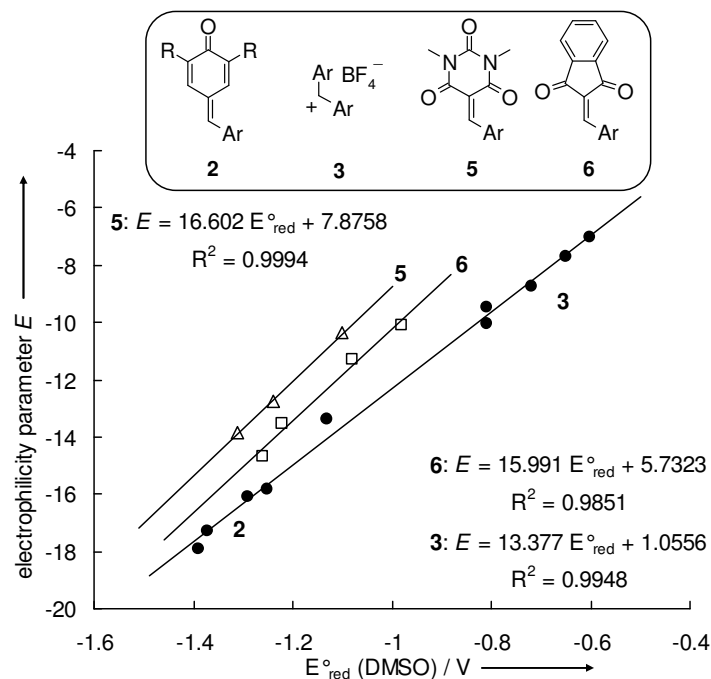
FIGURE 5.8: Plot of electrophilicity parameters *E* versus the one electron reduction potentials E°_{red} / V in DMSO of the reference electrophiles **2**, **3** and the Michael acceptors **5-6**.[35]

On the other side, when comparing electrophiles of similar reduction potentials E°_{red}, i.e., compounds with comparable LUMO energies,[36] the Michael acceptors **5**-**6** are more reactive than quinone methides **2** and diarylcarbenium ions **3**.

5.4 Conclusion

The nucleophilicity parameters for the benzenesulfonyl-stabilized carbanions (**1a**-**d**)¯ determined in this work can also be used to predict roughly the rates of their reactions with the ordinary Michael acceptors **4**-**6** within the postulated error limit of equation 5.1, i.e., a factor of 10-100. However, the observed second-order rate constants for the additions of (**1a**-**d**)¯ to the electrophiles **4**-**6** are generally smaller than predicted, indicating the operation of a special effect which we were unable to elucidate.

5.5 Experimental Section

^{1}H- and ^{13}C-NMR chemical shifts are expressed in ppm and refer to the corresponding solvents (d_6-DMSO: $\delta_H = 2.50$, $\delta_C = 39.5$ and CDCl$_3$: $\delta_H = 7.26$, $\delta_C = 77.2$). DEPT and HSQC experiments were employed to assign the signals. All reactions were performed under an atmosphere of dry argon. Dry DMSO for kinetics was purchased (< 50 ppm H$_2$O). Sulfones **1a**-**d** were synthesized from the corresponding benzyl bromides and sodium benzenesulfinate in DMSO according to ref. [37].

5.5.1 General procedure for the synthesis of anionic addition products

Under an argon atmosphere equimolar amounts of potassium *tert*-butoxide (~0.6 mmol) and sulfone **1** were dissolved in freshly distilled THF (10 mL). The electrophile (~0.6 mmol) was then added to this stirred solution and after 10 min the product was precipitated by adding Et$_2$O (10 mL).

7: Yellow crystals, isolated as a mixture of diastereomers (3:2), which contain 0.5 equivalents of THF (from ^{1}H-NMR), 41% yield. Major diastereomer: ^{1}H-NMR (400 MHz, d_6-DMSO): ^{1}H-NMR (400 MHz, d_6-DMSO): 2.78 (s, 3H, NCH$_3$), 2.78 (s, 6H, N(CH$_3$)$_2$), 2.87 (s, 3H,

NCH$_3$), 4.99 (d, ^3J = 12.0 Hz, 1H, C$^-$CH), 6.17 (d, ^3J = 12.0 Hz, 1H, CH), 6.30 (d, ^3J = 8.7 Hz, 2H, Ar), 7.24 − 7.64 (m, 11H, Ar). ^{13}C-NMR (100 MHz, d_6-DMSO): δ 26.3 (NCH$_3$), 27.0 (NCH$_3$), 40.3 (CH), 40.6 (N(CH$_3$)$_2$), 73.0 (CH), 88.5 (C$^-$), 112.0 (C$_{Ar}$-H), 123.7 (C$_{Ar}$-H), 125.7 (CF$_3$), 127.1 − 127.4 + 128.2 − 132.1 (5 × C$_{Ar}$-H), 127.6 ($\underline{C}_{Ar}$-CF$_3$), 132.3 − 140.8 (3 × C$_{Ar}$), 148.6 (C$_{Ar}$-N), 152.5 (CO), 160.6 (CO), 161.3 (CO). Minor diastereomer: ^{1}H-NMR (400 MHz, d_6-DMSO): 2.65 (s, 6H, N(CH$_3$)$_2$), 2.87 (s, 3H, NCH$_3$), 5.07 (d, ^3J = 11.9 Hz, 1H, C$^-$CH), 6.27 (d, ^3J = 8.7 Hz, 2H, Ar), 6.56 (d, ^3J = 11.9 Hz, 1H, CH), 7.11 (d, ^3J = 8.7 Hz, 2H, Ar), 7.24 − 7.64 (m, 9H, Ar). ^{13}C-NMR (100 MHz, d_6-DMSO): δ 26.3 (NCH$_3$), 27.0 (NCH$_3$), 40.3 (CH), 40.6 (N(CH$_3$)$_2$), 68.5 (CH), 86.8 (C$^-$), 111.6 (C$_{Ar}$-H), 124.3 (C$_{Ar}$-H), 125.5 (CF$_3$), 127.1 − 127.4 + 128.2 − 132.1 (5 × C$_{Ar}$-H), 127.9 ($\underline{C}_{Ar}$-CF$_3$), 132.3 − 140.8 (3 × C$_{Ar}$), 147.6 (C$_{Ar}$-N), 152.1 (CO), 160.6 (CO), 161.3 (CO).

8: Yellow crystals, isolated as a mixture of diastereomers (5:4), which contain 0.3 equivalents of THF (from ^{1}H-NMR), 81% yield. Major diastereomer: ^{1}H-NMR (400 MHz, d_6-DMSO): 2.78 (s, 3H, NCH$_3$), 2.78 (s, 6H, N(CH$_3$)$_2$), 2.87 (s, 3H, NCH$_3$), 4.97 (d, ^3J = 12.0 Hz, 1H, C$^-$CH), 6.12 (d, ^3J = 12.0 Hz, 1H, CH), 6.31 (d, ^3J = 8.8 Hz, 2H, Ar), 7.08 − 7.68 (m, 11H, Ar). ^{13}C-NMR (100 MHz, d_6-DMSO): δ 26.3 (NCH$_3$), 27.0 (NCH$_3$), 40.2 (CH), 40.6 (N(CH$_3$)$_2$), 73.2 (CH), 88.5 (C$^-$), 110.0 ($\underline{C}_{Ar}$-CN), 112.0 (C$_{Ar}$-H), 118.9 (CN), 127.1 − 132.2 (6 × C$_{Ar}$-H), 132.2 (C$_{Ar}$), 140.5 (C$_{Ar}$), 140.6 (C$_{Ar}$), 148.6 (C$_{Ar}$-N), 152.5 (CO), 160.5 (CO), 161.3 (CO). Minor diastereomer: ^{1}H-NMR (400 MHz, d_6-DMSO): 2.66 (s, 6H, N(CH$_3$)$_2$), 2.87 (s, 3H, NCH$_3$), 5.04 (d, ^3J = 11.8 Hz, 1H, C$^-$CH), 6.27 (d, ^3J = 8.9 Hz, 2H, Ar), 6.56 (d, ^3J = 11.9 Hz, 1H, CH), 7.10 (d, ^3J = 8.8 Hz, 2H, Ar), 7.08 − 7.68 (m, 9H, Ar). ^{13}C-NMR (100 MHz, d_6-DMSO): δ 26.3 (NCH$_3$), 27.0 (NCH$_3$), 40.2 (CH), 40.6 (N(CH$_3$)$_2$), 68.7 (CH), 86.7 (C$^-$), 110.0 ($\underline{C}_{Ar}$-CN), 111.5 (C$_{Ar}$-H), 118.7 (CN), 127.1 − 132.3 (6 × C$_{Ar}$-H), 132.8 (C$_{Ar}$), 139.9 (C$_{Ar}$), 140.5 (C$_{Ar}$), 147.7 (C$_{Ar}$-N), 152.1 (CO), 160.5 (CO), 161.3 (CO).

9: Orange crystals, isolated as a mixture of diastereomers (7:3), which contain 0.2 equivalents of THF (from ^{1}H-NMR), 69% yield. Major diastereomer: ^{1}H-NMR (400 MHz, d_6-DMSO): 2.78 (s, 6H, N(CH$_3$)$_2$), 4.53 (d, ^3J = 11.9 Hz, 1H, C$^-$CH), 5.97 (d, ^3J = 11.9 Hz, 1H, CH), 6.34 (d, ^3J = 8.9 Hz, 2H, Ar), 6.69− 7.63 (m, 15H, Ar). ^{13}C-NMR (100 MHz, d_6-DMSO): δ 40.2 (CH), 40.5 (N(CH$_3$)$_2$), 72.8 (CH), 106.8 (C$^-$), 109.9 ($\underline{C}_{Ar}$-CN), 112.1 (C$_{Ar}$-H), 115.9 (C$_{Ar}$-H), 118.7 (CN), 127.4−132.3 (6 × C$_{Ar}$-H), 132.0 (C$_{Ar}$), 140.0−140.6 (4 × C$_{Ar}$), 148.6 (C$_{Ar}$-N), 186.8 (2 × CO). Minor diastereomer: ^{1}H-NMR (400 MHz, d_6-DMSO): 2.65 (s, 6H, N(CH$_3$)$_2$), 4.57 (d, ^3J = 11.3 Hz, 1H, C$^-$CH), 6.27 − 6.35 (m, 3H, CH + Ar), 6.69−7.63 (m, 15H, Ar).

^{13}C-NMR (100 MHz, d_6-DMSO): δ 40.2 (CH), 40.2 (N(CH$_3$)$_2$), 69.5 (CH), 105.1 (C$^-$), 109.9 ($\underline{C}_{Ar}$-CN), 111.7 (C$_{Ar}$-H), 115.8 (C$_{Ar}$-H), 118.7 (CN), 127.4 − 132.3 (6 × C$_{Ar}$-H), 133.0 (C$_{Ar}$), 140.0 − 140.6 (4 × C$_{Ar}$), 148.7 (C$_{Ar}$-N), 187.3 (2 × CO).

5.5.2 Kinetic Experiments

During all kinetic studies the temperature of the solutions was kept constant (20 ± 0.1°C) by using a circulating bath thermostat. Dry DMSO for kinetics was purchased (< 50 ppm H$_2$O). For the evaluation of kinetics the stopped-flow spectrophotometer systems Hi-Tech SF-61DX2 or Applied Photophysics SX.18MV-R stopped-flow reaction analyzer were used. Rate constants k_{obs} (s^{-1}) were obtained by fitting the single exponential $A_t = A_0 \exp(-k_{obs}t) + C$ to the observed time-dependent electrophile absorbance (averaged from at least 4 kinetic runs for each nucleophile concentration). For the stopped-flow experiments 2 stock solutions were used: A solution of the electrophile in DMSO and a solution of the carbanion, which was generated by the deprotonation of the CH acid with 1.05 equivalents of base.

Reaction of **1a**$^-$ with **4a** (DMSO, KO^{t}Bu, 20 °C, stopped flow, 500 nm)

[E]$_0$ / M	[C$^-$]$_0$ / M	k_{obs} / s^{-1}
1.66×10^{-5}	2.63×10^{-4}	1.11×10^1
1.66×10^{-5}	9.85×10^{-4}	5.73×10^1
1.66×10^{-5}	1.31×10^{-3}	8.37×10^1
1.66×10^{-5}	1.64×10^{-3}	1.03×10^2
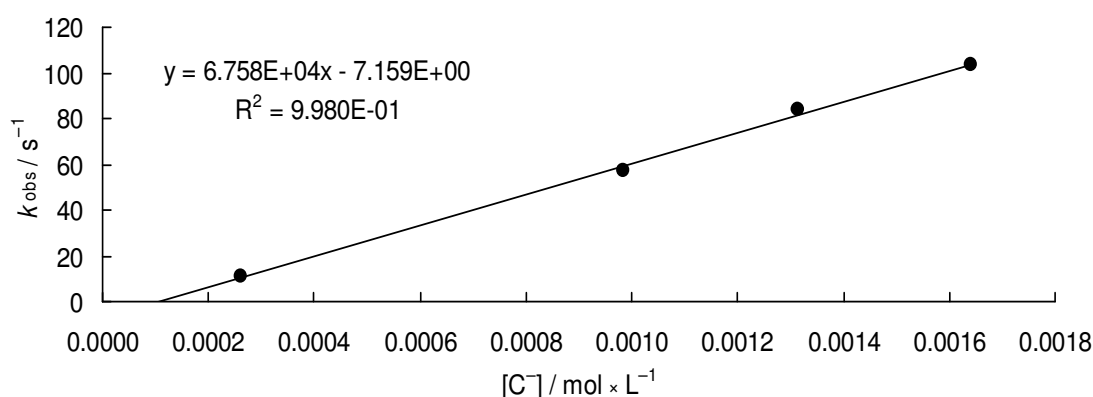
$k_2 = (6.76 \pm 0.21) \times 10^4$ M^{-1}s^{-1}

Reaction of **1a⁻** with **5a** (DMSO, KO^{t}Bu, 20 °C, stopped flow, 500 nm)

$[E]_0$ / M	$[C^-]_0$ / M	k_{obs} / s^{-1}
1.58×10^{-5}	2.63×10^{-4}	3.20×10^{1}
1.58×10^{-5}	9.85×10^{-4}	1.35×10^{2}
1.58×10^{-5}	1.31×10^{-3}	2.02×10^{2}
1.58×10^{-5}	1.64×10^{-3}	2.40×10^{2}

y = 1.539E+05x - 9.443E+00
R^2 = 9.940E-01
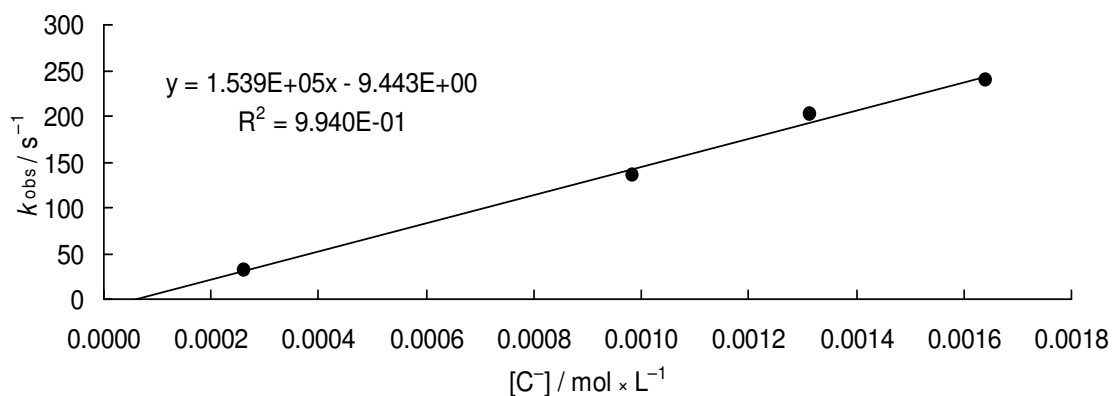
$$k_2 = (1.54 \pm 0.08) \times 10^5 \ \text{M}^{-1}\text{s}^{-1}$$

Reaction of **1a⁻** with **6a** (DMSO, KO^{t}Bu, 20 °C, stopped flow, 500 nm)

$[E]_0$ / M	$[C^-]_0$ / M	k_{obs} / s^{-1}
1.77×10^{-5}	2.63×10^{-4}	8.64
1.77×10^{-5}	9.85×10^{-4}	5.30×10^{1}
1.77×10^{-5}	1.31×10^{-3}	7.32×10^{1}
1.77×10^{-5}	1.64×10^{-3}	9.50×10^{1}

y = 6.239E+04x - 8.068E+00
R^2 = 9.997E-01
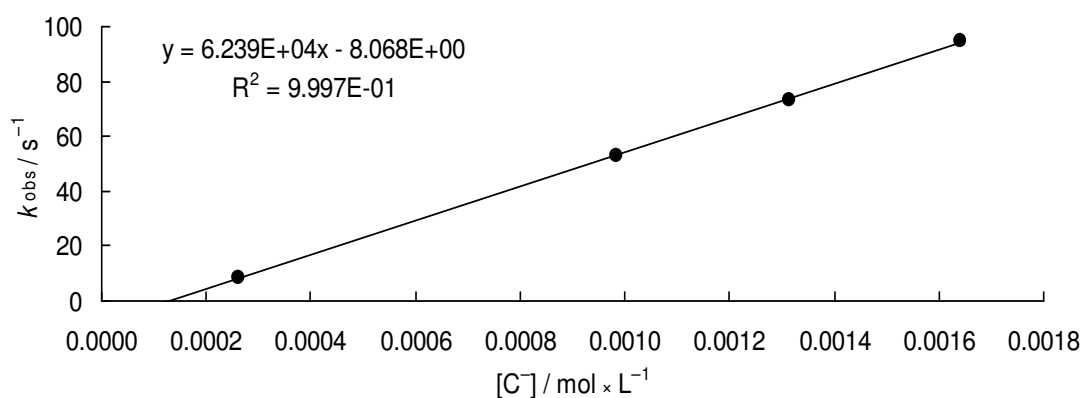
$$k_2 = (6.24 \pm 0.07) \times 10^4 \ \text{M}^{-1}\text{s}^{-1}$$

Reaction of **1a**$^-$ with **6b** (DMSO, KO^{t}Bu, 20 °C, stopped flow, 500 nm)

$[E]_0$ / M	$[C^-]_0$ / M	k_{obs} / s^{-1}
2.89×10^{-5}	6.43×10^{-4}	1.25×10^{2}
2.89×10^{-5}	9.65×10^{-4}	2.68×10^{2}
2.89×10^{-5}	1.29×10^{-3}	3.84×10^{2}
2.89×10^{-5}	1.61×10^{-3}	5.16×10^{2}
2.89×10^{-5}	1.93×10^{-3}	6.65×10^{2}

y = 412856x - 139.6
R^2 = 0.9984
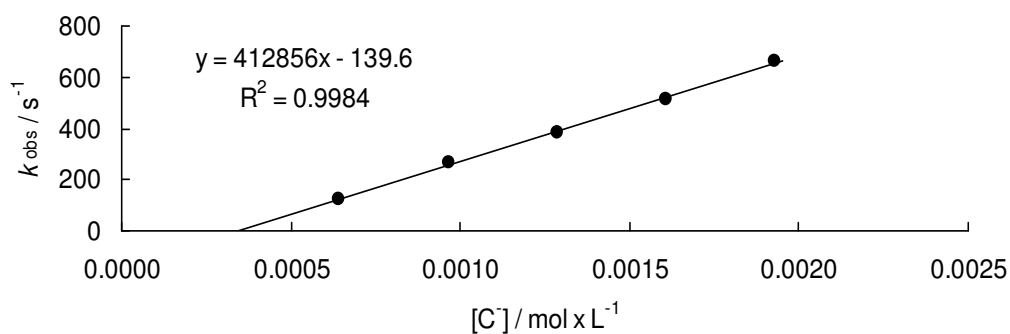
$k_2 = (4.13 \pm 0.09) \times 10^5$ M^{-1}s^{-1}

Reaction of **1b**$^-$ with **2a** (DMSO, KO^{t}Bu, 20 °C, stopped flow, 510 nm)

$[E]_0$ / M	$[C^-]_0$ / M	k_{obs} / s^{-1}
1.31×10^{-5}	2.50×10^{-4}	2.42×10^{-1}
1.31×10^{-5}	7.49×10^{-4}	1.24
1.31×10^{-5}	9.99×10^{-4}	1.78
1.31×10^{-5}	1.25×10^{-3}	2.20

y = 1.982E+03x - 2.435E-01
R^2 = 9.986E-01
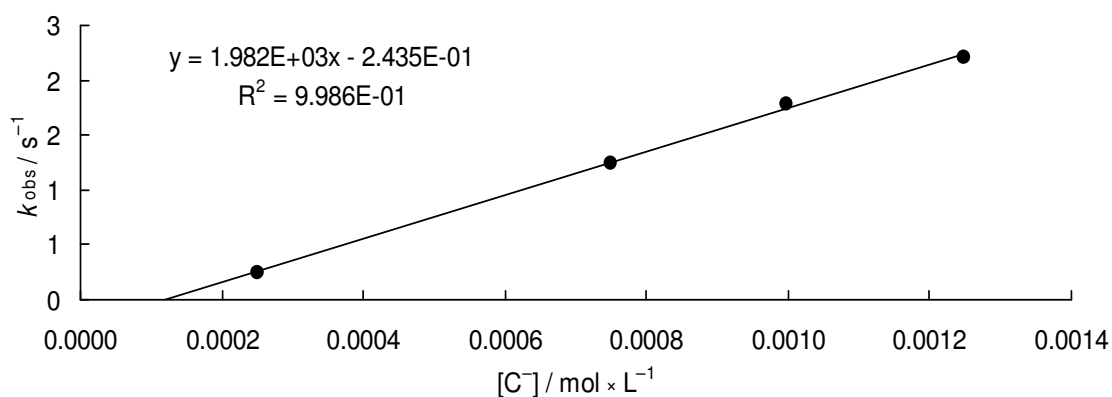
$k_2 = (1.98 \pm 0.05) \times 10^3$ M^{-1}s^{-1}

Reaction of **1b⁻** with **2b** (DMSO, KO^{t}Bu, 20 °C, stopped flow, 510 nm)

$[E]_0$ / M	$[C^-]_0$ / M	k_{obs} / s^{-1}
1.35×10^{-5}	2.50×10^{-4}	4.65×10^{-1}
1.35×10^{-5}	7.49×10^{-4}	2.40
1.35×10^{-5}	9.99×10^{-4}	3.45
1.35×10^{-5}	1.25×10^{-3}	4.11

$y = 3.723E+03x - 4.158E-01$
$R^2 = 9.948E-01$
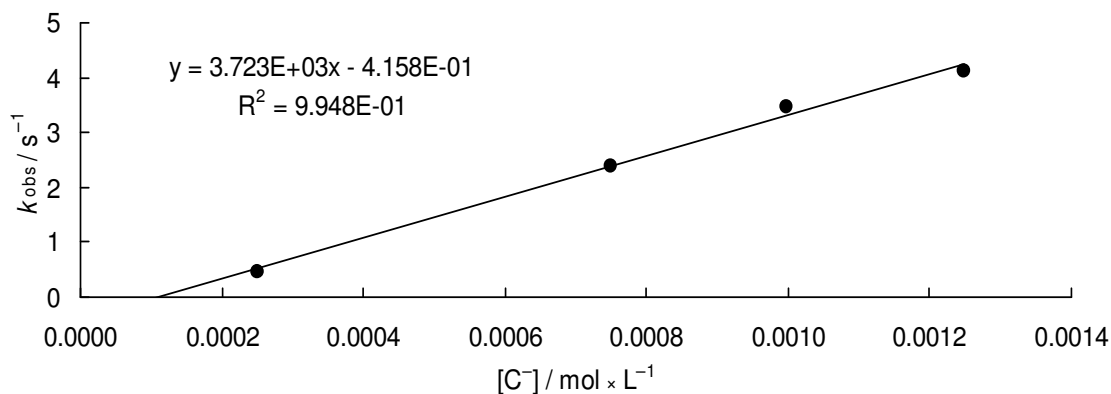
$$k_2 = (3.72 \pm 0.19) \times 10^3 \text{ M}^{-1}\text{s}^{-1}$$

Reaction of **1b⁻** with **2e** (DMSO, Verkade's base, 20 °C, stopped flow, 500 nm)

$[E]_0$ / M	$[C^-]_0$ / M	k_{obs} / s^{-1}
1.47×10^{-5}	5.92×10^{-4}	2.31×10^2
1.47×10^{-5}	8.88×10^{-4}	3.35×10^2
1.47×10^{-5}	1.18×10^{-3}	4.65×10^2
1.47×10^{-5}	1.48×10^{-3}	5.69×10^2

$y = 3.866E+05x - 7.000E-01$
$R^2 = 9.978E-01$

$$k_2 = (3.87 \pm 0.13) \times 10^5 \text{ M}^{-1}\text{s}^{-1}$$

Reaction of **1b⁻** with **4a** (DMSO, Verkade's base, 20 °C, stopped flow, 500 nm)

$[E]_0$ / M	$[C^-]_0$ / M	k_{obs} / s^{-1}
1.47×10^{-5}	2.96×10^{-4}	4.00
1.47×10^{-5}	5.92×10^{-4}	1.02×10^{1}
1.47×10^{-5}	8.88×10^{-4}	1.52×10^{1}
1.47×10^{-5}	1.18×10^{-3}	2.17×10^{1}
1.47×10^{-5}	1.48×10^{-3}	2.58×10^{1}

$y = 1.861E+04x - 1.146E+00$

$R^2 = 9.958E-01$
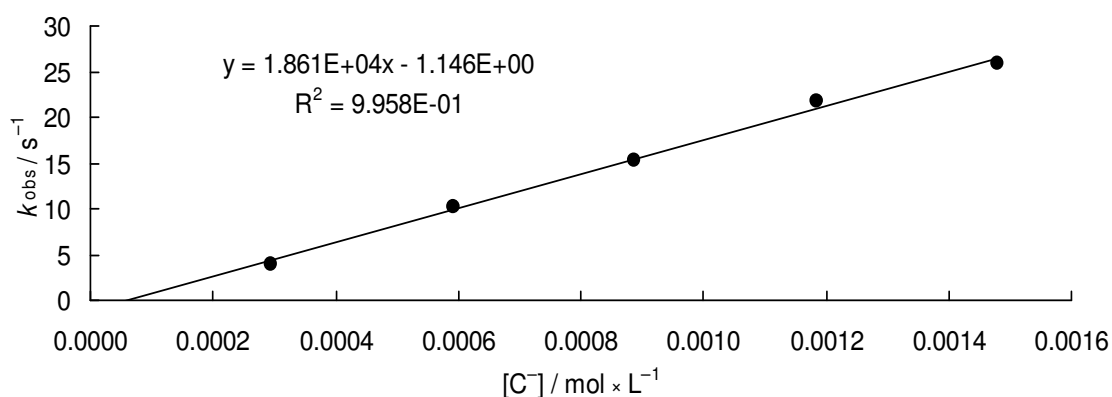
$$k_2 = (1.86 \pm 0.07) \times 10^4 \text{ M}^{-1}\text{s}^{-1}$$

Reaction of **1b⁻** with **5a** (DMSO, Verkade's base, 20 °C, stopped flow, 500 nm)

$[E]_0$ / M	$[C^-]_0$ / M	k_{obs} / s^{-1}
2.45×10^{-5}	2.96×10^{-4}	7.10
2.45×10^{-5}	5.92×10^{-4}	1.64×10^{1}
2.45×10^{-5}	8.88×10^{-4}	3.01×10^{1}
2.45×10^{-5}	1.18×10^{-3}	4.15×10^{1}
2.45×10^{-5}	1.48×10^{-3}	5.15×10^{1}

$y = 3.847E+04x - 4.850E+00$

$R^2 = 9.967E-01$
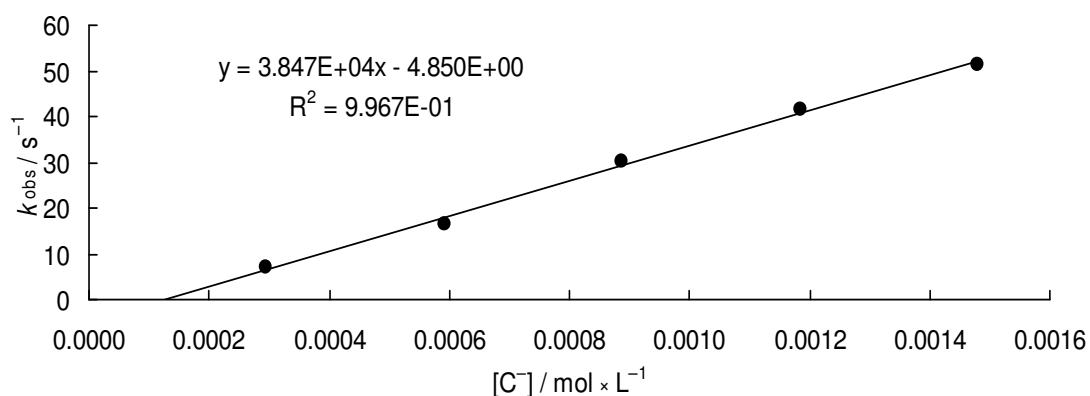
$$k_2 = (3.85 \pm 0.13) \times 10^4 \text{ M}^{-1}\text{s}^{-1}$$

Reaction of **1b⁻** with **5b** (DMSO, Verkade's base, 20 °C, stopped flow, 500 nm)

$[E]_0$ / M	$[C^-]_0$ / M	k_{obs} / s^{-1}
5.85×10^{-5}	5.56×10^{-4}	8.35×10^{1}
5.85×10^{-5}	7.79×10^{-4}	1.22×10^{2}
5.85×10^{-5}	1.00×10^{-3}	1.61×10^{2}
5.85×10^{-5}	1.45×10^{-3}	2.31×10^{2}

$y = 1.656E+05x - 7.207E+00$
$R^2 = 9.992E-01$
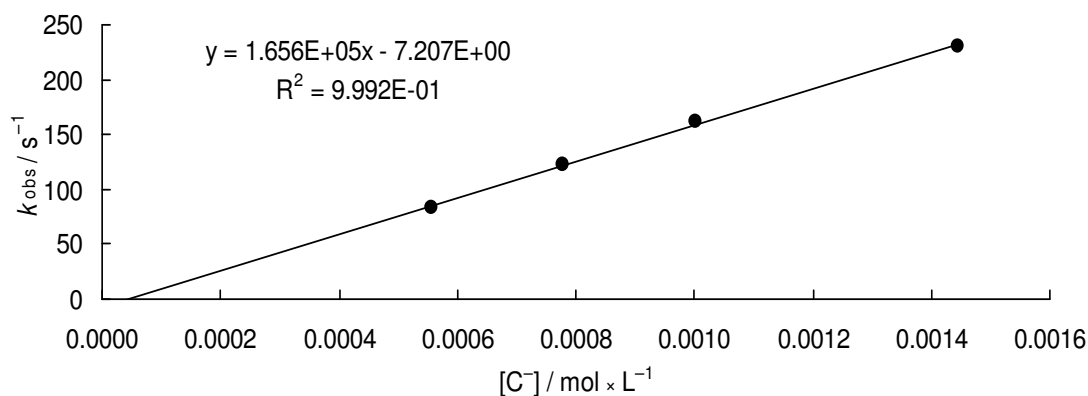
$$k_2 = (1.66 \pm 0.03) \times 10^5 \text{ M}^{-1}\text{s}^{-1}$$

Reaction of **1b⁻** with **6a** (DMSO, Verkade's base, 20 °C, stopped flow, 500 nm)

$[E]_0$ / M	$[C^-]_0$ / M	k_{obs} / s^{-1}
1.36×10^{-5}	2.96×10^{-4}	2.50
1.36×10^{-5}	5.92×10^{-4}	5.82
1.36×10^{-5}	8.88×10^{-4}	1.07×10^{1}
1.36×10^{-5}	1.18×10^{-4}	1.41×10^{1}
1.36×10^{-5}	1.48×10^{-4}	1.82×10^{1}

$y = 1.342E+04x - 1.648E+00$
$R^2 = 9.971E-01$

$$k_2 = (1.34 \pm 0.04) \times 10^4 \text{ M}^{-1}\text{s}^{-1}$$

Reaction of **1b⁻** with **6b** (DMSO, Verkade's base, 20 °C, stopped flow, 500 nm)

$[E]_0$ / M	$[C^-]_0$ / M	k_{obs} / s^{-1}
2.81×10^{-5}	4.45×10^{-4}	2.34×10^{1}
2.81×10^{-5}	5.56×10^{-4}	2.85×10^{1}
2.81×10^{-5}	7.79×10^{-4}	4.58×10^{1}
2.81×10^{-5}	1.00×10^{-3}	5.59×10^{1}
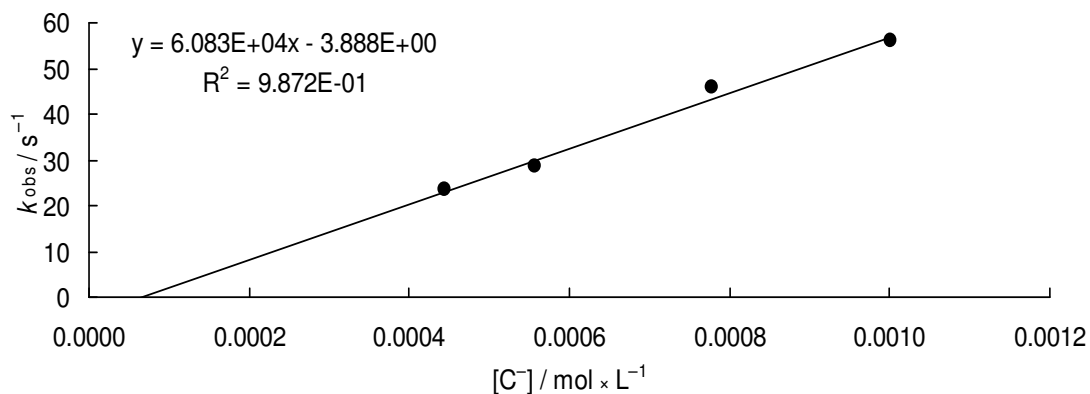
$$k_2 = (6.08 \pm 0.49) \times 10^4 \; M^{-1}s^{-1}$$

Reaction of **1c⁻** with **2b** (DMSO, KO^{t}Bu, 20 °C, stopped flow, 500 nm)

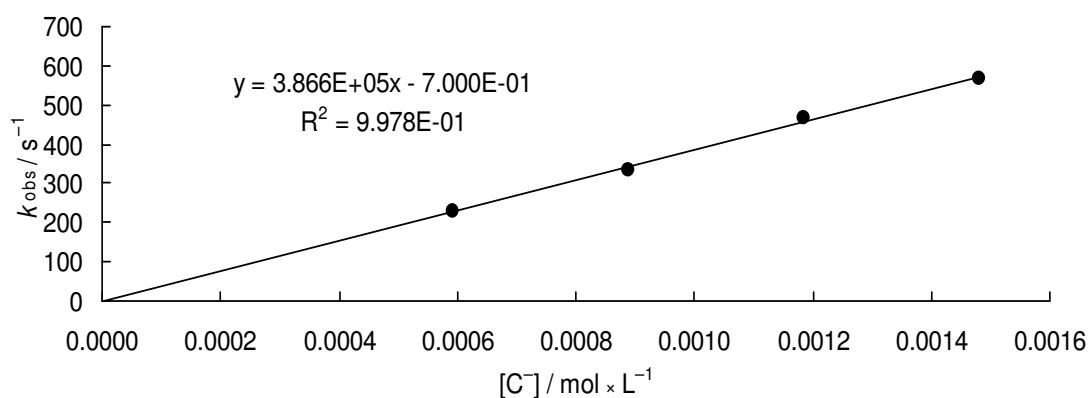| $[E]_0$ / M	$[C^-]_0$ / M	k_{obs} / s^{-1}
2.84×10^{-5}	6.39×10^{-4}	5.18×10^{-1}
2.84×10^{-5}	1.12×10^{-3}	1.02
2.84×10^{-5}	1.60×10^{-3}	1.53
2.84×10^{-5}	2.24×10^{-3}	2.20
2.84×10^{-5}	2.87×10^{-3}	2.83
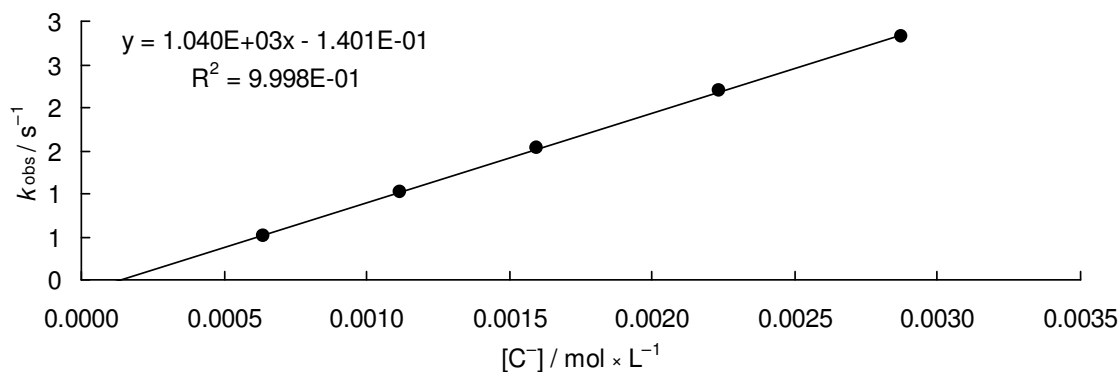
$$k_2 = (1.04 \pm 0.01) \times 10^3 \; M^{-1}s^{-1}$$

Reaction of **1c⁻** with **2e** (DMSO, KO^{t}Bu, 20 °C, stopped flow, 533 nm)

$[E]_0$ / M	$[C^-]_0$ / M	k_{obs} / s^{-1}
2.51×10^{-5}	2.95×10^{-4}	4.56×10^{1}
2.51×10^{-5}	5.16×10^{-4}	7.88×10^{1}
2.51×10^{-5}	7.37×10^{-4}	1.23×10^{2}
2.51×10^{-5}	1.03×10^{-3}	1.76×10^{2}
2.51×10^{-5}	1.47×10^{-3}	2.60×10^{2}

y = 1.840E+05x - 1.234E+01
R^2 = 9.989E-01
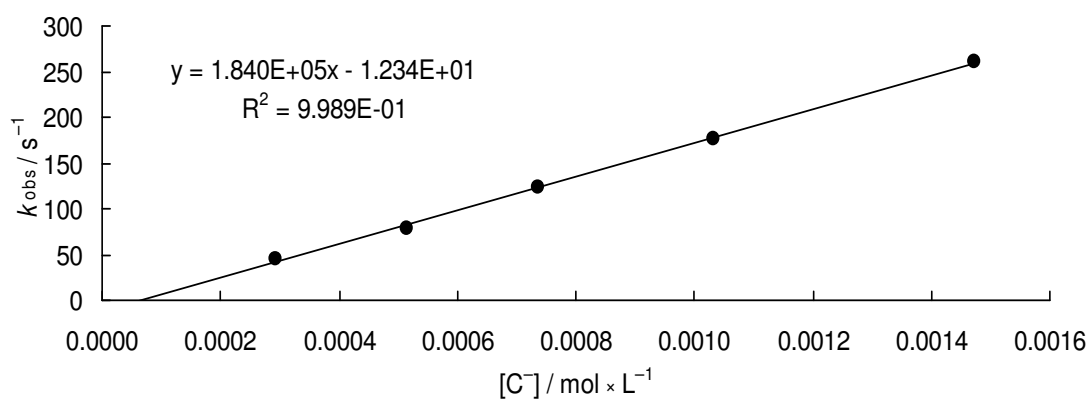
$$k_2 = (1.84 \pm 0.04) \times 10^5 \text{ M}^{-1}\text{s}^{-1}$$

Reaction of **1c⁻** with **4a** (DMSO, KO^{t}Bu, 20 °C, stopped flow, 500 nm)

$[E]_0$ / M	$[C^-]_0$ / M	k_{obs} / s^{-1}
1.66×10^{-5}	3.68×10^{-4}	2.72
1.66×10^{-5}	7.37×10^{-4}	7.02
1.66×10^{-5}	1.11×10^{-3}	9.58
1.66×10^{-5}	1.47×10^{-3}	1.42×10^{1}
1.66×10^{-5}	1.84×10^{-3}	1.83×10^{1}

y = 1.042E+04x - 1.145E+00
R^2 = 9.936E-01

$$k_2 = (1.04 \pm 0.04) \times 10^4 \text{ M}^{-1}\text{s}^{-1}$$

179
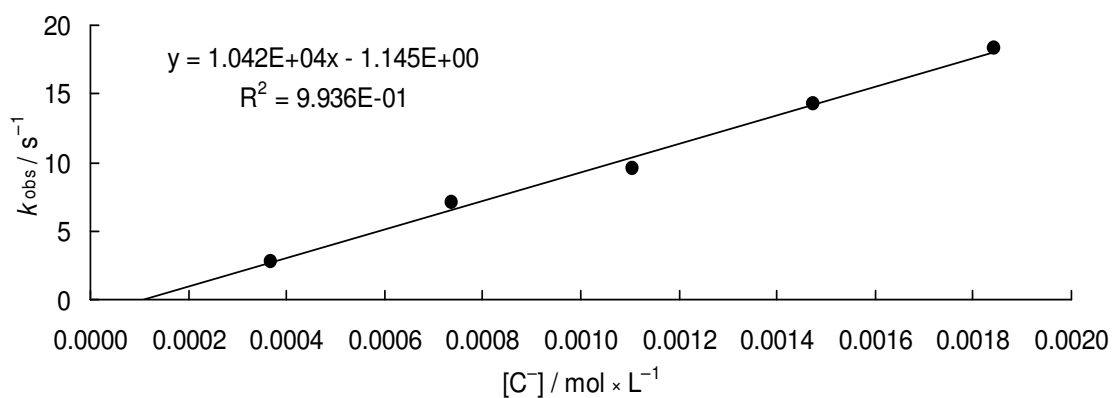
Reaction of **1c⁻** with **5a** (DMSO, Verkade's base, 20 °C, stopped flow, 495 nm)

$[E]_0$ / M	$[C^-]_0$ / M	k_{obs} / s^{-1}
1.84×10^{-5}	3.06×10^{-4}	3.14
1.84×10^{-5}	4.59×10^{-4}	5.49
1.84×10^{-5}	6.12×10^{-4}	8.25
1.84×10^{-5}	7.65×10^{-4}	1.05×10^1
1.84×10^{-5}	9.18×10^{-4}	1.19×10^1

$y = 1.479E+04x - 1.189E+00$
$R^2 = 9.897E-01$
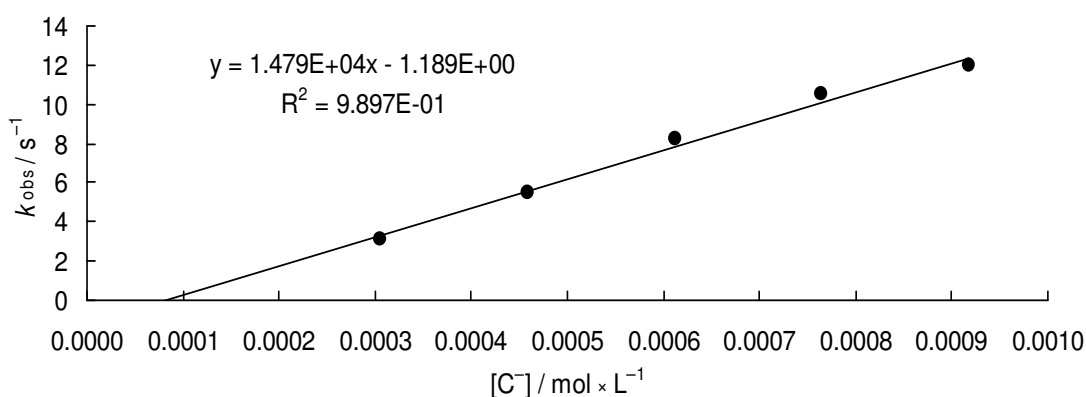
$k_2 = (1.48 \pm 0.09) \times 10^4$ M^{-1}s^{-1}

Reaction of **1c⁻** with **5a** (DMSO, KO^{t}Bu, 20 °C, stopped flow, 500 nm)

$[E]_0$ / M	$[C^-]_0$ / M	k_{obs} / s^{-1}
1.58×10^{-5}	3.68×10^{-4}	5.06
1.58×10^{-5}	7.37×10^{-4}	1.11×10^1
1.58×10^{-5}	1.11×10^{-3}	1.56×10^1
1.58×10^{-5}	1.47×10^{-3}	2.19×10^1
1.58×10^{-5}	1.84×10^{-3}	2.75×10^1

$y = 1.509E+04x - 4.502E-01$
$R^2 = 9.980E-01$
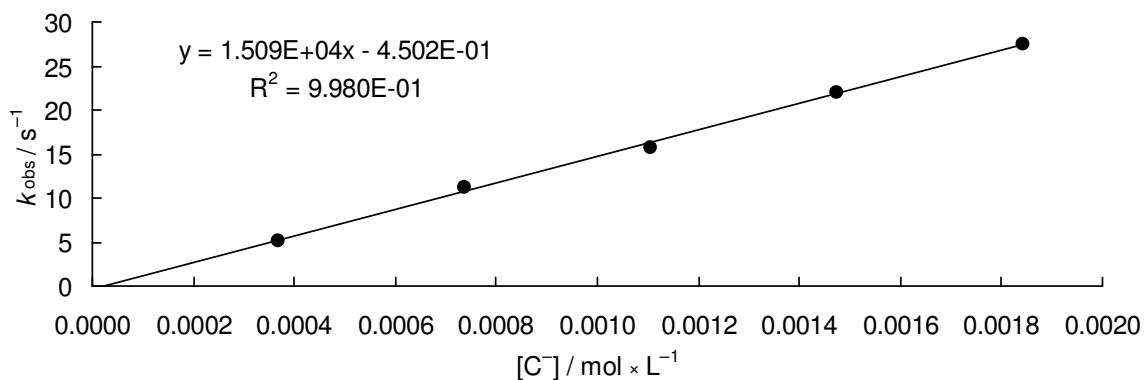
$k_2 = (1.51 \pm 0.04) \times 10^4$ M^{-1}s^{-1}

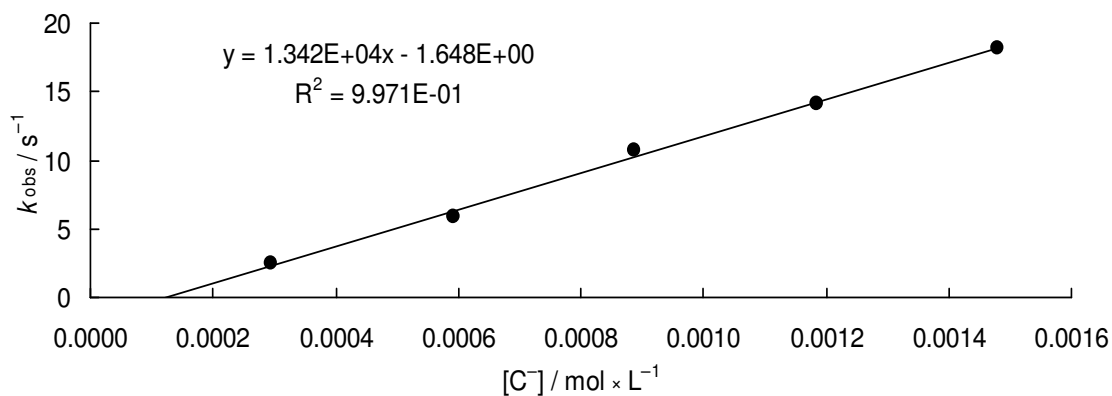Reaction of **1c⁻** with **5b** (DMSO, Verkade's base, 20 °C, stopped flow, 500 nm)

$[E]_0$ / M	$[C^-]_0$ / M	k_{obs} / s^{-1}
5.85×10^{-5}	6.86×10^{-4}	3.94×10^{1}
5.85×10^{-5}	9.43×10^{-4}	5.43×10^{1}
5.85×10^{-5}	1.20×10^{-3}	7.01×10^{1}
5.85×10^{-5}	1.37×10^{-3}	7.92×10^{1}
5.85×10^{-5}	1.71×10^{-3}	1.01×10^{2}

y = 5.971E+04x - 1.811E+00
R^2 = 9.995E-01
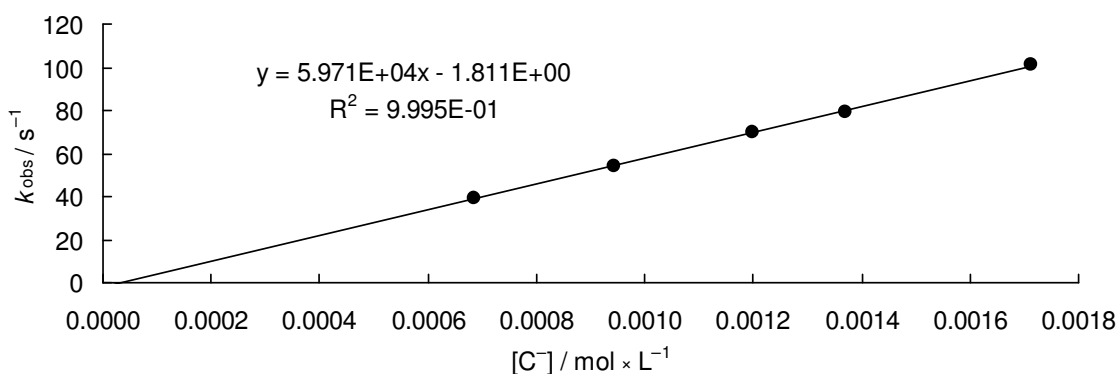
$$k_2 = (5.97 \pm 0.08) \times 10^4 \ \text{M}^{-1}\text{s}^{-1}$$

Reaction of **1c⁻** with **6a** (DMSO, KO^{t}Bu, 18-K-6, 20 °C, stopped flow, 500 nm)

$[E]_0$ / M	$[C^-]_0$ / M	k_{obs} / s^{-1}
1.77×10^{-5}	3.68×10^{-4}	1.62
1.77×10^{-5}	7.37×10^{-4}	3.87
1.77×10^{-5}	1.11×10^{-3}	5.46
1.77×10^{-5}	1.47×10^{-3}	7.64
1.77×10^{-5}	1.84×10^{-3}	1.01×10^{1}

y = 5.610E+03x - 4.688E-01
R^2 = 9.958E-01

$$k_2 = (5.61 \pm 0.08) \times 10^3 \ \text{M}^{-1}\text{s}^{-1}$$

181
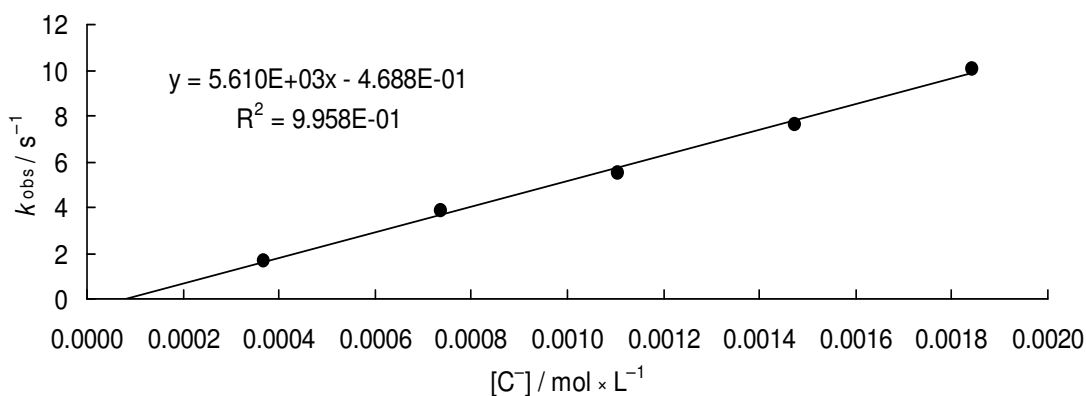
Reaction of **1c⁻** with **6a** (DMSO, KO^{t}Bu, 20 °C, stopped flow, 525 nm)

$[E]_0$ / M	$[C^-]_0$ / M	k_{obs} / s^{-1}
1.86×10^{-5}	3.06×10^{-4}	1.10
1.86×10^{-5}	4.59×10^{-4}	2.08
1.86×10^{-5}	6.12×10^{-4}	3.06
1.86×10^{-5}	7.65×10^{-4}	3.98
1.86×10^{-5}	9.18×10^{-4}	4.57

y = 5.771E+03x - 5.734E-01
R^2 = 9.924E-01
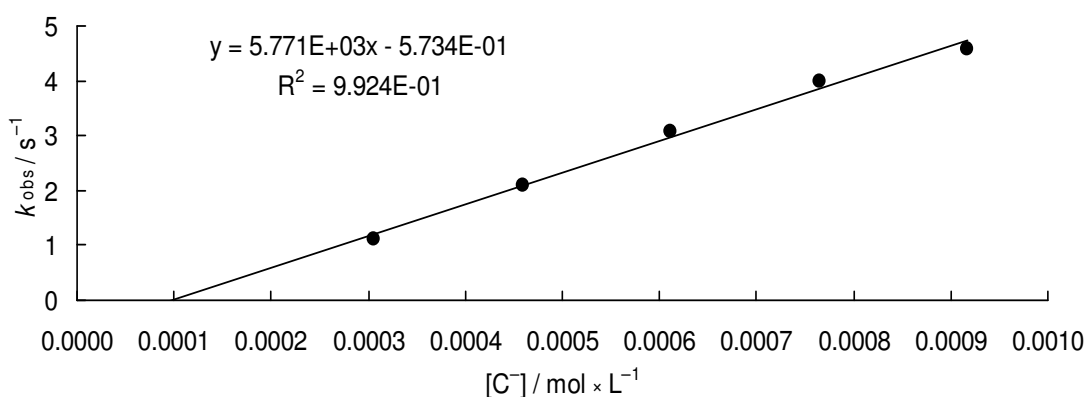
$$k_2 = (5.77 \pm 0.29) \times 10^3 \ \text{M}^{-1}\text{s}^{-1}$$

Reaction of **1c⁻** with **6b** (DMSO, Verkade's base, 20 °C, stopped flow, 500 nm)

$[E]_0$ / M	$[C^-]_0$ / M	k_{obs} / s^{-1}
2.81×10^{-5}	6.86×10^{-4}	1.69×10^{-1}
2.81×10^{-5}	9.43×10^{-4}	2.36×10^{-1}
2.81×10^{-5}	1.20×10^{-3}	2.93×10^{-1}
2.81×10^{-5}	1.37×10^{-3}	3.45×10^{-1}
2.81×10^{-5}	1.71×10^{-3}	4.29×10^{-1}

y = 2.527E+04x - 4.448E-01
R^2 = 9.988E-01
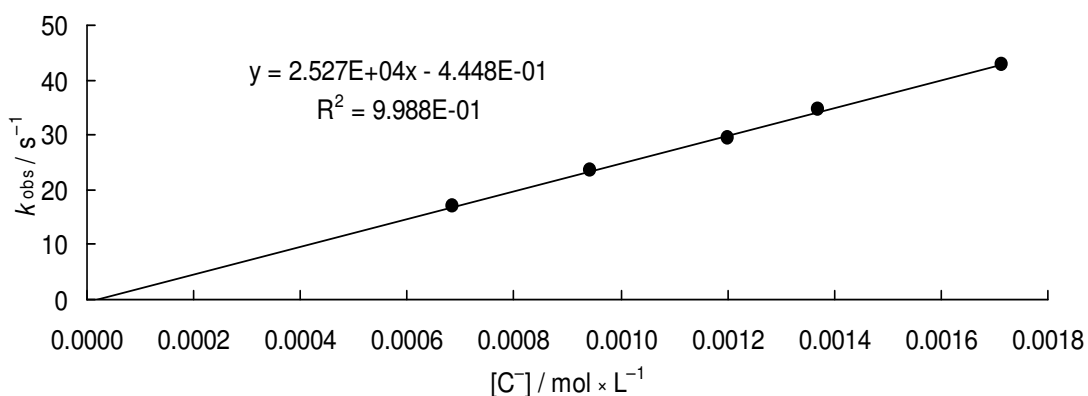
$$k_2 = (2.53 \pm 0.05) \times 10^4 \ \text{M}^{-1}\text{s}^{-1}$$

Reaction of **1d⁻** with **2c** (DMSO, Verkade's base, 20 °C, stopped flow, 400 nm)

$[E]_0$ / M	$[C^-]_0$ / M	k_{obs} / s^{-1}
4.85×10^{-5}	1.09×10^{-3}	7.40×10^{-2}
4.85×10^{-5}	1.36×10^{-3}	9.23×10^{-2}
4.85×10^{-5}	1.64×10^{-3}	1.11×10^{-1}
4.85×10^{-5}	1.91×10^{-3}	1.30×10^{-1}
4.85×10^{-5}	2.18×10^{-3}	1.47×10^{-1}

y = 6.736E+01x + 6.400E-04
R^2 = 9.997E-01
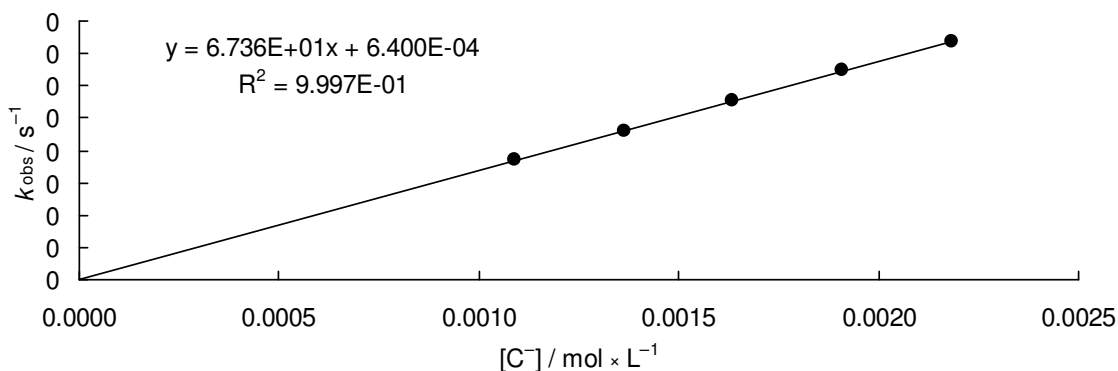
$k_2 = (6.74 \pm 0.07) \times 10^1 \ \text{M}^{-1}\text{s}^{-1}$

Reaction of **1d⁻** with **2d** (DMSO, Verkade's base, 20 °C, stopped flow, 400 nm)

$[E]_0$ / M	$[C^-]_0$ / M	k_{obs} / s^{-1}
4.64×10^{-5}	1.09×10^{-3}	1.22×10^{-1}
4.64×10^{-5}	1.36×10^{-3}	1.50×10^{-1}
4.64×10^{-5}	1.64×10^{-3}	1.82×10^{-1}
4.64×10^{-5}	1.91×10^{-3}	2.11×10^{-1}
4.64×10^{-5}	2.18×10^{-3}	2.41×10^{-1}

y = 1.096E+02x + 1.800E-03
R^2 = 9.997E-01

$k_2 = (1.10 \pm 0.01) \times 10^2 \ \text{M}^{-1}\text{s}^{-1}$

Reaction of **1d**$^-$ with **3a** (DMSO, Verkade's base, 20 °C, stopped flow, 640 nm)

$[E]_0$ / M	$[C^-]_0$ / M	k_{obs} / s^{-1}
1.01×10^{-5}	9.80×10^{-5}	6.91×10^2
1.01×10^{-5}	1.33×10^{-4}	9.90×10^2
1.01×10^{-5}	1.61×10^{-4}	1.10×10^3

y = 6.580E+06x + 6.772E+01
R^2 = 9.618E-01
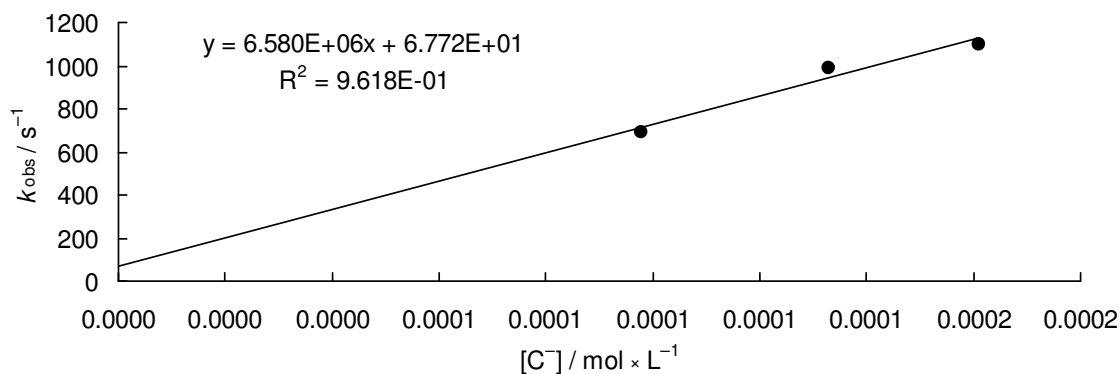
$$k_2 = (6.58 \pm 1.31) \times 10^6 \text{ M}^{-1}\text{s}^{-1}$$

Reaction of **1d**$^-$ with **3b** (DMSO, Verkade's base, 20 °C, stopped flow, 640 nm)

$[E]_0$ / M	$[C^-]_0$ / M	k_{obs} / s^{-1}
1.01×10^{-5}	9.80×10^{-5}	2.44×10^2
1.01×10^{-5}	1.33×10^{-4}	3.44×10^2
1.01×10^{-5}	1.61×10^{-4}	4.28×10^2
1.01×10^{-5}	1.96×10^{-4}	5.09×10^2
1.01×10^{-5}	3.50×10^{-4}	9.64×10^2

y = 2.853E+06x - 3.706E+01
R^2 = 9.993E-01
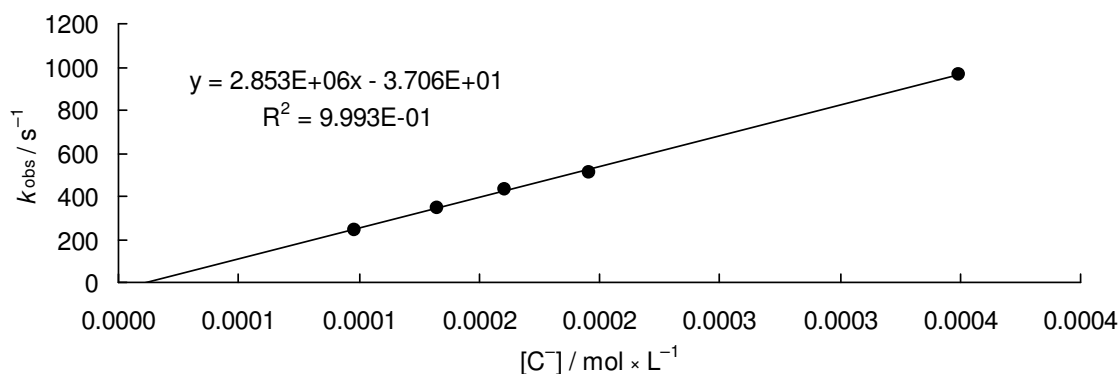
$$k_2 = (2.85 \pm 0.04) \times 10^6 \text{ M}^{-1}\text{s}^{-1}$$

Reaction of **1d⁻** with **5c** (DMSO, Verkade's base, 20 °C, stopped flow, 400 nm)
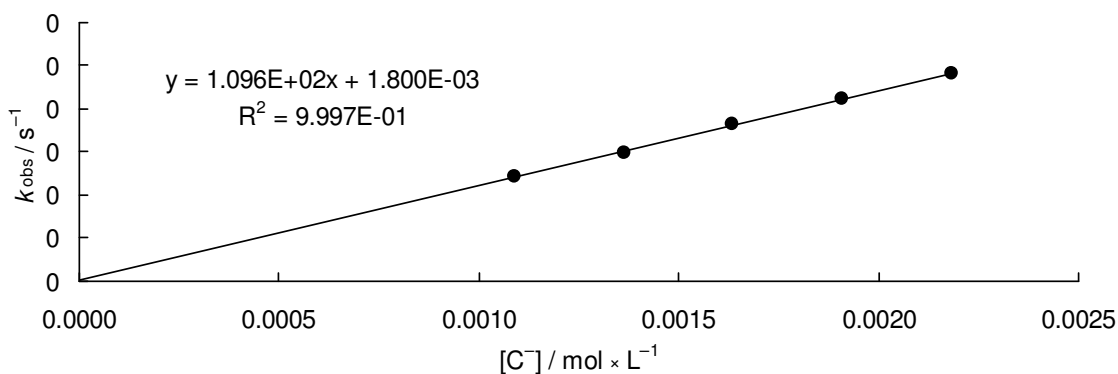
$[E]_0$ / M	$[C^-]_0$ / M	k_{obs} / s⁻¹
5.08×10^{-5}	1.09×10^{-3}	5.70×10^{1}
5.08×10^{-5}	1.36×10^{-3}	7.61×10^{1}
5.08×10^{-5}	1.64×10^{-3}	8.87×10^{1}
5.08×10^{-5}	1.91×10^{-3}	1.05×10^{2}
5.08×10^{-5}	2.18×10^{-3}	1.18×10^{2}

$y = 5.533E+04x - 1.580E+00$
$R^2 = 9.954E-01$
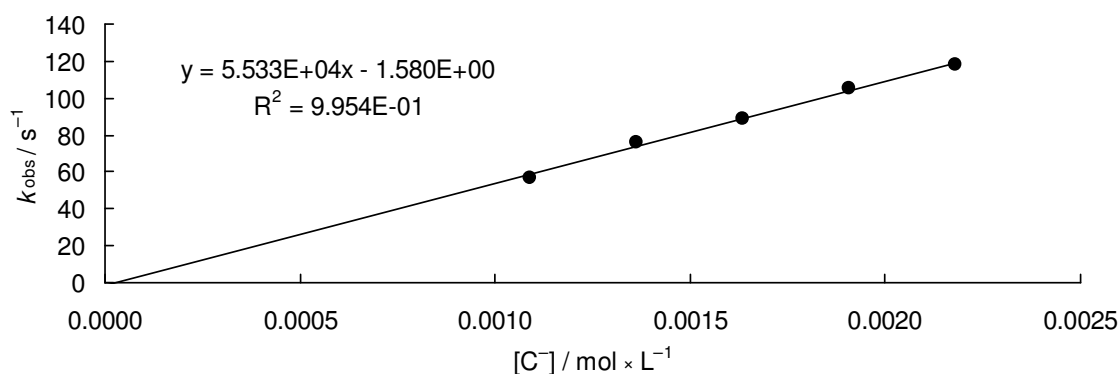
$k_2 = (5.53 \pm 0.22) \times 10^4 \text{ M}^{-1}\text{s}^{-1}$

Reaction of **1d⁻** with **6c** (DMSO, Verkade's base, 20 °C, stopped flow, 400 nm)

$[E]_0$ / M	$[C^-]_0$ / M	k_{obs} / s⁻¹
4.77×10^{-5}	1.09×10^{-4}	2.32×10^{1}
4.77×10^{-5}	1.64×10^{-3}	3.60×10^{1}
4.77×10^{-5}	1.91×10^{-3}	4.25×10^{1}
4.77×10^{-5}	2.18×10^{-3}	4.87×10^{1}

$y = 2.343E+04x - 2.329E+00$
$R^2 = 9.999E-01$
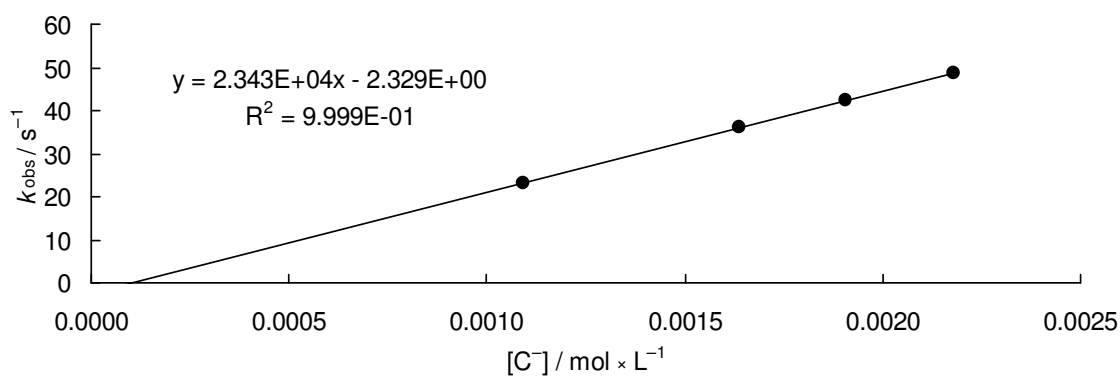
$k_2 = (2.34 \pm 0.01) \times 10^4 \text{ M}^{-1}\text{s}^{-1}$

Reaction of **1d**$^-$ with **6d** (DMSO, Verkade's base, 20 °C, stopped flow, 350 nm)

$[E]_0$ / M	$[C^-]_0$ / M	k_{obs} / s^{-1}
4.93×10^{-5}	1.09×10^{-3}	1.09×10^2
4.93×10^{-5}	1.36×10^{-3}	1.41×10^2
4.93×10^{-5}	1.64×10^{-3}	1.66×10^2
4.93×10^{-5}	1.91×10^{-3}	1.86×10^2
4.93×10^{-5}	2.18×10^{-3}	2.13×10^2
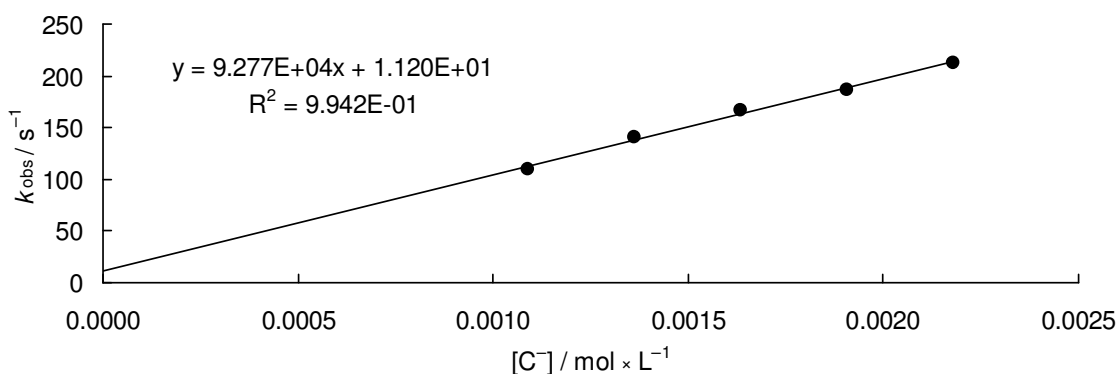
$$k_2 = (9.28 \pm 0.04) \times 10^4 \text{ M}^{-1}\text{s}^{-1}$$

5.5.3 Quantum Chemical Calculations

Cartesian coordinates of all calculated structures are deposited on CD-Rom and can be obtained from Dr. A. R. Ofial (armin.ofial@cup.uni-muenchen.de), Ludwig-Maximilians Universität München.

TABLE 5.6: Total Energies E_{tot} and enthalpies H_{298} at 298 K of all calculated conformers of quinone methides **2a**-**e** and Michael acceptors **4a**-**6d** and of the corresponding methyl anion adducts. If there is more than one conformer, the most stable is bold.

	B3LYP/6-31G(d,p)		B3LYP/6-311+G(d,p)//B3LYP/6-31G(d,p)		
	E_{tot} / a.u.	H_{298} / a.u.	E_{tot} / a.u.	"H_{298}" / a.u.	ΔE_0 / kJ mol^{-1}
Me$^-$	-39.7960283	-39.7643760	-39.8522797	-39.8206274	
2a_1	-1179.9954048	-1179.403485	-1180.243616	-1179.651696	
2a_2	-1179.9954301	-1179.403507	-1180.243675	-1179.651751	
2a_3	**-1179.9958291**	**-1179.403856**	**-1180.244140**	**-1179.652167**	
2a_4	-1179.9957606	-1179.403868	-1180.244082	-1179.652190	
2a-Me$^-$_1	-1219.9663664	-1219.336565	-1220.234603	-1219.604802	-346.5
2a-Me$^-$_2	-1219.9666028	-1219.336717	-1220.234884	-1219.604998	-347.0
2a-Me$^-$_3	**-1219.9688294**	**-1219.338898**	**-1220.237237**	**-1219.607306**	**-353.1**
2a-Me$^-$_4	-1219.9685960	-1219.338650	-1220.237033	-1219.607087	-352.5
2b	-1025.1275294	-1024.610344	-1025.349239	-1024.832054	
2b-Me$^-$	-1065.1012519	-1064.545975	-1065.343576	-1064.788299	-356.1

TABLE 5.6: Continued.

| | B3LYP/6-31G(d,p) | | B3LYP/6-311+G(d,p)//B3LYP/6-31G(d,p) | | |
	E_{tot} / a.u.	H_{298} / a.u.	E_{tot} / a.u.	"H_{298}" / a.u.	ΔE_0 / kJ mol^{-1}
2c	-1005.6766261	-1005.201928	-1005.899909	-1005.425211	
2c-Me$^-$	-1045.6552754	-1045.142233	-1045.899212	-1045.386170	-368.4
2d	-930.4712183	-930.002413	-930.6704427	-930.2016374	
2d-Me$^-$	-970.4513386	-969.944194	-970.6709209	-970.1637763	-371.5
2e_1	-1172.7186020	-1172.266884	-1172.977495	-1172.525777	
2e_2	**-1172.7189118**	**-1172.267146**	**-1172.978095**	**-1172.526329**	
2e_3	-1172.7189200	-1172.267121	-1172.977987	-1172.526188	
2e_4	-1172.7187532	-1172.267020	-1172.977801	-1172.526067	
2e-Me$^-$_1	-1212.7040705	-1212.213641	-1212.984737	-1212.494308	-386.9
2e-Me$^-$_2	-1212.7037578	-1212.213294	-1212.984582	-1212.494118	-386.4
2e-Me$^-$_3	-1212.7041236	-1212.213643	-1212.984844	-1212.494364	-387.0
2e-Me$^-$_4	**-1212.7038249**	**-1212.213436**	**-1212.984812**	**-1212.494423**	**-387.2**
5a_1	-1126.6983113	-1126.2944720	-1126.9646532	-1126.5608139	
5a_2	**-1126.6982865**	**-1126.2944520**	**-1126.9646791**	**-1126.5608446**	
5a-Me$^-$_1	-1166.6760383	-1166.2336200	-1166.9657153	-1166.5232970	-372.4
5a-Me$^-$_2	-1166.6758922	-1166.2335330	-1166.9655787	-1166.5232195	-372.2
5a-Me$^-$_3	**-1166.6786116**	**-1166.2360710**	**-1166.9685207**	**-1166.5259801**	**-379.4**
5a-Me$^-$_4	-1166.6784983	-1166.2359640	-1166.9684419	-1166.5259076	-379.2
5b	-971.8297699	-971.5008620	-972.0692802	-971.7403723	
5b-Me$^-$	-1011.8109402	-1011.4431310	-1012.0748336	-1011.7070244	-383.4
5c	-952.3773636	-952.0908080	-952.6181434	-952.3315878	
5c-Me$^-$	-992.3656122	-992.0399120	-992.6310331	-992.3053329	-402.0
6a_1	-1055.0380163	-1054.6571390	-1055.2755859	-1054.8947086	
6a_2	**-1055.0380378**	**-1054.6571880**	**-1055.2756547**	**-1054.8948049**	
6a-Me$^-$_1	-1095.0048755	-1094.5853530	-1095.2676748	-1094.8481523	-348.5
6a-Me$^-$_2	-1095.0046827	-1094.5851850	-1095.2674950	-1094.8479973	-348.0
6a-Me$^-$_3	**-1095.0073841**	**-1094.5877570**	**-1095.2703697**	**-1094.8507426**	**-355.3**
6a-Me$^-$_4	-1095.0072533	-1094.5876320	-1095.2702062	-1094.8505849	-354.8
6b	-900.1696164	-899.8636070	-900.3803348	-900.0743254	
6b-Me$^-$	-940.1396743	-939.7947670	-940.3765885	-940.0316812	-359.0
6c	-880.7179853	-880.4544120	-880.9299651	-880.6663918	
6c-Me$^-$	-920.6944779	-920.3916910	-920.9329348	-920.6301479	-375.8
6d	-766.1892969	-765.9609500	-766.3699630	-766.1416161	
6d-Me$^-$	-806.1704239	-805.9028400	-806.3778314	-806.1102475	-388.6

2a_3
0.0

2a_4
+0.06

2a_2
+1.15

2a_1
+1.30

2e_2
0.0

2e_3
+0.37

2e_4
+0.69

2e_1
+1.45

5a_2
0.0

5a_1
+0.02

6a_2
0.0

6a_1
+0.25
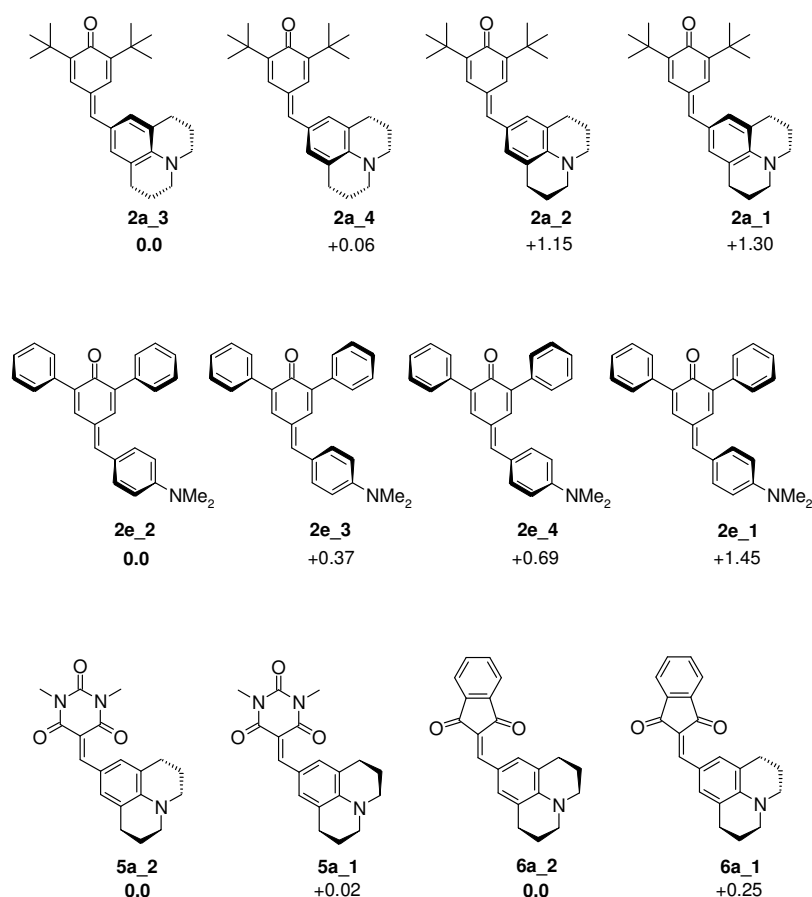
SCHEME 5.10: Relative energies (E_{tot} / kJ mol^{-1}) of the various conformers of Michael acceptors **5a**, **6a** and quinone methides **2a** and **2e**.

2a-me⁻_3
0.00

2a-me⁻_4
+0.58

2a-me⁻_2
+6.06

2a-me⁻_1
+6.58

2e-me⁻_3
0.00

2e-me⁻_1
+0.37

2e-me⁻_4
+0.69

2e-me⁻_2
+1.45
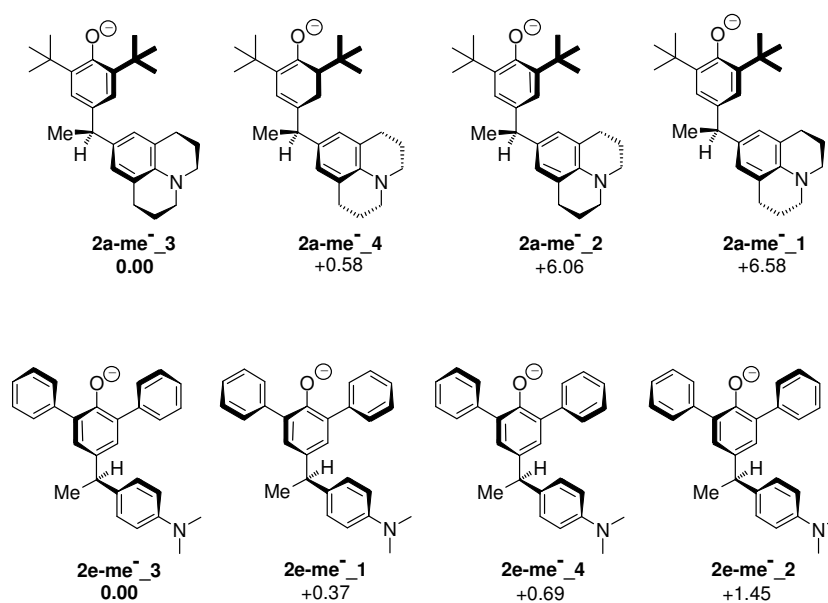
SCHEME 5.11: Relative energies (E_{tot} / kJ mol^{-1}) of the various conformers of methyl anion adducts of quinone methides **2a** and **2e**.
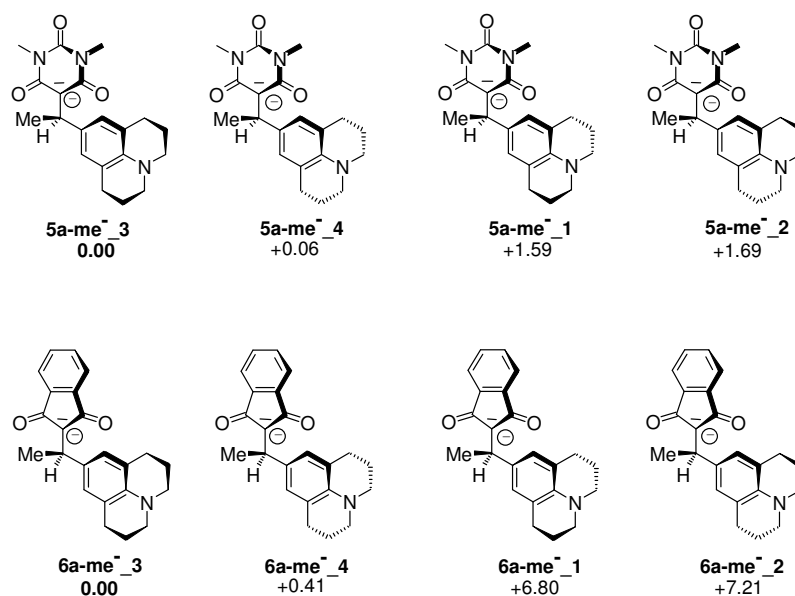
SCHEME 5.12: Relative energies (E_{tot} / kJ mol^{-1}) of the various conformers of methyl anion adducts of Michael acceptors **5a** and **6a**.

TABLE 5.7: Total Energies E_{tot} of the methanesulfonyl-ethyl anion adducts of quinone methide **2d**, benzylidenebarbituric acid **5c**, and 2-benzylidene-indan-1,3-dione **6d**.

	AM1	B3LYP/6-31G(d,p)	
	E_{tot} / a.u.	E_{tot} / a.u.	ΔE_0 / kJ mol^{-1}
1e$^-$		−667.1051834	
2d		−930.4712183	
14$^-$_111	−0.20889	−1597.6592324	−217.5
14$^-$_112	−0.21636	−1597.6683061	**−241.3**
14$^-$_113	−0.20522	−1597.6585625	−215.7
14$^-$_123	−0.20560	−1597.6601109	−219.8
14$^-$_131	−0.20665	−1597.6601109	−219.8
14$^-$_132	−0.20808	−1597.6610343	−222.2
14$^-$_133	−0.20550	−1597.6609755	−222.0
14$^-$_211	−0.19920	−1597.6502049	−193.8
14$^-$_212	−0.19982	−1597.6471783	−185.8
14$^-$_221	−0.20485	−1597.6552157	−206.9
14$^-$_231	−0.20910	−1597.6628868	−227.1
14$^-$_232	−0.21193	−1597.6628874	−227.1
14$^-$_233	−0.21150	−1597.6628842	−227.1
14$^-$_313	−0.20890	−1597.6592751	−217.6
14$^-$_323	−0.21638	−1597.6683061	−241.3
14*$^-$_111	−0.20634	−1597.6593164	−217.7
14*$^-$_112	−0.21457	−1597.6593162	−217.7
14*$^-$_121	−0.20882	−1597.6613684	−223.1
14*$^-$_131	−0.21061	−1597.6648803	−232.3

TABLE 5.7: Continued.

	AM1	B3LYP/6-31G(d,p)	
	E_{tot} / a.u.	E_{tot} / a.u.	ΔE_0 / kJ mol^{-1}
14*⁻_211	−0.21029	−1597.6631483	−227.8
14*⁻_223	−0.20712	−1597.6648779	−232.3
14*⁻_231	−0.19616	−1597.6631492	−227.8
14*⁻_311	−0.20304	−1597.6528610	−200.7
14*⁻_312	−0.20478	−1597.6590666	−217.0
14*⁻_322	−0.21399	−1597.6665334	**−236.6**
14*⁻_333	−0.21423	−1597.6665345	−236.6
5c		−952.3773636	
15*⁻_111	−0.34487	−1619.5771736	−248.4
15*⁻_121	−0.34904	−1619.5805798	−257.4
15*⁻_131	−0.34949	−1619.5839903	**−266.3**
15*⁻_132	−0.34931	−1619.5839903	−266.3
15*⁻_211	−0.33249	−1619.5616143	−207.6
15*⁻_212	−0.34220	−1619.5756971	−244.6
15*⁻_213	−0.20574	−1619.4311575	134.9
15*⁻_231	−0.33515	−1619.5691013	−227.2
15*⁻_232	−0.33128	−1619.5624386	−209.8
15*⁻_233	−0.34811	−1619.5839903	−266.3
15*⁻_311	−0.33680	−1619.5670214	−221.8
15*⁻_321	−0.34457	−1619.5790628	−253.4
15*⁻_322	−0.34440	−1619.5764561	−246.6
15*⁻_332	−0.34937	−1619.5826913	−262.9
15⁻_111	−0.35447	−1619.5856444	**−270.7**
15⁻_131	−0.34482	−1619.5782420	−251.2
15⁻_221	−0.34521	−1619.5856432	−270.7
15⁻_231	−0.35252	−1619.5822568	−261.8
15⁻_311	−0.33827	−1619.5618837	−208.3
15⁻_312	−0.33227	−1619.5618835	−208.3
15⁻_321	−0.33981	−1619.5743519	−241.0
15⁻_331	−0.34103	−1619.5746380	−241.8
15⁻_333	−0.33942	−1619.5750620	−242.9
6d		−766.1892969	
16*⁻_111	−0.17276	−1433.3814111	−228.2
16*⁻_121	−0.17664	−1433.3840415	−235.1
16*⁻_131	−0.17735	−1433.3881759	−246.0
16*⁻_133	−0.17722	−1433.3881757	−246.0
16*⁻_211	−0.16889	−1433.3814112	−228.2
16*⁻_221	−0.17668	−1433.3864318	−241.4
16*⁻_222	−0.17411	−1433.3815046	−228.5
16*⁻_231	−0.17978	−1433.3902228	**−251.4**
16*⁻_311	−0.16823	−1433.3738915	−208.5
16*⁻_321	−0.17565	−1433.3881759	−246.0
16*⁻_322	−0.17243	−1433.3820670	−230.0
16*⁻_333	−0.16307	−1433.3701559	−198.7
16⁻_111	−0.18347	−1433.3901586	**−251.2**

TABLE 5.7: Continued.

	AM1	B3LYP/6-31G(d,p)	
	E_{tot} / a.u.	E_{tot} / a.u.	ΔE_0 / kJ mol^{-1}
16⁻_113	−0.17193	−1433.3830877	−232.6
16⁻_131	−0.17412	−1433.3862026	−240.8
16⁻_211	−0.16436	−1433.3666787	−189.6
16⁻_212	−0.16339	−1433.3679824	−193.0
16⁻_221	−0.17113	−1433.3817466	−229.1
16⁻_222	−0.17017	−1433.3832461	−233.1
16⁻_223	−0.17015	−1433.3832460	−233.1
16⁻_231	−0.17232	−1433.3832460	−233.1
16⁻_321	−0.18040	−1433.3856286	−239.3
16⁻_331	−0.17276	−1433.3901603	−251.2

5.6 References

[1]   K. Schank, *Methoden der Organischen Chemie (Houben-Weyl), Vol. E11*, G Thieme, Stuttgart, **1985**.

[2]   P. D. Magnus, *Tetrahedron* **1977**, *33*, 2019-2045.

[3]   N. S. Simpkins, *Sulphones in Organic Synthesis*, Pergamon Press, Oxford, **1993**.

[4]   S. Patai, Z. Rappoport, *The Chemistry of Sulphones and Sulphoxides*, John Wiley and Sons, Chichester, UK, **1988**.

[5]   B. M. Trost, *Bull. Chem. Soc. Jpn.* **1988**, *61*, 107-124.

[6]   A. Solladie-Cavallo, D. Roche, J. Fischer, A. De Cian, *J. Org. Chem.* **1996**, *61*, 2690-2694.

[7]   M. Julia, *Pure Appl. Chem.* **1985**, *57*, 763-768.

[8]   T. Takeda, *Modern Carbonyl Olefination*, Wiley-VCH, Weinheim, **2004**.

[9]   K. Plesniak, A. Zarecki, J. Wicha, *Top. Curr. Chem.* **2007**, *275*, 163-250.

[10]   P. R. Blakemore, *J. Chem. Soc., Perkin Trans. 1* **2002**, 2563-2585.

[11]   F. G. Bordwell, J. C. Branca, T. A. Cripe, *Isr. J. Chem.* **1985**, *26*, 357-366.

[12]   H. Mayr, M. Patz, *Angew. Chem.* **1994**, *106*, 990-1010; *Angew. Chem. Int. Ed. Engl.* **1994**, *33*, 938-957.

[13]   H. Mayr, A. R. Ofial, *Pure Appl. Chem.* **2005**, *77*, 1807-1821.

[14]   F. G. Bordwell, M. J. Bausch, J. C. Branca, J. A. Harrelson, *J. Phys. Org. Chem* **1988**, *1*, 225-241.

[15]   F. Seeliger, S. T. A. Berger, G. Y. Remennikov, K. Polborn, H. Mayr, *J. Org. Chem.* **2007**, *72*, 9170-9180.

[16]   S. T. A. Berger, F. H. Seeliger, F. Hofbauer, H. Mayr, *Org. Biomol. Chem.* **2007**, *5*, 3020-3026.

[17]   O. Kaumanns, H. Mayr, *J. Org. Chem.* **2008**, accepted.

[18]   J.-L. Marco, I. Fernandez, N. Khiar, P. Fernandez, A. Romero, *J. Org. Chem.* **1995**, *60*, 6678-6679.

[19]   A. R. G. Ferreira, G. V. M. De Vilela, M. B. Amorim, K. P. Perry, A. J. R. Da Silva, A. G. Dias, P. R. R. Costa, *J. Org. Chem.* **2004**, *69*, 4013-4018.

[20]   E. Haslinger, P. Wolschann, *Org. Magn. Reson.* **1977**, *9*, 1-7.

[21]   L. Henning, M. Alva-Astudillo, G. Mann, T. Kappe, *Monatsh. Chem.* **1992**, *123*, 571-580.

[22] R. Bednar, E. Haslinger, U. Herzig, O. E. Polansky, P. Wolschann, *Monatsh. Chem.* **1976**, *107*, 1115-1125.

[23] F. Seeliger, **2004**, *Diploma Thesis*, Ludwig-Maximilians Universität München.

[24] R. Schwesinger, H. Schlemper, C. Hasenfratz, J. Willaredt, T. Dambacher, T. Breuer, C. Ottaway, M. Fletschinger, J. Boele, H. Fritz, D. Putzas, H. W. Rotter, F. G. Bordwell, A. V. Satish, G. Z. Ji, E. M. Peters, K. Peters, H. G. v. Schnering, L. Walz, *Liebigs Ann.* **1996**, 1055-1081.

[25] E. M. Arnett, L. E. Small, *J. Am. Chem. Soc.* **1977**, *99*, 808-816.

[26] M. A. H. Laramay, J. G. Verkade, *J. Am. Chem. Soc.* **1990**, *112*, 9421-9422.

[27] J. Tang, J. Dopke, J. G. Verkade, *J. Am. Chem. Soc.* **1993**, *115*, 5015-5020.

[28] Y. Tsuno, M. Fujio, *Advances in Physical Organic Chemistry* **1999**, *32*, 267-385.

[29] R. C. Gaussian 03, M. J. Frisch, G. W. Trucks, H. B. Schlegel, G. E. Scuseria, M. A. Robb, J. R. Cheeseman, J. A. Montgomery, Jr., T. Vreven, K. N. Kudin, J. C. Burant, J. M. Millam, S. S. Iyengar, J. Tomasi, V. Barone, B. Mennucci, M. Cossi, G. Scalmani, N. Rega, G. A. Petersson, H. Nakatsuji, M. Hada, M. Ehara, K. Toyota, R. Fukuda, J. Hasegawa, M. Ishida, T. Nakajima, Y. Honda, O. Kitao, H. Nakai, M. Klene, X. Li, J. E. Knox, H. P. Hratchian, J. B. Cross, V. Bakken, C. Adamo, J. Jaramillo, R. Gomperts, R. E. Stratmann, O. Yazyev, A. J. Austin, R. Cammi, C. Pomelli, J. W. Ochterski, P. Y. Ayala, K. Morokuma, G. A. Voth, P. Salvador, J. J. Dannenberg, V. G. Zakrzewski, S. Dapprich, A. D. Daniels, M. C. Strain, O. Farkas, D. K. Malick, A. D. Rabuck, K. Raghavachari, J. B. Foresman, J. V. Ortiz, Q. Cui, A. G. Baboul, S. Clifford, J. Cioslowski, B. B. Stefanov, G. Liu, A. Liashenko, P. Piskorz, I. Komaromi, R. L. Martin, D. J. Fox, T. Keith, M. A. Al-Laham, C. Y. Peng, A. Nanayakkara, M. Challacombe, P. M. W. Gill, B. Johnson, W. Chen, M. W. Wong, C. Gonzalez, and J. A. Pople, Gaussian, Inc., Wallingford CT, **2004**.

[30] H. Mayr, T. Bug, M. F. Gotta, N. Hering, B. Irrgang, B. Janker, B. Kempf, R. Loos, A. R. Ofial, G. Remennikov, H. Schimmel, *J. Am. Chem. Soc.* **2001**, *123*, 9500-9512.

[31] M. Baidya, S. Kobayashi, F. Brotzel, U. Schmidhammer, E. Riedle, H. Mayr, *Angew. Chem.* **2007**, *119*, 6288-6292; *Angew. Chem. Int. Ed.* **2007**, *46*, 6176-6179.

[32] M. Baidya, H. Mayr, *Chem. Commun.* **2008**, in print.

[33] B. H. M. Asghar, M. R. Crampton, *J. Phys. Org. Chem.* **2007**, *20*, 702-709.

[34] A. R. Ofial, K. Ohkubo, S. Fukuzumi, R. Lucius, H. Mayr, *J. Am. Chem. Soc.* **2003**, *125*, 10906-10912.

[35] A. R. Ofial, S. Fukuzumi, H. Mayr, unpublished results.

[36]   L. Eberson, H. Schäfer, *Organic Electrochemistry*, Springer, Berlin, **1971**.

[37]   J. P. Scott, D. C. Hammond, E. M. Beck, K. M. J. Brands, A. J. Davies, U. H. Dolling, D. J. Kennedy, *Tet. Lett.* **2004**, *45*, 3345-3348.

Chapter 6

Solvent Effects on the Rates of Electrophile-Nucleophile Combinations

6.1 Introduction

The nature of the solvent often plays an important role on the rate of chemical reactions. In particular processes, where the polarity changes from reactants to transition-state, for example ionization, displacement, elimination, and fragmentation reactions, often show a large dependence on the used solvent.[1, 2] Parker demonstrated the great influence of solvation in S_N2-type reactions. He reported that an increase in nucleophilicity up to the factor of 10^8 is observed, when dipolar aprotic solvents are used instead of hydrogen-bond donor solvents.[3]

In general, one can separate the enthalpy of interaction of two molecules into repulsive forces, induction interactions, dispersion interactions, and electrostatic interactions between permanent charge distributions of the two molecules.[4] The latter forces were found to play a dominant role in intermolecular interactions[5] and were the basis for the simple qualitative solvation model of Hughes and Ingold.[6-9] Their rules allow to qualitatively predict the effect of solvents on the rates of chemical reactions by comparing the polarities of the reactants and of the activated complex.

As already presented in the previous chapters, equation 6.1

$$\log k_2 \, (20 \, °C) = s \, (N + E) \tag{6.1}$$

is a helpful tool to calculate the rate constants k_2 at 20 °C of electrophile-nucleophile combinations.[10] The parameter E, which defines the electrophilic potential of a compound, is considered to be independent of solvent properties. In contrast, the reactivity parameters N and s for nucleophiles are committed to a definite solvent.

In previous work, it was demonstrated that the rates of the reactions of π-nucleophiles with carbocations are only slightly affected by the solvent polarity.[11-13] On the other hand, the reaction of 2-methylfuran (in CH_2Cl_2: $N = 3.61$, $s = 1.11$)[14] with the p-methoxy-substituted benzylidenebarbituric acid **2** ($E = -10.37$)[15] is almost four orders of magnitude faster in the polar aprotic solvent DMSO ($k_{2, exp} = 1.24 \times 10^{-4}$ L mol^{-1} s^{-1}) than calculated by equation 6.1 ($k_{2, calc} = 3.14 \times 10^{-8}$ L mol^{-1} s^{-1}).[16] This observation prompted me to investigate the effect of solvent polarity (Table 6.1) on the rate constants of electrophile-nucleophile combinations more deeply. Therefore, the addition reactions of anionic and neutral nucleophiles to both carbocations and uncharged Michael acceptors were studied.

TABLE 6.1: Commonly used solvent polarity scales.[17]

| solvent	$E_T(30)$ / kcal mol^{-1}	Z / kcal mol^{-1}	ε_r / As Vm^{-1}
MeOH	55.4	83.6	32.6
DMSO	45.1	70.2	46.7
DMF	43.2	68.4	36.7
CH_2Cl_2	40.7	64.7	9.10
THF	37.4	58.8	7.58

Increasing polarity

6.2 Results and Discussion

*6.2.1 Reactions of 1-pyrrolidinocyclopentene (**1**) with charged and uncharged electrophiles in dichloromethane and DMF*

The addition reactions of 1-pyrrolidinocyclopentene (**1**) to benzylidenebarbituric acid **2**, diarylcarbenium ion **3**, and quinone methide **4** have been studied in DMF and dichloromethane at 20 °C (Scheme 6.1).
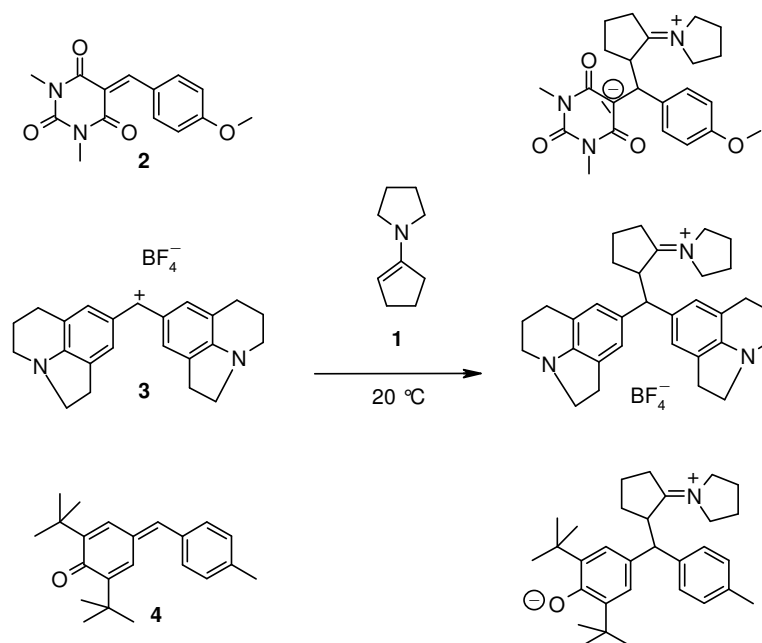
SCHEME 6.1: Reaction of 1-pyrrolidinocyclopenten (**1**) with benzylidenebarbituric acid **2**, diarylcarbenium ion **3**, and quinone methide in various solvents at 20 °C.

All reactions depicted in Scheme 6.1 proceeded quantitatively, so that the solutions were completely decolorized. The kinetic experiments were performed under pseudo-first-order conditions using a high excess of enamine **1**. From the exponential decays of the UV-Vis absorbances of the electrophiles the pseudo-first-order rate constants were determined. The second-order rate constants k_2 (Table 6.2) where then obtained as the slopes of $k_{1\Psi}$ versus [**2**] correlations, as already illustrated in the previous chapters.

TABLE 6.2: Second-order rate constants k_2 (20 °C) of the reactions of 1-pyrrolidino-cyclopenten (**1**) with electrophiles **2-4**.

elec.	solvent	k_2 (L mol^{-1} s^{-1})
2	DMF	$(9.24 \pm 0.13) \times 10^4$
	CH$_2$Cl$_2$	$(1.37 \pm 0.09) \times 10^5$
3	DMF	$(5.34 \pm 0.12) \times 10^4$
	CH$_2$Cl$_2$	$(1.52 \pm 0.10) \times 10^5$
4	DMF	6.75 ± 0.06
	CH$_2$Cl$_2$	1.60 ± 0.10

From Figure 6.1, which illustrates the results of Table 6.2, one can see that the second-order rate constants of the addition of enamine **1** to Michael acceptor **2** and carbocation **3** are

slightly larger in dichloromethane than in DMF, in contrast to the reaction of **1** with quinone methide **4**. The reactivity parameters of compound **1** were exclusively, those of **3** and **4** were predominantly determined in CH_2Cl_2. Thus, calculated k_2-values for the additions of **1** to **3** and **4** in dichloromethane (indicated by the triangles (▲) in Figure 6.1) are in good agreement with the obtained experimental numbers in this solvent. Possibly, the small deviation of experimental and calculated rate constant of the addition of **1** to benzylidenebarbituric acid **2** is due to the fact that the *E*-parameter of **2** was derived from reactions in DMSO solution only.
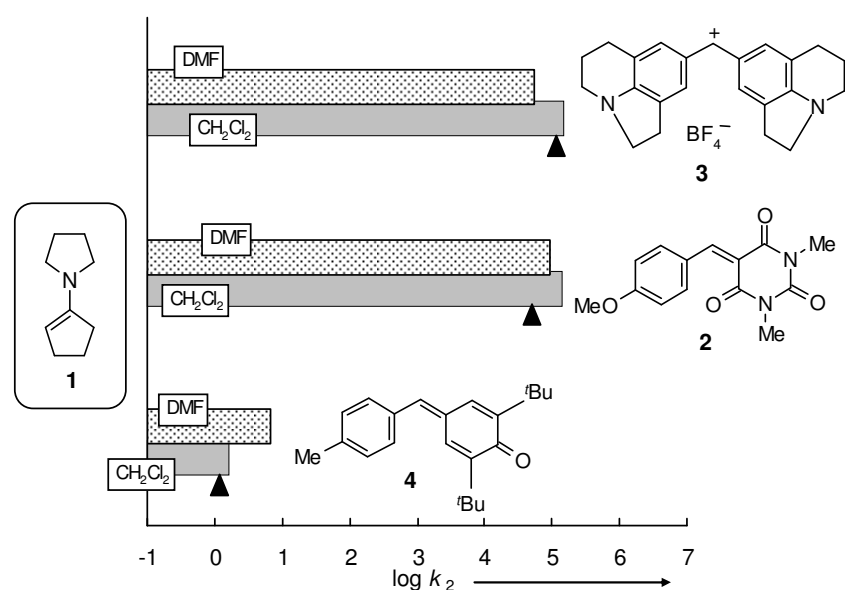

FIGURE 6.1: Solvent effect on the rate k_2 of the reaction of 1-pyrrolidinocyclopentene (**1**) with diarylcarbenium ion **3** (top)**,** benzylidenebarbituric acid **2** (middle), and quinone methide **4** (bottom) at 20 °C. The triangles (▲) indicate the calculated log k_2-values (equation 6.1) based on reactivity parameters *N*, *s* of **1** determined in CH_2Cl_2.

The charge of the activated complex formed upon the attack of a neutral nucleophile (like **1**) to a carbocation (e.g., **3**) is more dispersed than in the initial reactants. Therefore, a change to a more polar aprotic solvent will decrease the rate of this reaction due to a better stabilization of the reactants than of the activated complex.[6] Consequently, the reaction of enamine **1** with diarylcarbenium ion **3** in DMF ($k_2 = 5.34 \pm 0.12 \times 10^4$ L mol^{-1} s^{-1}) is approximately 3 times slower than in dichloromethane ($k_2 = 1.52 \times 10^5$ L mol^{-1} s^{-1}).

On the other side, reactions will be accelerated by more polar aprotic solvents, if the activated complex possesses a larger dipole moment than the initial reactants. For the addition of **1** to quinone methide **4** this is obvious: In DMF ($k_2 = 6.75$ L mol^{-1} s^{-1}) the reaction is about 4 times faster than in the less polar dichloromethane ($k_2 = 1.60$ L mol^{-1} s^{-1}). In contrast, the attack of 1-pyrrolidinocyclopentene (**1**) to benzylidenebarbituric acid **2** is slightly faster in dichloromethane than in the more polar DMF (Figure 6.1).

6.2.2 Reactions of the dimedone anion (**5⁻**) with charged and uncharged electrophiles in various solvents

The anion of dimedone (in DMSO:[18] $N = 16.27$, $s = 0.77$; in water:[19] $N = 11.77$, $s = 0.63$) was chosen as model compound for the investigation of carbanion reactivity in different solvents. Dimedone was deprotonated by the use of the sterically hindered amidine base diaza-1,3-bicyclo[5.4.0]undecane (DBU) in DMSO, DMF, and MeOH. In the less polar solvents dichloromethane and THF, DBU does not deprotonate dimedone completely. Thus, the potassium salt of dimedone anion mixed with equimolar amounts of crown ether was studied in these solvents. The neutral organic Lewis acid **2** ($E = -10.37$)[15] and the diarylcarbenium ion **3** ($E = -10.04$)[14] are comparable in their electrophilicity and served as reaction partners in this study (Scheme 6.2).
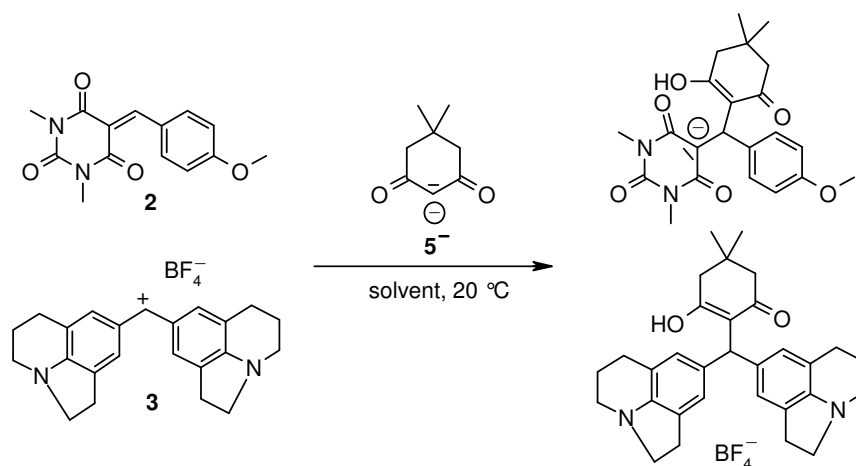
SCHEME 6.2: Reaction of dimedone anion (**5⁻**) with benzylidenebarbituric acid **2** and diarylcarbenium ion **3** in various solvents at 20 °C.

The second-order rate constants (Table 6.3) for the reactions shown in Scheme 6.2 were measured photometrically by the stopped-flow method as described in the previous chapters.

TABLE 6.3: Second-order rate constants k_2 (20 °C) of the reactions of dimedone anion (5^-) with electrophiles **2-3** in various solvents.

elec	solvent	counter ion	k_2 (L mol^{-1}s^{-1})
2	MeOH	DBUH$^+$	$(7.50 \pm 0.37) \times 10^1$
	DMSO	DBUH$^+$	$(4.51 \pm 0.02) \times 10^4$
	DMF	DBUH$^+$	$(5.27 \pm 0.09) \times 10^4$
	CH$_2$Cl$_2$	K$^+$ (18-C-6)	$(2.88 \pm 0.11) \times 10^3$
	THF	K$^+$ (18-C-6)	$(7.26 \pm 0.26) \times 10^4$
3	MeOH	DBUH$^+$	$(5.14 \pm 0.03) \times 10^1$
	DMSO	DBUH$^+$	$(5.39 \pm 0.05) \times 10^4$
	DMF	DBUH$^+$	$(1.79 \pm 0.03) \times 10^5$
	CH$_2$Cl$_2$	K$^+$ (18-C-6)	-[b]
	THF[a]	K$^+$ (18-C-6)	-[b]

[a] The reaction mixture contains 0.5 % (vol.) of CH$_2$Cl$_2$. [b] The reaction is to fast to be followed with the stopped-flow technique.

The reactions of the dimedone anion (5^-) with benzylidenebarbituric acid **2** and diarylcarbenium ion **3** are considerably more influenced by solvent properties than afore discussed reactions of enamine **1** with the same electrophiles. In dipolar aprotic solvents, like DMSO and DMF, the rate constants of the reactions of 5^- with **2** and **3** are similar and fairly well described by equation 6.1 (Figure 6.2).
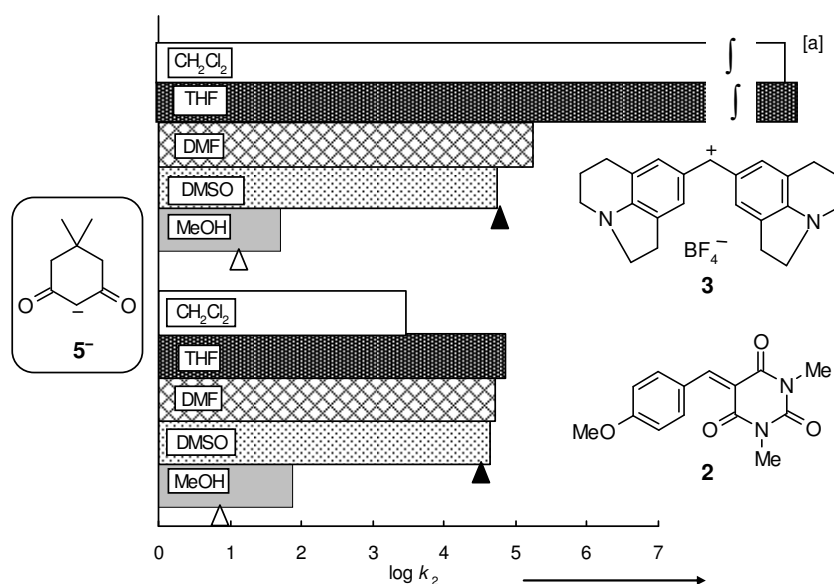
FIGURE 6.2: Solvent effects on the rate k_2 of the reactions of dimedone anion (5^-) with diarylcarbenium ion **3** (top) and benzylidenebarbituric acid **2** (bottom) at 20 °C. The filled

triangles (▲) indicate the calculated log k_2-values (equation 6.1) in DMSO, unfilled triangles (Δ) represent the corresponding values in water. − [a] The reactions of 5^- with 3 in THF and CH_2Cl_2 are too fast to be measured with the stopped-flow method.

In methanol the reaction rates of the addition of carbanion 5^- to 2 and 3 are clearly lower than in all other solvents examined in this study. This tremendous reduction of the nucleophilic reactivities of 5^- is most likely caused by the ability of MeOH to form stabilizing hydrogen bonds, as it was also found for other carbanions.[20, 21]

In more apolar solvents like dichloromethane and THF it is not possible to determine the rate constant of the carbanion-carbocation combination $5^- + 3$ with the stopped-flow method. As it is expected for reactions where charges are destroyed, this addition is strongly accelerated.

In contrast, one can study the kinetics of the addition of carbanion 5^- to Michael acceptor 2 in THF and dichloromethane, though electrophiles 2 and 3 possess nearly the same electrophilicity parameters E. The reaction of dimedone anion (5^-) with benzylidenebarbituric acid 2 in THF is slightly faster than in the more polar solvents DMF and DMSO (Table 6.1) and clearly slower in dichloromethane.
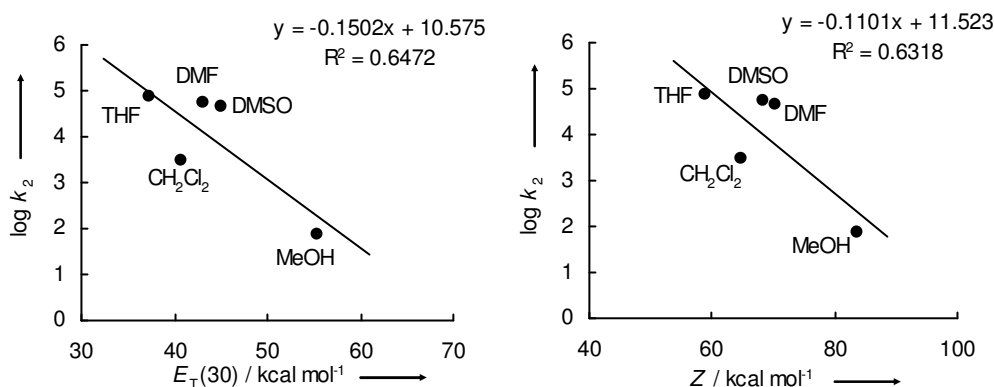

FIGURE 6.3: Correlation of log k_2 versus $E_T(30)$ (left) and versus Z (right) for the reaction of dimedone anion (5^-) with benzylidenebarbituric acid 2 in different solvents.

Figure 6.3 shows the poor correlations of the logarithmic second-order rate constants log k_2 versus $E_T(30)$[17] (left) and Z (right)[17] for the reaction of 5^- with 2, indicating that these solvent polarity scales derived from UV-Vis-spectroscopic experiments describe the influence of the solvent on this reaction improperly.
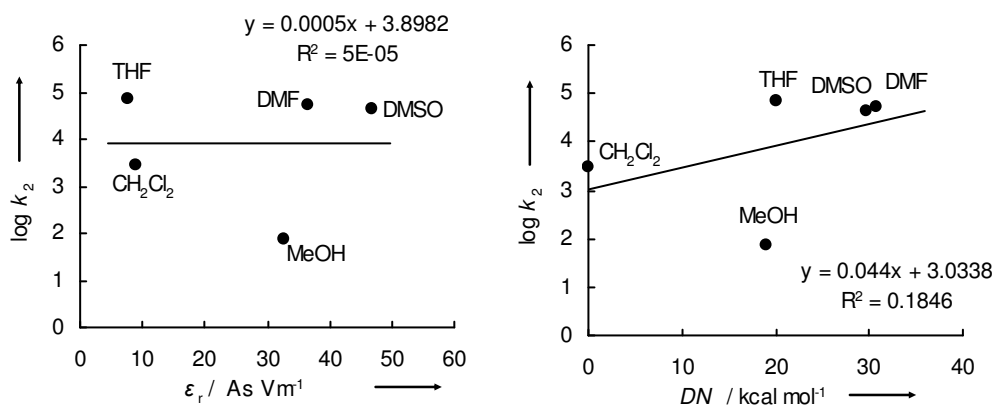
FIGURE 6.4: Correlation of log k_2 versus dielectric constants ε_r (left) and versus Gutmann's donor number DN (right) for the reaction of dimedone anion (**5$^-$**) with benzylidenebarbituric acid **2** in different solvents.

Analogous correlations with the relative permittivity ε_r or the donor number DN [22] are even worse (Figure 6.4). The so-called acceptor number AN, which was introduced by Gutmann and Mayer *et al.* in 1975,[23] is better in describing the effect of solute-solvent interactions on the reaction rates of **5$^-$ + 2** (Figure 6.5, left). The nondimensional AN values express the Lewis acidity of a solvent in relation to SbCl$_5$, which is also the standard for the donor number scale. Acceptor numbers are obtained from the ^{31}P-NMR chemical shift of triethylphosphane oxide in the solvent under consideration (Scheme 6.3).
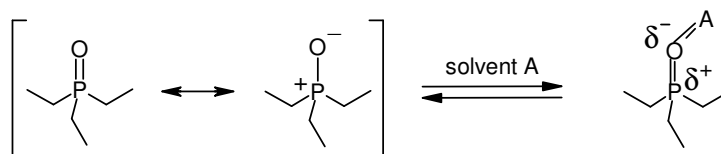
SCHEME 6.3: Interaction of a solvent A with triethylphosphane oxide (AN scale).[23]

The AN scale is set up by defining $AN = 0$ for *n*-hexane and $AN = 100$ for the 1:1 complex of Et$_3$PO$-$SbCl$_5$ dissolved in 1,2-dichloroethane.
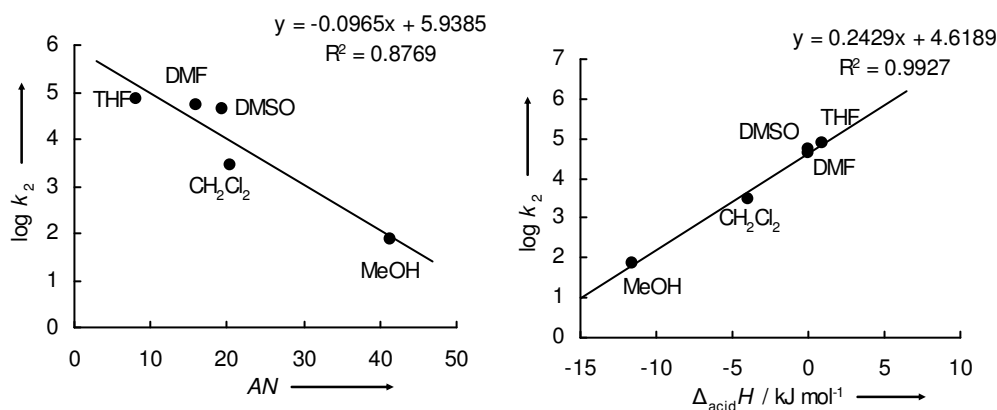
202

FIGURE 6.5: Correlation of log k_2 versus the acceptor-number AN (left)[23] and versus the hydrogen-bond acidity $\Delta_{acid}H$ (right)[24, 25] for the reaction of dimedone anion (**5$^-$**) with benzylidenebarbituric acid **2** in different solvents.

An excellent relationship ($R^2 = 0.993$) is found between the logarithmic second-order rate constants of the reaction of the Michael acceptor **2** with carbanion **5$^-$** and Catalan's hydrogen-bond acidity value of the solvent (Figure 6.5, right).[24, 25] The enthalpy term $\Delta_{acid}H$ characterizes the electron pair accepting abilities of a solvent and equals the difference of the solvation enthalpies of *N*-methylimidazole and *N*-methylpyrrole in the solvents under consideration.

The correlations shown in Figures 6.3 - 6.5 indicate that the rate of the addition of the dimedone anion (**5$^-$**) to benzylidenebarbituric acid **2** is dominated by the carbanion-solvent interactions. Strong hydrogen-bond-donor solvents (i.e., MeOH) stabilize the negative charge delocalized over the *β*-diketo function and, therefore, decrease the nucleophilicity of the carbanion **5$^-$**. Thus, the hydrogen-bond donor ability of dichloromethane is the prime reason for the low reaction rate of **5$^-$** + **2** in this solvent.

6.3 Conclusion

Equation 6.1 predicts second-order rate constants of electrophile-nucleophile combinations with accuracy better than a factor of 100, provided that the formation of a *σ*-bond is the rate-determining step. The reactions of 1-pyrrolidinocyclopentene (**1**) with benzyldidene-barbituric acid **2**, diarylcarbenium ion **3**, and quinone methide **4** in dichloromethane and DMF confirm the negligible solvent effect on the rates of the reactions of *π*-nucleophiles with

diarylcarbenium ions found previously. When exploring carbanion reactivity the situation changes. The reaction rates of the attack of dimedone anion (5^-) at the uncharged Michael acceptor **3** considerably depend on the hydrogen-bond donor abilities of the used solvent and can be properly correlated with the solvent acidity scale of Catalan. Nevertheless, this relationship has to be proved with other neutral electrophiles (e.g., quinone methide **4**).

The high reactivity of the carbanion-carbocation combination 5^- + **2** in the more apolar solvents dichloromethane and THF can be rationalized in terms of electrostatic interactions and clearly point out that equation 6.1 cannot be used to describe the reactions of oppositely charged reactants in apolar solvents.

6.4 Experimental Section

The temperature of the solutions during all kinetic studies was kept constant ($20 \pm 0.1°C$) by using a circulating bath thermostat. Dry DMSO, DMF, and MeOH for kinetics were purchased (< 50 ppm H_2O). Dichloromethane was freshly distilled over CaH_2, THF was freshly distilled over sodium before use.

For the evaluation of kinetics the stopped-flow spectrophotometer system Applied Photophysics SX.18MV-R stopped-flow reaction analyzer was used. Rate constants k_{obs} (s^{-1}) were obtained by fitting the single exponential $A_t = A_0\exp(-k_{obs}t) + C$ to the observed time-dependent electrophile absorbance (averaged from at least 4 kinetic runs for each nucleophile concentration).

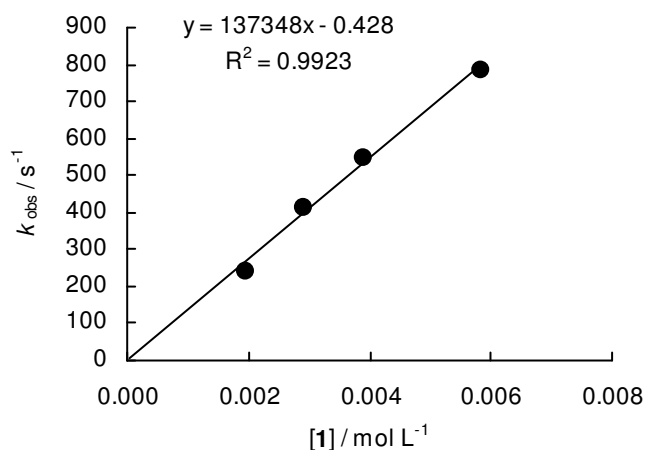Reaction of **2** with **1** (DMF, 20 ° C, stopped-flow, $\lambda = 400$ nm)

$[2]_0$ / M	$[1]_0$ / M	k_{obs} / s^{-1}
3.83×10^{-5}	1.41×10^{-3}	1.32×10^{2}
3.83×10^{-5}	1.98×10^{-3}	1.80×10^{2}
3.83×10^{-5}	3.11×10^{-3}	2.88×10^{2}
3.83×10^{-5}	3.53×10^{-2}	3.26×10^{2}

$$k_2 = (9.24 \pm 0.13) \times 10^{4} \text{ L mol}^{-1} \text{ s}^{-1}$$
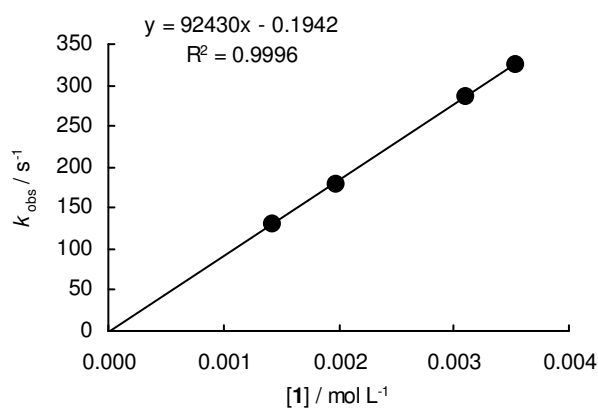
Reaction of **2** with **1** (CH$_2$Cl$_2$, 20 ° C, stopped-flow, $\lambda = 400$ nm)

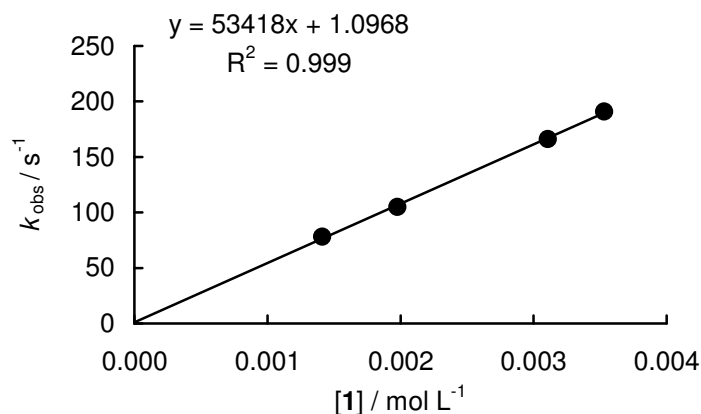| $[2]_0$ / M	$[1]_0$ / M	k_{obs} / s^{-1}
9.04×10^{-5}	1.94×10^{-3}	2.45×10^{2}
9.04×10^{-5}	2.91×10^{-3}	4.14×10^{2}
9.04×10^{-5}	3.88×10^{-3}	5.51×10^{2}
9.04×10^{-5}	5.82×10^{-3}	7.85×10^{2}

$$k_2 = (1.37 \pm 0.09) \times 10^{5} \text{ L mol}^{-1} \text{ s}^{-1}$$

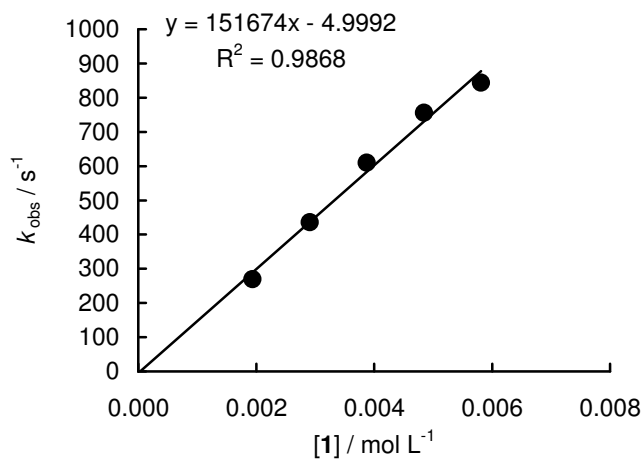Reaction of **3** with **1** (DMF, 20 ° C, stopped-flow, $\lambda = 600$ nm)

$[3]_0$ / M	$[1]_0$ / M	k_{obs} / s^{-1}
2.59×10^{-5}	1.41×10^{-3}	7.80×10^{1}
2.59×10^{-5}	1.98×10^{-3}	1.05×10^{2}
2.59×10^{-5}	3.11×10^{-3}	1.66×10^{2}
2.59×10^{-5}	3.53×10^{-2}	1.91×10^{2}

$$k_2 = (5.34 \pm 0.12) \times 10^4 \text{ L mol}^{-1} \text{ s}^{-1}$$

$y = 53418x + 1.0968$
$R^2 = 0.999$

Reaction of **3** with **1** (CH$_2$Cl$_2$, 20 ° C, stopped-flow, $\lambda = 600$ nm)

$[3]_0$ / M	$[1]_0$ / M	k_{obs} / s^{-1}
2.21×10^{-5}	1.94×10^{-3}	2.69×10^{2}
2.21×10^{-5}	2.91×10^{-3}	4.36×10^{2}
2.21×10^{-5}	3.88×10^{-3}	6.10×10^{2}
2.21×10^{-5}	4.85×10^{-3}	7.56×10^{2}
2.21×10^{-5}	5.82×10^{-3}	8.44×10^{2}

$$k_2 = (1.52 \pm 0.10) \times 10^5 \text{ L mol}^{-1} \text{ s}^{-1}$$

$y = 151674x - 4.9992$
$R^2 = 0.9868$

Reaction of **4** with **1** (DMF, 20 ° C, stopped-flow, $\lambda = 400$ nm)

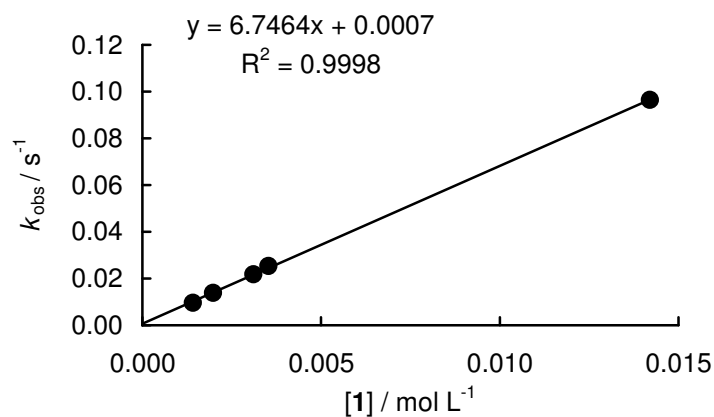| $[\mathbf{4}]_0$ / M	$[\mathbf{1}]_0$ / M	k_{obs} / s^{-1}
3.50×10^{-5}	1.41×10^{-3}	9.62×10^{-3}
3.50×10^{-5}	1.98×10^{-3}	1.38×10^{-2}
3.50×10^{-5}	3.11×10^{-3}	2.18×10^{-2}
3.50×10^{-5}	3.53×10^{-3}	2.54×10^{-2}
3.50×10^{-5}	1.42×10^{-2}	9.64×10^{-2}

$$k_2 = (6.75 \pm 0.06) \text{ L mol}^{-1} \text{ s}^{-1}$$

Reaction of **4** with **1** (CH$_2$Cl$_2$, 20 ° C, stopped-flow, $\lambda = 400$ nm)

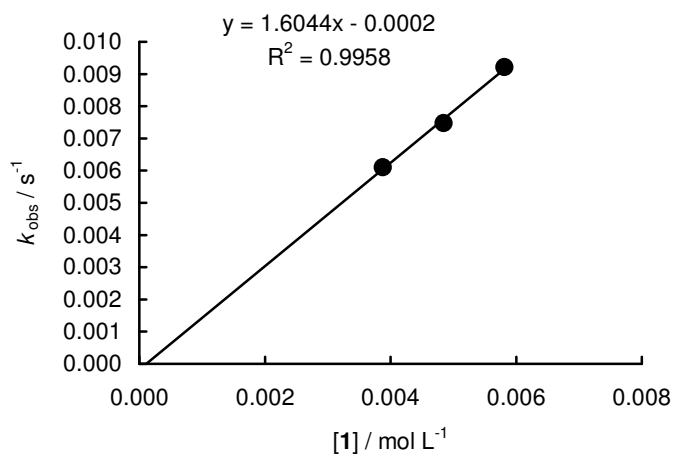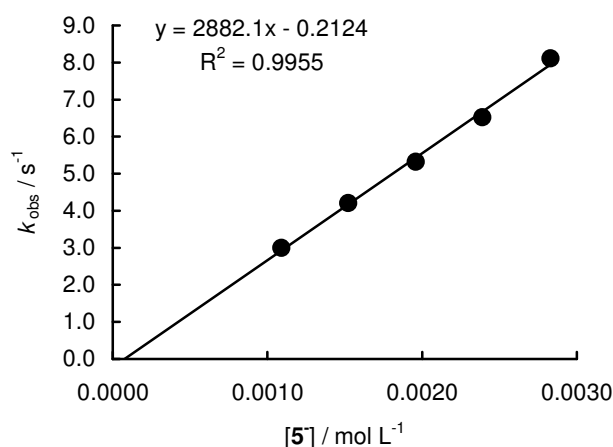| $[\mathbf{4}]_0$ / M	$[\mathbf{1}]_0$ / M	k_{obs} / s^{-1}
6.61×10^{-5}	3.88×10^{-3}	6.10×10^{-3}
6.61×10^{-5}	4.85×10^{-3}	7.48×10^{-3}
6.61×10^{-5}	5.82×10^{-3}	9.21×10^{-3}

$$k_2 = (1.60 \pm 0.10) \text{ L mol}^{-1} \text{ s}^{-1}$$

Reaction of **2** with **5⁻** (employed as potassium salt, CH_2Cl_2, 20 °C, stopped-flow, $\lambda = 375$ nm)

$[2]_0$ / M	$[5^-]_0$ / M	[18-C-6]	k_{obs} / s^{-1}
4.96×10^{-5}	1.09×10^{-3}	1.19×10^{-3}	3.00
4.96×10^{-5}	1.52×10^{-3}	1.66×10^{-3}	4.21
4.96×10^{-5}	1.96×10^{-3}	2.14×10^{-3}	5.32
4.96×10^{-5}	2.39×10^{-3}	2.61×10^{-3}	6.52
4.96×10^{-5}	2.83×10^{-3}	3.08×10^{-3}	8.11

$$k_2 = (2.88 \pm 0.11) \times 10^3 \text{ L mol}^{-1} \text{ s}^{-1}$$

Reaction of **3** with **5⁻** (DMF, 20 ° C, stopped-flow, $\lambda = 600$ nm)

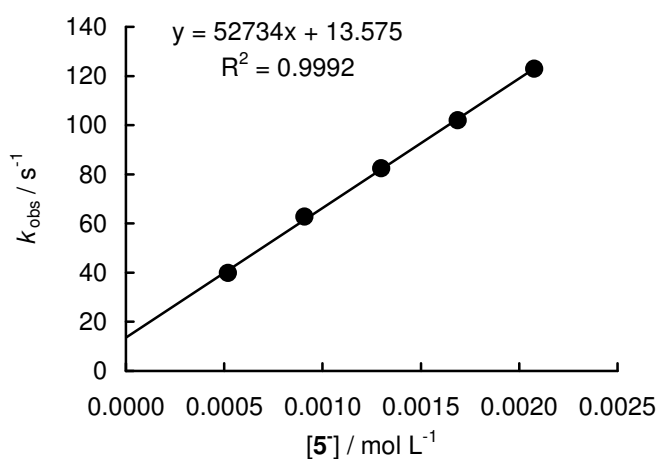| $[3]_0$ / M	$[5^-]_0$ / M	k_{obs} / s^{-1}
2.19×10^{-5}	5.19×10^{-4}	1.16×10^2
2.19×10^{-5}	9.09×10^{-4}	1.86×10^2
2.19×10^{-5}	1.30×10^{-3}	2.57×10^2
2.19×10^{-5}	1.69×10^{-3}	3.20×10^2
2.19×10^{-5}	2.08×10^{-3}	3.97×10^2

$$k_2 = (1.79 \pm 0.03) \times 10^5 \text{ L mol}^{-1} \text{ s}^{-1}$$
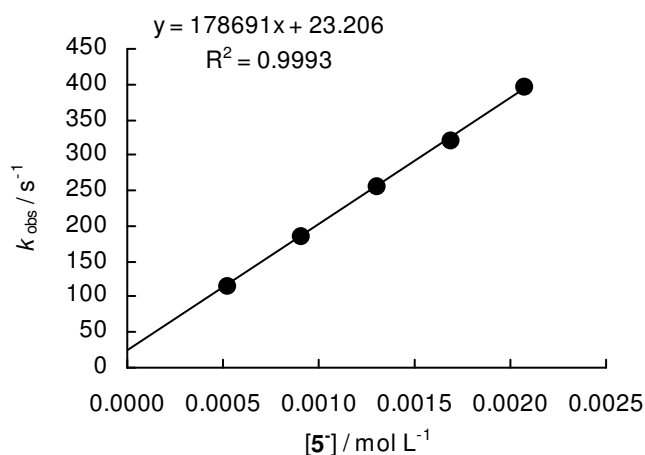
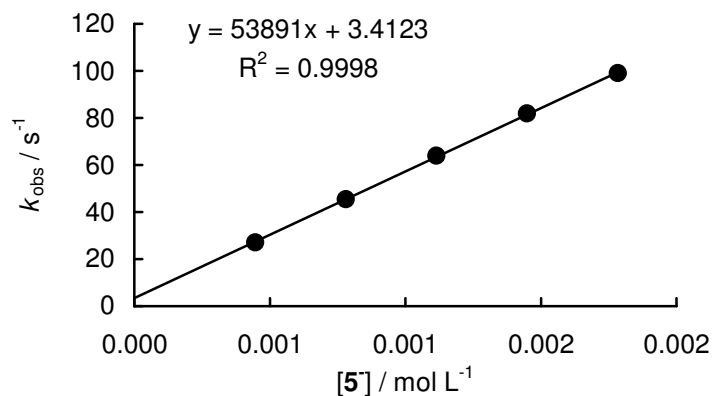Reaction of **2** with **5**$^-$ (DMF, 20 ° C, stopped-flow, λ = 375 nm)

$[\mathbf{2}]_0$ / M	$[\mathbf{5}^-]_0$ / M	k_{obs} / s^{-1}
3.33×10^{-5}	5.19×10^{-4}	3.99×10^{1}
3.33×10^{-5}	9.09×10^{-4}	6.28×10^{1}
3.33×10^{-5}	1.30×10^{-3}	8.25×10^{1}
3.33×10^{-5}	1.69×10^{-3}	1.02×10^{2}
3.33×10^{-5}	2.08×10^{-3}	1.23×10^{2}

$$k_2 = (5.27 \pm 0.09) \times 10^4 \text{ L mol}^{-1} \text{ s}{-1}$$

Reaction of **3** with **5**$^-$ (DMSO, 20 ° C, stopped-flow, λ = 600 nm)
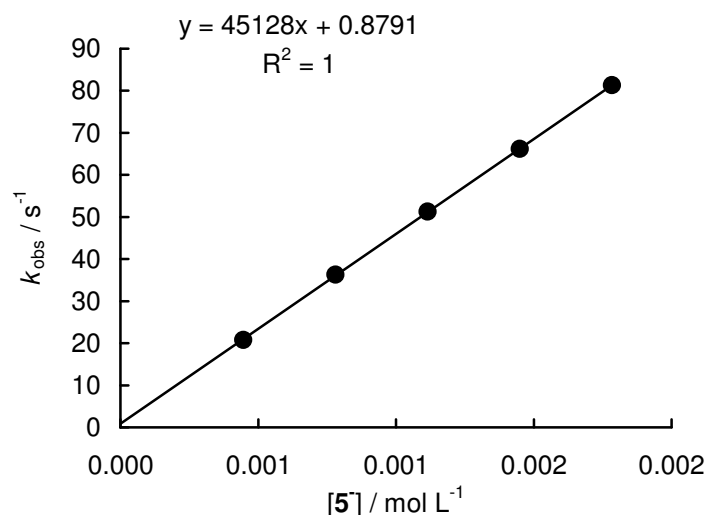
$[\mathbf{3}]_0$ / M	$[\mathbf{5}^-]_0$ / M	k_{obs} / s^{-1}
2.21×10^{-5}	4.46×10^{-4}	2.71×10^{1}
2.21×10^{-5}	7.80×10^{-4}	4.55×10^{1}
2.21×10^{-5}	1.12×10^{-3}	6.39×10^{1}
2.21×10^{-5}	1.45×10^{-3}	8.19×10^{1}
2.21×10^{-5}	1.78×10^{-3}	9.90×10^{1}

$$k_2 = (5.39 \pm 0.05) \times 10^4 \text{ L mol}^{-1} \text{ s}^{-1}$$

209

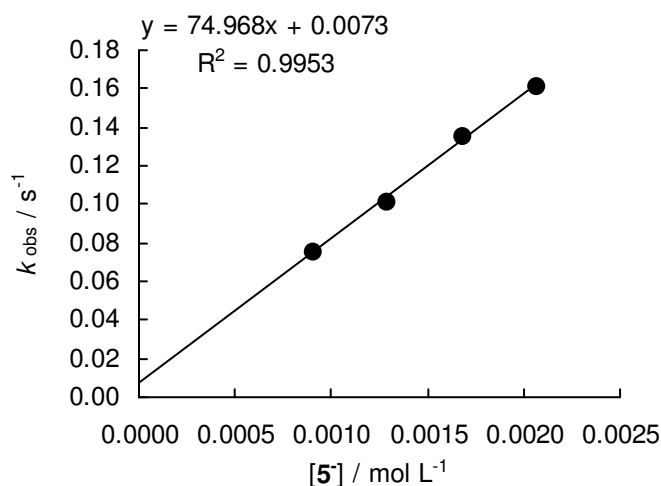Reaction of **2** with **5**⁻ (DMSO, 20 ° C, stopped-flow, λ = 375 nm)

$[\mathbf{2}]_0$ / M	$[\mathbf{5}^-]_0$ / M	k_{obs} / s^{-1}
3.28×10^{-5}	4.46×10^{-4}	2.08×10^{1}
3.28×10^{-5}	7.80×10^{-4}	3.63×10^{1}
3.28×10^{-5}	1.12×10^{-3}	5.13×10^{1}
3.28×10^{-5}	1.45×10^{-3}	6.62×10^{1}
3.28×10^{-5}	1.78×10^{-3}	8.13×10^{1}

$$k_2 = (4.51 \pm 0.02) \times 10^4 \text{ L mol}^{-1} \text{ s}^{-1}$$

$y = 45128x + 0.8791$
$R^2 = 1$

Reaction of **3** with **5**⁻ (MeOH, 20 ° C, stopped-flow, λ = 600 nm)

$[\mathbf{3}]_0$ / M	$[\mathbf{5}^-]_0$ / M	k_{obs} / s^{-1}
2.02×10^{-5}	5.16×10^{-4}	2.43×10^{-2}
2.02×10^{-5}	9.03×10^{-4}	4.44×10^{-2}
2.02×10^{-5}	1.29×10^{-3}	6.41×10^{-2}

$$k_2 = (5.14 \pm 0.03) \times 10^1 \text{ L mol}^{-1} \text{ s}^{-1}$$

$y = 51.448x - 0.0022$
$R^2 = 1$
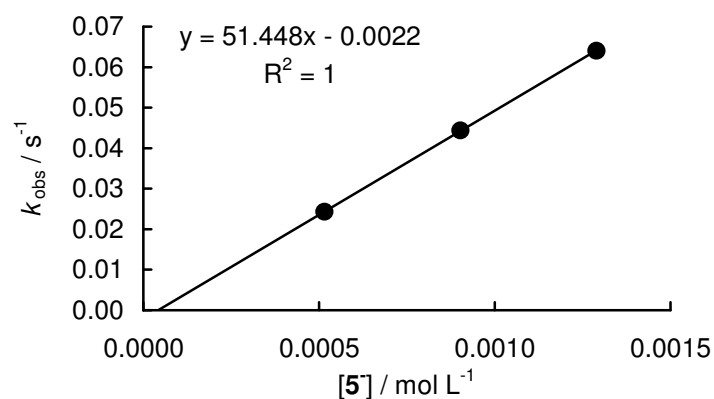
Reaction of **2** with **5**$^-$ (MeOH, 20 ° C, stopped-flow, λ = 375 nm)

$[\mathbf{2}]_0$ / M	$[\mathbf{5}^-]_0$ / M	k_{obs} / s^{-1}
3.50×10^{-5}	9.03×10^{-4}	7.60×10^{-2}
3.50×10^{-5}	1.29×10^{-3}	1.01×10^{-1}
3.50×10^{-5}	1.68×10^{-3}	1.36×10^{-1}
3.50×10^{-5}	2.06×10^{-3}	1.61×10^{-1}

$$k_2 = (7.50 \pm 0.37) \times 10^1 \text{ L mol}^{-1} \text{ s}^{-1}$$

y = 74.968x + 0.0073
R^2 = 0.9953

Reaction of **2** with **5**$^-$ (employed as potassium salt, THF, 20 ° C, stopped-flow, λ = 375 nm)

$[\mathbf{2}]_0$ / M	$[\mathbf{5}^-]_0$ / M	[18-C-6]	k_{obs} / s^{-1}
4.83×10^{-5}	1.12×10^{-3}	1.22×10^{-3}	7.80×10^1
4.83×10^{-5}	1.56×10^{-3}	1.70×10^{-3}	1.10×10^2
4.83×10^{-5}	2.01×10^{-3}	2.19×10^{-3}	1.39×10^2
4.83×10^{-5}	2.46×10^{-3}	2.68×10^{-3}	1.70×10^2
4.83×10^{-5}	2.90×10^{-3}	3.16×10^{-3}	2.10×10^2

$$k_2 = (7.26 \pm 0.26) \times 10^4 \text{ L mol}^{-1} \text{ s}^{-1}$$

y = 72632x - 4.5908
R^2 = 0.9961
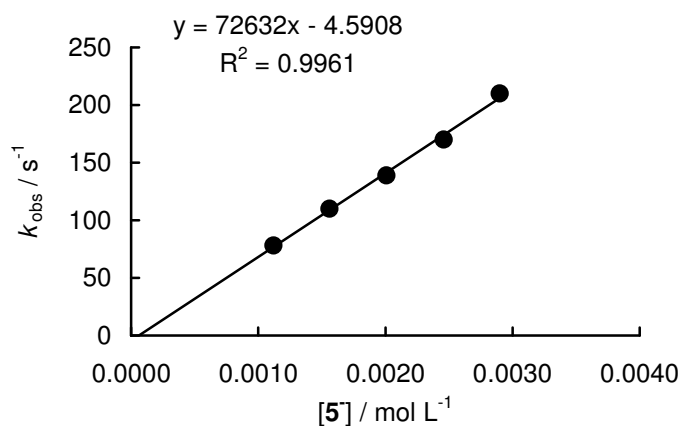
6.5 References

[1]   C. Reichardt, *Pure Appl. Chem.* **1982**, *54*, 1867-1884.

[2]   C. Reichardt, *Solvents and Solvent Effects in Organic Chemistry*, 3rd Ed. Wiley-VCH Weinheim, **2003**.

[3]   A. J. Parker, *Chem. Rev.* **1969**, *69*, 1-32.

[4]   M. Rigby, E. B. Smith, W. A. Wakeham, G. C. Maitland, *The Forces Between Molecules*, Clarendon, Oxford, **1986**.

[5]   C. A. Hunter, *Angew. Chem. Int. Ed.* **2004**, *43*, 5310-5324.

[6]   C. K Ingold: *Structure and Mechanism in Organic Chemistry*, 2. Ed., Cornell University Press, Ithaca / N.Y., and London, **1969**, p. 457ff. and 680ff.

[7]   E. D. Hughes, C. K. Ingold, *J. Chem. Soc.* **1935**, 244-255.

[8]   E. D. Hughes, C. K. Ingold, *Trans. Farady Soc.* **1941**, *37*, 657-685.

[9]   E. D. Hughes, C. K. Ingold, *Trans. Farady Soc.* **1941**, *37*, 603-631.

[10]   H. Mayr, A. R. Ofial, *Pure Appl. Chem.* **2005**, *77*, 1807-1821.

[11]   H. Mayr, R. Schneider, C. Schade, J. Bartl, R. Bederke, *J. Am. Chem. Soc.* **1990**, *112*, 4446-4454.

[12]   H. Mayr, N. Basso, G. Hagen, *J. Am. Chem. Soc.* **1992**, *114*, 3060-3066.

[13]   B. Kempf, *Dissertation* **2003**, Ludwig-Maximilians-Universität München.

[14]   H. Mayr, T. Bug, M. F. Gotta, N. Hering, B. Irrgang, B. Janker, B. Kempf, R. Loos, A. R. Ofial, G. Remennikov, H. Schimmel, *J. Am. Chem. Soc.* **2001**, *123*, 9500-9512.

[15]   F. Seeliger, S. T. A. Berger, G. Y. Remennikov, K. Polborn, H. Mayr, *J. Org. Chem.* **2007**, *72*, 9170-9180.

[16]   See Scheme 2.5 in chapter 2 (p. 29).

[17]   From ref. [2].

[18]   R. Lucius, R. Loos, H. Mayr, *Angew. Chem.* **2002**, *114*, 97-102; *Angew. Chem. Int. Ed.* **2002**, *41*, 91-95.

[19]   T. Bug, H. Mayr, *J. Am. Chem. Soc.* **2003**, *125*, 12980-12986.

[20]   T. B. Phan, H. Mayr, *Eur. J. Org. Chem.* **2006**, 2530-2537.

[21]   For an inverse effect, where the reactivity of carbanions is larger in MeOH than in DMSO, see: S. T. A. Berger, A. R. Ofial, H. Mayr *J. Am. Chem. Soc.* **2007**, *129*, 9753-9761.

[22]   Y. Marcus, *J. Sol. Chem.* **1984**, *13*, 599-624.

[23]   U. Mayer, V. Gutmann, W. Gerger, *Monatsh. Chem.* **1975**, *106*, 1235-1257.

[24]   J. Catalan, A. Couto, J. Gomez, J. L. Saiz, J. Laynez, *J. Chem. Soc. Perkin Trans. 2* **1992**, 1181-1185.

[25]   J. Catalan, J. Gomez, J. L. Saiz, A. Couto, M. Ferraris, J. Laynez, *J. Chem. Soc. Perkin Trans. 2* **1995**, 2301-2305.

Chapter 7

Miscellaneous Experiments

7.1 Combinatorial Kinetics

7.1.1 Introduction

The idea of combinatorial chemistry is the parallel synthesis of structurally different products, using the same reaction conditions and reaction vessels. With this approach, it is possible to make a large amount of compounds at the same time. Combinatorial chemistry, therefore, is often applied in the pharmaceutical industry, in order to amplify the productivity of drug screenings.[1]

As already introduced in the previous chapters, the linear-free-enthalpy-relationship 7.1

$$\log k_2 \ (20 \ °C) = s \ (N + E) \tag{7.1}$$

is a helpful tool to estimate polar organic reactivity.[2] With known nucleophilicity parameters N, s and electrophilicity parameters E, it is possible to predict the rate of electrophile-nucleophile combinations within accuracy of two orders of magnitude. However, there are still many classes of compounds, for example carbonyl compounds, for which reactivity parameters are inadequately or even not determined.

For reliable s- and N-parameters of nucleophiles, the rate constants of at least three reactions with reference electrophiles have to be measured. Till now, chemists in our group execute one kinetic experiment after the other.

In order to save time and consumables during this process, it was of high interest for us to transfer the idea of combinatorial chemistry to our daily business of measuring reaction kinetics. Since UV-Vis spectroscopy is usually the method of choice, it is obvious that a simple analysis of multicomponent reactions is only possible, if UV-Vis spectra of reactants and products do not interfere.

214

7.1.2 Results

The proof of principle was performed by combining with the anion of dimedone (1^-, $N = 16.27$, $s = 0.77$)[3] with three different colored electrophiles **2**, **3a**, and **3b** in DMSO solution (Scheme 7.1).
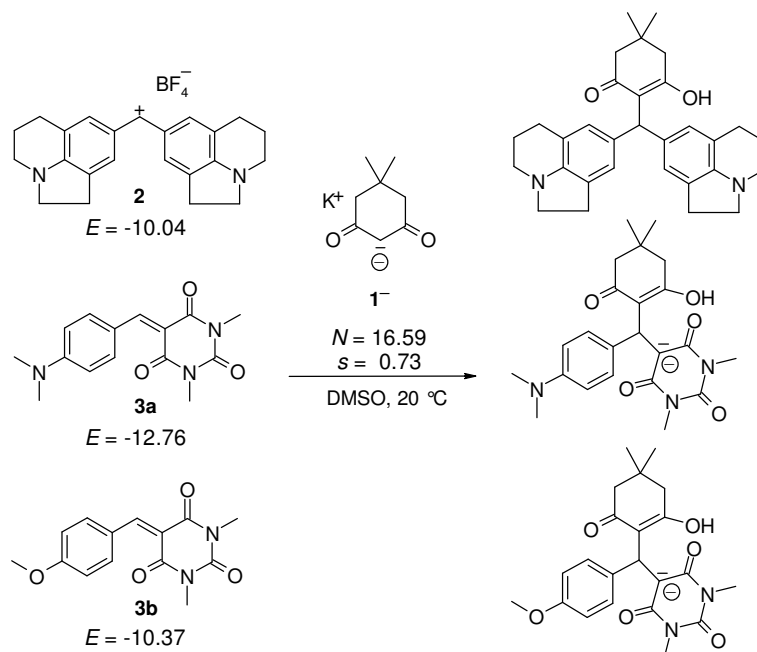
SCHEME 7.1: Combinatorial reactions of carbanion 1^- (6.10×10^{-4} M) with electrophiles **2** (3.13×10^{-6} M), **3a** (6.29×10^{-6} M), and **3b** (1.74×10^{-5} M) in DMSO at 20 °C.

Figure 7.1 shows the resultant UV-Vis spectrum of the green mixture of electrophiles **2**, **3a-b**. The absorption bands of the blue diarylcarbenium ion **2** (λ_{max} = 643 nm), the red benzylidenebarbituric acid **3a** (λ_{max} = 469 nm), and the yellow benzylidenebarbituric acid **3b** (λ_{max} = 378 nm) are separated and do not overlap significantly. Neither the anion of dimedone (1^-) nor the formed adducts (Scheme 7.1) absorb at wavelengths larger than 300 nm and do not interfere with the UV-Vis spectrum in Figure 7.1.

In order to guarantee pseudo-first-order conditions during the reactions, the nucleophile 1^- was used in high excess over each of the electrophiles.
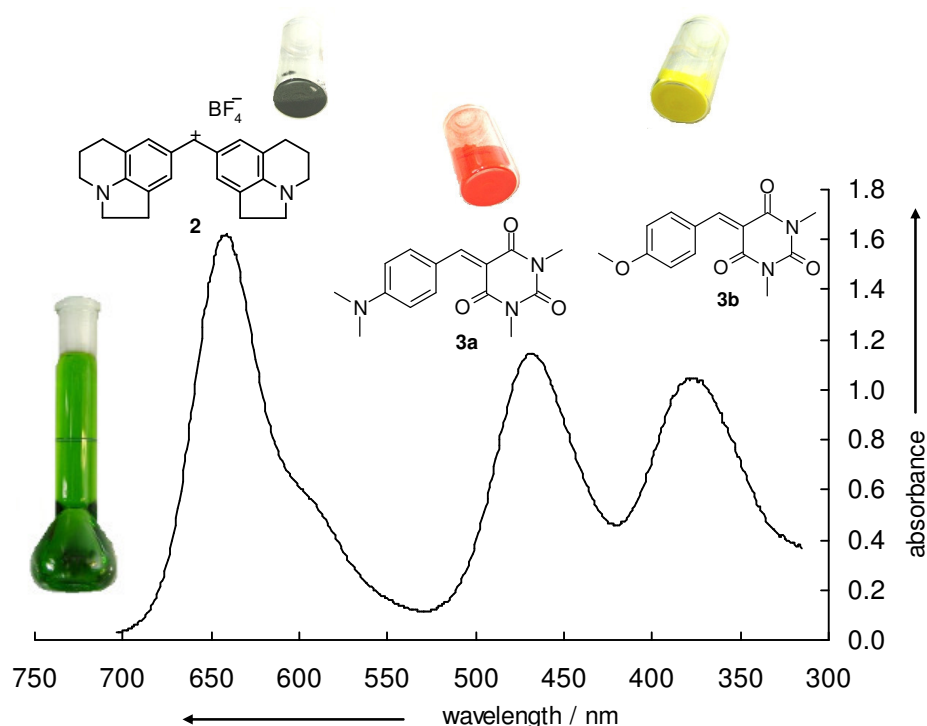
215

FIGURE 7.1: UV-Vis spectrum of a solution of diarylcarbenium ion **2** (3.13×10^{-6} M) and Michael acceptors **3a** (6.29×10^{-6} M) and **3b** (1.74×10^{-5} M) in DMSO.

The green solution of the electrophiles **2**, **3a-b** was mixed with a solution of the carbanion **1**⁻ in a stopped flow instrument, equipped with a diode array detector, and the three reactions depicted in Scheme 7.1 were monitored simultaneously. From Figure 7.2, which exactly displays the first 0.3 seconds of this experiment, one can see that the reactions of **2** with **1**⁻ (orange area) and of **3b** with **1**⁻ (purple area) are already finished within 0.1 seconds. In contrast, the reaction of benzylidenebarbituric acid **3a** with carbanion **1**⁻ (blue to green area of Figure 7.2) has not come to an end during this time. This observation is in agreement with the *E*-parameters of the studied electrophiles: Methoxy-substituted benzylidenebarbituric acid **3b** ($E = -10.37$)[4] and diarylcarbenium ion **2** ($E = -10.04$)[3] are similar in their electrophilicity, whereas Michael acceptor **3a** ($E = -12.76$)[4] is more than two orders of magnitude less electrophilic.

When the time scale of Figure 7.2 is zoomed out to a maximum of three seconds, one can also see the nearly complete reaction of **3a** with dimedone anion (**1**⁻, Figure 7.3).
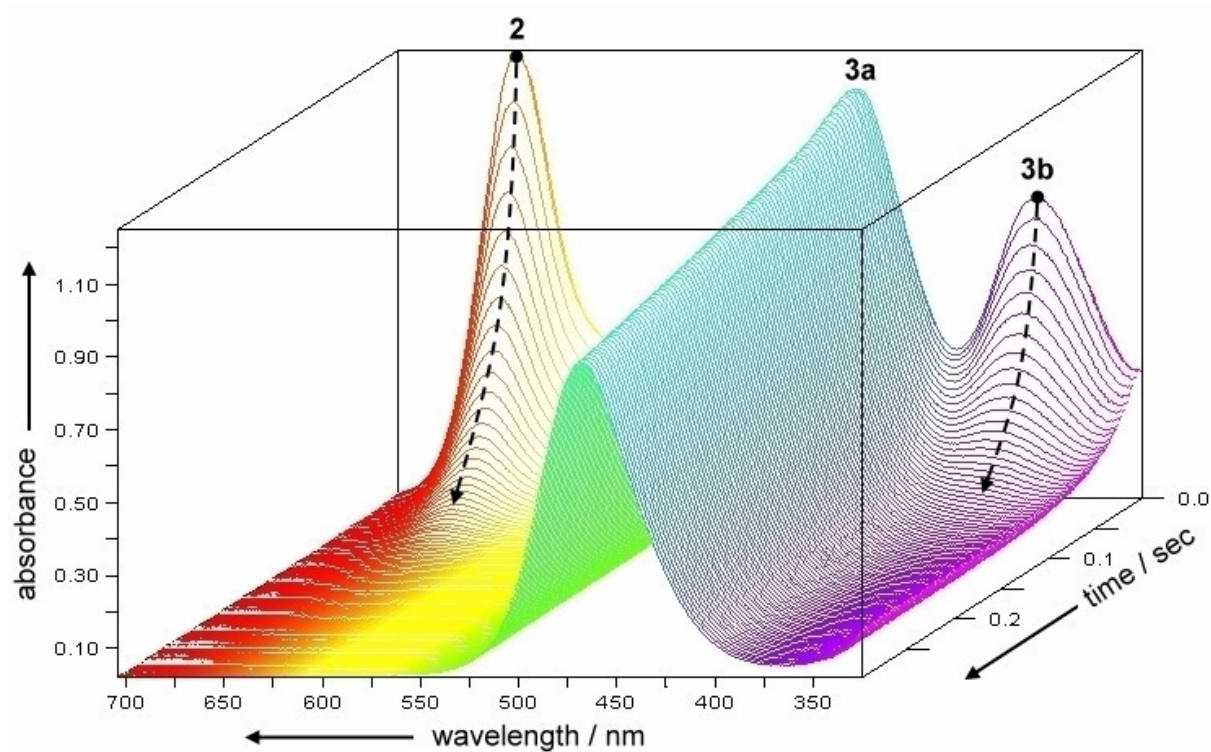
216

FIGURE 7.2: The first 0.3 s of the multicomponent reaction of **1⁻** with electrophiles **2**, **3a**-**b** monitored by stopped-flow UV-Vis spectroscopy.
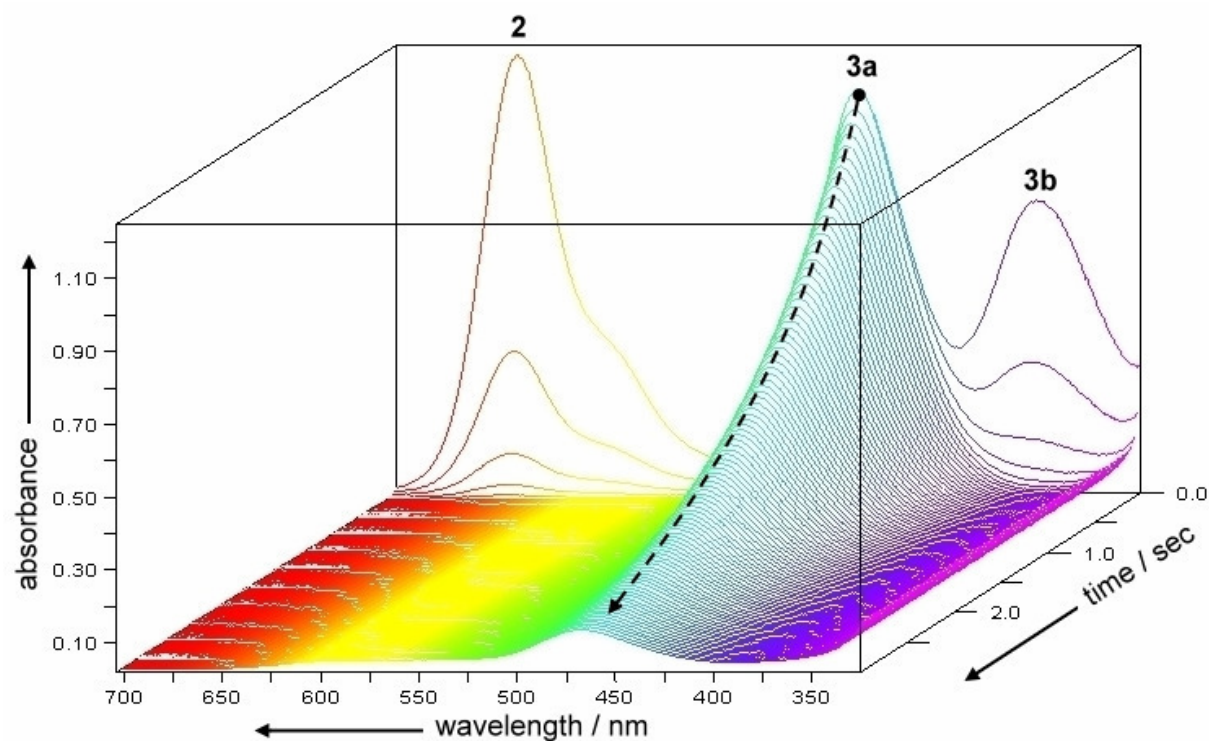

FIGURE 7.3: Complete multicomponent reaction of **1⁻** with electrophiles **2**, **3a**-**b** monitored by stopped-flow UV-Vis spectroscopy.

The observed exponential decays of absorbance were extracted for each reaction at λ_{max} of the corresponding electrophile (Figure 7.4), in order to obtain the pseudo-first-order rate constants k_{obs}, listed in Table 7.1.
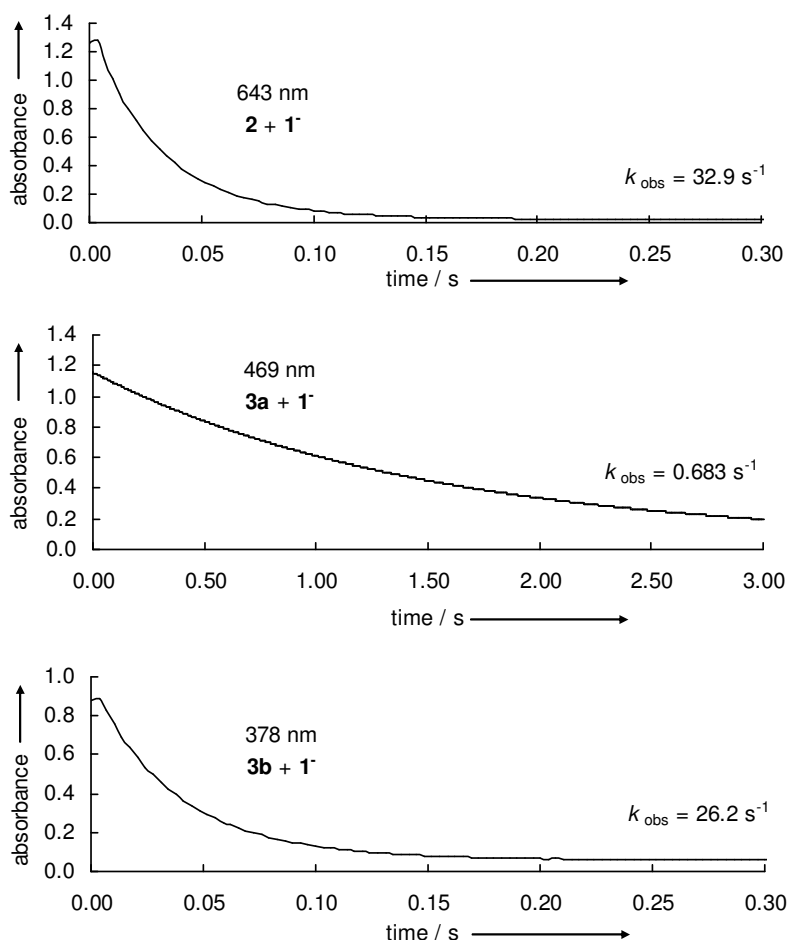

FIGURE 7.4: Exponential decays of absorbance at 643 nm (reaction of **2** with **1**⁻, top), 469 nm (reaction of **3a** with **1**⁻, middle), and 378 nm (reaction of **3b** with **1**⁻, bottom).

TABLE 7.1: Pseudo-first-order rate constants k_{obs} and derived second-order rate constants k_2 of the reactions of dimedone anion (**1**⁻) with electrophiles **2**, **3a**-**b**, compared with corresponding k_2 values from literature.

elec	E	k_{obs} / s^{-1}	$k_2 / M^{-1} s^{-1}$ [a]	k_2 lit. $/ M^{-1} s^{-1}$
2	-10.04[b]	3.29×10^1	5.39×10^4	6.08×10^4 [b]
3a	-12.76[c]	6.83×10^{-1}	1.12×10^3	1.04×10^3 [c]
3b	-10.37[c]	2.62×10^1	4.30×10^4	4.83×10^4 [c]

[a] $k_2 = k_{obs} / [\mathbf{1}^-]$; with $[\mathbf{1}^-] = 6.10 \times 10^{-4}$ M. [b] From ref. [3]. [c] From ref. [4].

The second-order rate constants k_2 determined by the combinatorial approach differ -11 % ($\mathbf{2} + \mathbf{1}^-$ and $\mathbf{3b} + \mathbf{1}^-$) and $+8$ % ($\mathbf{3a} + \mathbf{1}^-$) from conventionally obtained rate constants k_2. However, one has to keep in mind that the latter values were at least determined by four pseudo-first order experiments (analysis of the k_{obs} versus [$\mathbf{1}^-$] correlations) and therefore are likely to be more accurate. Thus, the observed deviations shall not be over-interpreted.

7.1.3 Conclusion

The kinetic investigation of the combinatorial reactions of dimedone anion ($\mathbf{1}^-$) with Michael acceptors $\mathbf{3a}$-$\mathbf{b}$ and diarylcarbenium ion $\mathbf{2}$ shows that in principle it is possible to determine three pseudo-first order rate constants k_{obs} with only one experiment. N and s parameters, which will be determined with the introduced electrophile mixture in the future, have to be considered as preliminary numbers, due to the small utilized electrophilicity range [from $E = -10.04$ ($\mathbf{2}$) to $E = -12.79$ ($\mathbf{3a}$)].

Nevertheless, further development of new multicomponent mixtures will make kinetic investigations, e.g., determination of reactivity parameters, faster and more efficient particularly for screening experiments with nucleophiles of unknown reactivity.

7.2 Reactivity of the 2-(*p*-Nitrophenyl)-propionitrile Anion

7.2.1 Introduction

Due to the carbanion-stabilizing power of an α-cyano group,[5] phenylacetonitriles and their α-methylated analogues are deprotonated by strong bases (e.g., potassium *tert*-butoxide) in DMSO solution (Scheme 7.2).

R = Me, X = *p*-NO$_2$: **4**
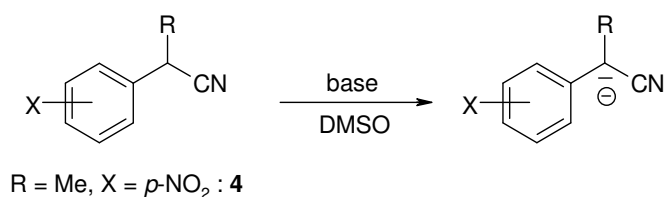
SCHEME 7.2: Deprotonation of phenylalkylnitriles in DMSO.

Substituents X in the benzene ring highly influence the pK_a values of phenylalkylnitriles in DMSO.[6] The acidity of 2-(*p*-nitrophenyl)acetonitrile (pK_a $_{DMSO}$ = 12.3)[6] is comparable to that of acetylacetone (pK_a $_{DMSO}$ = 13.3),[7] whereas the corresponding *p*-dimethylamino-substituted analogue is more then ten orders of magnitude less acidic (pK_a $_{DMSO}$ = 24.6).[6] Despite the weak correlation of nucleophilicity versus basicity (Figure 7.5),[8] one can expect that carbanions of donor-substituted phenylalkylnitriles are among the strongest nucleophiles, which have been characterized by equation 7.1. Therefore, these compounds can serve as important references in the investigation of weak electrophiles.

Furthermore, carbanions derived from phenylalkylnitriles absorb in the visible region of light. The 2-(*p*-Nitrophenyl)-propionitrile anion (**4**⁻) has a broad absorption band in DMSO solution (λ_{max} = 549 nm, Figure 7.6), which corresponds to a deep red color. This general attribute makes anions of phenylalkylnitriles ideal candidates to study the reactivity of colorless electrophiles by UV-Vis spectroscopy.
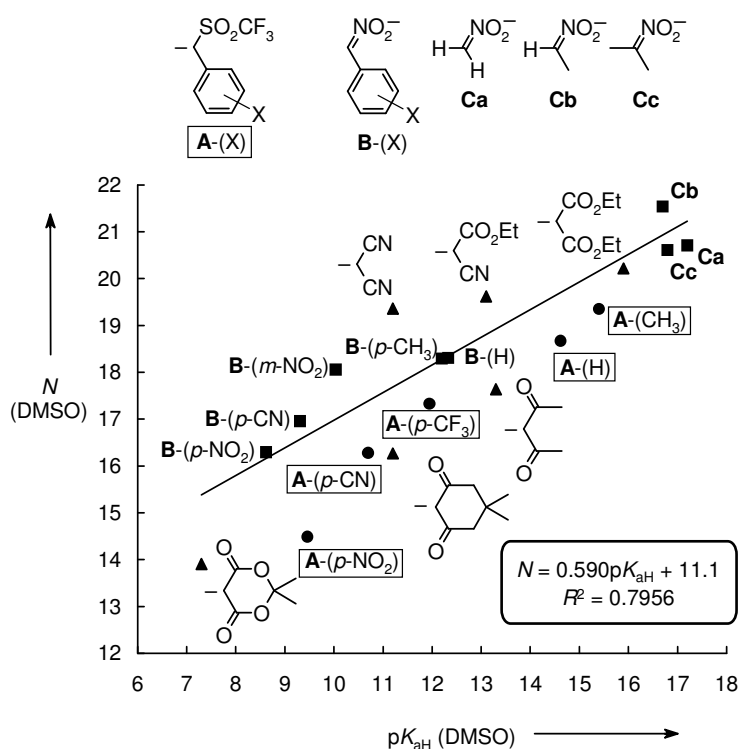
FIGURE 7.5: Brønsted plot for the reactions of different carbanions with benzhydrylium ions and quinone methides in DMSO, taken from ref. [8].
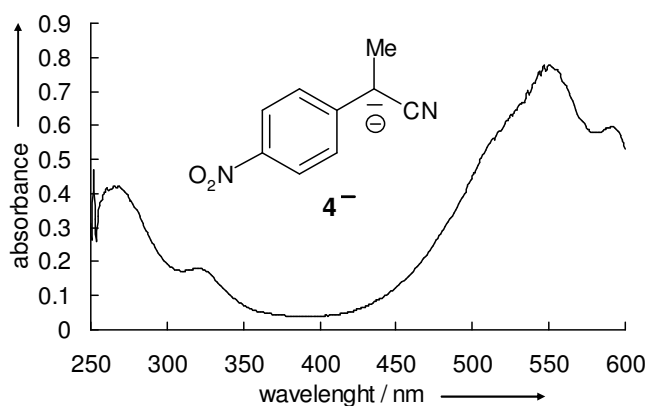

FIGURE 7.6: UV-Vis spectrum of the 2-(p-nitrophenyl)-propionitrile anion (4^-) in DMSO.

In a collaborative effort, the anions of phenylalkylnitriles were characterized according to equation 7.1. Reactions of the 2-(p-nitrophenyl)-propionitrile anion (4^-) with quinone methides have been already studied by T. Lemek,[9] and it was my task to investigate the reactivity of 4^- towards Michael acceptors, like benzylidenebarbituric acids and benzylideneindan-1,3-diones.

221

7.2.2 Product Study

In order to prove the assumed attack of the carbanionic center to the β-position of the Michael acceptor, the representative reaction of 4^- with the benzylidenebarbituric acid $3b$ (Scheme 7.3) was investigated by ^{1}H-NMR spectroscopy (Figure 7.7).
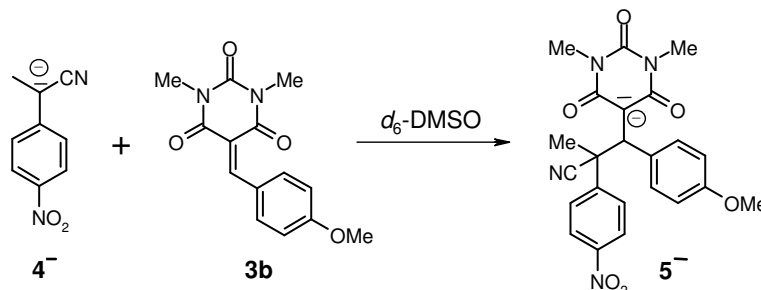
SCHEME 7.3: Reaction of carbanion 4^- with benzylidenebarbituric acid $3b$ in d_6-DMSO.

Addition product 5^- is obtained as a 7:4 mixture of diastereomers (from ^{1}H-NMR, Figure 7.7) in d_6-DMSO solution. Characteristic for the addition product 5^- is the benzylic proton (attributed with "d" in Figure 7.7), which absorbs as a singlet at δ 4.59 ppm (major diastereomer). The high upfield shift of the ^{1}H-NMR signal of the vinylic proton in compound $3b$ (δ 8.47 ppm)[10] to δ 4.59 ppm in product 5^- clearly indicates the nucleophilic attack in β-position of the Michael acceptor.
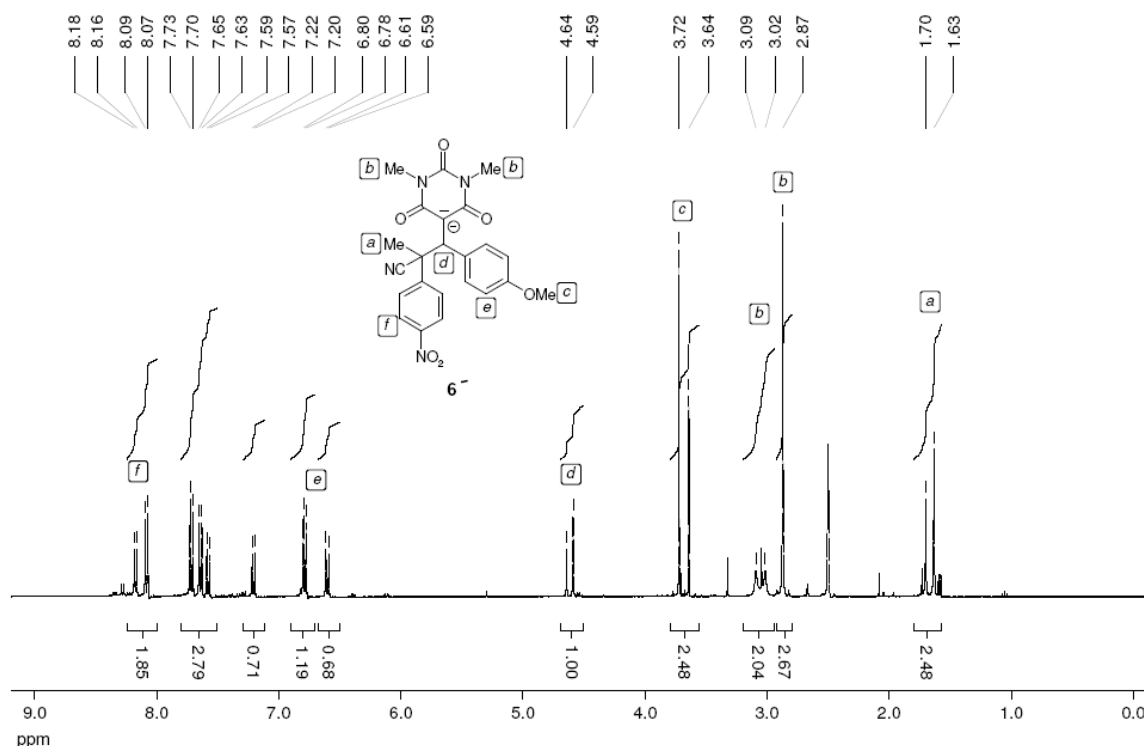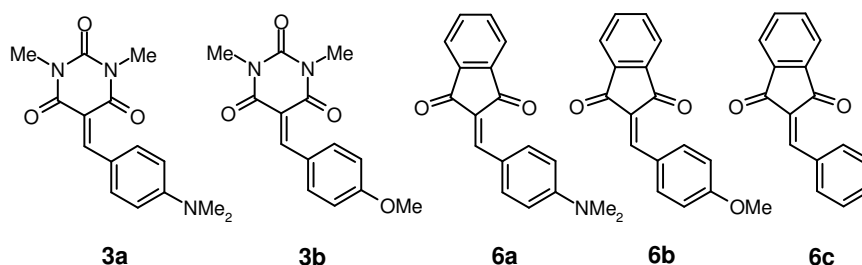

FIGURE 7.7: ^{1}H-NMR spectrum (200 MHz, d_6-DMSO) of 5^- (addition product of $3b$ and 4^-).

7.2.3 Kinetic Experiments

The Benzylidenebarbituric acids **3a** and **3b**[4] and the benzylideneindan-1,3-diones **6a-c**[11] have been used as a basis in this study of the nucleophilic behavior of the 2-(*p*-nitrophenyl)-propionitrile anion (**4⁻**).

3a   **3b**   **6a**   **6b**   **6c**

Kinetic experiments were performed as described in chapters 2 and 3, but using the electrophiles **3a**-**b**, and **6a**-**c** in excess over carbanion **4⁻**. Thus, the decrease of the absorbance of **4⁻** was monitored at $\lambda = 590$ nm.

The reactions of **K⁺-4⁻** with **3a**-**b**, and **6b**-**c** proceeded quantitatively, indicated by constant absorbances ($\lambda = 590$ nm) at the end. The reaction of **4⁻** with **6a** shows a positive intercept of the k_{obs} versus [**6a**] correlation, which indicates an equilibrium process. Accordingly, the end-absorbances ($\lambda = 590$ nm) of the different pseudo-first-order runs considerably depend on the electrophile concentration. With the absolute value of the positive intercept and the obtained second-order rate constant one calculates an equilibrium constant $K = 2.48 \times 10^3$ L mol⁻¹ for the reaction of **4⁻** with **6a**.[12]

TABLE 7.2: Second-order rate constants k_2 for the reactions of the Michael acceptors **3** and **6** with the 2-(*p*-nitrophenyl)-propionitrile anion (**4⁻**) in DMSO at 20 °C.

elec	E	k_2 / L mol⁻¹ s⁻¹ [a]
6a	−13.56[b]	3.15×10^3
3a	−12.76[c]	9.12×10^3
6b	−11.32[b]	1.15×10^5
3b	−10.37[c]	1.88×10^5
6c	−10.11[b]	5.22×10^5

[a] Decrease of the absorbance of **4⁻** is followed, carbanion **4⁻** is used as potassium salt. [b] From ref. [11]. [c] From ref.[4].

7.2.4 Discussion

In order to determine the nucleophilicity parameters N and s for the 2-(p-nitrophenyl)-propionitrile anion ($\mathbf{4}^-$), the logarithmic second-order rate constants log k_2 were plotted versus the electrophilicity parameters E of the corresponding electrophiles (Figure 7.8). From the slope of the resultant linear correlation one derives a nucleophile-specific slope-parameter of $s = 0.60$. According to equation 7.1, the intercept with the abscissa equals $-N$. Hence, a nucleophilicity-parameter for the anion of 2-(p-nitrophenyl)-propionitrile ($\mathbf{4}^-$) of $N = 19.54$ is obtained.
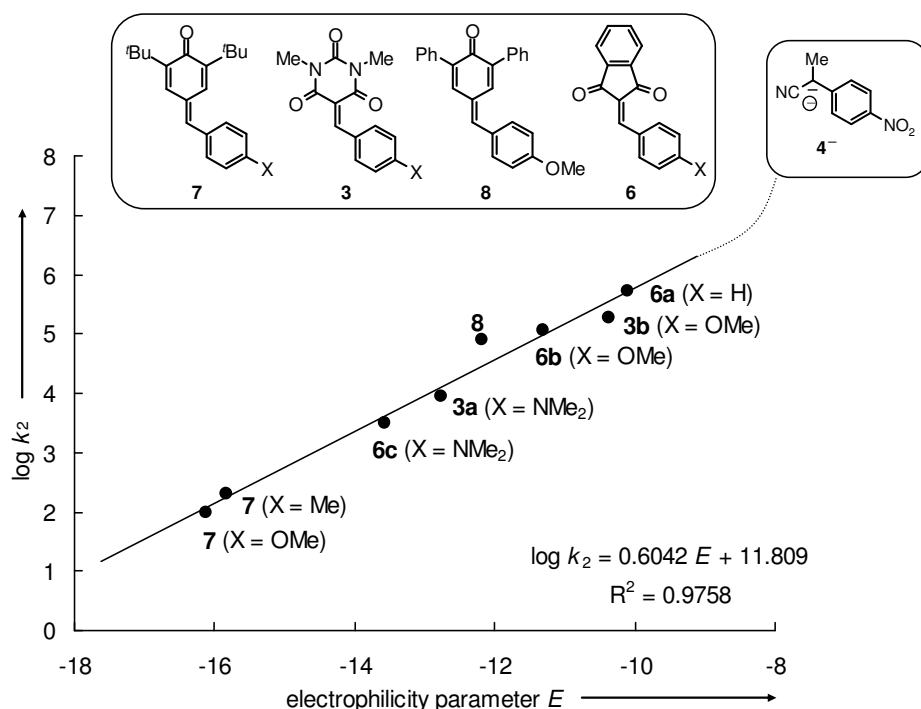
FIGURE 7.8: Plot of log k_2 versus E for the reactions of the 2-(p-nitrophenyl)-propionitrile anion ($\mathbf{4}^-$) with electrophiles $\mathbf{3}$, $\mathbf{6}$, $\mathbf{7}$, and $\mathbf{8}$.

The nucleophilicity of 2-(p-nitrophenyl)-propionitrile ($\mathbf{4}^-$) is therefore ranked between the reactivities of other cyano-stabilized carbanions, e.g., malononitrile ($N = 19.36$)[3] and ethyl cyanoacetate ($N = 19.62$).[3]

7.2.5 Experimental Section

7.2.5.1 Synthesis of the potassium salt of 2-(p-nitrophenyl)-propionitrile anion (**K⁺-4⁻**)

A solution of 2-(p-nitrophenyl)-propionitrile (**4**, 500 mg, 2.84 mmol) and KO^{t}Bu (318 mg, 2.84 mmol) in dry ethanol (10 mL) was stirred for one hour. The brown precipitate was filtered off, washed with dry ethanol (2 × 10 mL), and finally dried in vacuum. Everything was done under inert gas. 89 % yield. ^{1}H-NMR (CDCl$_3$, 300 MHz): δ 1.73 (s, 3H, CH$_3$), 6.12 (d, ^3J = 12 Hz, 1H, Ar-H), 6.39 (d, ^3J =12 Hz, 1H, Ar-H), 7.35 (d, ^3J = 12 Hz, 1H, Ar-H) 7.39 (d, ^3J = 10 Hz, 1H, Ar-H).

7.2.5.2 Synthesis of **5⁻** for ^{1}H-NMR analysis

The potassium salt of 2-(p-nitrophenyl)-propionitrile anion (**K⁺-4⁻**, 10.0 mg, 4.67 × 10^{-2} mmol) and benzylidenebarbituric acid **3b** (10.6 mg, 3.86 × 10^{-2} mmol) were dissolved in d_6-DMSO (0.7 mL), which yielded **5⁻** as a mixture of diastereomers (7:4, from ^{1}H-NMR). ^{1}H-NMR (CDCl$_3$, 200 MHz), major diastereomer: δ 1.63 (s, 3H, CH$_3$), 2.87 (s, 6H, NCH$_3$), 3.72 (s, 3H, OCH$_3$), 4.59 (s, 1H, CH), 6.79 (d, ^3J = 8.8 Hz, 2H, Ar-H), 7.64 (d, ^3J = 8.8 Hz, 2H, Ar-H), 7.72 (d, ^3J = 8.8 Hz, 2H, Ar-H) 8.08 (d, ^3J = 8.8 Hz, 2H, Ar-H). Minor diastereomer: δ = 1.70 (s, 3H, CH$_3$), 3.02 (s , br., 3H, NCH$_3$), 3.09 (s, br., 3H, NCH$_3$), 3.64 (s, 3H, OCH$_3$), 4.64 (s, 1H, CH), 6.60 (d, ^3J = 8.8 Hz, 2H, Ar-H), 7.21 (d, ^3J = 8.8 Hz, 2H, Ar-H), 7.58 (d, ^3J = 8.8 Hz, 2H, Ar-H) 8.17 (d, ^3J = 8.8 Hz, 2H, Ar-H).

7.2.5.3 Kinetic Experiments

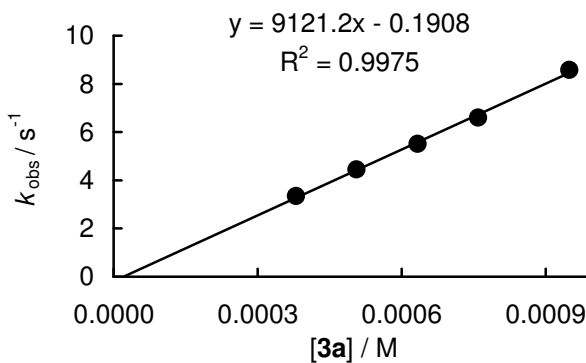Reaction of **6a** with **4⁻** (DMSO, 20 ° C, stopped-flow, λ = 590 nm)

Nr.	$[\mathbf{4^-}]_0$ / M	$[\mathbf{6a}]_0$ / M	k_{obs} / s^{-1}
03-1	2.65×10^{-5}	9.18×10^{-4}	4.19
03-2	2.65×10^{-5}	7.71×10^{-4}	3.69
03-3	2.65×10^{-5}	6.61×10^{-4}	3.31
03-4	2.65×10^{-5}	5.14×10^{-4}	2.90
03-5	2.65×10^{-5}	2.94×10^{-4}	2.21

$$k_2 = 3.15 \times 10^3 \, \text{L mol}^{-1} \, \text{s}^{-1}$$
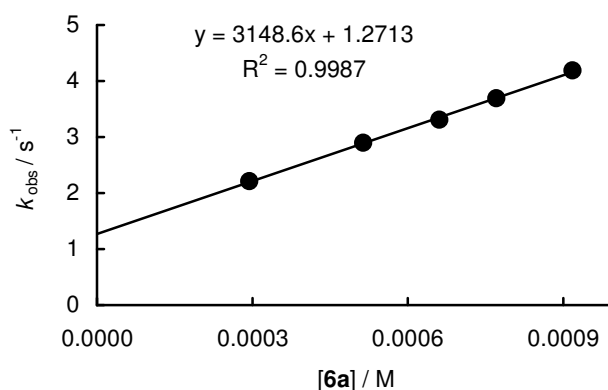
Reaction of **3a** with **4⁻** (DMSO, 20 ° C, stopped-flow, λ = 590 nm)

Nr.	$[\mathbf{4^-}]_0$ / M	$[\mathbf{3a}]_0$ / M	k_{obs} / s^{-1}
04-1	2.50×10^{-5}	9.49×10^{-4}	8.58
04-2	2.50×10^{-5}	7.59×10^{-4}	6.60
04-3	2.50×10^{-5}	6.33×10^{-4}	5.51
04-4	2.50×10^{-5}	5.06×10^{-4}	4.45
04-5	2.50×10^{-5}	3.80×10^{-4}	3.34

$$k_2 = 9.12 \times 10^3 \, \text{L mol}^{-1} \, \text{s}^{-1}$$

226

Reaction of **6b** with **4**$^-$ (DMSO, 20 $^\circ$ C, stopped-flow, λ = 590 nm)

Nr.	$[\mathbf{4^-}]_0$ / M	$[\mathbf{6b}]_0$ / M	k_{obs} / s^{-1}
05-1	2.50×10^{-5}	8.92×10^{-4}	1.03×10^{2}
05-2	2.50×10^{-5}	7.43×10^{-4}	8.53×10^{1}
05-3	2.50×10^{-5}	6.13×10^{-4}	7.14×10^{1}
05-4	2.50×10^{-5}	5.02×10^{-4}	5.87×10^{1}
05-5	2.50×10^{-5}	3.72×10^{-4}	4.25×10^{1}

$$k_2 = 1.15 \times 10^5 \, \text{L mol}^{-1} \, \text{s}^{-1}$$

y = 115224x + 0.2342
R^2 = 0.9994
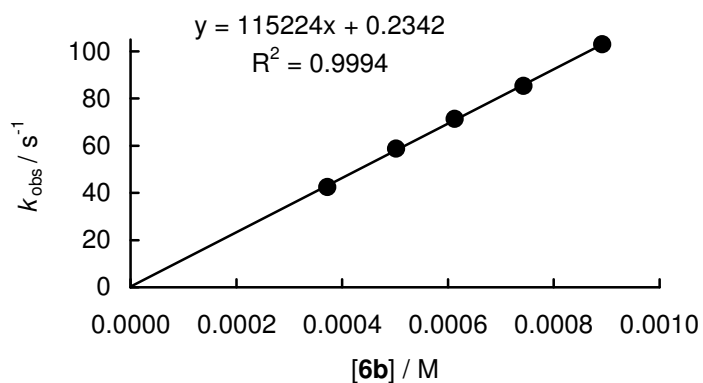
Reaction of **3b** with **4**$^-$ (DMSO, 20 $^\circ$ C, stopped-flow, λ = 590 nm)

Nr.	$[\mathbf{4^-}]_0$ / M	$[\mathbf{3b}]_0$ / M	k_{obs} / s^{-1}
06-1	2.50×10^{-5}	9.86×10^{-4}	1.92×10^{2}
06-2	2.50×10^{-5}	7.49×10^{-4}	1.49×10^{2}
06-3	2.50×10^{-5}	6.31×10^{-4}	1.27×10^{2}
06-4	2.50×10^{-5}	4.73×10^{-4}	9.66×10^{1}
06-5	2.50×10^{-5}	3.55×10^{-4}	7.32×10^{1}

$$k_2 = 1.88 \times 10^5 \, \text{L mol}^{-1} \, \text{s}^{-1}$$

y = 188140x + 7.3764
R^2 = 0.9996

227
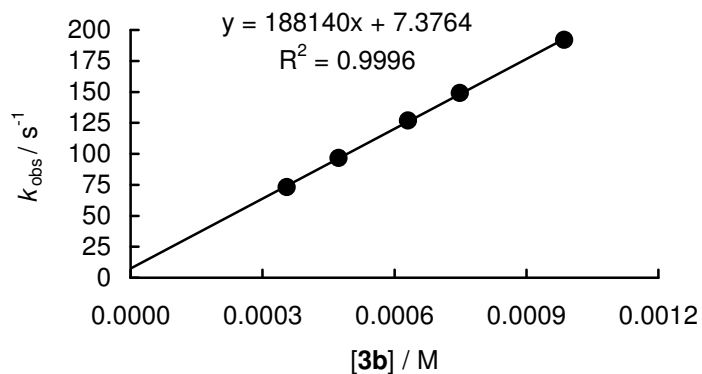
Reaction of **6c** with **4**$^-$ (DMSO, 20 ° C, stopped-flow, λ = 590 nm)

Nr.	$[4^-]_0$ / M	$[6c]_0$ / M	k_{obs} / s^{-1}
07-1	2.21×10^{-5}	6.38×10^{-4}	3.60×10^2
07-2	2.21×10^{-5}	5.32×10^{-4}	3.10×10^2
07-3	2.21×10^{-5}	4.36×10^{-4}	2.67×10^2
07-4	2.21×10^{-5}	3.30×10^{-4}	2.03×10^2
07-5	2.21×10^{-5}	2.66×10^{-4}	1.66×10^2

$$k_2 = 5.22 \times 10^5 \text{ L mol}^{-1} \text{ s}^{-1}$$

y = 521830x + 31.386
R^2 = 0.9958
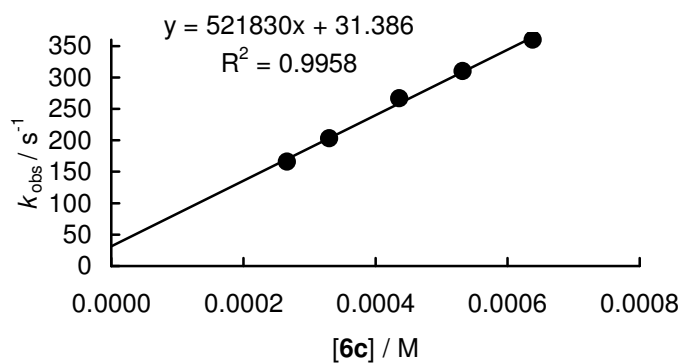
7.3 References

[1]   F. Darvas, G. Dorman, L. Urge, I. Szabo, Z. Ronai, M. Sasvari-Szekely, *Pure Appl. Chem.* **2001**, *73*, 1487-1498.

[2]   H. Mayr, A. R. Ofial, *Pure Appl. Chem.* **2005**, *77*, 1807-1821.

[3]   R. Lucius, R. Loos, H. Mayr, *Angew. Chem.* **2002**, *114*, 97-102; *Angew. Chem. Int. Ed.* **2002**, *41*, 91-95.

[4]   F. Seeliger, S. T. A. Berger, G. Y. Remennikov, K. Polborn, H. Mayr, *J. Org. Chem.* **2007**, *72*, 9170-9180.

[5]   A. Abbotto, S. Bradamante, G. A. Pagani, *J. Org. Chem.* **1993**, *58*, 449-455.

[6]   F. G. Bordwell, J. P. Cheng, M. J. Bausch, J. E. Bares, *J. Phys. Org. Chem.* **1988**, *1*, 209-223.

[7]   W. N. Olmstead, F. G. Bordwell, *J. Org. Chem.* **1980**, *45*, 3299-3305.

[8]   S. T. A. Berger, A. R. Ofial, H. Mayr, *J. Am. Chem. Soc.* **2007**, *129*, 9753-9761.

[9]   T. Lemek, **2004**, unpublished results.

[10]   R. Bednar, E. Haslinger, U. Herzig, O. E. Polansky, P. Wolschann, *Monatsh. Chem.* **1976**, *107*, 1115-1125.

[11]   S. T. A. Berger, F. H. Seeliger, F. Hofbauer, H. Mayr, *Org. Biomol. Chem.* **2007**, *5*, 3020-3026.

[12]   This method is not exact. For a more reliable number one has to determine the equilibrium constant from a UV-Vis spectroscopic titration experiment.

Curriculum Vitae

Persönliche Daten:

Name:	**Florian Hendrik Seeliger**
Geburtsdatum:	02.08.1977
Geburtsort:	Hamburg
Familienstand:	Verheiratet
Nationalität:	Deutsch
Adresse:	Alter Elbdeich 42, 21217 Seevetal

Schule: 1987–1996 Alexander von Humboldt Gymnasium, Hamburg

Abschluss: Allgemeine Hochschulreife 12.06.1996

Ausbildung: 09/1993–01/1997 Gymnasium Altona, Hamburg und Berufsfachschule für Chemisch-technische Assistenz, Hamburg

Abschluss: Staatlich geprüfter Chemisch Technischer Assistent

Ersatzdienst: 03/1997–03/1998 Rettungssanitäter DRK, Hamburg

Studium: Chemie (Diplom)

Grundstudium: 10/1998–10/2000 Technische Universität München

Hauptstudium: 11/2000–11/2004 Ludwig-Maximilians-Universität München

Diplomarbeit: Physikalisch Organische Chemie:

„Nucleophile Reaktivität Sulfonyl-stabilisierter Carbanionen" Betreuung durch Prof. Dr. Herbert Mayr

Promotion: 12/2004-04/2008 *„Reactions of Carbanions with Michael Acceptors and Electron-deficient Arenes: Quantifying Polar Organic Reactivity"*, betreut von Prof. Dr. Herbert Mayr.

Auslandsaufenthalte: 08/2006–11/2006 Institute of Organic Chemistry, Polish Academy of Sciences, Warschau, Polen

Mitarbeit im Arbeitskreis von Prof. Dr. Mieczyslaw Makosza

München, 25.04.2008